Alma Mater Studiorum – Università di Bologna

DOTTORATO DI RICERCA IN

Scienze Ambientali: Tutela e Gestione Delle Risorse Naturali

Ciclo XXV

**Settore Concorsuale di afferenza:** 03/A1 – CHIMICA ANALITICA

**Settore Scientifico disciplinare:** CHIM/12 - CHIMICA DELL'AMBIENTE E DEI BENI CULTURALI

TITOLO TESI

# Advanced spectroscopic techniques and chemometric analysis for atmospheric organic aerosol characterization and source apportionment

**Presentata da: Dott. MARCO PAGLIONE**

**Coordinatore Dottorato:**
**Prof. Enrico Dinelli**

**Tutore:**
**Emilio Tagliavini**

**Relatore:**
**Dott. Stefano Decesari**

**Esame finale anno 2013**

# Table of contents

# Executive summary of the thesis

**by Marco Paglione**

Atmospheric aerosol particles directly impact air quality, visibility and atmospheric transparency, through scattering and absorption of light (i.e., direct climate forcing effect) and by modulating the formation and properties of clouds (i.e., indirect climate forcing effect) which in turns contribute to control the climate system at both regional and global scales (Ravishankara, 2005; IPCC, 2007; Ghan, 2007). Organic Aerosol (OA) in general accounts for a large fraction (10–90%) of the global submicron (PM1) particulate mass (Kanakidou et al., 2005; Zhang et al., 2007) whereas the rest of the mass consists of soot, inorganic salts, metals and elements. The inorganic and elemental fraction of the particle mass has been quite well characterized, while much less is known about the composition of the organic fraction. The characterization of OA chemical composition and mass concentration is limited by analytical challenges arising from the fact that atmospheric OA is a complex mixture of thousands of organic compounds characterized by vastly different properties, such as oxidation state, volatility and hygroscopicity, and extremely diverse sources and atmospheric reactions.

Organic particles are either emitted directly into the atmosphere as primary organic aerosol (POA) or form in the atmosphere as secondary organic aerosol (SOA) due to the photochemical conversion of gaseous precursors, including both anthropogenic and biogenic species (Pankow, 1994; Kroll and Seinfield, 2008; Calvert, 2002; Atkinson and Arey, 2003). Current atmospheric chemical transport models estimate that SOAs dominate the aerosol organic composition at the global scale (Baltensperger et al., 2005; Lanz et al., 2007). Nevertheless, current estimates of global SOA production remain extremely uncertain due to the lack of observations capable to constrain the contributions from the various SOA sources.

In general, OA measurement methods can be divided into two broad categories: off-line and on-line. Off-line techniques, e.g., gas chromatography/mass spectrometry (GC/MS), liquid chromatography/MS (LC/MS), nuclear magnetic resonance (NMR) and Fourier transform infrared (FTIR) spectroscopy, provide detailed information on individual chemical species or functional groups but require large amounts of sample, resulting in low time resolution (hours to days). On-line techniques (e.g., aerosol mass spectrometry, AMS, or Proton-Transfer-Reaction Mass Spectrometry, PTR-MS) usually provide less specific information on composition, with little details

on individual species concentrations, but benefit from fast acquisition times, providing near real-time data (Saarikoski et al., 2012; Duarte and Duarte, 2011).

A universal technique for atmospheric organic aerosol analysis does not exist, and trade-offs between specificity or resolution and recovery have to be applied, resulting in a certain degree of complementariness between the analytical techniques (Hallquist et al., 2009). For this reason, a comprehensive characterization can be attempted by employing suitable combinations of techniques. This approach, however, involves the problem of treating heterogeneous chemical datasets with a large number of variables, up to $10^2$ - $10^3$ in the case of mass spectra or high resolution NMR. In order to reduce the database complexity, algorithms for multivariate statistical analysis and factor analysis are increasingly used for the identification of "hidden" information in the datasets and for explanation of the variability in the chemical records obtained at a given site using a limited number of relevant variables ("receptor modelling") (Viana et al., 2008).

Multivariate statistical techniques, overall called Factor Analysis, such as Positive Matrix Factorization (PMF) (Paatero and Tapper, 1994; Paatero, 1999) and Multivariate Curve Resolution (Terrado et al., 2010) are used to deconvolve a time series of simultaneous measurements into a set of "factors" or "components", representing groupings of chemical species that correlate in time, and their time-dependent concentrations. These factors can be related to specific emission sources or atmospheric reactions, on the basis of chemical tracer profiles or of the links between time trends and atmospheric transport (e.g., wind direction respect to sources). Because receptor models require no a priori knowledge of source-specific emission inventories, they are ideal for use in locations where emission inventories are poorly characterized or where atmospheric processing and secondary formation play a major role.

Several publications in last years dealt with factor analysis applied to datasets of OA chemical compositions from both off-line and on-line measurements. Most consistent results are based on the deconvolution of AMS mass spectra and allowed the separation of OA components into a few chemical classes: oxygenated OA (OOA), hydrocarbon-like OA (HOA), and sometimes other components such as biomass burning OA (BBOA) (Zhang et al., 2011). It was found that the majority of OA mass is accounted for by OOA which can be further decomposed into a more oxidized component, the low-volatility OOA (LV-OOA), and a less oxidized one, the semi-volatile OOA (SV-OOA) (Ng et al., 2010). Moreover, there is strong evidence that most atmospheric OOA is of secondary origin since its concentration is strongly correlated to photochemical activity tracers (Volkamer et al., 2006). Laboratory and field observations and state-of-the-art gas-to-particle partitioning models suggest that atmospheric OOA are a highly dynamic system, tightly coupled to gas-phase oxidation chemistry (Jimenez et al., 2009). Examination of a large AMS dataset for

Northern Hemisphere environments (Ng et al. 2010) showed that in spite of the great variability in compositions in near-source areas, all compositions tend to converge to highly oxidized LV-OOA at background sites and whose composition is confined in a relatively narrow range of the most characteristics mass fragments, that must be considered as an endpoint of OA transformation ("ageing") in the troposphere. Nevertheless, the relative contribution of POA and SOA to the overall OA budget remains controversial due to the persistent discrepancies between measured OA concentrations and predictions of atmospheric chemistry models. Finally, preliminary comparison of the AMS groupings for OA with those emerging from other techniques (i.e. FT-IR or NMR) indicates that the actual diversity of aerosol organic chemical classes (and especially of its secondary fraction) is greater than suggested by AMS alone, and hence it requires information from complementary analytical techniques.

Chemometric methods for sample source identification are used in many disciplines, but contrary to other scientific fields, methods relying on the analysis of NMR datasets are rarely used in atmospheric sciences. This thesis work is a first attempt to fill this gap. It provides **an original application of NMR-based chemometric methods to atmospheric aerosol source apportionment.** The method was tested on chemical composition databases obtained from sample sets collected at both pristine and polluted environments in Europe, hence exploring the impact of a great diversity of natural and anthropogenic sources. In this work, we focused on sources of water-soluble organic aerosols, for which the NMR analysis provides substantial advantages compared to alternative methods. Moreover, aerosol water-soluble organic carbon (WSOC) represents a fraction of aerosol organic matter for which the traditional source apportionment methods, relying on the GC/MS analysis of tracer compounds, is less reliable and for which the development of new methods, more suitable for the analysis of very polar compounds, is advisable.

In recent years, progress in the application of NMR techniques to the analysis of atmospheric aerosols showed that:

a) the sensitivity of proton-NMR (H-NMR) analysis of atmospheric samples conducted in strong magnetic fields (≥ 400 MHz) is not inferior to that of GC/MS analysis, making H-NMR suitable for the analysis of full time series of samples collected during experimental field campaigns;

b) the availability of new spectral datasets from laboratory studies, like in reaction chambers ("smog" chambers) provided the basis for the assignment of NMR spectral fingerprints to specific aerosol sources.

In this context, this thesis work starts from nine NMR datasets for submicron aerosol WSOC samples collected during field campaigns of the research project EUCAARI, characterized by

different levels of complexity and source variability. Standard factor analysis algorithms are then applied and compared. A minimum spread in the results from the various mathematical algorithms was indicative of genuine solutions, suitable for the estimation of specific source contributions to the WSOC mass concentrations. Most of the following discussion will deal with the interpretation of factor "profiles" and "contributions". While profiles represent the characteristic NMR spectra for each factor and are interpreted on the basis of the underlying functional group composition and by comparing with libraries of NMR spectra, the contributions are the time trends and contributing amounts to the total aerosol concentrations. Comparison of factor time trends with those of tracer compounds derived by ancillary techniques, such as ion chromatography, supported the assignment of factors to specific sources.

The factor analysis techniques, applied independently to the NMR datasets from the various field campaigns, allowed the identification of recurrent source contributions to the aerosol WSOC in the European background lower troposphere:

1. Marine SOA, containing methane-sulphonate (MSA) and found at coastal stations and in Mediterranean countries;
2. Aliphatic amines from ground sources (soil respiration, agricultural activities, waste management, etc.) which were found in northern countries and in the Po Valley;
3. Biomass burning POA, containing tracers of cellulose and lignine pyrolysis and occurring especially in samples collected in the cold seasons and at both rural and urban sites;
4. Biogenic SOA from terpene oxidation, with spectral features matching those of SOA generated in smog chamber experiments starting from monoterpene ozonolysis and photooxidation, and occurring at forest sites in Scandinavia and central Europe;
5. "Aged" SOAs, of unclear biogenic/pyrogenic origin, characterized by polysubstitued aliphatic compounds including humic-like substances (HULIS) and which were found at *all* European sites;
6. Other factors found at the forest sites, possibly including contributions from Primary Biological Aerosol Particles (PBAPs), and during summer at SPC, possibly representing the products of cooking activities.

The contributions of such factors varied considerably between stations and according to the period of the year. POA from biomass burning accounted for more than 50% of the water-soluble organic carbon in the winter months, even in the urban station (Zürich). Aged SOA associated with HULIS was predominant during the spring-summer at rural background stations (> 75%), suggesting that secondary sources and transboundary transport become more important with respect to local sources

in determining concentration levels of organic aerosol (oxygenated) in Europe in spring and summer.

The complex aerosol measurements carried out during the EUCAARI field campaigns, involving several foreign research groups, provided the opportunity to compare the source apportionment results obtained by NMR analysis in this thesis with those provided from modern, more widespread techniques and in particular from the Aerodyne aerosol mass spectrometers (AMS). Factor analysis methods applied to AMS datasets have now provided categorization schemes of atmospheric organic aerosols (the above mentioned OOAs, HOA, etc.) which are becoming a standard for atmospheric chemists. The results emerging from this thesis work partly confirm the AMS classification and partly challenge it. In particular, NMR factors for aerosol WSOC were linked to AMS oxidized organic aerosol (OOA) types in some environments: HULIS compounds, found at all continental polluted sites, were linked to the AMS Low-Volatility OOA, while the biogenic SOA from terpenes oxidation, found at forest stations by NMR analysis, was linked to less oxidized AMS OOA types. Finally, the biomass burning POA NMR factor overlaps with the AMS biomass burning aerosols (BBOA), even if a better match of total biomass burning source contributions from AMS respect to NMR was found when accounting for oxygenated compounds believed to form by atmospheric chemical reactions in biomass burning plumes, hence of secondary origin (SOA). Fewer similarities were observed between the other classes of organic aerosol components identified separately by AMS and NMR factor analysis, with no simple scheme of assignment. Reasons for these discrepancies are discussed in the final sections of this thesis. In brief, the different sensitivities of AMS and NMR to specific chemical structures and functional groups have an impact on the variables determining the results of factor analysis. Therefore, even if AMS and NMR spectroscopies exhibit much greater recoveries in the analysis of complex matrices with respect to gaschromatographic techniques, differences in analytical selectivity between spectroscopic methods remains an issue for receptor modeling of organic aerosols. In conclusion, this study shows that the picture of the chemical composition of the organic fraction of the aerosol is more complex than AMS or NMR can individually explain. Conversely, identification of "factors" in *multiple methods*, provides better chances that the chemical structures underlying factors correspond to "real" chemical classes rather than being mere collections of spectral signals extracted by statistical algorithms. Therefore, the use of complementary spectroscopic techniques during field experiments is a powerful tool to test and constrain the conceptual schemes of particulate organic compound categorization and evolution in the atmosphere which have been proposed in the recent literature.

## Papers on the international refereed literature originating from this thesis

- Decesari S., Finessi E., Rinaldi M., **Paglione M.**, Fuzzi S., Stephanou E. G., Tziaras T., Spyros A., Ceburnis D., O'Dowd C., Dall'Osto M., Harrison R. M., Allan J., Coe H., Facchini M. C., Primary and secondary marine organic aerosols over the north Atlantic Ocean during the MAP experiment, J. Geophys. Res. A, doi:10.1029/2011JD016204, 2011.

- Finessi E., Decesari S., **Paglione M.**, Giulianelli L., Carbone C., Gilardoni S., Fuzzi S., Saarikoski S., Raatikainen T., Hillamo R., Allan J., Mentel Th. F., Tiitta P., Laaksonen A., Petäjä T., Kulmala M., Worsnop D. R., and Facchini M. C., Determination of the biogenic secondary organic aerosol fraction in the boreal forest by NMR spectroscopy, *Atmos. Chem. Phys.*, 12, 941-959, 2012.

- Landi T. C., Curci G., Carbone C., Menut L., Bessagnet B., Giulianelli L., **Paglione M.** and Facchini M. C, Simulation Of The Size-Segregated Aerosol Chemical Composition Over Northern Italy, accepted and under press on *Atmospheric Reaserch*.

- **Paglione M.**, Kiendler-Scharr A., Mensah A., Finessi E., Giulianelli L., Sandrini S., Facchini M.C., Fuzzi S., Schlag P., Piazzalunga A., Tagliavini E., Decesari S., Identification of humic-like substances (HULIS) in oxygenated organic aerosols using NMR and AMS factor analyses and liquid chromatographic techniques, under submission to *Atmos. Chem. Phys. Discuss.*

- **Paglione M.**, Decesari S., Finessi E., Giulianelli L., Carbone C., Facchini M. C., Moretti F., Tagliavini E., Hillamo R., Carbone S., Saarikoski S., Worsnop D., Canagaratna M., Prevot A., Swietlicki E., Fuzzi S., Primary and secondary biomass burning aerosols determined by proton nuclear magnetic resonance ($^1$H-NMR) spectroscopy during the 2008 EUCAARI campaign in the Po Valley (Italy), in preparation.

# 1 - Atmospheric Aerosol

## 1.1 Definition

Atmospheric aerosol is generally defined as a suspension of liquid or solid particles in the air, with particle diameters in the range of $10^{-9}$–$10^{-4}$ m (lower limit: molecules and molecular clusters; upper limit: rapid sedimentation). The most evident examples of aerosols in the atmosphere are clouds, which consist primarily of condensed water with particle diameters on the order of approximately 100 μm. In atmospheric science, however, the term aerosol is most often restricted to refer to suspended to solid particles or to particles in which condensed water occurs in lower concentrations respect to the other chemical constituents, whereas clouds are considered as separate phenomena, even if aerosol and clouds are linked by a very fundamental process in the atmosphere which is cloud droplet nucleation (as explained below).

Atmospheric aerosol particles originate from a wide variety of natural and anthropogenic sources. Primary particles are directly emitted from sources such as biomass burning, incomplete combustion of fossil fuels, volcanic eruptions, and mechanical processes resulting from the friction of wind over land and sea surfaces leading to the suspension of mineral dust, sea salt, and biological materials (plant fragments, microorganisms, pollen, etc.). In urban environments, (re-)suspension of particles can be also promoted by traffic. Secondary particles, conversely, are formed by the transformation of reactive gases into particulate matter in the atmosphere caused by chemical reactions or upon cooling of the air mass (*gas-to-particle conversion*).

As illustrated in Figure 1.1, airborne particles undergo various physical and chemical transformations (atmospheric *aging*), encompassing changes of particle size, shape, structure, and composition. Cloud formation can also lead to fast aerosol ageing, as particles are scavenged into cloud droplets, gas absorption and chemical reactions occur in the aqueous phase and eventually droplet can re-evaporate producing particles with modified chemical composition with respect to the original aerosols. Such phenomenon is often referred as *cloud processing*. In cloud systems, aerosol particles can be scavenged either by direct nucleation of water vapor onto particles forming new droplets or by collision with cloud droplets. In the first case, aerosols serve as cloud condensation nuclei (CCN) or ice nuclei (IN).

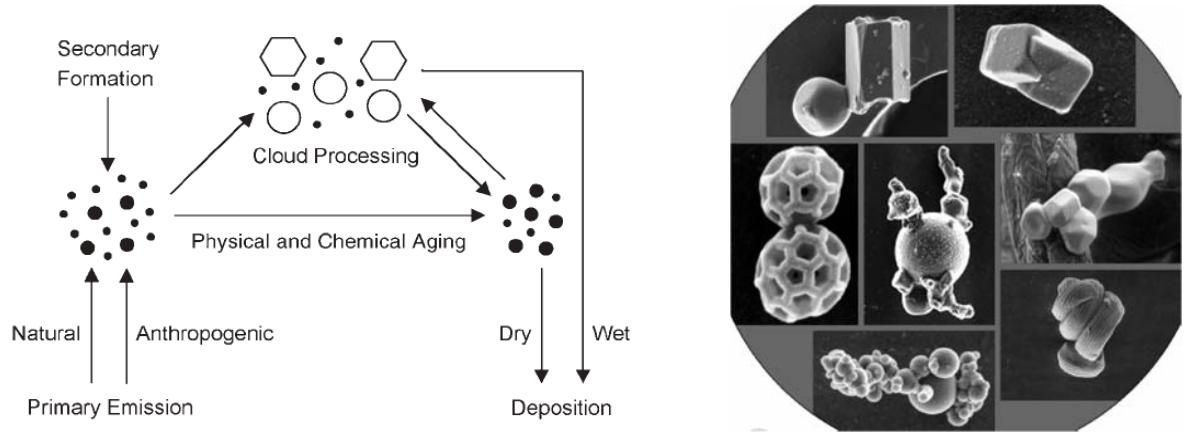


**Figure 1.1**: Atmospheric cycling of aerosols and examples of common aerosol shapes and compositions as observed by scanning electron microscopy, SEM (from Poschl, 2005).

In precipitating clouds, not only the condensation nuclei but also other aerosol particles are scavenged on the way to the surface and removed from the atmosphere. This process, termed "wet deposition", is actually the main sink of submicrometric atmospheric particulate matter. Particle deposition without precipitation of hydrometeors that is, "dry deposition" by convective transport, diffusion, and adhesion to the Earth's surface – is less important for fine aerosol fluxes at the global scale, but cannot be neglected at the urban scale.

Depending on aerosol properties and meteorological conditions, the characteristic residence times of aerosol particles in the atmosphere range from hours to weeks. The concentration, composition, and size distribution of atmospheric aerosol particles are temporally and spatially extremely variable. In the lower atmosphere (troposphere) the total particle number and mass concentrations typically vary in the range of about $10^2$–$10^5$ $cm^{-3}$ and 1–100 $\mu gm^{-3}$, respectively.

## 1.2 Size distribution

The atmospheric aerosol particles size distribution spans over several orders of magnitude from a few nanometers (nm; 1nm = $10^{-9}$m) to about a hundred micrometers (μm; 1μm = $10^{-6}$m). To appreciate this wide size range one just needs to consider that the mass of a 10 μm diameter particle is equivalent to the mass of one billion 10 nm particles. As result of particle formation and removal processes, the atmospheric aerosol size distribution is characterized by multiple relative maxima or modes, corresponding to different populations of particles, generally classified as nucleation, accumulation and coarse mode particles (Figure 1.2).

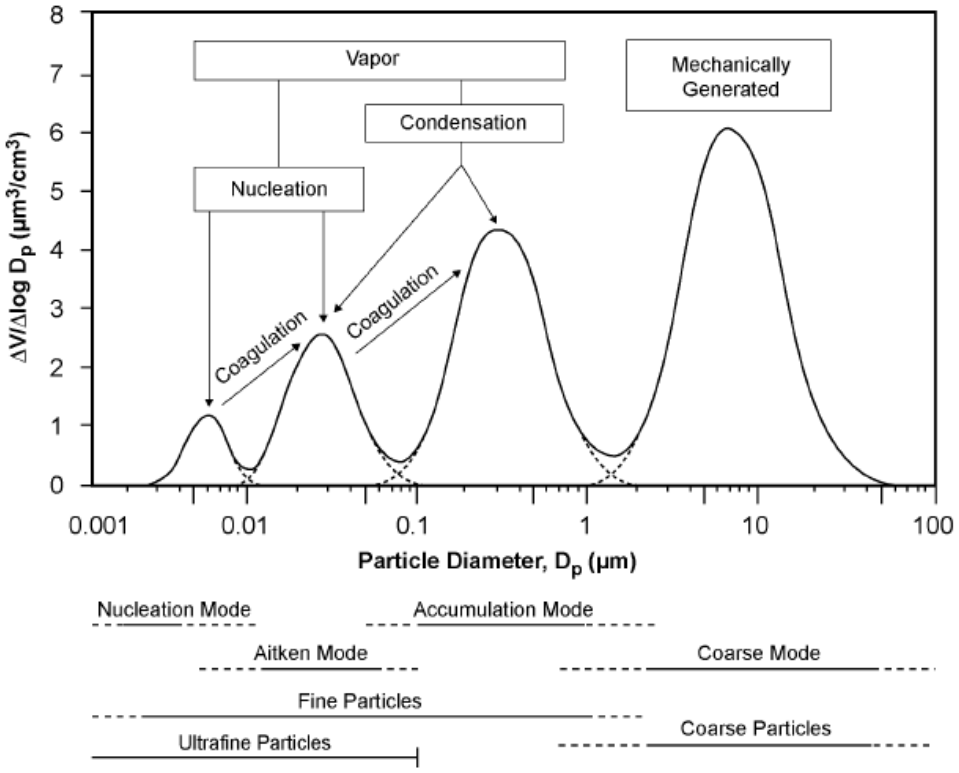


**Figure 1.2**: ideal size distribution with their four principal modes. The diagram also shows the main mechanisms of formation and growth of particles acting in the various size ranges.

These modes are generally found in to the following size ranges, defined on the basis of particle aerodynamic diameter ($D_a$[1]) (Whitby, 1978):

- Nucleation and Aitken mode ($D_a < 0.1\mu m$);
- Accumulation mode ($0.1 < D_a < 1\mu m$);
- Coarse mode ($D_a > 1\mu m$).

A more general distinction is made between "fine" and "coarse" aerosol: fine aerosol is made up of particles of the first two modes (PM1 with $D_a < 1\mu m$), whereas coarse one of those with larger size (PM10 with $D_a < 10\mu m$,). Other categorizations are provided by air quality regulations, the most popular being PM2.5, which is based on the deposition properties of aerosol particles in the human respiratory system.

The distinction between fine and coarse particles is fundamental in any discussion of the physics, chemistry, measurement, or health effects of aerosol because very different formation,

[1] Aerodynamic diameter is the diameter that a particle with ideal unitary density should have to sediment at the same speed of a particle with its real density and diameter.

transformation and removal processes characterize the submicron and supermicron regimes (Seinfeld&Pandis, 1998) (Figure 1.3).

Coarse particles are formed mainly by mechanical processes like dust suspension or re-suspension or sea spray. Coarse particles have sufficiently large sedimentation velocities to make them settle by dry deposition within a few hours of transport in the lower troposphere, although longer transport (> 1 day) are possible at high elevations. Coarse particles never account for more than a few percent of the particles by number concentration, even if they can account for a large fraction in term of particulate mass.

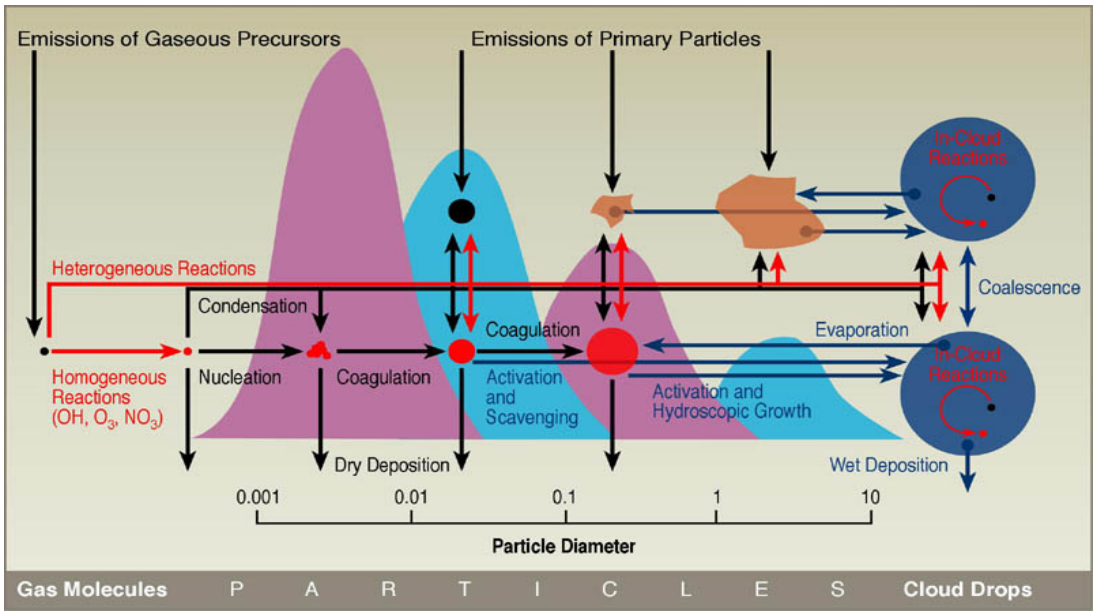


**Figure 1.3**: microphysical processes that affect size distribution and chemical composition of atmospheric aerosol. The diagram shows the wide size range of particles and as the aerosol participates in processes through atmospheric chemical reactions in homogeneous and heterogeneous phase or within clouds.

Conversely, fine particles are mainly produced by secondary processes such as gas-to-particle conversion mechanisms and by primary sources mostly represented by various types of combustion (open burning, vehicular emissions, etc.). The nucleation mode is the result of nucleation of new particles from rapid gas condensation. This occurs during the rapid cooling of an exhaust upon dilution in the background air, but may happen also at ambient temperature through photochemical reactions. The Aitken mode results from condensation of vapors onto nucleation mode particles and from their coagulation, as well as from primary combustion emissions. In turns, the accumulation mode typically results from prolonged condensation of vapors on Aitken particles and from the formation of particle mass by chemical reactions in non-precipitating cloud droplets. Since sedimentation is not effective for fine aerosols and coagulation is too slow for aerosol > 0.1 μm, particles in the accumulation mode tend to accumulate in the atmosphere and usually account for

most of the aerosol surface area. They also provide an equivalent or greater contribution to total aerosol mass with respect to coarse particles.

Fine particles, given their small size, penetrate deeply into the human respiratory system with detrimental effects on human health (as better explained in the section 1.5.2). Moreover, because of their long residence time, accumulation mode particles contribute to transboundary air pollution transport and to the modification of atmospheric transparency over vast geographical areas.

For these reasons my PhD and this thesis have been mainly focused on fine (submicron or PM1) particles which are the most representative of aerosol background concentrations and compositions in diverse environments.

## 1.3 Chemical composition

Respect to long-lived greenhouse gases, tropospheric aerosol exhibits a chemical composition characterized by a great spatial and temporal variability, reflecting the variety of sources, transformation, and removal processes. In general, aerosol particles consist of complex mixtures of inorganic and carbonaceous species, the most important classes being inorganic water-soluble salts such as sulfates, nitrates, ammonium salts and sea salt, soluble and insoluble carbonaceous material, and insoluble inorganic compounds from soil particles and combustion ash.

Carbonaceous particles are found in the troposphere as elemental (black) carbon (EC), organic carbon (OC) and carbonate carbon, the latter being negligible in the submicron size range. Produced solely by combustion processes, EC strongly absorbs light and was put in relation with degraded visibility (Bond and Bergstrom, 2006). Organic carbon is formed by both primary sources and gas-to-particle conversion (Castro et al., 1999).

Aerosol compounds derived from combustion or from gas-to-particle conversion, such as sulphate, ammonium, elemental and organic carbon, are found predominantly in fine particles whereas coarse particles are generally associated with sea salt and crustal species emitted by mechanical processes at the Earth surface. However, heterogeneous chemical reactions at particle surface may lead some compounds, like nitrate, to form by condensation in both fine and coarse modes. An overview of the average chemical composition of European tropospheric aerosols in the different size ranges was published by Putaud and co-workers (2003) and more recent studies provided detailed phenomenologies of the aerosol chemical composition for many specific European sites (Putaud et al., 2004 and 2010).

## 1.4 Organic Aerosol (OA)

Particulate organic compounds are widespread in all environments and represent a large, sometimes dominant fraction of atmospheric fine particles accounting for 20-90% of aerosol mass in the lower troposphere (Kanakidou et al., 2005; Zhang et al., 2005; Jimenez, 2009). Figure 1.4 shows the average mass concentrations of aerosol particles in the fine mode determined by aerosol mass spectrometric measurements across the Northern Hemisphere. The fractional abundance of sulphate (red) nitrate (blue), ammonium (orange) and organics (OM, green) is given in the pie charts, showing an OM significant fraction in all measurements independent of location.

While it is relatively easy to get insights to the physical properties such as size distribution or refractive index of aerosol particles, compositional analysis especially of the organic fraction is still very challenging. Although a substantial amount of new data on organic aerosol composition emerged from a number of dedicated studies in the last decade, the current understanding of OA chemical composition and on the relative importance of natural vs. anthropogenic sources remain unsatisfactory (Fuzzi et al., 2006).

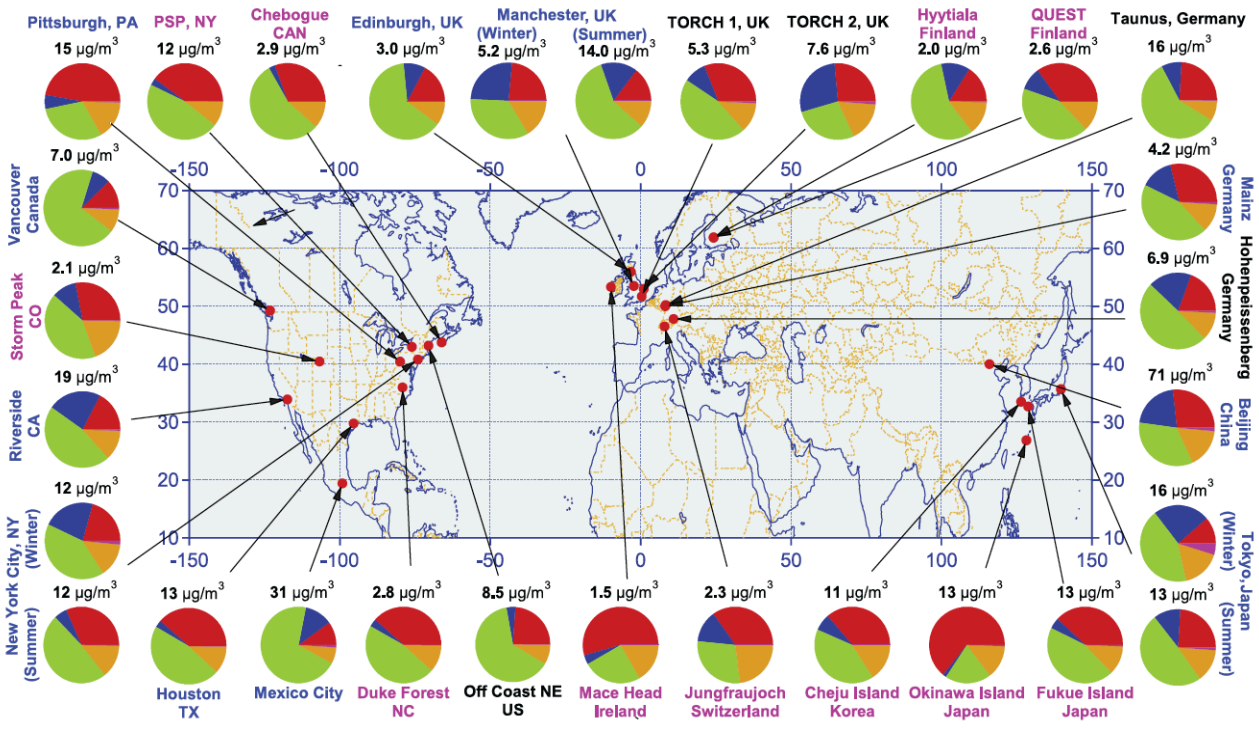


**Figure 1.4**: Aerosol mass spectrometric measurements of the fine particulate aerosol fraction. Colors for the study labels indicate the type of sampling location: urban areas (blue), <100 miles downwind of major cities (black, and rural/remote areas >100 miles downwind (pink). Pie charts show the average mass concentration and chemical composition: organic matter (organics, green), sulphate (red), nitrate (blue), and ammonium (orange) [Zhang et al., 2007].

A wide range of both natural and anthropogenic sources for ambient OA were identified, including combustion of fossil fuels, direct injection of un-burnt fuel and lubricants, industrial emissions, plant matter, biomass burning, and biogenic emissions (Jacobson et al., 2000).

Organic aerosols can be separated into primary (**POA**) and secondary (**SOA**) depending on their process of formation (Figure 1.5). POA consists of particles that are directly emitted into the atmosphere such as organic compounds associated to elemental carbon formed by combustion processes (contributing mostly to the fine fraction of OA) or plant debris from biogenic sources (more representative of the coarse fraction). Spray of organic-rich liquid surfaces may inject primary organic particles also in the submicron mode. Such mechanism can contribute to the formation of submicron organic particles over high biologically productive oceanic waters (O'Dowd et al., 2004).

SOA in contrast is mainly formed by gas-to-particle conversion of volatile organic compounds (VOC) after their oxidation and participates almost entirely to the fine OA fraction. The global VOC budget is dominated by biogenic emissions, which are estimated to be at the order of 1150 Tg C/yr, almost tenfold the flux of anthropogenic volatile organic compounds (Guenther et al., 1995). However SOA in the broad sense can be generated in the atmosphere also by chemical transformation (aging) of primary components in the condensed phase that can lead to the formation of multiple generations of secondary chemical components.

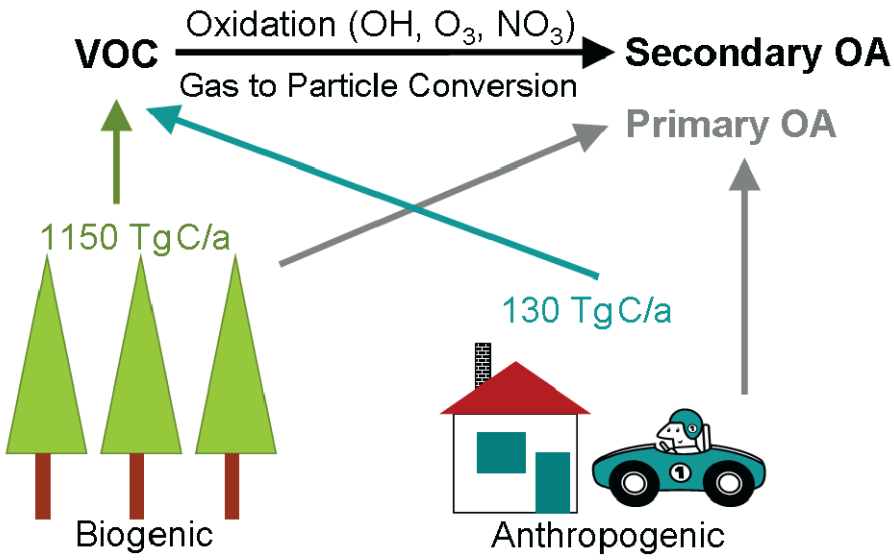


**Figure 1.5**: Sources of organic aerosol particles. Emission rates are taken from (Guenther et al., 1995).

Recent estimations of primary and secondary, biogenic and anthropogenic emissions are reported in the table below (Table 1.1). Nevertheless, the relative contribution of POA and SOA to the overall OA budget and the determination of their main sources remain controversial due to the persistent

discrepancies between measured OA concentrations and predictions of atmospheric chemistry models often showing an underestimation of the real concentrations.

Particle emission/production and burdens estimated for the year 2000

| | Mass emission | | | Mass Burden | Number Prod. | Number Burden |
|---|---|---|---|---|---|---|
| | "Best guess" | Min | Max | | | |
| | | Tg $a^{-1}$ | | Tg | $a^{-1}$ | |
| *Carbonaceous aerosols* | | | | | | |
| Primary organic (0–2 µm) | 95 | 40 | 150 | 1.2 | – | $310 \cdot 10^{24}$ |
| Biomass burning | 54 | 26 | 70 | – | $7 \cdot 10^{27}$ | – |
| Fossil fuel | 4 | 3 | 9 | – | – | – |
| Biogenic | 35 | 15 | 70 | 0.2 | – | – |
| Black carbon (0–2 µm) | 10 | 8 | 14 | 0.1 | – | $270 \cdot 10^{24}$ |
| Open burning and biofuel | 6 | 5 | 7 | – | – | – |
| Fossil fuel | 4.5 | 3 | 6 | – | – | – |
| Secondary organic | 28 | 2.5 | 83 | 0.8 | – | – |
| Biogenic | 25 | 2.5 | 79 | 0.7 | – | – |
| Anthropogenic | 3.5 | 0.05 | 4.0 | 0.08 | – | – |
| *Sulfates* | 200 | 107 | 374 | 2.8 | $2 \cdot 10^{28}$ | – |
| Biogenic | 57 | 28 | 118 | 1.2 | – | – |
| Volcanic | 21 | 9 | 48 | 0.2 | – | – |
| Anthropogenic | 122 | 69 | 214 | 1.4 | – | – |
| *Nitrates* | 18 | 12 | 27 | 0.49 | – | – |
| *Industrial dust, etc.* | 100 | 40 | 130 | 1.1 | – | – |
| *Sea salt* | | | | | | |
| $d$<1 µm | 180 | 60 | 500 | 3.5 | $7.4 \cdot 10^{26}$ | – |
| $d$=1–16 µm | 9940 | 3000 | 20,000 | 12 | $4.6 \cdot 10^{26}$ | – |
| Total | 10,130 | 3000 | 20,000 | 15 | $1.2 \cdot 10^{27}$ | $27 \cdot 10^{24}$ |
| *Mineral (soil) dust* | | | | | | |
| <1 µm | 165 | – | – | 4.7 | $4.1 \cdot 10^{25}$ | – |
| 1–2.5 µm | 496 | – | – | 12.5 | $9.6 \cdot 10^{25}$ | – |
| 2.5–10 µm | 992 | – | – | 6 | – | – |
| Total | 1600 | 1000 | 2150 | 18±5 | $1.4 \cdot 10^{26}$ | $11 \cdot 10^{24}$ |

**Table 1.1**: Particles emission/production burdens estimated for the year 2000 (taken from Andreae and Rosenfeld, 2008). Range reflects estimates reported in the literature.

Therefore, in order to improve models simulations and to develop strategies of reduction or mitigation of the aerosol potential adverse effects on environment and human health, it is very crucial to delve into the knowledge of sources, transformation mechanisms and chemical features of organic primary and secondary aerosols.

## 1.5 Aerosol and Climate: Direct and Indirect Effects

Anthropogenic aerosol modifies the transparency of the atmosphere, hence exerting a *radiative forcing*. Radiative forcings are changes in the energy fluxes of solar radiation (short-wave) and terrestrial radiation (long wave) in the atmosphere, induced by anthropogenic modifications of

atmospheric composition and Earth surface respect to pre-industrial times. Negative forcings such as the scattering and reflection of solar radiation by aerosols tend to cool the Earth's surface whereas positive forcings such as the absorption of terrestrial radiation by greenhouse gases warm it (greenhouse effect). Figure 1.6 illustrates the distinction between direct and indirect aerosol effects and some major feedback loops in the climate system. Direct forcings of aerosols are due to their effect on atmospheric transparency because of light scattering and absorption by aerosol particles, whereas indirect forcings refer to the modifications induced by aerosol on other actors of the climate system, such as clouds (cloud brightness is influenced by the availability of aerosol particles acting as CCN and IN).

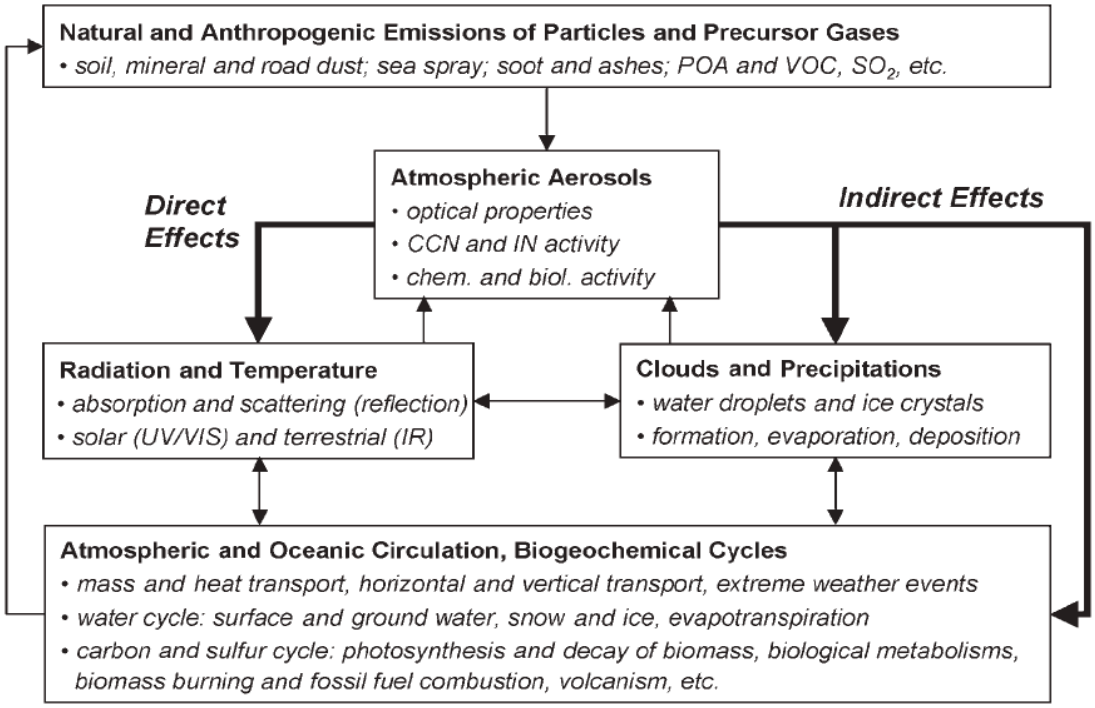


**Figure 1.6**: Direct and indirect aerosol effects and major feedback loops in the climate system.

The optical properties relevant for the direct effects (scattering and absorption coefficients or extinction cross-section and single scattering albedo, etc.) as well as the ability to act as CCN or IN are determined by the aerosol size-distribution, morphology and chemical composition. Such characteristics depends in turn on aerosol sources as well as on the atmospheric processes outlined above (coagulation, condensation, sedimentation, chemical transformation, cloud processing).

The climate feedback loops in Figure 1.6 illustrate the complexity of the possible interactions of atmospheric aerosols with solar and terrestrial radiation, clouds and precipitation, atmospheric circulation and the hydrological cycle. Each interaction highlighted in Figure 1.6 comprises a

multitude of physicochemical processes that depend on atmospheric composition and meteorological conditions and are largely not quantitatively characterized. Thus the actual climate system responses and feedback to natural or anthropogenic perturbations such as industrial and traffic-related greenhouse gas and aerosol emissions, volcanic eruptions, etc. are highly uncertain. In many cases, even the sign or direction of the feedback effect is unknown, that is, it is not clear whether a perturbation will be reinforced (positive feedback) or dampened (negative feedback).

For example, enhanced deposition and uptake of aerosol particles and trace gases on vegetation, soil, or surface water can lead to an increase or decrease in biogenic POA and SOA precursor emissions, depending on the fertilizing, toxic, or reproductive biological activity of the aerosol and trace gas components. The increase in atmospheric $CO_2$ and global warming is expected to enhance photosynthesis, biogenic emissions of VOC, and the formation of SOA particles, which may act as CCN, increase cloudiness, and lead to a cooling effect (negative feedback). On the other hand, the negative feedback mechanism could be counteracted by temperature-related biological stress and eutrophication effects which may lead to a decrease in photosynthesis, biomass production, VOC emissions, SOA formation, and cloudiness, and further enhance global warming (positive feedback). A recent review article by Lohmann and Feichter (2005) provides an overview of indirect aerosol effects, their estimated magnitude, and climatic implications.

Overall, the current aerosol radiative forcing relative to that in preindustrial times is estimated to be around -0.7 [from -1.8 to -0.3] W $m^{-2}$, as opposed to a total forcing of about +1.6 [from +0.6 to +2.4] W $m^{-2}$, as evaluate by the last report of the Intergovernmental Panel on Climate Change (IPCC) elaborating in 2007 (Figure 1.7).

Owing to the limited understanding of the numerous feedbacks, however, it is still unclear if clouds provide a positive or negative feedback to an increase in atmospheric carbon dioxide and other greenhouse gases. The uncertainties of aerosol, cloud, and precipitation interactions and feedback effects are among the main reasons for the high uncertainty of climate sensitivities and for the projected global mean surface temperature increase over the next century (1–6 °C or more). My doctoral work and this thesis, although not specifically addressing the climate change issues, deals with the scientific question of the aerosol *source apportionment*, by contributing to the development of experimental techniques aimed to assess the anthropogenic vs. natural fractions of atmospheric aerosol particles. It is worth to remind that, if *all* aerosol particles including desert dust and marine seasalt particles exert en effect on atmospheric transparency, only anthropogenic particles or the perturbations in the amount of natural particles due to anthropogenic activities are counted as forcings. In the case of the organic aerosols, object of this thesis, it is not trivial to discriminate between the anthropogenic and natural (e.g., biogenic) contributions. However, the concept of

climate forcing requires a clear split between the anthropogenic contribution and the natural background.

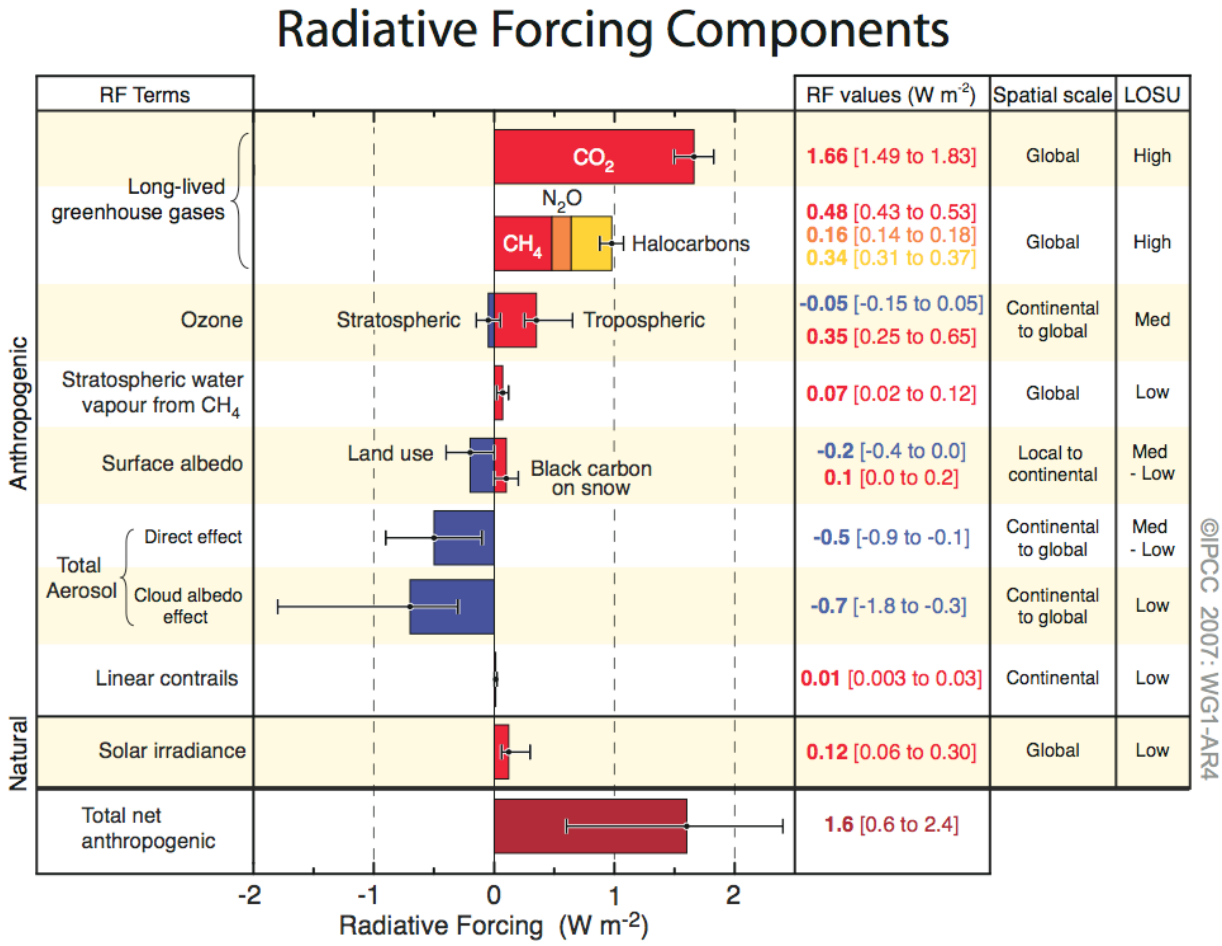


**Figure 1.7**: Global average radiative forcing (RF) estimated in 2005 for the carbon dioxide ($CO_2$), methane ($CH_4$), nitrous oxide ($N_2O$) and other anthropogenic important agents and mechanisms, together with the range reported IGT (scale space) of the forcing and the level of scientific understanding reached (LOSU - Level Of Scientific Understanding). It also shows the net anthropogenic radiative forcing. These forcing require an estimate with sums of factors asymmetric and can not be obtained by simple addition of the individual terms. Forcing additional factors not included in this chart are considered to have a low LOSU. The contribution of volcanic aerosols and other additional natural forcing are not included in this figure due to their episodic nature.

## 1.6 Aerosol Health Effects and Air Quality

Numerous epidemiological studies show that fine air particulate matter and traffic-related air pollution are correlated with severe health effects, including enhanced mortality, cardiovascular, respiratory, and allergic diseases (Bernstein et al. 2004; Gauderman et al., 2004; Katsouyanni et al., 2001; Pope et al., 2004; Samet et al., 2005).

Moreover, toxicological investigations in vivo and in vitro have demonstrated substantial pulmonary toxicity of model and real environmental aerosol particles, but the biochemical mechanisms and molecular processes that cause the toxicological effects such as oxidative stress and inflammatory response have not yet been resolved. Among the parameters and components

potentially relevant for aerosol health effects are the specific surface, transition metals, and organic compounds (Bernstein et al. 2004; Bommel et al., 2003; Donaldson et al., 2003; Schinset al., 2004). Some of the possible mechanisms by which air particulate matter and other pollutants may affect human health are summarized in Table 1.2.

Ultrafine particles ($D_a$<100 nm) are suspected to be particularly hazardous to human health, because they are sufficiently small to penetrate the membranes of the respiratory tract and enter the blood circulation or be transported along olfactory nerves into the brain (Oberdorster et al. 2004; Nemmar et al., 2002; Oberorster et al., 2005). Neither for ultrafine nor for larger aerosol particles, however, it is clear which physical and chemical properties actually determine their adverse health effects (particle size, structure, number, mass concentration, solubility, chemical composition, and individual components, etc.).

| |
|---|
| pulmonary inflammation induced by PM or $O_3$ |
| free radical and oxidative stress generated by transition metals or organic compounds (e.g. PAHs) |
| covalent modification of key intracellular proteins (e.g. enzymes) |
| inflammation and innate immune effects induced by biological compounds such as endotoxins and glucans |
| stimulation of nocioreceptor and autonomic nervous system activity regulating heart-rate variability and airway reactivity |
| adjuvant effects in the immune system (e.g. DPM and transition metals enhancing responses to common environmental allergens) |
| procoagulant activity by ultrafine particle accessing the systemic circulation |
| suppression of normal defense mechanisms (e.g. suppression of alveolar macrophage functions) |

**Table 1.2**: some of the possible mechanisms by which aerosol particles and other air pollutants may affect human health (Poschl, 2005).

Particularly little is known about the relations between allergic diseases and air quality. Nevertheless, traffic-related air pollution with high concentration levels of fine air particulate matter, nitrogen oxides, and ozone is one of the prime suspects besides non-natural nutrition and excessive hygiene practices, which may be responsible for the strong increase of allergies in industrialized countries over the past decades. A molecular rationale for the promotion of allergies by traffic-related air pollution has been proposed by Franze et al. (2003; 2005).

Efficient control of air quality and related health effects requires a comprehensive understanding of

the identity, sources, atmospheric interactions, and sinks of hazardous pollutants.. In this context, my doctoral work and this thesis, though not focused on assessing aerosol health impacts, contributes to a) the development of experimental and statistical tools to discriminate the contribution of pollution sources to ambient PM2.5 levels, which can inform the evaluation of new regulatory actions for air quality control; and to b) the chemical characterization of the aerosol water-soluble organic carbon (WSOC), not including "traditional" micropollutants (such as PAHs) and for which inflammatory effects mediated by redox reactions have already been shown (Varma et al. 2009), but whose toxicological effects certainly require to be fully clarified and linked to specific sources.

The techniques of aerosol source apportionment developed in my doctoral work have been introduced and employed in the scientific project "Supersito", started in 2011 and coordinated by ARPA-ER, and focusing on the aerosol health effects in Emilia-Romagna.

# 2 - Measurement of organic aerosol (OA) chemical composition

## 2.1 Overview

The determination of OA composition covers a wide range of analytical techniques and a number of reviews have been published in recent years on this topic (McMurry, 2000; Hoffmann and Warnke, 2007; Rudich et al., 2007). The aim of this section is to present some of the most recent advances in OA and SOA analysis extracted from the work of Hallquist et al. (2009), but with a focus on the characteristics and applications of the main technique employed in this study, i.e. proton-nuclear magnetic resonance spectroscopy ($^1$H-NMR).

One of the main limitations to complete characterization of OA, and especially SOA, is the sheer number of individual species present. Most of the OA mass is accounted for by complex mixtures of compounds, including many isomeric forms, and each occurring in very low concentrations. Goldstein and Galbally (2007) showed that for alkanes with 10 carbons there are about 100 possible isomers, increasing to well over 1 million $C_{10}$ organic species when all typical heteroatoms are included. For this reason, the recovery of particulate compound measurements varies dramatically between techniques: methods for individual compounds analysis cannot cope with the full molecular complexity of the samples and generally exhibits low recoveries ($\leq$ 10%), while spectroscopic methods for functional group determination provides a more complete analysis, since for the same chemical composition the number of functionalities is much smaller than the number of individual compounds.

Methods for OA chemical analysis are generally classified into **off-line** and **on-line techniques**.

Off-line high complexity techniques, e.g., gas chromatography/mass spectrometry (GC/MS), liquid chromatography/MS (LC/MS), nuclear magnetic resonance (NMR) and Fourier transform infrared (FTIR) spectroscopy, provide detailed information on individual chemical species or functional groups in OA but generally require large amounts of sample, resulting in low time resolution (hours to days) and low aerosol size resolution. On-line techniques (e.g., aerosol mass spectrometry, AMS) usually provide less specific information on composition (with respect to chromatographic techniques), i.e., some level of chemical characterization with less details on individual species, but have the advantage of fast acquisition times, providing near real-time data.

Figure 2.1 highlights how some of the most important techniques suitable for field applications compare in respect to completeness, chemical resolution, and time/size resolution.

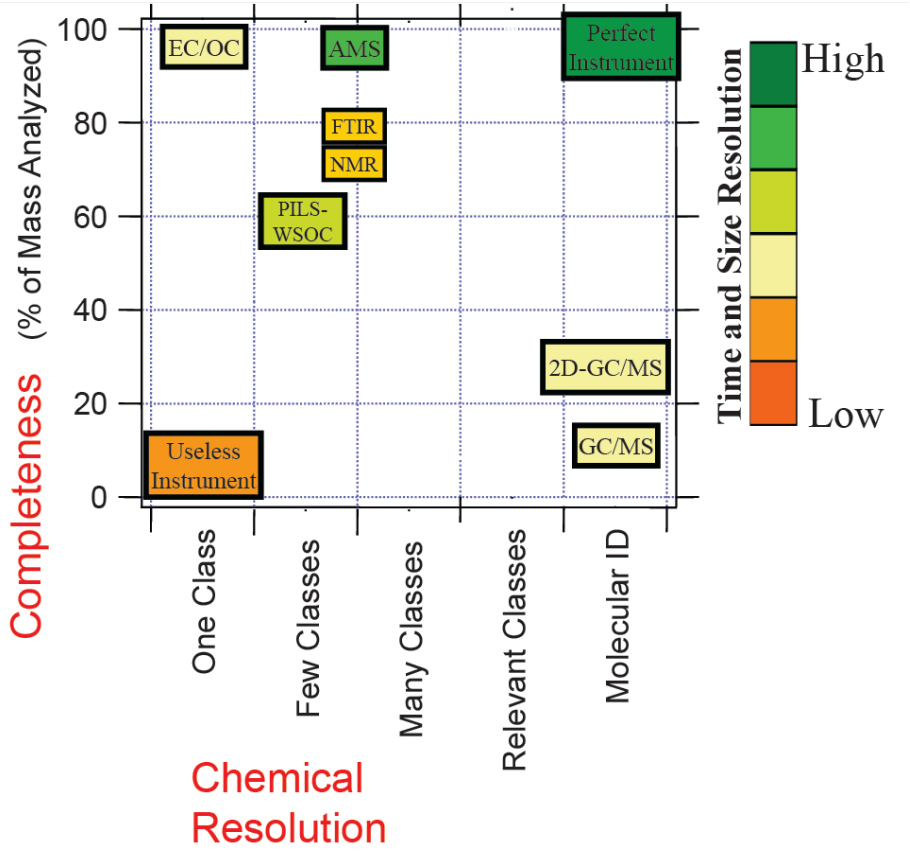


**Figure 2.1**: Three-dimensional representation of some techniques currently used for the analysis of the organic content of aerosol, highlighting their complementary nature. Definition of the acronyms is provided in the text and in the list of abbreviations.

As described above, techniques that provide molecular speciation, represented by GC/MS in the figure, can only do so for a small mass fraction of the OA (of the order of 10%) present in ambient aerosol. Time resolution is typically of many hours although automatic GC/MS systems for semi-continuous measurements, increasing time resolution up to 1 h, are now available (Williams et al., 2006, 2007). Improvements in this type of speciation techniques are highly desirable and are being actively pursued (e.g. Goldstein et al., 2008) but it is very unlikely that in the foreseeable future a single technique will provide full quantitative speciation of OA with a high time resolution.

Thermal-optical EC/OC analyzers can quantify total OC with 1 h time resolution but without size-resolution. The PILS-WSOC technique, which involves the use of a particle-into-liquid sampler (PILS) combined with analysis for water-soluble organic compounds (WSOC), can be used to quantify water-soluble OC with a time resolution of minutes and without size resolution (and also water-insoluble OC by difference from e.g. a thermal-optical instrument, but then limited to 1 h time resolution).

Spectroscopic techniques, like AMS, FTIR and NMR, can be employed to improve completeness of analysis by exploiting their selectivity to specific chemical classes or functional groups. Mass

spectrometric methods, like AMS, benefit of a much higher time and size resolution respect to the other techniques (e.g. DeCarlo et al., 2008) and are suitable for on-line elemental analysis (Aiken et al., 2008). Conversely, FTIR and NMR analysis can be carried out at a reduced time resolution but the resulting spectral data provide a much clearer information on functional group distribution with respect to AMS (e.g. Maria et al., 2003; Decesari et al., 2007).
In conclusion, a perfect field instrument does not exist, and at present a combination of techniques is required for a more complete characterization of OA and in particular of SOA.

## 2.2 Off-line high-resolution OA measurements

Generally the detailed analysis of OA is performed in the laboratory using aerosol samples collected onto filters followed by standard solvent extraction (Cheng and Li, 2004), supercritical fluid extraction (Chiappini et al., 2006) or thermal desorption (Greaves et al., 1985; Veltkamp et al., 1996). A range of solvents and pre-treatments of the analytes can be used, including chemical derivatization, to increase the range of species analyzed. The specific solvent is often used as an empirical definition for fractions of aerosol organic carbon e.g., the "water-soluble organic carbon" (WSOC).
Thermal desorption has gained increasing popularity over the last few years for the measurement of semivolatile, thermally stable organic aerosol components and can be used without any sample preparation when combined with high resolution chromatographic techniques (Hays and Lavrich, 2007).
Solvent extraction or thermal desorption methods allow to extract the majority of particulate organic compounds from the sample, though rarely > 80%, but the real bottleneck in the analysis is the recovery and resolution of the chromatographic techniques. Because of the tremendous molecular complexity, the majority of the eluted mass being present as an "unresolved complex mixture" (e.g., Williams et al., 2007). In addition, the large amounts of oxygenated organic compounds present in ambient samples, and especially in SOA, cannot be resolved by conventional GC analysis, although recovery and resolution can be increased by adopting suitable derivatization techniques (e.g., Yu et al., 1998, 1999; Kubàtovà et al., 2000; Docherty and Ziemann, 2001; Ho and Yu, 2002; Edney et al., 2003, 2005; Claeys et al., 2004a, b, 2007; Jaoui et al., 2005; Surratt et al., 2006; Szmigielski et al., 2007a, b; Healy et al., 2008)). Liquid chromatography (LC) is becoming increasingly popular for the analysis of polar compounds in aerosol and is routinely used for the analysis of carboxylic acids (Anttila et al., 2005; Römpp et al., 2006; Warnke et al., 2006). LC is particularly suited to high-MW species and very polar molecules, without the need for derivatization prior to analysis.

Ion chromatography (IC) is also suitable for the separation of organic aerosol components, especially for the analysis of very acidic, short-chain carboxylic or dicarboxylic acids, such as oxalic acid and glyoxylic acid (Jaffrezo et al., 1998; Kerminen et al., 2000; Röhrl and Lammel, 2001). Mass spectrometric detection is rarely coupled to IC, because of the necessity to use buffers that are often not compatible with MS detection. However, some IC-MS techniques were explored to investigate the composition of SOA in reaction chambers (Fisseha et al., 2004).

Semi-preparative ion-exchange chromatography was to separate WSOC fractions prior to proton NMR analysis (Decesari et al., 2000, 2001). This method allowed the characterization of very polar polycarboxylic acids, including high-molecular weight compounds. The NMR spectra of aerosol polyacids were found to be similar to those characteristic of terrestrial fulvic acids, for example Suwannee River fulvic acid (SRFA, Cappiello et al., 2003). Standards of fulvic acids were often used as surrogates for ambient aerosol in studies of physiochemical properties (Parsons et al., 2004; Topping et al., 2005b; Dinar et al., 2006b).

As already mentioned, functional group analysis using spectroscopic techniques can be used to reduce the complexity of the analysis and improve recovery. The most popular application among the off-line methods is the collection of aerosol on impactors or filters followed by analysis by FTIR spectroscopy to determine the concentration of organic functional groups such as saturated aliphatic (C-C-H), unsaturated aliphatic (C=C-H), aromatic (C=C-H), organosulfur (C-O-S), carbonyl (C=O), organic hydroxyl (COH), etc. (Blando et al., 1998; Havers et al., 1998a; Maria et al., 2003; Sax et al., 2005; Polidori et al., 2008). The strength of this technique is the ability to measure the total concentrations of certain functional groups, such as amines or organosulfur species, which are difficult to quantify with alternative methods. FTIR spectroscopic analysis was applied during many field campaigns (e.g. Maria et al., 2003; Polidori et al., 2008; Coury and Dillner, 2008, 2009; Russell et al., 2009). Maria et al. (2003) used aerosol concentrators to obtain sub- 1 h time resolution for employ onboard research aircrafts. The OA concentration determined by FTIR spectroscopy showed good agreement with co-located AMS measurements in several studies (Gilardoni et al., 2007; Russell et al., 2009). Sequential solvent rinsing can be used to further separate the organic compounds by polarity (Maria et al., 2002, 2003; Polidori et al., 2008). The OM/OC ratio can also be estimated from these measurements (Gilardoni et al., 2009).

NMR techniques were also used in numerous studies (comprising this that I am writing). Both solid and liquid NMR techniques were explored, and the analysis was performed with or without chemical derivatization aimed to increase selectivity to specific functional groups such as carboxylic acids and ketones (Tagliavini et al., 2006, Moretti et al., 2008). Proton NMR

spectroscopy was successfully used to characterize biomass burning aerosols in tropical environments (Decesari et al., ACP 2006), and was also proposed as a tool for source attribution of water-soluble organic aerosol including biomass burning, marine and SOA particles (Decesari et al., ES&T 2007). A better description of NMR techniques applied to aerosol samples will be carried out in next sections 2.4 and 2.5.

## 2.3 On-line techniques

The analytical techniques described above are suitable for time-integrated samples (using filters, impactors, etc.) analysed off-line (i.e., in laboratory). This implies the risk of positive and negative artifacts due to adsorption, evaporation, and chemical reactions during sampling, storing or during analysis in laboratory (e.g., Turpin et al., 2000; Schauer et al., 2003; Subramanian et al., 2004; Dzepina et al., 2007). Off-line techniques are particularly problematic when used on mobile observatories (e.g., research aircrafts). Therefore, on-line techniques, which provide real-time measurements, have revolutionized the chemical analysis of aerosols. The two main types of online techniques currently in use are PILS-WSOC and AMS with a growing interest in TD-PTR-MS ones.

Particle-into-liquid-samplers (PILS) collect particles into water for subsequent analysis (e.g., IC) (Weber et al., 2001; Orsini et al., 2003; Sullivan et al., 2004; Sorooshian et al., 2006a). A liquid TOC analyzer for continuous measurement of WSOC with a time resolution of a few minutes was coupled to a PILS instrument and deployed in several aircraft campaigns (e.g., Sorooshian et al., 2006a, b, 2007a, b; Peltier et al., 2007a; Weber et al., 2007).

Since the first studies using aerosol mass spectrometers (McKeown et al., 1991), the number of on-line MS techniques has rapidly increased, and scientific achievements of the AMS have been subject of several reviews (Noble and Prather, 2000; Sullivan and Prather, 2005; Canagaratna et al., 2007; Murphy et al., 2007). The operating principle of AMS involves the introduction of airborne particles into the instrument, followed by vaporization and ionization of the material before analysis of the ions using MS. Particle beams can be introduced in the ion source under vacuum using nozzles, capillaries or aerodynamic lenses. The AMS instruments commercialized by Aerodyne Inc. were proven to be very useful for fast quantitative determination of non-thermally refractory aerosol chemical components (Jayne et al., 2000; Jimenez et al., 2003; Canagaratna et al., 2007). The AMS combines thermal desorption (flash evaporation) of the aerosol components and ionization of the desorbed components by electron impact (EI). Quantitative data for sulfate, nitrate, ammonium, chloride and organic matter concentrations can be achieved through standard AMS operations (Allan et al., 2003; Jimenez et al., 2003). The EI ionization at 70 eV upon vaporization at 600 °C

results in significant fragmentation of the OA fraction with complete loss of molecular ions. For this reason, individual compounds can hardly be identified by AMS. Conversely, the AMS provides the distribution of major molecular fragments, which can be linked to the *bulk* composition (e.g., the functional groups) of OA, in an analogous manner to some of the off-line techniques such as FTIR and NMR spectroscopy. On the other hand, the derivation of functional group distribution from the AMS fragmentation patterns is less straightforward with respect to the other two techniques.

Recently, the quadrupole in the AMS instrument was replaced by a time-of-flight mass analyzer (ToF-AMS) (Drewnick et al., 2005; DeCarlo et al., 2006). The high-resolution version (up to $m/\Delta m \approx 5000$) of the ToF-AMS, or HR-ToF-AMS, allows the separation of isobaric ions. This facilitates the identification of mass fragments containing heteroatoms such as N or, and provides better differentiation of spectra of POA respect to SOA, resulting in improved accuracy of factor analysis for OA source apportionment (Ulbrich et al., 2009). The elaboration of HR-TOF-AMS data allows the determination of O/C, N/C, and H/C atomic ratios of organic matter directly and with high time resolution (Aiken et al., 2007).

Many of the above characteristics of AMS are unparalleled by any other aerosol instrument. The AMS has therefore become a standard for aerosol chemical observations, and the classification of observed AMS spectral patterns provided a new paradigm in categorizing ambient OAs. However, the information on OA chemical composition derived by the AMS is limited by the fact that the ionization method is highly destructive and complex chemical structure as well as the molecular weight distributions are completely lost during the analysis.

Over the last decade, alternative methods of desorption and ionization were investigated. Some of these designs were tested in field studies, while others were mainly employed in laboratory applications, primarily due to sensitivity limitations. The most promising technique is the Proton-Transfer Reaction Mass Spectrometry (PTR-MS, Holzinger et al., 2007) which was recently introduced to evaluate both the bulk composition and volatility of organic aerosol. In particular, the new Thermal-Desorption version of the instrument (TD-PTR-MS, Holzinger et al., 2010) consists of a modified commercial PTR-MS (Ionicon Inc., Innsbruck, Austria) equipped with both a gas and an aerosol inlet. The use of PTR-MS as detector for aerosol compounds is highly advantageous for the following various reasons: 1) PTR-MS is a relatively soft ionization technique and so many compounds do not fragment and are detected at their protonated mass (molecular weight +1); 2) PTR-MS is very sensitive and therefore low detection limits in aerosol analysis can be achieved; 3) virtually all compounds constituting the “organic carbon” fraction in aerosols can be detected, and 4) although compounds are only identified by their mass to charge ratio in the mass spectrometer

they can still be quantified at the ≈ 30% accuracy level because of the well-defined conditions in the drift tube and the fact that proton-transfer reaction rates are usually close to the ion-molecule collision rate when a reaction is energetically possible. Other techniques, such as the thermal desorption particle beam mass spectrometer (TDPBMS), capture particles in a cryo-cooled surface and then desorbs them by slow heating allowing volatility separation before MS analysis (Docherty and Ziemann, 2003; Lim and Ziemann, 2005). Finally laser-ablation mass spectrometers can analyze individual particles by using a laser to vaporize and ionize single particles followed by TOFMS (McKeown et al., 1991; Noble and Prather, 1996; Murphy, 2007) and allow the analysis of positive and negative ions simultaneously (Hinz et al., 1996). An instrument of this type, the aerosol TOF mass spectrometer (ATOFMS), is commercially available from TSI Inc. The OA fraction produces characteristic fragmentation patterns, but matrix effects make quantification difficult. Under certain conditions (e.g., matrix composition, instrument tuning), fragmentation in laser-ablation instruments can be reduced and higher-MW compounds, such as oligomers formed in chamber experiments, can be identified with this technique (Gross et al., 2006; Denkenberger et al., 2007).

## 2.4 Introduction to $^{1}$H-NMR analysis of organic aerosol

Despite its widespread application in all disciplines involving organic chemistry, Nuclear Magnetic Resonance (NMR) spectroscopy was rarely applied to the analysis of atmospheric aerosol. In fact, the relatively poor sensitivity with respect to mass spectrometric techniques makes NMR challenging for the analysis of μg-levels of airborne particulate organic matter. Nevertheless, starting from the pioneering studies of Havers et al. (1998) and Suzuki et al., (1998), the technique has gained interest in the last decade, especially for overcoming specific limitations inherent to the more diffused MS and FTIR methodologies.

Nuclear Magnetic Resonance Spectroscopy (NMR) is an analytical technique that allows obtaining detailed information on the molecular structure of organic compounds. It measures the electromagnetic radiation absorbed and released by spinning nuclei in molecules immersed in a strong magnetic field. $^{1}$H and $^{13}$C are the most common nuclei, but there are many others like $^{31}$P, $^{17}$O, $^{15}$N, $^{19}$F, etc.. Studies on aerosol samples were so far focused on mono-dimensional proton-NMR ($^{1}$H-NMR) whereas the inherent low sensitivity of NMR based on nuclei other than $^{1}$H prevents at the moment their routinely implementation, although some tests with solid and liquid 13C-NMR techniques have been carried out.

In NMR spectroscopy, chemical information about molecular structures is inferred by observing the behavior of spinning atomic nuclei: depending on the electron density distribution around them,

nuclei absorb electromagnetic pulses with different frequencies allowing to distinguish adjacent functional groups contributing to the "chemical environment" of the nuclei. . The signal intensity in $^1$H-NMR spectra is proportional to the number of hydrogen atoms that generate it. Therefore, provided a sufficiently long relaxation time (a few seconds), it is therefore possible to perform a qualitative analysis or organic hydrogen in specific chemical structures starting from the integrals of the $^1$H -NMR peaks and using an a-specific internal standard.

The horizontal scale in $^1$H-NMR spectra reports the *chemical shift* (δ), which is the frequency difference of the signals of a defined proton compared to a reference signal:

$$\delta_i = (\nu_i - \nu_s)/ \nu_s * 10^6$$

where $\nu_i$ and $\nu_s$ are the resonance frequencies of the proton i and of the reference proton s respectively. The reference signal is most often provided by an internal standard. Examples are tetramethyl-silane (TMS) for organic solutions and sodium 3-(trimethyldilyl-)-2,2,3,3-d4-proponiate (TSPd4) in the case of aqueous solutions. The frequency difference is very small, and is measured in parts per million (ppm). As already mentioned, the integrals of NMR bands is directly related to the moles of organic protons in the sample.

The advantage of $^1$H-NMR on vibrational spectroscopy (like IR or Raman) are:

a) little interference from inorganic salts and water. The resonance for H atoms from $H_2O$, HDO, $OH^-$, $H_3O^+$ (H-O groups) occur at 4.8 ppm from that of the internal standard. In water solutions the acidic H atoms from inorganic ions like sulfate and ammonia are exchanged with the molecules of the solvent and also contribute to the peak at 4.8 ppm. By contrast, the organic protons bound to carbon atoms do not exchange protons with water and exhibit response signals in a broader range (0 to 10 ppm), resulting in a spectrum which is only marginally affected by the signal of O-H. The main difficulty is encountered when the concentration of organic proton is much lower than that of O-H, because the strong signal from O-H lowers the detector gain, decreasing total sensitivity. This is typically the case for the analysis of atmospheric samples, in which large amounts of water are present while the amount of organic compounds is much lower. Increased sensitivity may be obtained by instrumental techniques, which suppress the H-O signal. This can be achieved by selective excitation of protons at 4.8 ppm (presaturation), followed by acquisition of the spectrum before the H-O signal relaxes. In this way, the solvent signal is suppressed or strongly attenuate in the final spectrum.

b) high resolution, which allows to distinguish individual compounds within the same chemical class. Contrary to IR, NMR analysis of mixtures of different compounds is straightforward. For $^1$H-

NMR spectra at 300 MHz the peak width is typically 1 to 3 Hz, while the total spectrum frequency window is about 3 KHz. It follows that an high resolution $^{1}$H-NMR spectrum of a pure compound consists of sharp lines, allowing its identification also within a fairly complex mixture. Resolution is higher for the most powerful instruments employing very strong magnetic fields (400 to 900 MHz proton resonance).

c) easier standardization for quantitative determinations. In fact, providing sufficient relaxation time to H nuclei, the integrated area of the spectrum is proportional to the moles of protons present in the sample (Derome, 1987; Braun et al., 1998). Therefore, any compound present in known amount is suitable for internal standardization. In particular, the same reference standard for the chemical shift, TSPd4, was normally used for the quantitative analysis.

Besides these major advantages, important restrictions also exists for liquid $^{1}$H-NMR analysis in $D_2O$ solution. Since organic acidic H atoms exchange with molecules of the solvent, alcohols, acids and amines can be present (depending on pH of the extract) as deuterated derivates (ROD, RCOOD, $RND_2$), and only the non-acidic protons bound to carbon atoms (C-H) can directly observed. These are called *non-exchangeable protons*. Therefore liquid $^{1}$H-NMR essentially provides information about the skeletal structures of organic molecules, and only indirect information on the oxygenated functional groups, that can be integrated just with long and time-consuming procedures of derivatization of carbonyl and carboxyl groups (Tagliavini et al., 2006 ). In addition, NMR suffers from intrinsically low sensitivity, due to the low energy of the radiation employed. This drawback can partially be overcome through time-averaged accumulation of the signal. In the most cases, we found that the analysis of samples containing around 100 μgC of aerosol WSOC needs an accumulation time of approximately 4h at 400 MHz (which can be 12-13h in case of concentrations of the order of 30 – 40 μgC).

Taking into account the inherent potential and drawbacks of NMR spectroscopy for environmental sample analysis, increasing efforts have been dedicated in the last decade to formulate applications for atmospheric aerosol analysis, and specifically according to three strategies:

1) for the analysis of specific tracers, similarly to GC/MS,

2) for the analysis of functional groups, in the same way of FTIR techniques, and

3) for recognizing spectral fingerprints and their use in factor analysis, like AMS.

### 2.4.1 NMR analysis of specific tracers

$^{1}$H-NMR analysis provides unambiguous identification and quantification of some molecular tracers into aerosol complex organic mixture, like levoglucosan (biomass combustion tracer) or methanesulfonic acid (MSA) and low-molecular weight alkyl amines (like MMA, DMA, TMA and

DEA and TEA) of prevalent marine biogenic origin (Facchini et al. 2008), etc. Figure 2.2 shows an example of NMR resolution power for identification of marine biogenic amines.

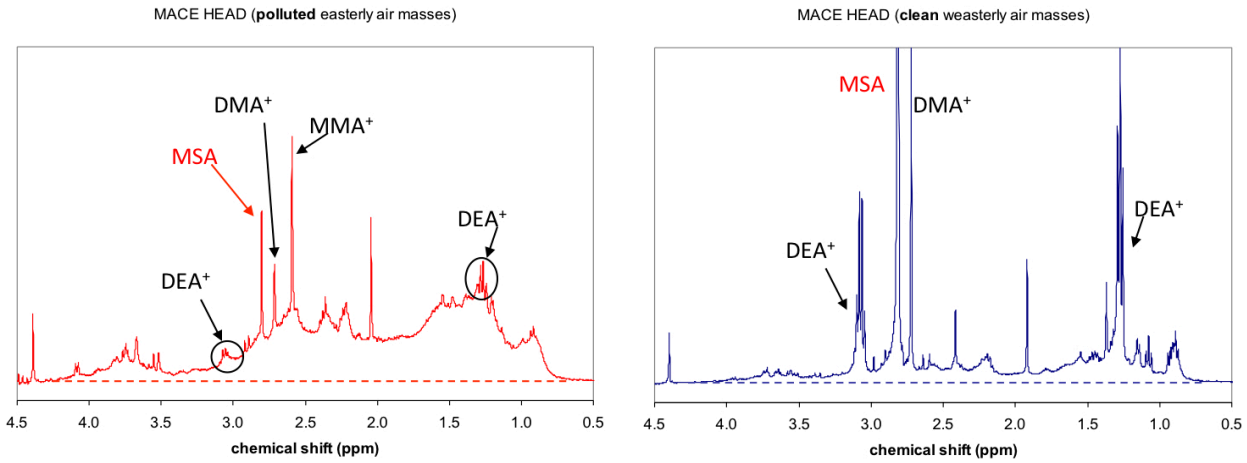


**Figure 2.2**: $^{1}$H-NMR spectra of aerosol samples collected at Mace Head (Ireland) measurement station in two different period: one of marine clean sector and other one of "polluted" terrestrial air masses: MSA and some different low molecular weight alkyl-amines were identified based one their narrow characteristic peaks in the spectral region between 2.5 and 3.2. More specifically: MSA=MethaneSulfonic Acid (2.82 ppm); MMA=Mono-Methyl Amine (2.60 ppm); DMA=Di-Methyl Amine (2.72 ppm); DEA=Di-Ethyl Amine (1.28 and 3.08 ppm).

### 2.4.2 NMR analysis of functional groups and related source apportionment

The rationale for functional group analysis of atmospheric WSOC is based on the approach followed for over two decades for the analysis of terrestrial and aquatic humic substances. Like humic substances, atmospheric WSOC shows $^{1}$H-NMR spectra with four main bands corresponding to the functional groups, as shown in typical $^{1}$H-NMR spectrum of an atmospheric aerosol water extract reported in Figure 2.3. The most evident feature of the spectrum is the presence of very broad, poorly resolved peaks, deriving from the overlap of a very large number of individual minor contributions. Peaks attributable to individual compounds (amines, MSA, etc.) contribute to a lesser extent to the total integrated area. The broad signals apparently cannot be resolved even by most powerful NMR instruments (Suzuki et al., 1998), leading to the same analytical constraints encountered by GC/MS: only a small number of organic compounds occurring in relatively high concentrations can be identified, the rest appearing as an unresolved mixture of minor constituents. On the other hand, contrary to the GC/MS, NMR spectroscopy provides an important insight into the average chemical structure of the unresolved portion, since the complex mixture produces spectral bands, which can be attributed to a few categories of functional groups. An overview of these spectral regions is reported below and summarized in Figure 2.3 and in Table 2.1.

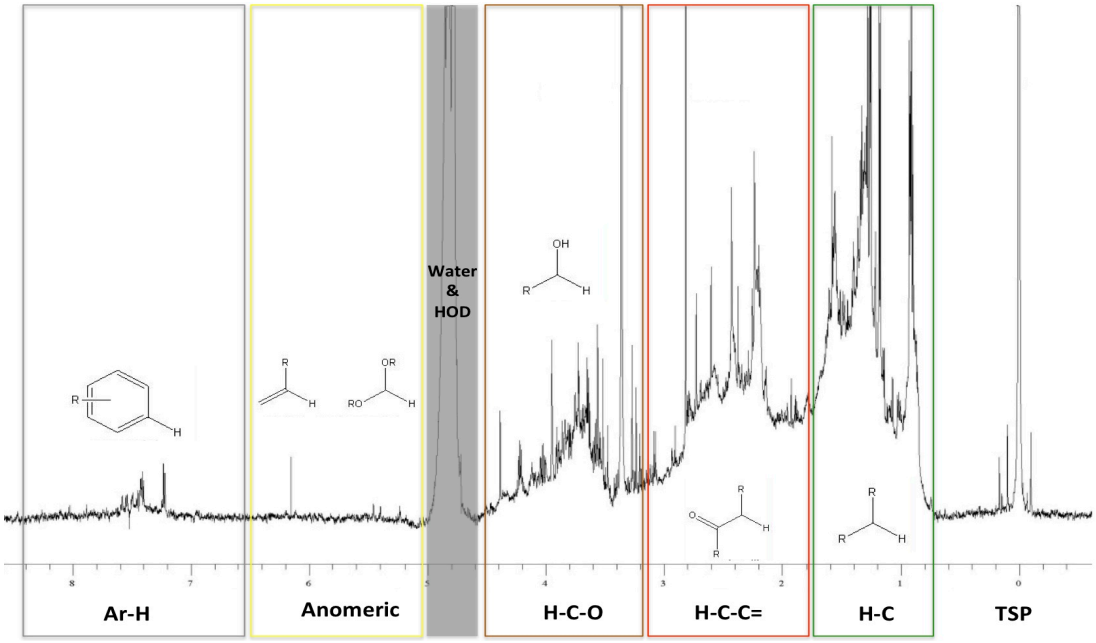


**Figure 2.3**: $^{1}$H-NMR spectrum of an aerosol sample collected in Po' Valley (Italy) and recorded with a Varian INOVA 600 MHz spectrometer in $D_2O$ solvent. Solvent peak (4.6-5 ppm) was attenuated with a presaturation sequence (PRESAT). Signal at 0 ppm is that of internal standard TSP. Rectangles of different colors evidence the main spectral bands or region characteristics of different functional groups.

Aromatic protons appear in the spectral region between 6.7 and 8.3 ppm as a weak continuous band. The maximum is located at 7.5-7.6 ppm, suggesting that electron-withdrawing substituents (carbonyl-, carboxyl-, and nitro-) are more abundant than electron-donor substituents (hydroxyl-, methoxyl-, alkyl-, amino-). Aldehydic protons were not observed (9-10 ppm). A relatively intense continuous spectrum of aliphatic protons appears between 0.7 and 4.2 ppm. Aliphatic protons are particularly abundant in the following regions: 0.7-1.0 ppm (methyl groups), 1.2-1.8 ppm (chain methylene and methyne groups), 2.1-2.8 ppm (aliphatic protons on carbon atoms adjacent to carbonyl groups or aromatic rings), 3.4-4.0 ppm (alcohols and ethers). Strong signals in the 3.4-4.0 ppm evidence a high concentration of hydroxyl- and/or ether- functionalities. Contributions from olefins (4.5-7 ppm), and organic nitrates (4.1-4.5 ppm) cannot be observed, whereas the peak at 5.4 ppm is due to the anomeric proton of levoglucosan. Besides the above main functionalities, formylic (H-C=O), acetalic (O-CH-O), and sulfonic (H-C-S=O) groups were also sporadically detected (Graham et al., 2002; Cavalli et al., 2006; Balasubramanian et al., 2003).

Finally it should be noted that the peak of residual water and HDO derived from the solvent prevents the investigation of the spectral region from 4.5 to 5.0 ppm, where signals of hydrated aldehydes occur.

In summary, the most representative categories of functional groups in $^{1}$H-NMR spectra can be listed as follows:

- Ar-H (6.5 – 8.5 ppm): aromatic protons;
- Anomeric and/or vinyl protons (O-CH-O) (5 – 6 ppm): signals singlets, sometimes so low as to be confused with the background noise, due to the vinyl protons, of not completely oxidized isoprene and terpenes derivatives (Claeys et al. 2004), and anomeric protons of sugars derivatives (levoglucosan, glucuronic acid, etc.) in the furaneidic form (O-CH-O). The most studied compound of this family is levoglucosan (see Figure 2.4), a marker of cellulose combustion that can be easily identified, isolated and integrated by NMR, thanks to the peak of its anomeric proton (δ = 5.45 ppm) (Schkolnik & Rudich, 2005).
- H-C-O (3.2 – 4.4 ppm): protons bound to oxygenated aliphatic carbon atoms (hydroxyl and alkoxy groups): aliphatic alcohols, ethers, and esters;
- H-C-C= (1.8 – 3.2 ppm): protons bound to aliphatic carbon atoms adjacent to unsaturated groups like alkenes (allylic protons), carbonyl or imino groups (heteroallylic protons) or aromatic rings (benzylic protons);
- H-C (0.9 – 1.8 ppm): unfunctionalized alkylic protons.

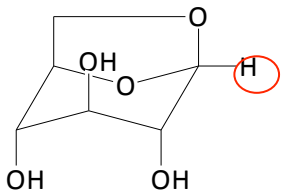


**Figure 2.4**: Levoglucosan with its anomeric proton highlighted: absorption at ~5.45 ppm.

The abundance of these structural units expressed as organic hydrogen content is measured by the integral of the above bands and calibrated on the integral of the signal of the internal standard. Therefore this method provides a chemical characterization of the unresolved fraction of WSOC on a quantitative base with no need of specific standards.

Although $^{1}$H-NMR spectroscopy measures concentrations of organic hydrogen, H/C ratios based on the expected stoichiometry of each functional group allow the conversion of the data into OC concentrations, which are more easily compared with the most common concentration metrics for OA which are usually expressed as µg of carbon per cubic meter or air. The choice of conversion ratios has been made based on structural general considerations on the molecules actually found in WSOC but presents a certain degree of uncertainty.
The H/C molar ratios mostly used are:

- Aliphatic chains (0.9-1.8 ppm): **H/C = 2** corresponding to an average between the ratios of methyls ($CH_3$), methylenes ($CH_2$), and methynes (CH). Notice that in the aliphatic moietes methyls are usually accompained by methynes; thus, the average H/C ratio for branched structures does not differ from that of linear chains rich in methylenes;
- H-C-C= (1.8-3.2 ppm): **H/C = 2**, since they consisting mainly of methylenes;
- H-C-O (3.2-4.4 ppm) **H/C = 1.1-1.2**, according to the simple hypothesis that hydroxyls can be found more frequently on an internal position of the molecule rather than in a terminal position;
- Anomeric and vinylic protons (5-6 ppm): **H/C = 1**, assuming that the contribution of vinyl protons is negligible;
- Ar-H (6.5-8.5 ppm): **H/C = 0.4**: each carbon in an aromatic ring may form a single bond; to obtain an average H/C ratio it needs to determine the degree of substitution of the aromatic rings. It was decided to take lignin (possible precursor of humic acids) as a model for aerosol aromatic compounds. Lignin in each ring is tri- or tetra- substituted and so, by averaging these possibilities, it is obtained a ratio of 0.4.

| **Groups** | **Chemical Shift (δ)** | **H/C** |
|---|---|---|
| **Aliphatics (H-C)** | 0.9-1.8 | 2 |
| **In α to unsaturated (H-C-C=)** | 1.8-3.2 | 2 |
| **In α to heteroatoms (H-C-O)** | 3.2-4.4 | 1.1-1.2 |
| **Anomeric (O-CH-O)** | 5-6 | 1 |
| **Aromatics (H-Ar)** | 6.5-8.5 | 0.4 |

**Table 2.1**: identification of the NMR spectral regions representative for different functional groups and their H/C ratios

The NMR characterization of unresolved organic mixture in term of functional groups composition demonstrated to have the potential to be a simple tool for the assignment of functional group distributions to specific types of WSOC sources, like biomass burning, marine and secondary (biogenic and anthropogenic) sources (as shown in Figure 2.5, from Decesari et al., 2007). Compared to tracer analysis, indeed, the $^1$H-NMR functional group composition has less specificity, but is representative of the bulk properties of the organic mixture in ambient aerosol samples.

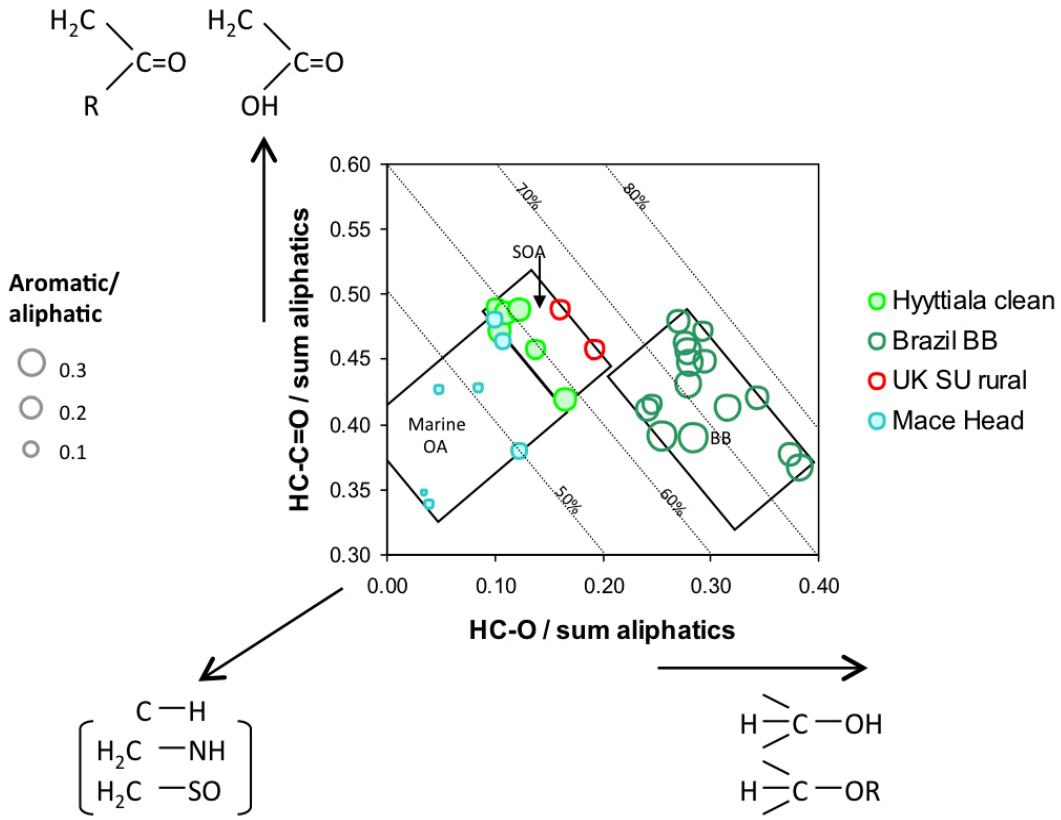


**Figure 2.5**: Functional group distribution of WSOCs samples characteristic of specific aerosol sources. Diagonal lines represent the percentage fraction of total oxygenated groups (H–C–O + HC–C=O). The boundaries of the regions assigned to marine OA, SOA, and biomass burning (BB) aerosols are specified in Decesari et al. 2007.

At the same time, compared to other methods measuring the integral properties of aerosol OC (e.g., isotopic analysis, OC/EC ratios), $^{1}$H-NMR spectra carry out more chemical information and provide a more direct linkage to the physiochemical properties of the organic mixtures, that is usually considered a side issue in source apportionment studies, but actually is of primary importance for chemical transport and climate models, which need to assign physiochemical properties (e.g., density and water activity) to each aerosol type (produced by specific sources) (Decesari et al., 2007).

With respect to other spectroscopic techniques for organic aerosol analysis, like AMS (that give information on the bulk structure of molecules and about their oxidation state) or FT-IR spectroscopy (useful for discrimination of carbonyls and hydroxyl functional groups), NMR spectroscopy is able to provide a better discrimination between aromatic and aliphatic structures (Figure 2.6), which can be critical for the identification and quantification of different oxidized organic aerosol classes and for the discrimination between biogenic and anthropogenic compounds (like biomass burning products).

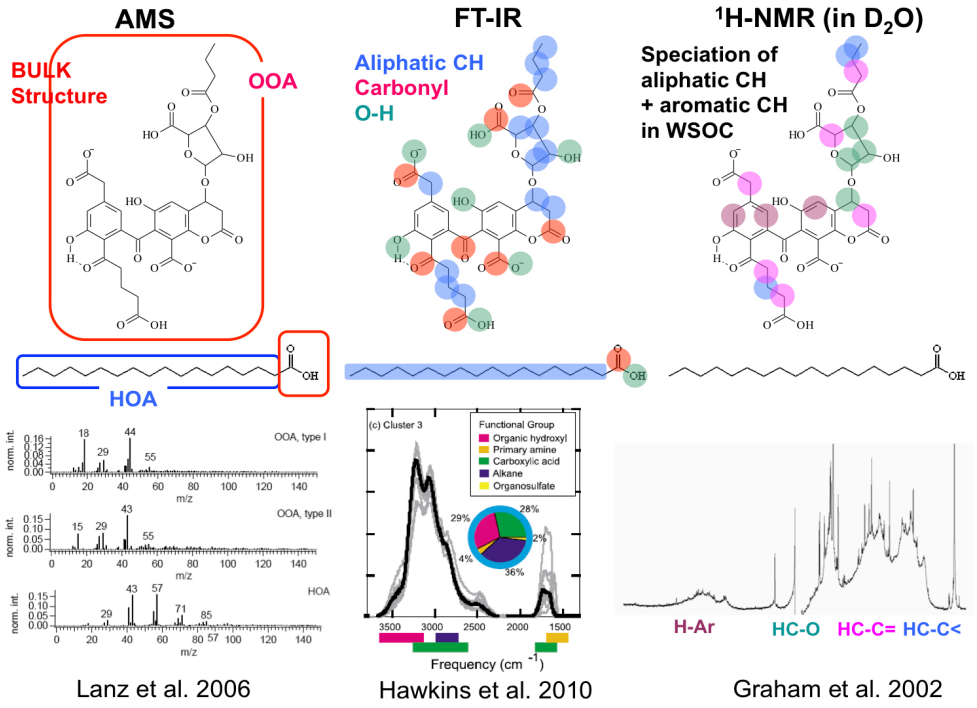


**Figure 2.6**: schematic representation of complementary information profitably extractable by different advanced spectroscopic techniques for organic aerosol analysis.

The limits of $^{1}$H-NMR functional groups distributions for source attribution of aerosol WSOC are already illustrated in Figure 2.5: The compositions of biogenic and anthropogenic SOA fall in the same region of the graph. Clearly, this apportionment schemes, employing three metrics derived from the concentrations of the five major functionalities in Figure 2.2, is not specific enough to distinguish all the major categories of atmospheric oxygenated organic compounds of interest..

### 2.4.3 NMR fingerprints and factor analysis for identification of OOA types

A new approach based on statistical analysis of NMR spectra series was developed for the first time in this thesis, at least to our knowledge, in order to exploit the full information brought by high-resolution (400 MHz) $^{1}$H-NMR spectra. The method is based on multivariate statistical techniques, overall called Factor Analysis, such as Positive Matrix Factorization (PMF) (Paatero and Tapper, 1994; Paatero, 1999) and Multivariate Curve Resolution (Terrado et al., 2010) are used here, following a "receptor model" approach already used in many atmospheric studies, to deconvolve time series of simultaneous measurements obtained at given "receptor" sites into a set of "factors" or "components", representing groupings of chemical species that correlate in time. These factors may then be related to emission sources, chemical composition and/or atmospheric processing, depending on their specific spectral characteristics and on the phenomenology of concentrations (as better explained in next sections).

Moreover, comparison of results from this new NMR spectral source apportionment with those from other techniques of OA analysis (like AMS and FT-IR) and from other chemical and meteorological data was attempted in order to develop a complementary and integrate characterization of the main organic aerosol sources.

Next sections will present an overview of the existent source apportionment, in particular receptor-modeling approaches to aerosol analysis and then their application on NMR-spectra dataset.

# 3 – Source apportionment of atmospheric aerosol

## 3.1 Overview on source apportionment models of atmospheric aerosol

In the field of atmospheric sciences, source apportionment (SA) models aim to re-construct the impacts of emissions from different sources of atmospheric pollutants, e.g., particulate matter (PM), based on ambient data registered at monitoring sites (Bruinen de Bruin, Koistinen, Yli-Tuomi, Kephalopoulos, & Jantunen, 2006; Hopke & Song, 1997; Watson et al., 2002). The review by Viana et al. (2008) provides a clear distinction between three main SA approaches:

(a) **Methods based on the evaluation of monitoring data**. Basic numerical data treatment is used to identify sources. Examples are: (1) correlation of wind direction with levels of measured components to identify source locations (Henry, Chang, & Spiegelman, 2002); (2) the correlation of gaseous pollutants with PM components to identify source associations; (3) subtraction of levels measured at regional background from those obtained at urban background and/or roadside levels to identify the contributions from the regional background, the city background and the monitored street (Lenschow et al., 2001), or (4) quantification of natural PM contributions (e.g., African dust) by subtracting PM levels at regional background sites from those at urban background locations for specific days (Escudero et al., 2007). The main advantage is the simplicity of the methods and the consequent low impact of mathematical artifacts due to data treatment.

(b) **Methods based on emission inventories and/or dispersion models** to simulate pollutant emission, formation, transport and deposition (Eldering & Cass, 1996; Visser, Buring, & Breugel, 2001). These models require detailed emission inventories that are not always available, and they are limited by the accuracy of emission inventories, especially when natural emissions are important. A significant advantage of these methods is that they may be used in scenario studies to evaluate the impact of emission abatement strategies on the anthropogenic contribution to ambient PM concentrations.

(c) **Methods based on the statistical evaluation of chemical data acquired at receptor sites (receptor models)**. The fundamental principle of receptor modeling is that mass and species conservation can be assumed and a mass balance analysis can be used to identify and apportion sources of general pollutants and more specifically airborne PM in the atmosphere (Hopke et al., 2006). An overview of the wide range of statistical models and modeling approaches, which are currently available in the literature, is shown in Figure 3.1. As shown

in the graph, one of the main differences between models is the degree of knowledge required about the pollution sources prior to the application of receptor models. The two main extremes of receptor models are chemical mass balance (CMB) and multivariate models.

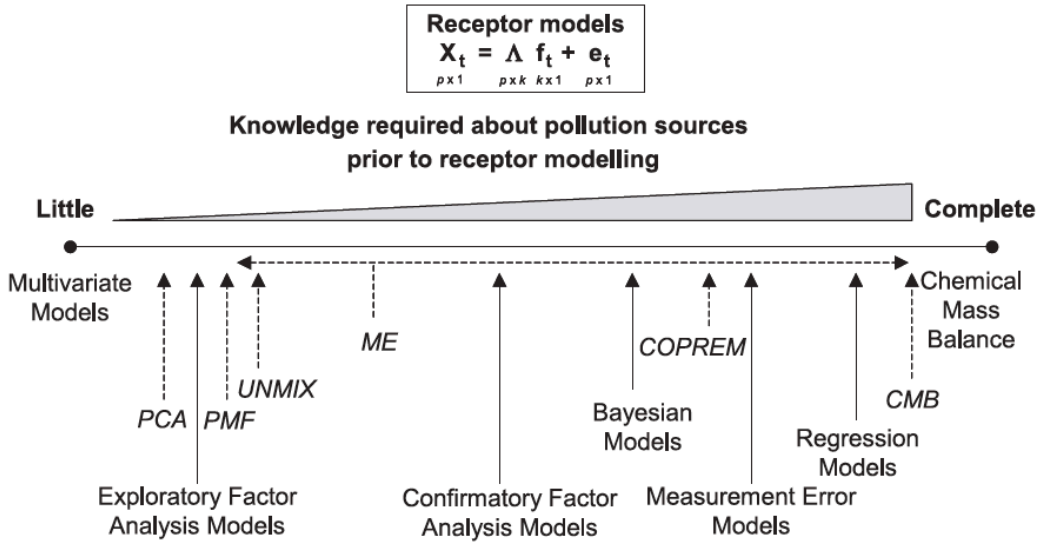


**Figure 3.1**: approaches for estimating pollution source contributions using receptor models (modified from Schauer et al., 2006). Specific models are shown in italics and with dotted arrows (Viana et al., 2008).

Receptor models use multivariate analysis (Principal Component/Factor analysis) to estimate source of pollutants on the basis of the mixture of chemicals measured at the receptor. They require low computational intensity and are independent from emission inventories and meteorological data. These are commonly used tools, because software to perform this type of analysis is widely available and detailed prior knowledge of the sources and source profiles are not required. The choice of the model dimension and the search for non-negative solutions by axis rotations can be based entirely on mathematical criteria. It is a common problem that the resulting components or factors may represent mixtures of emission sources, as opposed to clearly independent source profiles. Source signatures that change with time are a limitation for this and other types of receptor models. Moreover, since they resolve a mass balance equation are not appropriate for reactive species and perform better in areas relatively close to the sources. For that reason are suitable for urban and regional scales. The type of receptor model to be used depends on the available knowledge about the source profiles. When the sources are well known a chemical mass balance approach is preferred while pure factor analysis is the choice when no information about the sources is available. Hybrid models (Wåhlin, 2003; Lanz et al., 2007) can combine both types of approaches.

An increasing number of scientific papers have been published on source apportionment studies used this kind of models. Moreover they have been extensively used in the identification of pollution sources in support to the implementation of the European Air Quality Legislation.

Review papers (Viana et al., 2008; Fragkou et al., 2010) indicate that the most common receptor models in Europe have been PCA (and modifications), Chemical Mass Balance (CMB) and Positive Matrix Factorization (PMF) (Paatero and Tapper, 1994). The reliability of receptor model outputs depends on appropriate data collection, in terms of data capture and kind of chemical species, and, for PMF, proper expression of uncertainty in the input data. In addition, determining the number of relevant sources and establishing the correspondence between factors and sources still appear as critical steps. Moreover, little is known about the comparability between the output of different models or between different implementations of a model.

Performing intercomparison exercises and compiling quality assurance protocols, to reduce the influence of expert subjectivity to a minimum, could achieve improving comparability and reliability of receptor models (Viana et al., 2006; Larsen et al., 2008; Laupsa et al., 2009; Favez et al., 2010). Further improvements in the performance of Receptor Models are expected from the application of advanced tools, which make it possible to combine chemical data with other kind of information (e.g., meteorological data). More effort should be done to extend the range of the chemical species used as explanatory variables (e.g. VOCs, inorganic gases, organic markers, etc.). Finally, receptor models have also good prospects in the study of the impact of pollutants on human health. Combining source identification with toxicological and epidemiological data is a promising approach to evaluate air pollution mitigation measures. (Belis & Karagulian, 2011)

## 3.2 Source Apportionment of OA environmental data

### 3.2.1 Overview of OA source apportionment techniques

Several source apportionment techniques have been proposed specifically for organic aerosol (OA). A most simple one estimates the fractions of primary and secondary OA on the basis of the ratio between elemental and organic carbon (EC/OC) measured on aerosol filter samples (Turpin and Huntzicker, 1991), and assuming that primary OA concentrations are proportional to those of EC.

Techniques based on carbon isotopic ratios ($^{14}C/^{12}C$) have recently received attention because they provide quantification of the fossil fuel combustion contribution to ambient levels of OA, but their widespread application is limited by the relative few number of laboratories capable to handle atmospheric samples, by the high costs and by the reduced sensitivity (Szidat et al., 2006; Gilardoni et al., 2011).

OA source apportionment based on multivariate statistical approach, such as that general described in previous section, has been developed in last years: factor analysis of time and compositionally-resolved OA data enables the extraction of "factors" or "components" representing species that correlate in time. Each factor extracted in this way typically corresponds to many individual molecules and contains information about their sources, processing histories, and/or chemical properties. The most common application of multivariate statistical methods to OA source apportionment is the chemical mass balance (CMB), which employs as explanatory variables the concentrations of molecular markers measured by GC-MS (Schauer et al., 1996). Several sources with unique markers can be identified, but source profiles must be known a priori and in generally only primary (e.g., combustion) OA sources are accounted for by this method.

### 3.2.2 Factor analysis of OA chemical datasets

Factor analysis includes a wide set of multivariate statistical techniques, including Principal Component Analysis (PCA), although non-negative methods are most often used for the analysis of spectroscopic data and concentrations matrixes. Basically, regardless of the specific constraints imposed and of the different algorithms, all the different methods of factor analysis are based on the same bilinear model:

$$x_{ij} = \sum_{k=1}^{p} g_{ik} f_{kj} + e_{ij} \qquad \textbf{(1)}$$

where $x_{ij}$ refers to a particular experimental measurement of concentration species ***j*** (one of the analites or, here, one point of the mass or NMR spectrum) in one particular sample ***i***. Individual experimental measurements are decomposed into the sum of ***p*** contributions or sources, each one of which is described by the product of two elements, one ($f_{kj}$) defining the relative amount of the considered variable *j* in the source composition (loading of this variable on the source) and another ($g_{ik}$) defining the relative contribution of this source in that sample *i* (score of the source on this sample). The sum is extended to k=1,…,p sources, leaving the measurement unexplained residual stored in $e_{ij}$.

Equation (2) describes the same model in a more compact way using matrix algebra notation.

$$X = G \cdot F + E \qquad \textbf{(2)}$$

The data matrix of measurements X is decomposed into the product of two factor matrices, the loadings matrix (F) defining the chemical composition of the sources, and the score matrix (G)

related to the contributions or distribution of these between samples. The noise matrix E contains the experimental error as well as unmodelled variance sources not included in the p components.

Several publications reported factor analysis of speciated OA data from filter samples (Shrivastava et al., 2007; Jaeckels et al., 2007; Dutton et al., 2010; Sun et al., 2011) collected at low time resolution (typically 24 or 12h). In recent years, the development of on-line aerosol chemical measurements employing mass spectrometers (e.g. AMS, see Chapter 2) enabled chemical analysis in near-real time allowing to collect complex datasets of OA compositions with a high time-resolution (seconds to minutes) and a large number of variables (up to $10^2$ - $10^3$ in the case of mass spectra). Thanks to the fast sampling rate and high sensitivity, the AMS measurements allowed for the first time tracing the aerosol chemical composition at time scales typical of meteorology (~ minutes). At present, the most numerous and consistent results of multivariate models in OA source apportionment are based on the deconvolution of AMS spectra that allowed the separation of OA components into a few chemical classes: oxygenated OA (OOA) associated with secondary fraction (SOA), hydrocarbon-like OA (HOA) linked to primary emissions (POA), and sometimes other components such as biomass burning OA (BBOA) connected to biomass combustion sources (Zhang et al., 2011).

In addition to factor analysis of AMS datasets, deconvolution of FTIR spectra was used to identify groupings of functionalities (aliphatic, carboxylic, carbonyl, hydroxyl, organosulphate, and organonitrate groups) attributable to specific aerosol sources (Russell et al., 2010 & 2011).

In this context, NMR spectroscopy with its ability of functional groups identification and (see sections 2.4) has the potential to become a new critical application in OA source apportionment, in particular for the discrimination between biogenic and anthropogenic SOA. However, NMR spectral deconvolution in atmospheric aerosol studies is still in its infancy and this thesis represents the first attempt of extensive application of factor analysis methods for direct deconvolution of aerosol NMR spectra with a receptor modeling approach and subsequent source apportionment of organic aerosol.

# 4 - Experimental

In the present study, proton-nuclear magnetic resonance ($^1$H-NMR) spectroscopy was employed to investigate the chemical composition of atmospheric fine particulate matter ambient samples collected at several sites in Europe. A receptor modeling approach of source apportionment based on factor analysis of $^1$H-NMR spectra was used for the first time with the aim of identification of the main chemical components present in ambient aerosols and of their quantification and attribution to specific sources (primary and/or secondary, biogenic and/or anthropogenic, etc.). In order to reach these purposes, NMR spectroscopic analysis was supported by chemical analyses provided by various off-line and on-line analytical techniques. Specifically, elemental analysis by thermal methods (TOC) and ion chromatography (IC) were used as ancillary techniques with the aim of closing the mass balance and of identifying chemical tracers; high-performance liquid chromatography (HPLC) provided chemical classes of substances for comparison with the NMR factors; finally on-line aerosol mass spectroscopic (AMS) data and their PMF-resulting factors, representing nowadays the standard in categorizing ambient OAs, were used for direct comparison with NMR-factors.

During my doctoral work, I took care of NMR analysis of the samples from 3 of the field experiments described below, plus other 2 which await elaboration and are not included in this thesis. I carried out the factor analysis of *all* the NMR datasets discussed in this thesis. I also performed the TOC analyses, and the HPLC fractionation of the samples from the Cabauw stations (see Chapter 7). The IC data were provided by the CNR-ISAC laboratories and the AMS data were furnished by foreign partners involved in the project EUCAARI.

Sampling sites description and analytical protocols will be reported in the following sections.

## 4.1 Sampling sites

Ambient aerosol samples analyzed within this thesis were mostly collected during various intensive field experiments set up in the frame of the EU-funded EUCAARI project.

### 4.1.1 Overview of the EUCAARI project

The European Aerosol Cloud Climate and Air Quality Interactions (EUCAARI) project, involving 48 partners from Europe and other non-EU countries, was a multidisciplinary study of air pollution and climate interactions. More specifically, the project aimed to halve the uncertainty of the impact of aerosol particles on climate and to quantify the relationships between regional air quality and

anthropogenic aerosols. The project was coordinated by the University of Helsinki (Finland) and lasted from 2007 to 2010.

The project dealt with processes occurring at wide spatial and temporal scales (from nanometres to global scale and from seconds to years) and employed extensively modeling tools supported by some new laboratory and field observations. These measurements were also complemented with intensive air pollution monitoring activities regarding aerosols, which were carried out in particular in May 2008, but also in 2007 and 2009, making use of ground stations and research aircrafts.

### 4.1.2 EUCAARI sampling sites and Intensive Observation Periods analyzed

The measurements campaigns analyzed in this thesis were carried out at nine European sites selected on the basis of their different typology of aerosol emission patterns and pollution levels. Referring to the criteria used by Putaud and coworkers for Europe (Putaud et al., 2003), e.g. the distance from pollution sources, the sites can be classified into: marine background, natural background, rural background, near-city background or urban background. Sampling sites position and main characteristics are reported in Table 4.1.

| ID | site | position | altitude (m asl) | typology | operated by |
|---|---|---|---|---|---|
| MHD | Mace Head, Ireland | 53° 19' N, 09° 53' W | 5 | marine background | National University of Ireland, Galway |
| HYY | Hyytiälä, Finland | 61° 51' N, 24° 17' E | 181 | natural continental background | University of Helsinki |
| KPZ | K-Puszta, Hungary | 46° 58' N, 19° 33' E | 125 | rural background | Hungarian Meteorological Service and ACUV |
| CBW | Cabauw, Netherlands | 51° 18' N, 04° 55' E | 60 | rural background | KNMI |
| SPC | San Pietro Capofiume, Italy | 44° 39' N, 11° 37' E | 11 | rural or near-city background | CNR-ISAC and regional environmental protection agency |
| MPZ | Melpitz, Germany | 51° 32' N, 12° 54' E | 87 | Rural polluted background | Leibniz Institute for Tropospheric Research |
| ZW | Zürich, Switzerland | 47° 22' N, 08° 31' E | 410 | near-city background | Paul Scherrer Institute (PSI), Villigen, Switzerland |
| BCN | Barcelona, Spain | 41° 23' N, 02° 06' E | 80 | urban background | Consejo Superior de Investigaciones Científicas (CSIC) - Barcelona, Spain |
| MSY | Montseny, Spain | 41° 46' N, 02° 21' E | 720 | rural background | Consejo Superior de Investigaciones Científicas (CSIC) - Barcelona, Spain |

**Table 4.1**: Synthetic description of the sites

Intensive observing periods (IOP) of the field measurement campaigns analyzed in this thesis are reported on map in Figure 4.1 and Table 4.2 along with number and type of the collected samples.

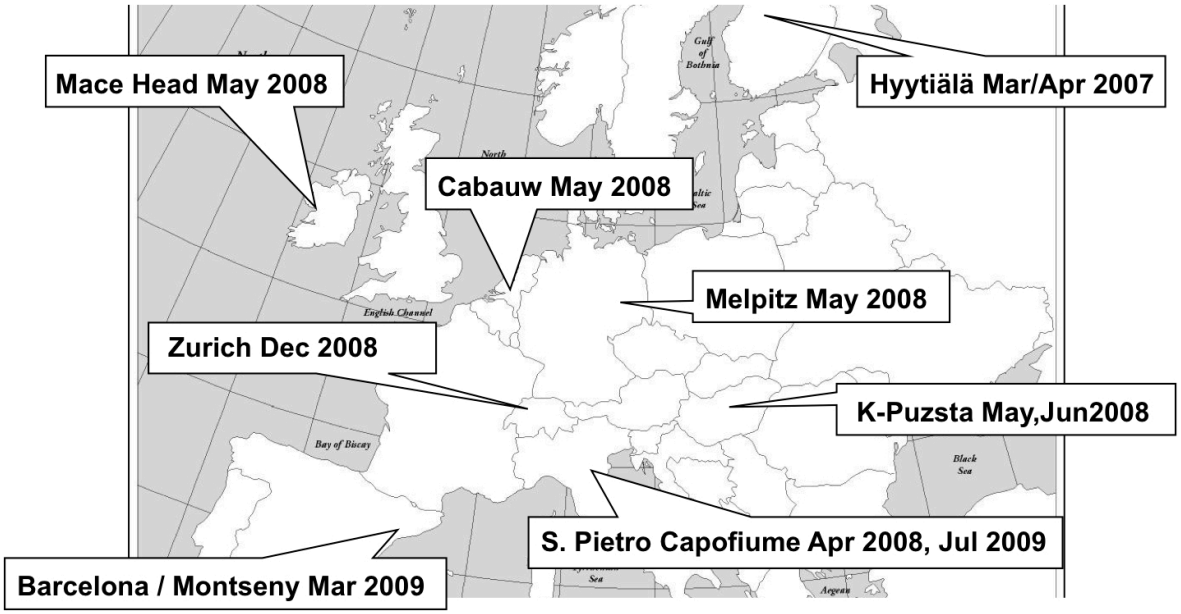


**Figure 4.1**: map of EUCAARI IOPs sites considered in this thesis.

| site (year) | IOP | | samples n° | aerosol type |
|---|---|---|---|---|
| | start exp. date | stop exp. date | | |
| HYY (2007) | 29/03/2007 | 18/04/2007 | 22 | $PM_1$ |
| SPC (2008) | 31/03/2008 | 20/04/2008 | 34 | $PM_1$ and $PM_{1-10}$ |
| CBW (2008) | 08/05/2008 | 26/05/2008 | 30 | $PM_1$ and $PM_{1-10}$ |
| MPZ (2008) | 01/05/2008 | 31/05/2008 | 15 | $PM_{2.5}$-$PM_{2.5-10}$ |
| MHD (2008) | 17/05/2008 | 10/06/2008 | 7 | $PM_{1.5}$-$PM_{1.5-10}$ |
| KPZ (2008) | 26/05/2008 | 14/08/2008 | 10 | $PM_{2.5}$ |
| ZW (2008) | 30/11/008 | 17/12/2008 | 10 | $PM_1$ |
| SPC (2009) | 27/06/2009 | 15/07/2009 | 100 (29+71) | $PM_1$ and $PM_{1-10}$ |
| BCN&MSY (2009) | 27/02/2009 | 23/03/2009 | 14 (7+7) | $PM_1$ |

**Table 4.2:** Sampling periods.

A more detailed description of the sites is reported in the following sub-sections.

#### *4.1.2.1 Mace Head*

The atmospheric research station of Mace Head is located on the west cost of Ireland, offering a westerly exposure to the North Atlantic ocean. The climate is prevalently dominated by maritime air masses: on average over 60% of air masses arrive to the site from a *clean sector* (180° through west to 300°). In fact, it has been shown that this site can be representative of clean background marine air (Rinaldi et al., 2009). By contrast, when easterly air masses reach the station, aerosols characteristic of the European pollution background are observed. More details on the station are available on the official web site (http://macehead.nuigalway.ie/).

**Figure 4.2**: Mace Head Atmospheric Research Station. Department of Experimental Physics National University of Ireland, Galway.

#### *4.1.2.2 Hyytiälä*

The Finnish Station for Measuring Forest Ecosystem-Atmosphere Relations (SMEAR II) is located in Hyytiälä, Finland. This forestry station is situated in the middle of a more than 40-years old Scots pine stand (*Pinus Sylvetrsis L.*) which surrounds homogeneously the site for about 200 m in all directions and it extends up to 1.2 km towards the North. Tampere is the largest city nearby and it is situated more than 60 km S-SW far. In fact, it has been shown that this site can be representative of the boreal coniferous forest. More details on the station are available on the official web site (http://www.mm.helsinki.fi/hyytiala/english/eng_index.htm).

**Figure 4.3**: Landscape surrounding the Hyytiälä forestry field station (SMEAR II). Faculty of Agriculture and Forestry, Helsinki University.

#### *4.1.2.3 K-Puszta*

K-Puszta is a central European site located in the middle of the Hungarian plain. The station is surrounded by coniferous forests spaced out with clearings. The station resides at 80 km south-east far from Budapest. The largest nearby town (Kecskemét, 110,000 inhabitants) is 15 km far from the station, S-E direction. Thus the site can be representative of the European rural background as well as more polluted air masses depending on the meteorological conditions.

#### *4.1.2.4 Cabauw*

The Cabauw Experimental Site for Atmospheric Research (CESAR) is located in flat rural area in the western part of The Netherlands. The North Sea is more than 50 km away from the site in the N-W direction.

**Figure 4.4**: Landscape surrounding the CESAR observatory. The Royal Netherlands Meteorological Institute.

The region nearby the site is predominantly agricultural although the station is not very far from

large cities such as Amsterdam and Utrecht. Hence the site offers the opportunity to study a variety of air masses from clean maritime to continental polluted ones. More details on the station are available on the official web site (http://www.cesar-database.nl/About.do ).

#### *4.1.2.5 San Pietro Capofiume*

The Italian field station is located at San Pietro Capofiume in a flat rural area in the river Po Valley region. The Adriatic Sea is more than 60 km away from the site in the east direction. The closest large cities are Bologna and Ferrara which are each roughly 40 km far from the site. This region is overall characterized by a high population density and by intensive agricultural as well industrial activities. Moreover major highways cross this area. Hence according to EMEP (European Monitoring and Evaluation Programme under the Convention on Long-range Transboundary Air Pollution) conventions this site can be classified as a rural background site, although in the winter season, when aerosol dispersion is reduced, the site behaves more as a urban background location.

**Figure 4.5**: Atmospheric research station "G. Fea", San Pietro Capofiume. CNR-ISAC.

#### *4.1.2.6 Melpitz*

The IFT-Melpitz ground-based research station is located in the river Elbe Valley in Germany. Melpitz is a small village surrounded by agricultural land interspersed by edges of forest and it is far from the city of Leipzig about 40 km in the southwest direction. Nevertheless major highways cross the region at a minimum distance of 1.5 km. Moreover during high pressure conditions dry air masses are transported from the north-east area where coal heated power plants and old industries with poor exhaust treatments still operate. Anyway air masses reaching the station come predominantly from the south-west direction after crossing part of western Europe. Hence Melpitz can be described as a rural polluted continental site.

**Figure 4.6**: IFT-Melpitz atmospheric research station.

#### *4.1.2.7 Zurich*

The sampling site was located at the well-described urban courtyard site in Zurich Kaserne, Switzerland (Hueglin et al., 2005; Lanz et al., 2007) in the center of the metropolitan area of Zurich with about half a million inhabitants. The location is considered as an urban background site as far as traffic emissions are concerned and is one of the Swiss NABEL long-term monitoring stations.

#### *4.1.2.8 Barcelona & Montseny*

The BCN and MSY sites are located respectively inside Barcelona (in the university campus in the western side of the city close to Diagonal Avenue, one of the main traffic roads) and at about 50 Km away from that. They are run by CSIC-IES within the framework of the Catalan atmospheric network. Montseny is located far from any local source of pollution and the air is representative of regional background. Montseny is equipped with PM1, PM2.5 and PM10 continuous measurements, and PM10 and PM2.5 Hivol samplers that are involved also in the EUSAAR (European Supersites for Atmospheric Aerosol Research) network.

The Barcelona geographical area is affected by convergence of air masses with different characteristics: the cold air coming down from medium and high latitudes, and the warm air coming up from tropical and subtropical latitudes. The former mainly dominates during the winter months, while the latter, characterized by anticyclones in the middle and upper layers of the troposphere, is predominantly observed during the summer. For this reason, the summer season is dry while the rest of the year is moderately humid (Clavero et al., 1997). The mountain ranges surrounding the Mediterranean Sea act as a sharp climate barrier protecting the Mediterranean basin from more extreme continental weather conditions. Thus, the coastal and pre-coastal zones present a winter regime characterized by low precipitation, a warm and dry summer and a rainy autumn. The major orographic features that influence the flows to BCN are the Pyrenees Mountains and the Ebro Valley, acting as a natural barrier of the flows and producing important orographic forcings into the

low troposphere. In a local scale, BCN is dominated by the coastal depression, coastal mountain range, pre-coastal depression and pre-coastal mountain range where the MSY site is located. There are two main river valleys perpendicular to the coast limiting the BCN area. These valleys contain highways and roads that link the Barcelona urban area and its outlying towns with the cities in the pre-coastal depression. Many industries are located around these urban areas. The development of thermally-driven flows and forced channelization of synoptic flows have important effects in the dispersion of the pollutants emitted within the area.

**Figure 4.7**: Barcelona city landscape and Montseny research station (EUSAAR).

## 4.2 Samples handling and analysis

### 4.2.1 Sampling methods

Within this work aerosol samples have been prevalently collected on quartz micro-fiber filters (QMA grade purchased by Whatman or Pall). The quartz fiber filters were washed with Milli-Q water and fired for 1h at 800 °C before sampling in order to reduce their blank values.

Various high volume samplers have been employed in aerosol sampling depending on the instrument availability on the site. During the intensive observing periods held in the SPC and CBW stations was employed a dichotomous high volume sampler from MSP Corporation (Universal Air Sampler, model 310) working at a constant nominal air flow rate of 300 L/min. The dichotomous sampler allowed to collect atmospheric aerosols in their PM1 and PM10 fractions. A Sierra Andersen high volume sampler, segregating PM1.5 and PM1.5-10 particles, was used in the MHD station. $PM_{2.5}$ and $PM_{2.5\text{-}10}$ fractions of atmospheric aerosol were obtained in the MPZ station using a Digitel high volume sampler. In the HYY and KPO stations were employed two high volume samplers working at 600 and 850 L/min and configured to remove particles with aerodynamic diameter larger than 1 and 2.5 μm respectively.

A sampling tandem configuration consisting in the use two piled filters, one front (F) and one back up (BU) filter, in separate filter holders, was adopted when possible in order to assess sampling artifacts on OA concentrations due to absorption of organic vapors (Cheng et al., 2009; Vecchi et

al., 2009).

After sampling the aerosol samples were stored in a freezer until the analyses.

### 4.2.2 Analytical methods

A scheme of the analytical protocol employed to chemically characterize the aerosol samples collected on quartz fiber filters at the various sites and to compare them with on-line measurements is reported below (figure 4.8).

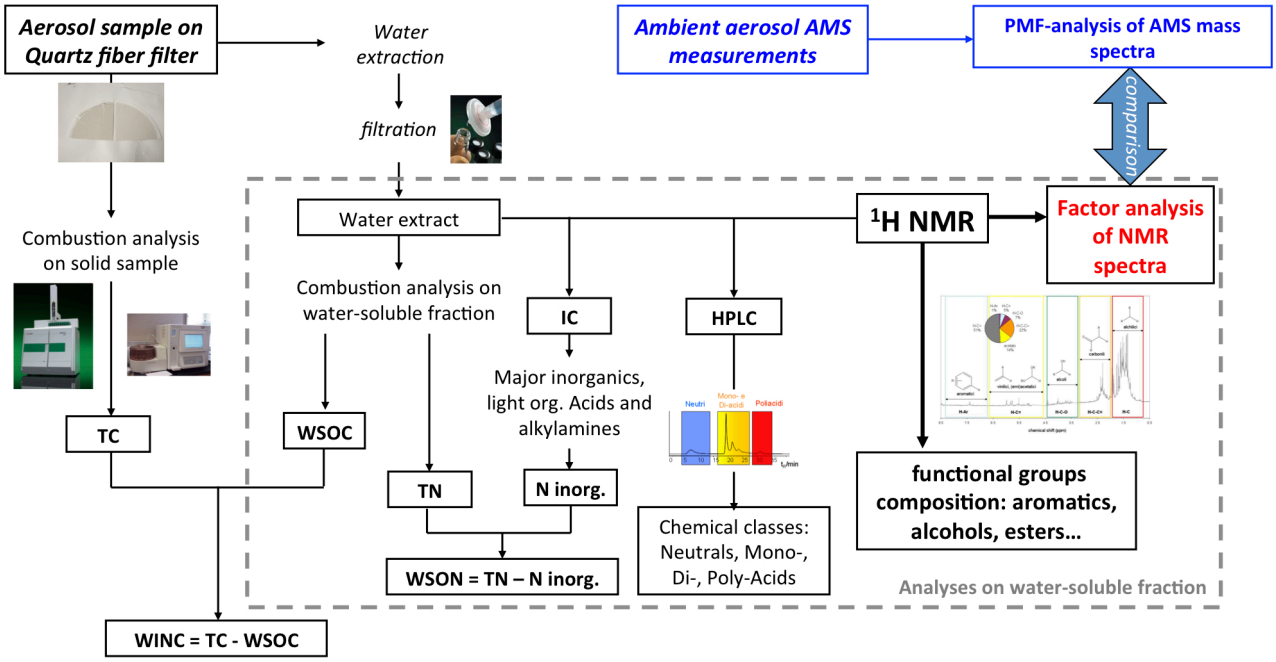


**Figure 4.8**: Scheme of the analytical protocol deployed to characterize aerosol samples. In red the main innovation of this work; in blue analyses not carried results from other research groups and used here for comparison. Grey dotted rectangle encompasses all the analyses on water-soluble aerosol fraction.

Small portion of the samples was directly subjected to high temperature combustion analysis in order to measure their Total Carbon (TC) content. The leftover filter portions underwent extraction with ultrapure mQ water (Millipore, 18.2 mOhm cm water resistivity): about 1 mL of mQ water per filter's $cm^2$ has been generally employed. The extraction procedure was performed using an ultrasonic bath on quartz fiber filters for 30 minutes. After sonication, water extracts were filtered on PTFE membranes (pore size 0.45 μm) in order to remove suspended particles. After filtration the water extract was split into aliquots devoted to the various analyses on the dissolved water-soluble organic matter as schematically reported in figure 4.1. Additional analytical details will be reported in the following sections.

#### *4.2.2.1 Total Carbon (TC) analysis*

Total carbon content was directly measured on a small portion of the quartz fiber filters (about 1 $cm^2$) by evolved gas analysis. Measurements were performed by a Multi N/C 2100 elemental analyser (Analytik Jena, Germany) equipped with a furnace suited for solid samples. Inside the furnace samples were exposed to increasing temperature (up to 950 °C) in a pure oxygen carrier gas. Under these conditions all carbonaceous matter (Organic Carbon, Carbonate Carbon and Elemental Carbon) is converted in CO2 (Gelencser et al., 2000). TC is measured as total evolved $CO_2$ by a non-dispersive infrared (NDIR) analyser. The instrumental detection limit was 0.2 μgC and the accuracy resulted better than 5% for 1 μgC.

#### *4.2.2.2 Water Soluble Organic Carbon (WSOC) analysis*

WSOC content was measured by the liquid module of the above-mentioned Multi N/C 2100 total organic carbon analyser. For each aqueous sample parallel measurements of carbonate carbon (CC) and total soluble carbon (TSC) were carried out. The measure of the TSC is performed by catalytic high temperature combustion in a pure oxygen carrier gas (up to 800 ° C in presence of Pt as catalyst) and a NDIR detector. The measure of the CC content is provided by the acidification of the sample before its combustion. The difference between the measured total soluble carbon and inorganic carbon results in WSOC (Rinaldi et al., 2007). Replicate analysis of standard solutions showed reproducibility within 5% for both TSC and carbonate carbon at the concentrations typically employed for samples extracts (i.e. between 0.5 and 5 ppmC).

#### *4.2.2.3 Ion Chromatography (IC)*

The inorganic water soluble fraction of the ambient aerosol samples has been characterized by means of Ion Chromatography (IC). Inorganic ions ($NH_4^+$, $Na^+$, $K^+$, $Mg^{2+}$, $Ca^{2+}$, $Cl^-$, $NO_2^-$, $NO_3^-$, $SO_4^{2-}$ ) were identified along with light organic acids ions such as acetate (Ace), formate (For), oxalate (Oxa) and methanesulfonate (MSA). Even light alkyl ammonium ions were identified such as mono-, di- and tri-methyl ammonium ions ($MMA^+$, $DMA^+$, $TMA^+$), and mono-, di- and tri-ethyl ammonium ions ($MEA^+$, $DEA^+$, $TEA^+$).

A Dionex instrument (ICS-2000) equipped with a conductivity detector, a gradient pump and a self –regenerating suppressor has been used to separate and quantify the above-listed ions. Anions were specifically analyzed by the ion chromatograph, equipped with IonPac AG11 2x50mm Dionex guard column, IonPac AS11 2x250mm Dionex separation column and ASRS ULTRA II self-regenerating suppressor. A solution of KOH was used as eluent. Its concentration increased from 0.1 mM to 38 mM, in a 25 minutes long run (0.1 mM for 8 min, 5 mM reached at 12 min, 10 mM at

17 min and 38 mM at 25 min). The flow rate was 0.25 mL/min. Cations were analyzed with the same ion chromatograph, equipped with IonPac CG16 3x50 mm Dionex guard column, IonPac CS16 3x250mm Dionex separation column and CSRS ULTRA II self-regenerating suppressor. The analyses were performed isocratically with a 30 mM solution of MSA as eluent held for 35 min. The flow rate was 0.36 mL/min.

The detection limit for the analyzed inorganic ions corresponds to an average air concentration of 4 ng/$m^3$, except for sodium, nitrite and calcium for which it is 45 ng/$m^3$.

#### *4.2.2.4 Water Soluble Organic Nitrogen (WSON)*

The above-mentioned Multi N/C elemental analyzer has been even employed to measure also the Total Soluble Nitrogen (TSN) content of the water-soluble fraction of the aerosol. The instrument's module for nitrogen analysis is equipped with a chemo-luminescence detector to measure the $NO_x$ evolved from the high temperature combustion (800 ° C, 100% $O_2$) of the samples. The elemental analyzer resulted sensitive to nitrogen regardless to its chemical form. TSN was quantified against calibration curves obtained using sodium nitrate as standard compound. The instrumental reproducibility resulted very good (better than 2%) at concentration of 1 ppmN but increases at lower concentrations (8% at 300 ppbN).

Once determined the TSN, the Water Soluble Organic Nitrogen (WSON) content was calculated subtracting the inorganic nitrogen content derived by ion chromatography (i.e. the sum of nitrate, nitrite and ammonium).

#### *4.2.2.5 WSOC separation by High Performance Liquid Chromatography (HPLC)*

A new liquid chromatography method has been applied to simplify the initial complex mixture of water soluble organics into few main chemical classes according to their neutral/acidic character (Mancinelli et al., 2007). An anion exchange HPLC method coupled to WSOC analysis was specifically exploited to quantitatively resolving water soluble organics into: neutral compounds (N), mono- and di-acids (MA and DA), and poly-acids (PA, i.e. compounds carrying more than two carboxylic groups).

The analyses were performed on a HPLC instrument from Agilent (Model 1100), equipped with a TSK-GEL® DEAE-5PW column (7.5mm i.d. . 7.5 cm length, Tosoh Bioscience), an autosampler, UV detector and a fractions collector. The selected injection volume, flow rate and wavelength were respectively 1 mL, 0.7 mL/min and 260 nm. The mobile phase consisted of A) mQ water and B) a $ClO_4$-/$PO_4^{3-}$ buffer solution at pH 7 ($NaClO_4$ 0.5 M, $KH_2PO_4$ 0.05 M, NaOH 0.044 M) whose composition changed towards an increasing ionic strength within the eluition program . The mobile

phase composition changed as follows: A 100 % isocratically from 0 to 8 min; first gradient from 8 to 15 min reaching B 10 %; B 10 % isocratically from 15 to 21 min; second gradient from 21 to 26 min reaching B 100 %; final gradient back to A from 26 to 31 min. N, MA, DA and PA compounds were subsequently eluted and collected on the bases of time intervals chosen depending on the minima between the UV peaks in the chromatogram (7-20 min for N, 20-23 min for MA, 23-30 min for DA and 30-37 min for PA). Avoiding organic additives, the mobile phase does not interfere with the measure of the dissolved organic carbon in the HPLC collected fractions thus allowing the direct WSOC analyses after the collection (before the elemental analysis PA fractions were acidified with 50 μL HCl conc. and purged with $CO_2$ free-air to remove the carbonates due to the mobile phase).

The instrumental detection limits of the NB, MA, DA and PA fractions were 2.2, 1.0, 1.3 and 3.2 μgC, respectively.

#### *4.2.2.6 WSOC characterization by proton-Nuclear Magnetic Resonance ($^1$H-NMR) spectroscopy*

$^1$H-NMR spectroscopy in deuterium oxide ($D_2O$) solution was exploited for functional group characterization of water-soluble organics. Aliquots of water extracts were dried under vacuum and re-dissolved in 650 μL $D_2O$. Sodium 3-trimethylsilyl-(2,2,3,3-$d_4$) propionate (TSP-$d_4$) was prevalently used as referred internal standard adding 50 μL of a TSP-$d_4$ 0.05 % (w/w) solution in $D_2O$ (1.455 μmol H belonging to the standard in the probe) following the protocol reported by Decesari (Decesari et al., 2000; Tagliavini et al., 2006) and already described in Chapter 2. In some cases, methanol (MeOH) was used as alternative internal standard (0.5 μmol H belonging to the standard in the probe). The $^1$H-NMR spectra were acquired with a Varian spectrometer working at 400 MHz (Mercury 400) in 5 mm probes. Pre-saturation of the HDO signal was always performed..

A minimum amount of 80 μg of WSOC in 5 mm NMR tube provides a good signal-to-noise ratio even for the least abundant functionalities (like the aromatics) at 400 MHz and upon a few hours of acquisition. The different bands of the spectra were integrated providing molar concentrations of the organic hydrogen atoms associated with the various functional groups. Different functional group bands and their respective H:C ratios for conversion in carbon molar concentration are those descried in Chapter 2.

## 4.3 Factor Analysis of NMR spectra

### 4.3.1 General description of factor analysis procedure and algorithms

Collections of NMR spectra were processed using factor analysis methodologies in order to find

contributions and spectral profiles (loadings) of major components of WSOC. The carbon fraction not soluble in water (WINC) was not analyzed by NMR in this study and therefore was not accounted for by this factor analysis.

The original NMR spectra were subjected to several pre-processing steps prior to undergo to factor analysis in order to remove spurious sources of variability. A polynomial fit was applied to baselines and subtracted from the spectra. Careful horizontal alignment of the spectra was performed using the TSP-d4 singlet as reference position. Peaks overlapping with blank signals were removed. The spectral regions containing only sparse signals ($\delta H < 0.5$ ppm; $4.7 < \delta H < 5.2$ ppm; and $\delta H > 8.5$ ppm) were omitted from the data set. Binning over ≈0.030 ppm of chemical shift intervals was applied to remove the effects of peak position variability caused by matrix effects. Low-resolution (200 or 400 points depending on specific dataset) spectra were finally obtained, and were allowed to be processed by factor analysis. A scheme of the NMR factor analysis steps is reported in figure 4.8.

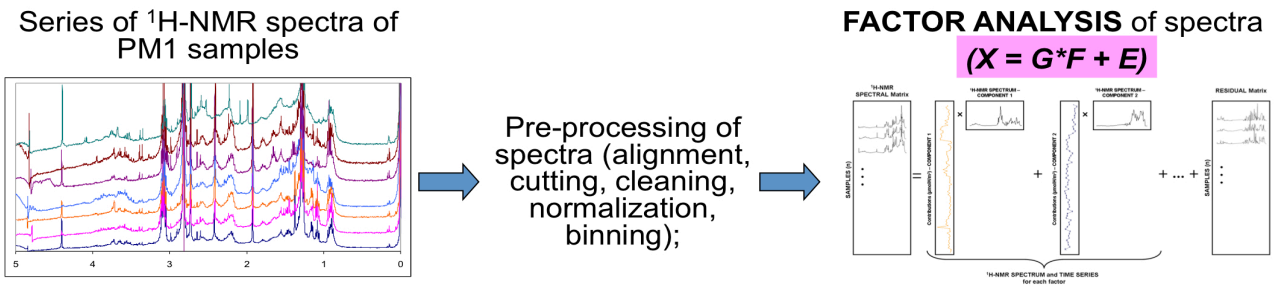


**Figure 4.8**: schematic protocol for NMR factor analysis.

Since these statistical approaches had never been applied to the analysis of atmospheric organic aerosol samples before the present study, 5 different methods of non-negative factor analysis were tested and intercompared in my doctoral work: The EPA open-source software EPA-PMF v3.0 was used for PMF analysis. Two different algorithms were used for N-NMF, employing a projected gradient bound-constrained optimization (Lin, 2007), or a multiplicative update approach (Lee and Seung, 2001). MCR was run according to two different algorithms: the classical alternating least square approach (MCR-ALS, Tauler 1995, Jaumot et al., 2005) and a weighted alternating least square method (MCR-WALS, Wentzell et al., 2006). The five methods, based on the same bilinear model described in section 3.2.2 but with different algorithms, are listed in table 4.3.

| | |
|---|---|
| **EPA-PMF 3.0v** | Positive Matrix Factorization of US Environmental Protection Agency (EPA) software 3.0v with Multilinear Engine (ME) algorithm |
| **N-NMF_ Projected Gradient** | Non-negative Matrix Factorization with Projected gradient bound-constrained optimization |
| **N-NMF_ Multiplicative** | Non-negative Matrix Factorization with multiplicative update approach |
| **MCR-ALS** | Multivariate Curve Resolution-Alternating Least Squares |
| **MCR-WALS** | Multivariate Curve Resolution-Weighted Alternating Least Squares |

**Table 4.3**: multivariate statistical methods exploit for NMR-factor analysis.

The mathematical goal of every model is to find values of $g_{i,k}$, $f_{k,j}$ and p that best reproduce $x_{i,j}$.
For this purpose the values of G and F are iteratively fitted to the data using a least-squares algorithm, minimizing the fit parameter called "Q". Q may be defined in different ways depending on model's approach:

- **EPA-PMF** defines Q as:

$$Q(\mathbf{E}) = \sum_{i=1}^{m} \sum_{j=1}^{n} \left[\frac{e_{ij}}{s_{ij}}\right]^2 \quad \textbf{(3)}$$

where
$\mathbf{s_{ij}}$ is the uncertainty of the $j^{th}$ species concentration in sample i,
**n** is the number of samples and
**m** is the number of species.

It is also possible to use EPA PMF in a "**Robust mode**" which reduces the weight of outliers in the data matrix: when Robust mode is used the uncertainties of measurements for which the scaled residuals ($e_{ij}/s_{ij}$) are greater than a certain parameter (called "outlier distance" or α) are increased in order to downweigh their influence on the PMF solution. Most PMF analyses of PM data report α values give a value of **α=4**.

When Robust mode is used, Q is defined as:

$$Q_{Robust} = \sum_{i=1}^{n} \sum_{j=1}^{m} \left( \frac{e_{ij}}{h_{ij} s_{ij}} \right)^2 \quad \textbf{(4)}$$

where $h_{ij} = 1$ for $|e_{ij}/s_{ij}| \leq \alpha$

$h_{ij} = |e_{ij}/s_{ij}|/\alpha$ for $|e_{ij}/s_{ij}| > \alpha$

In Robust mode the PMF algorithm attempts to minimize $Q_{Robust}$ rather than Q as defined in eq. 3 (so called $Q_{True}$).

The uncertainty matrix ($s_{ij}$) is the most characteristic for PMF respect to other methods, and it allows to reduce the actual impacts of specific values or variables (e.g., outliers or anomalous data) on the results of factor analysis.

The uncertainty matrix was derived in this study on the basis of the baseline noise in the NMR spectra (see following sections).

- **N-NMF Projected Gradient & Multiplicative** define Q as:

$$Q^2 = \frac{1}{2} \sum_{i=1}^{n} \sum_{j=1}^{m} (X_{i,j} - G_{i,k} * F_{k,j})^2 \quad \textbf{(5)}$$

In this equation there is not any term referred to uncertainty and the Q-value depends only on the difference between the measurements ($X_{i,j}$) and model's results ($G_{i,k}*F_{k,j}$).

- **MCR-ALS**, finally, defines Q as:

$$Q^2 = \sum_{i=1}^{m} \sum_{j=1}^{n} (X_{i,j} - X'_{i,j})^2 \quad \textbf{(6)}$$

Q is similar to N-NMF methods, without uncertainty term.

Each factor analysis model can provide solutions with an arbitrary number of factors: the user must select the solution with the factor number that "best" explains the data. This is often the most subjective and least quantitative step of factor analysis and relies greatly on the experience of the modeler (Engel-Cox and Weber, 2007; Reff et al., 2007). In addition, mathematical deconvolution of a dataset often yields non-unique solutions, in which linear transformations (colloquially referred

to as “rotations”) of the factors are possible while the positivity constraint is maintained. The necessity of choosing a number of factors and a particular rotation often complicates the interpretation of the solutions. Criteria for reducing subjectivity and variability in the application of factor analysis (in particular on NMR data) will be provided in Chapter 5 (section 5.2).

## 4.4 Aerosol Mass Spectrometer (AMS)

AMS data are reported in this thesis with aim of comparison with NMR analysis. AMS measurements were operated by partners of the EUCAARI project, not by the writer of this thesis. Nevertheless it is worthwhile to provide here a general overview on the AMS operation principle and set up, because AMS measurements accompanied filter sampling for NMR analysis during all the EUCAARI field campaigns and the AMS-NMR comparison became a key topic of this doctoral work.

The Aerodyne Aerosol Mass Spectrometer (AMS) (Canagaratna et al., 2007; Jayne et al., 2000; Jimenez et al., 2003) is an online particle measurement system which allows the mass spectrometric analysis of aerosol particle composition after separation from the gas phase. The AMS is built up in four sections: an aerodynamic lens as inlet, a differentially pumped vacuum particle sizing chamber, a vaporization/ionization region and a mass spectrometer (MS).

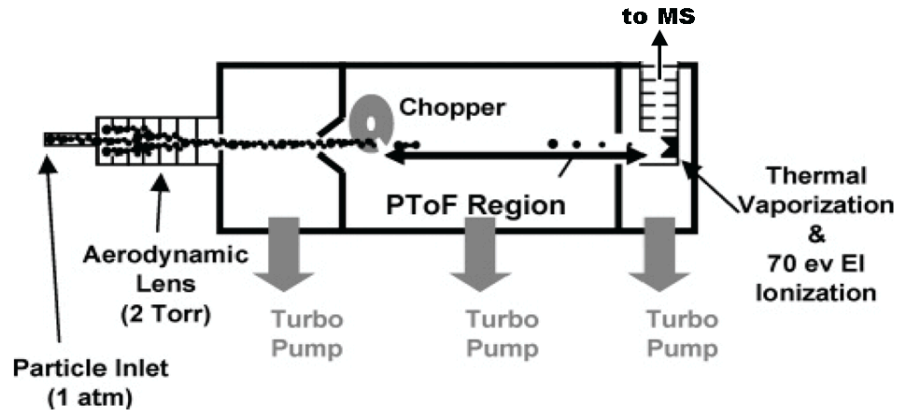


**Figure 4.9**: Schematic drawing of an AMS (partly taken from (DeCarlo et al., 2006)).

An aerosol stream of 80 mL/min passes through a Liu type aerodynamic lens (Liu et al., 1995a; b). The lens reduces the gas phase to particle phase concentration by a factor of 107. It focuses the particle stream to a narrow beam of about 1 mm diameter and has an almost 100 % transmission efficiency for particles between 70 nm and 500 nm. Particles in the size ranges of 30 nm to 70 nm and 500 nm to 2500 nm are still substantially transmitted, with a 50 % transmission efficiency for particles of 1 μm (Jayne et al., 2000; Zhang et al., 2004). Hence, the AMS is referred to as PM1 instrument (Canagaratna et al., 2007).

The particles are accelerated at the exit of the lens and fly through a particle sizing chamber with a pressure within the chamber of approximately $10^{-3}$ Pa. The particle sizing is achieved by measuring the particles time of flight (PToF) between entering the chamber and detection, since the particles velocity is directly proportional to their aerodynamic diameter. A spinning disk that has two radial slits chops the particle beam at the exit of the aerodynamic lens. The recording of the flight time starts when the particles pass through one of the slits, detected by an LED and a photodiode, and ends when ion signal is detected.

After passing through the PToF chamber the particle beam strikes a conic tungsten surface, the so called vaporizer. The vaporizer consists of porous tungsten and has an inverted conical shape, to achieve optimum particle collection efficiency. The temperature of the vaporizer can be modulated from about 150 °C to about 950 °C and is chosen such that maximum signal is obtained. In general, the vaporizer is operated at approximately 600°C causing the non-refractory components of the particles to flash evaporate on the surface (Jayne et al., 2000).

The evaporated molecules are ionized by 70 eV Electron Impact (EI). The required electrons are emitted by a filament that is located millimeters beside the vaporizer. The ionized molecules are then extracted into the MS for compositional analysis. EI ionization is a standard ionization method. Acquired mass spectra can therefore be compared to data base spectra like the public available data base from the National Institute for Standards and Technology (NIST). One must keep in mind, that the flash evaporation of the particles introduces additional internal energy which in turn leads to a high degree of fragmentation when the molecules are ionized.

Quadrupole AMS (Q-AMS) and High Resolution Time of Flight AMS (HR-ToF-AMS) results from various EUCAARI measurement campaigns were used in this work for a comparison with filters measurements. The major difference between these two instruments is the mass spectrometer. The quadrupole mass spectrometer (Q-MS) consecutively scans a defined range of mass to charge ratios (m/z's) with only a narrow mass range reaching the detector at a given time. The scan of a mass range of 300 m/z's requires about 300 ms (Drewnick et al., 2007). Opposite to this, the HR-ToF mass spectrometer acquires all m/z's in one ion extraction, which occurs about every 30 µs in V-mode and ever 50 µs in W-mode. V- and W- mode refer to the flight path of the ions within the MS. V-mode is a single reflection flight path and W-mode is a triple reflection flight path of 1.3 m and 2.9 m, respectively (DeCarlo et al., 2006) resulting in a high mass resolution.

The application of PMF analysis to the organic fraction of AMS mass spectra can be used for source apportionment of organic aerosol, which is an important part of field data interpretation (Aiken *et al.*, 2009; Huffman *et al.*, 2009; Lanz *et al.*, 2007). Details regarding the application of PMF to AMS data can be found in Ulbrich *et al.*, 2009. Briefly, the rows of the matrix ($\mathbf{X}_{ij}$)

represent the averaged mass spectra obtained at each single measurement point and the columns represent the time series of the individual *m*/*z* measured. The rows of the $\mathbf{F}_{pj}$ matrix are the factor profiles (mass spectra) and the columns of matrix $\mathbf{G}_{ip}$ represent the time dependent contribution of each factor to the solution. The number of factors is chosen based on residuum analysis for a range of solutions together with correlation analysis of the factors with each other both in terms of mass spectral and time dependent similarities (Ulbrich et al., 2009). Each factor needs to be validated based on the knowledge of the mass spectrum characteristics and/or by correlation of the time dependence to so called tracers. Tracers are time series of compounds a) measured by the AMS itself e.g. $NO_3$, $SO_4$, $NH_4$, and Cl, b) data of gas phase species like $O_3$, $SO_2$, CO, and $NO_x$, or c) particulate species like black carbon (BC) or elemental carbon (EC) acquired by co-located instruments. Most common factors arising from PMF-AMS (OOA, HOA, etc.) were already mentioned in Section 2.

# 5 - Characterization and source apportionment of atmospheric organic aerosols during the EUCAARI measurement campaigns by means of nuclear magnetic resonance (NMR) spectroscopy

This chapter reports the main results of the chemical analyses carried out at nine different European sites during the EUCAARI project campaigns and of the source apportionment techniques presented in previous chapter. The field sites are located at different altitudes ranging from sea level to several hundreds of meters above sea level (a.s.l.), are distanced 500-1000 Km each other and represent a wide variety of environments, such as marine, coastal, remote continental, suburban and rural, hence being representative for very different local emissions. Nevertheless, being this study focused on PM1 aerosol particles, dominated by accumulation mode aerosols having characteristic lifetimes of 1 - 5 days in the lower-mid Troposphere (Williams et al., 2002), the chemical composition at the various sites in Europe is expected to be considerably impacted by transboundary transport. Therefore, the comparison between samples collected even at stations distanced 500 – 1000 km is informative of the source contributions building up the OA background concentrations at regional-to-continental scale.

## 5.1 Analyses of NMR datasets from the EUCAARI intensive observation periods (IOPs)

Collections of $^{1}$HNMR spectra of WSOC were recorded for each EUCAARI measurement campaign following the procedures described in Chapter 4. Figure 5.1 shows examples of $^{1}$H-NMR spectra recorded during the EUCAARI experiments.

As shown in the figure, NMR spectra of ambient aerosol can show very different features depending on sampling site and measurement period, even if all spectra exhibited a complex spectral structure with presence of very broad, poorly resolved peaks, deriving from the overlap of a very large number of individual minor contributions (as already described in Chapter 2). In order to reduce complexity and to identify and characterize the contributions of possible organic aerosol sources, the unresolved mixtures of molecular structures were decomposed into distributions of main classes of functional groups according to the criteria presented by Decesari et al 2007, and the results from all NMR spectra collected in EUCAARI campaigns are reported in the graph in Figure 5.2. The figure takes into account only the samples collected in continental or marine polluted conditions.

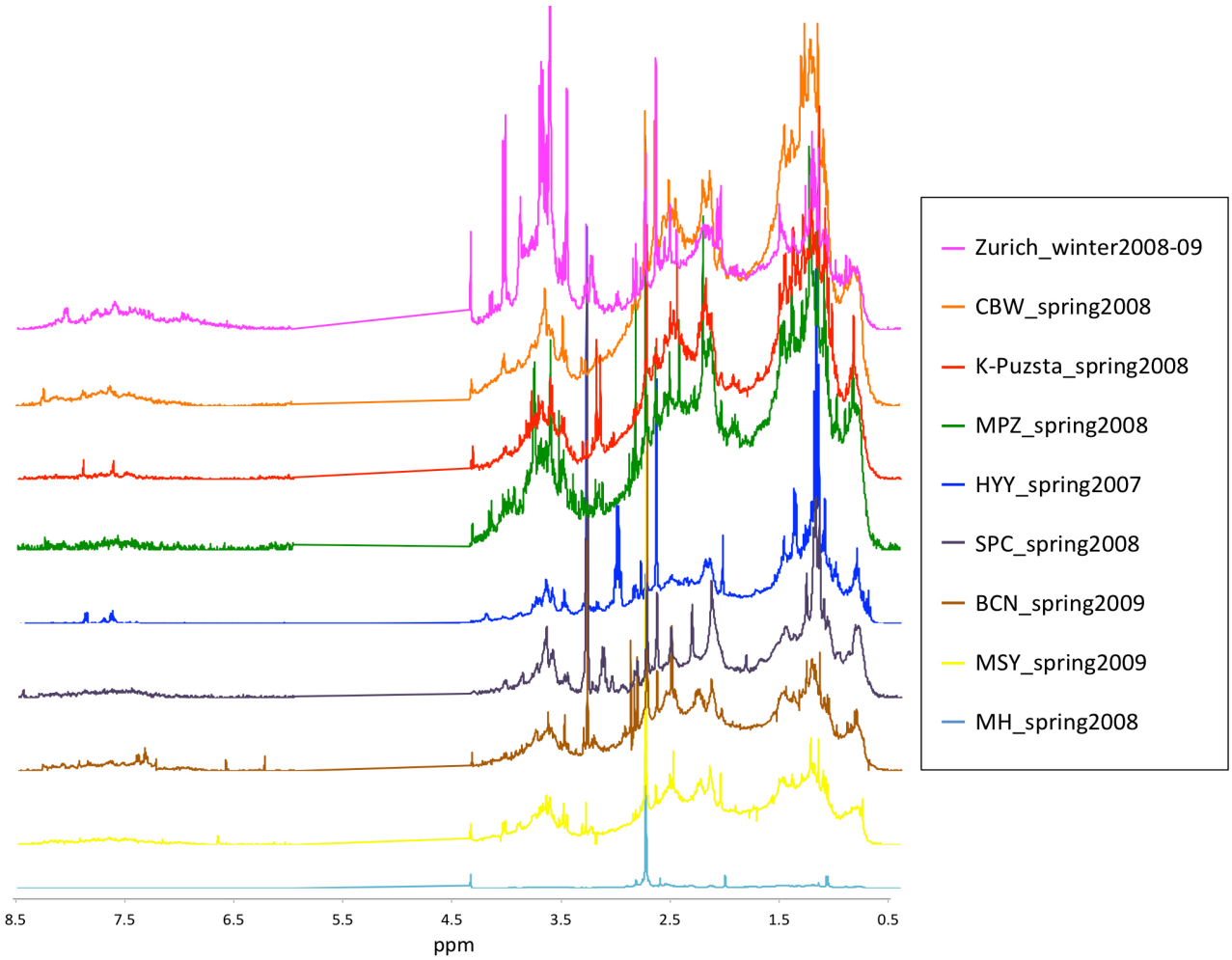


**Figure 5.1**: examples of H-NMR spectra of ambient aerosol samples from the different EUCAARI campaigns. Spectra total signals here are normalized to aerosol concentrations in the air. Y-axis reports arbitrary unit linked with signal intensity; x-axis reports chemical shift expressed in ppm.

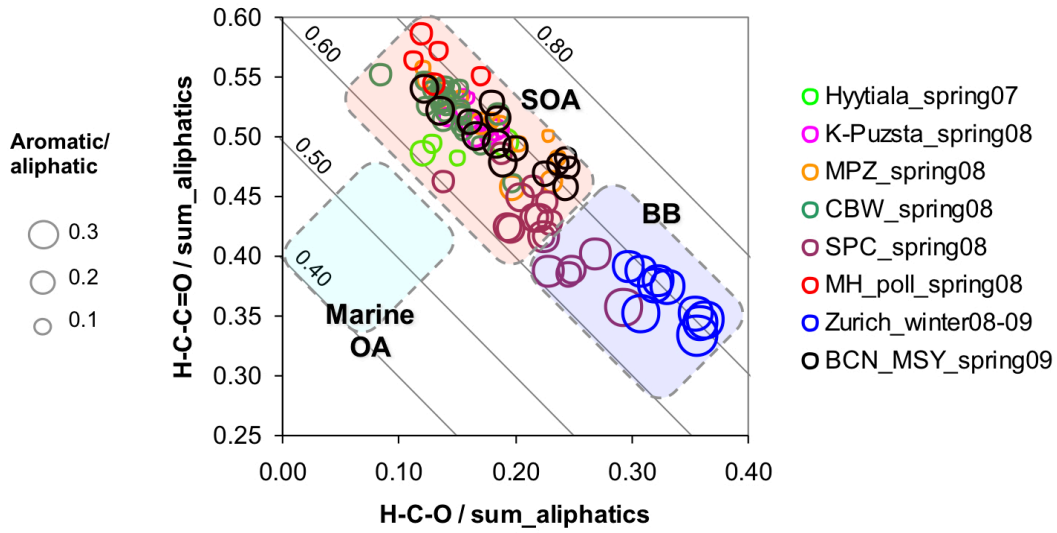


**Figure 5.2**: characterization of unresolved organic mixture in term of functional groups composition from all samples collected and analyzed by H-NMR in the frame of EUCAARI project. MH samples directly impacted by Atlantic air masses were excluded (only polluted cases are considered)

The figure shows a continuum of compositions between two groups: those dominated by biomass burning (BB) and those labelled as "SOA" in the broad sense (enriched in carbonyls or carboxyls). As already explained in Chapter 2, $^{1}$H-NMR analysis without chemical derivatization does not differentiate between carbonyls and carboxyls, therefore the "SOA" cluster actually encompasses compositions of fresh and aged OA without a clear distinction. Conversely, biomass burning OA, enriched in alcohols and in aromatics are clearly identified.

## 5.2 Application of factor analysis to the EUCAARI NMR datasets

In addition to the analysis of functional groups and analogously to more established methodologies employing mass spectrometric techniques, factor analysis of NMR spectra were exploited for the identification of a small number of recurrent chemical classes characterized by source-specific NMR features. We used the five techniques of non-negative factor analysis introduced in Chapter 4. First of all, attempting to address the major issues inherent to factor analysis and its application to NMR (see Chapter 4), an explorative factor analysis was carried out on a subset of NMR data (section 5.2.1) before application to the whole EUCAARI dataset (section 5.3).

### 5.2.1 Choosing the number of factors

Choosing the best modeled number of factors for a dataset is the most critical decision to the interpretation of the PMF results. Mathematically consistent matrix decompositions into scores and loadings do not guarantee that the solutions have a physical sense. Therefore, the selection of appropriate solutions implies a certain degree of subjectivity (e.g. by Li et al., 2004; Buset et al., 2006; Lanz et al., 2007, 2008a,b). Nevertheless, mathematical diagnostics can be profitably exploited to inform decision on factor number and to identify spurious sources of variability.. Several mathematical metrics were eventually used in this work:

***- Q-value Analysis***

A first standardized criterion is the calculation of **Q-value**, the total sum of the squares of scaled residuals (Paatero et al., 2002). If all points in the matrix are fit to within their expected error, then abs $(e_{ij})/\sigma_{ij}$ is ≈ 1 and the expected Q (Qexp) equals the degrees of freedom of the fitted data = $mn-p(m+n)$ (Paatero et al., 2002). If the assumptions of the bilinear model are appropriate for the problem (i.e., the dataset is the sum of variable amounts of components having characteristic constant "profiles") and the estimation of the uncertainties in the input data is accurate, solutions with numbers of factors that give Q/Qexp near 1 should be obtained. In PMF method values of Q/Qexp >> 1 indicate underestimation of the uncertainty or variability in the factor profiles that

cannot be simply modeled as the sum of the given number of components. If Q/Qexp << 1, the errors of the input data are probably overestimated.

Schematically:

**Q/Qexp≈($e_{i,j}$/$s_{i,j}$)/cost ➔ as higher is $s_{i,j}$ as Q/Qexp is lower ➔**

**-if Q/Qexp<1 => OVERESTIMATION of unc. ;**

**-if Q/Qexp≙1 => APPROPRIATE ESTIMATION of unc.;**

**-if Q/Qexp>1 => UNDERESTIMATION of unc.**

Anyway Q/Qexp ratio is expected to decrease with the number of factor, as additional factors explain bits of variance with a general improvement of the fit. However, spurious solutions provide only minor decreases in Q, whereas genuine factors explain a significant fraction of the total variance and their inclusion is generally reflected by a marked decrease in Q/Qexp ratio. Therefore, the visual inspection of the curve Q/Qexp versus number of factor often provides a straightforward manner to highlight to number of "genuine factors" (Paatero and Tapper, 1993).

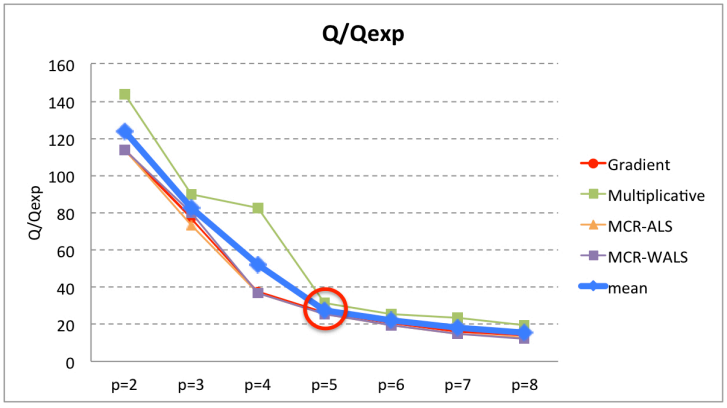


**Figure 5.3**: an example of Q/Qexp versus the number of factors p for the NMR-factor analysis of data from SPC 2008 IOP**.** Blu line represents average values between four methods applied. Red circle denotes the chosen solution (p=5).

Moreover the comparison between factor analysis algorithms allows identification of solutions in which different methods perform similarly, which is also useful for the determination of the best number of factors: as shown in Figure 5.3 referring to SPC 2008 campaign, results from the different algorithms show a significant improvement of their agreement passing from p=4 solution to p=5 one.

***- Preliminary Principal Components Analysis (PCA)***

Preliminary PCA can be run to identify the best number of factors as function of explained variance: the number of factors that explains the majority of the total variance (i.e. 90%), and beyond which the model explains only a further percentage, probably represents a good number of

factor also for other non-negative factor analysis methods. E.g., for Cabauw IOP NMR-dataset, the PCA model with three factors already explains 92% of the total variance. A fourth factor explains only a further 1% indicating a probable spurious solution.

***-Residuals analysis***

Another evaluation method to identify a reasonable number of factors is the analysis of residuals resulting from subtracting the concentrations provided by the sum of the scores calculated by the model from those directly measured by the instrument. The contribution of residuals to total concentrations is expected to decrease with the number of factor, as each additional factor introduces a general improvement of the fit. When the addition of one more factor does not decrease the percentage of residuals, it is most probably the case of a spurious solution. Therefore, the inspection of the dependence of the correlation coefficient (between modeled and measured data) on factor number provides an alternative diagnostic to Q analysis. An example referring to application of EPA-PMF on the Cabauw 2008 NMR dataset (Figure 5.4) shows that better fit is obtained by increasing the number of factors from three to four. In this case, a plateau is reached at four factors (R=0.9996) even if already with only three factors the model fit was excellent (R>0.99) and residuals represent just 0.5% of the reconstructed data.

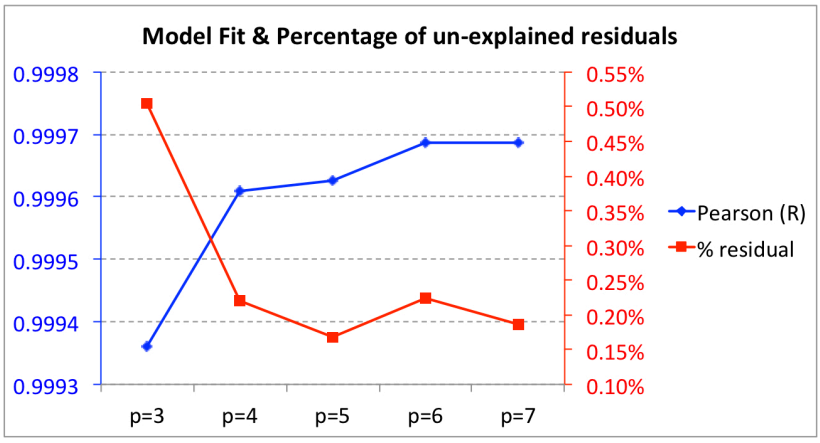


**Figure 5.4**: the model fit and percentage of un-explained residuals as function of the number of factor: blue line represents the Pearson correlation coefficient (R) (on blue left y-axis); red line represents the percentage of model residuals with respect to the sum of concentrations explained by factors modeled.

***- Uniqueness of NMR spectral profiles and contribution***

Genuine factors are normally characterized by distinct profiles. Inversely, very high correlation coefficients between two or more factor profiles point to probable spurious solutions. An example regarding Cabauw 2008 campaign shows that in the solution with p = 4 the spectra of two factors result very similar and difficult to distinguish between each other. Table 5.1 shows the correlation between profiles for the p=4 solution: very high values of correlation coefficient between F2 and

F3, F2 and F4, F3 and F4 (respectively 0.81, 0.78 and 0.93) suggested that the split into four factors was artificial.

| p=3 | R | F1 | F2 | F3 |
|---|---|---|---|---|
| | F1 | 1 | | |
| | F2 | 0.64 | 1 | |
| | F3 | 0.62 | 0.82 | 1 |

| p=4 | R | F1 | F2 | F3 | F4 |
|---|---|---|---|---|---|
| | F1 | 1 | | | |
| | F2 | 0.53 | 1 | | |
| | F3 | 0.53 | 0.81 | 1 | |
| | F4 | 0.71 | 0.78 | 0.93 | 1 |

**Table 5.1**: Pearson correlation coefficients (R) between spectral profiles of NMR-factors for p=3 and p=4 solutions in Cabauw 2008 EUCAARI campaign. The high correlation between two factors (F3 and F4) in the p=4 solution is highlighted in bright red. Other shades of red indicate different levels of correlation, smaller but still significant.

***- Comparison with chemical and meteorological metadata***

Finally, even if mathematical diagnostics are very useful to exclude spurious factors and to describe the mathematical aspect of the models explanatory power, metadata analysis is also used to discriminate between ambiguous solutions and to facilitate the interpretation of the physical sense of the factors (e.g., Lanz et al. 2008). In this study, NMR factor contributions were compared, for instance, with the concentration time trends of proxies for primary (e.g. CO, NOx, BC, EC) and secondary (e.g. gaseous oxidants, particulate nitrate and sulphate etc.) sources in the troposphere. The calculated scores were also examined in parallel with air-masses origin study to determine prevalent origin area and to link them to specific activities and sources.

### 5.2.2 Input uncertainty determination

As already mentioned in Chapter 4, a matrix of uncertainties ($s_{ij}$), with values defined for each entry in the measurement matrix, must also be supplied as input to EPA-PMF. Quantification of the uncertainty is often very important for the outcomes of PMF analysis and it is always critical for calculating the diagnostic Q defined in eq. (3) (see Chapter 4). The estimation of uncertainty starting from the method detection limit and other sources of analytical uncertainty can be derived according to different equations, as exemplified by Reff et al. (2007). Since PMF had never been applied to NMR spectral datasets before the present study, several approaches for building up the uncertainty matrix for PMF have been pursued:

- ***DLx2***: The signal-to-noise ratio was calculated in the 6 - 7 ppm region, which is typically free of the sample signals for each spectrum, and the detection limit (DL) was derived from the noise amplitude. Uncertainty for PMF was then defined as twice the detection limit (DL x 2), in order to take into account additional sources of variability respect to the instrumental noise.
  DLx2 may differ between spectra, but it is constant in each spectrum.

E.g.: DLx2= [ 0.9 0.9 … 0.9
0.3 … … 0.3
… … … …
0.7 … … 0.7 ];

- ***Relative uncertainty***: after DL calculation (or Instrument Precision (IP)), the uncertainty is defined as follows:
  - if the concentration is lower than DL (or IP), an uncertainty equal to DLx2 is assigned:

$$s_{ij} \equiv 2 \times \mathrm{IP}, \quad \text{if} \quad x_{ij} \leq \quad \mathrm{IP}$$

  - if the concentration is higher than DL (or IP) we assign an uncertainty which is also a function of the relative error (percentage):

$$s_{ij} \equiv \sqrt{(\text{percentage} \times x_{ij})^2 + (IP)^2}, \quad \text{if} \quad x_{ij} > \quad \mathrm{IP}$$

    where $s_{i,j}$ and $x_{i,j}$ are respectively the total uncertainty and concentration in the $j^{th}$ species during the $i^{th}$ sample, and IP is the Instrument Precision calculated in different possible ways.

This kind of uncertainty varies between spectra and within each spectrum along the scale of the chemical shifts:

E.g.: WilliamDL=[0.9 0.8 … 1.2
0.6 … … 1.3
… … … …
0.7 … … 1.0 ];

Although uncertainty definitions taking into account relative errors on the measurements are in principle more correct than those relying on the DL quantification alone, in this particular study the definition of uncertainties had no clear impact on the determination of the factors and on results of NMR spectra factor analysis. On the contrary, EPA-PMF, regardless of the criteria adopted for uncertainty definition, behaved very similarly to the other algorithms in treating the NMR datasets. For this reason, in this work a simple DLx2 uncertainty was finally selected (section 4.4.1).

### 5.2.3 Rotational problems

Despite the constraint of non-negativity, PMF and factor analysis solutions may not be univocally determined even for the same factor number: there may be many possible linear transformations ("rotations") of the factors profiles and contributions that result in an identical fit to the data, such that:

$$GF = GTT^{-1}F$$

Where T is a transformation matrix and $T^{-1}$ is its inverse. A given $t_{i,j}>0$ would create a rotation by adding the profiles (F) and subtracting the contributions (G) of factors *i* and *j*, while $t_{i,j}<0$ would create a rotation by subtracting the profiles (F) and adding the contributions (G) of factors *i* and *j*. An infinite number of "rotations" may exist and still meet the non-negativity constraint. It should be noted that orthogonal or "solid body" geometric rotations of the factors are only a subset of the possible linear transformations.

With EPA-PMF 3.0v (like with PMF2 and ME, the most widespread software for PMF), once the best number of factors has been determined, a subset of the rotational freedom of the solution can be explored by changing the FPEAK parameter. Of greatest interest are FPEAK values for which Q does not increase significantly over $Q_{FPEAK=0}$, meaning that the PMF model is still satisfied with little additional error. Some researchers recommend exploring a range of FPEAKs such that Q/Qexp increase from its minimum to e.g. 10% (P.K. Hopke, personal communication, 2007; Paatero and Hopke, 2009). Solutions reported in the literature generally have an FPEAK value between -1 and +1 (Reff et al., 2007). Taking into account these recommendations, a range of FPEAK results were explored for every PMF analysis of NMR dataset and solutions such that Q/Qexp increase from its minimum by e.g. 10% were studied. An example of this rotational ambiguity analysis (relative to CBW) is reported in Figure 5.5.

Overall, the effect of positive FPEAK is to generate a greater number of values close to zero in the profiles (F) and to decrease the number of near-zero values in the contributions (G), while the opposite is observed for negative FPEAK parameters.

Another possible way used to optimize rotation is to maximize the correlation of factor contributions with external tracers (metadata). This method was also used in some cases in this study.

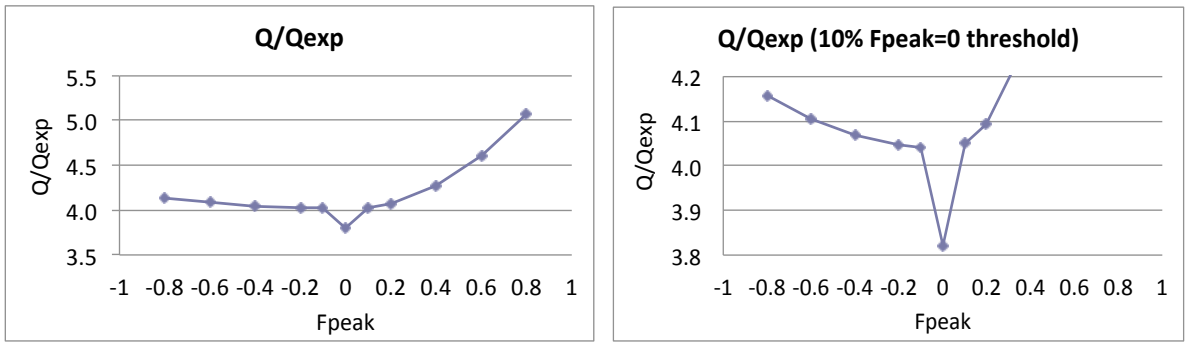


**Figure 5.5**: Q/Qexp ratio values as function of different FPEAK parameter, useful for the rotational ambiguity analysis: solutions reported refers to Cabauw 2008 campaign and examine FPEAK values between -0.8 and +0.8 (in the left graph) and just the range of FPEAKs such that Q/Qexp increase from its minimum to 10% max (in the right graph).

## 5.3 Factor analysis of NMR-datasets from individual EUCAARI campaigns (IOPs)

Factor analysis on NMR spectra was applied to individual Intensive Observation Period datasets presented before. There is a general good overlap between results from different methods of factor analysis that suggests a feasible robust solution for each campaign dataset. Table 5.2 shows an overview of the results of the NMR factor analysis for each IOP by reporting the best solutions identified according to the criteria described above.

Interpretation of spectral profiles from factor analysis and their attribution to specific sources was based on the comparison with a unique library of **reference spectra** recorded during laboratory studies or in the field at near-source stations.

From the independent factor analysis of each IOP data, some recurrent factors were identified in different sites and experiments, listed below using a subjective classification:

- "**MSA-containing" factor**: the peak of methane-sulphonate (MSA) at 2.81 ppm of chemical shift is most characteristic for this factor and represents on average 17% of the total factor spectral profile. Other spectral features include aliphatic chains with methylenes and terminal methyls peaks at respectively 1.3 and 0.8 ppm of chemical shift. The occurrence of MSA as major tracer compound and the characteristics of concentration time trends assign this NMR-factor to *marine WSOC sources* and was found at coastal (MH, CBW) stations and in Mediterranean countries (SPC, BCN/MSY);

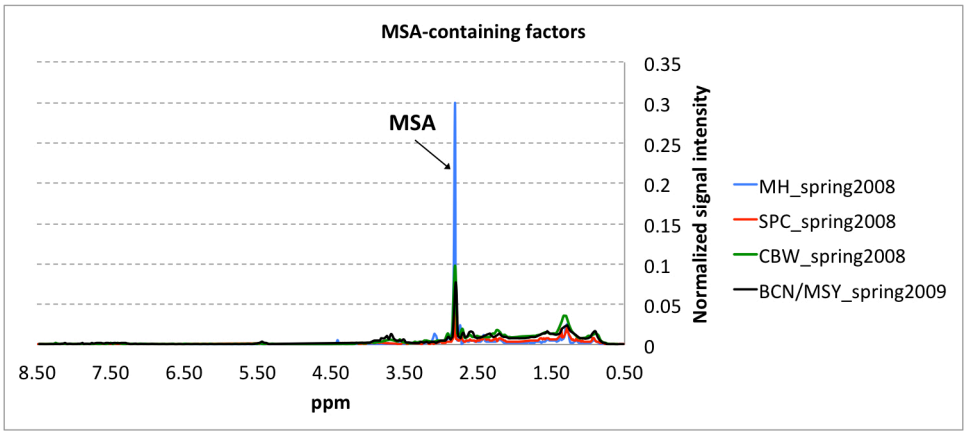


**Figure 5.6**: spectral profiles of "MSA-containing" factors from EUCAARI campaigns where they are identified (as reported by legend).

- **Amine factor**: characterized by peaks of low-molecular weight alkyl-amines, including monomethyl-, dimethyl-, trimethyl-, diethyl- and/or triethyl-amines (MMA, DMA, TMA, DEA and/or TEA), was found in HYY and SPC (both in spring and in summer) and it is probably linked with biogenic and anthropogenic sources from anaerobic processes and agriculture activity;

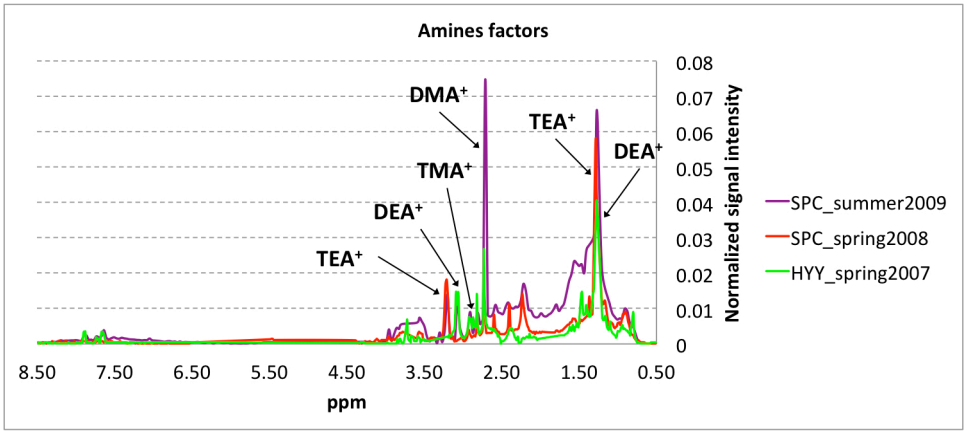


**Figure 5.7**: spectral profiles of Amines factors from EUCAARI campaigns where they are identified (as reported by legend).

- **Biomass Burning factor**: showed spectral profile with clear signatures from aromatic compounds and polyols and carrying **levoglucosan** (singlets at 5.45 and 4.15 ppm). Its profile is very similar to the spectrum of biomass burning POA obtained in chamber experiments and field observations of open burning (as shown later in figure 5.11). It occurs especially in samples from winter and early spring (Zurich, SPC, BCN/MSY, HYY);

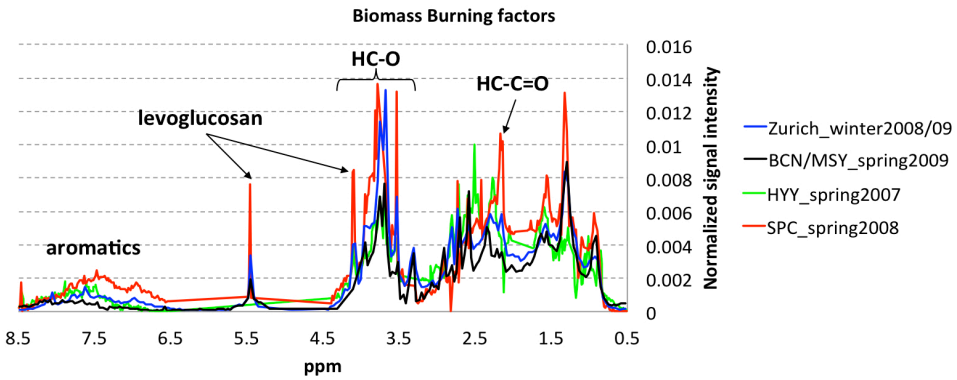


**Figure 5.8**: spectral profiles of Biomass Burning factors from EUCAARI campaigns where they are identified (as reported by legend).

- **<u>bioSOA-like factor</u>**: main distinguishing features of this factor are the presence of singlets overlapping the background signal in the region between 0.7–1.8 ppm which comprises un-functionalized alkyls (HC-C), e.g. methyl or methylene groups. Aliphatic alcohols and ethers/esters (HC-O) also contribute to characterizing the profile of this factor in the range of chemical shifts between 3.3–4.5 ppm. By comparing the spectral profile of this factor with reference $^{1}$H-NMR spectra of ambient and laboratory-generated water-soluble aerosols, the best match was found with the biogenic SOA produced in the SAPHIR simulation chamber (*Jülich Research Centre*) during photo-oxidation and ozonolysis of terpene mixtures (Figure 5.11). In particular, the closest similarity was found with BSOA generated with mixtures of monoterpenes (MT) and sesquiterpenes (SQT), including: α/β-pinene, limonene, $\Delta^3$-carene, ocimene, β-caryophyllene and α-farnesene. This NMR factor was observed at the forest sites (HYY, MPZ);

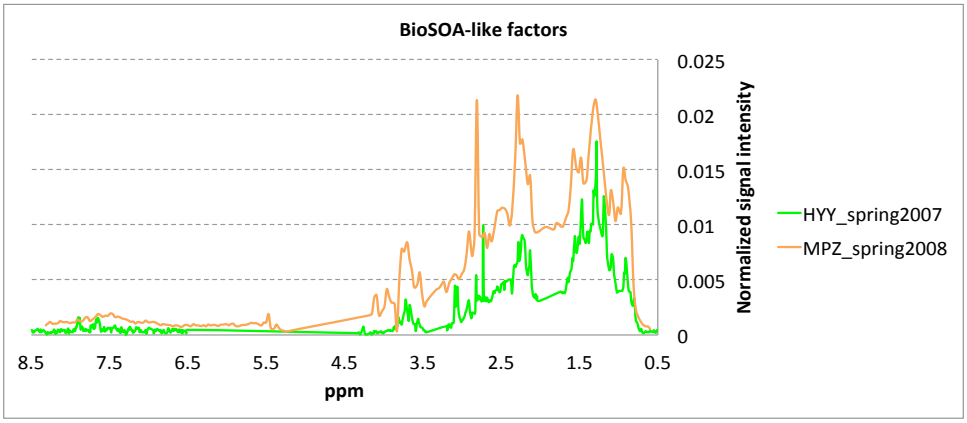


**Figure 5.9**: spectral profiles of BioSOA-like factors from EUCAARI campaigns where they are identified (as reported by legend).

- **<u>polysubstitued aliphatic compounds factor</u>**: its spectral characteristics are attributable to branched/cyclic and polysubstituted aliphatic compounds. Aliphatic chains with terminal

methyls are almost absent and also the hydroxyl groups account for a very small fraction (6% on average) of the detected WSOC. Conversely, the aliphatic groups substituted with C=C and C=O groups (between 1.8 and 3.2 ppm) represent on average 50% of the total functionalities on a carbon basis. Such spectral features were already reported for WSOC in environments impacted by continental anthropogenic emissions (Decesari et al., 2000, 2007, 2011; Finessi et al., 2012). Most interestingly, they overlap well with the $^{1}$H-NMR spectrum of Suwannee river fulvic acid (Figure 5.11) and can be considered characteristic of atmospheric Humic-Like Substances. This factor profile was found at *all* EUCAARI stations;

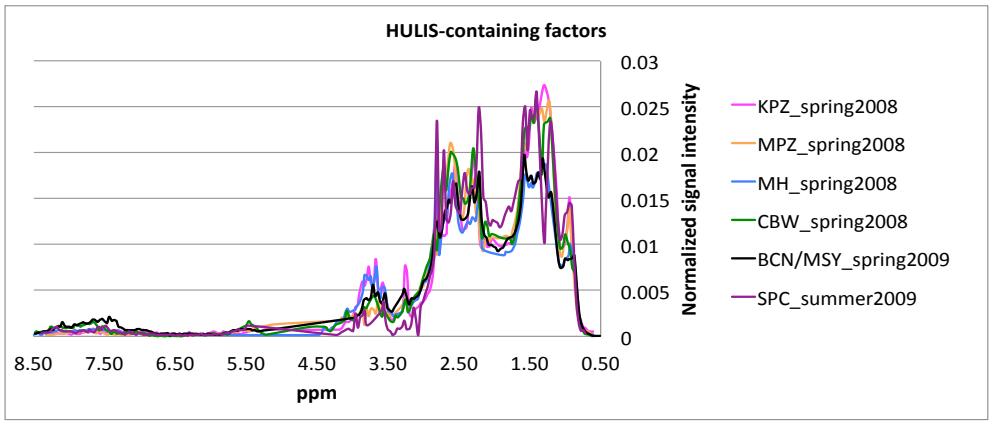


**Figure 5.10**: spectral profiles of "HULIS-containing" factors from EUCAARI campaigns where they are identified (as reported by legend).

- **unclassified factors** found at the forest sites (HYY, MPZ), possibly including contributions from Primary Biological Aerosol Particles (PBAPs), and during summer at SPC, possibly representing the products of cooking activities.

The fact that some of these factors were found at some stations not in others does not mean that they were completely missing in the latter. On the contrary, they could be rather mixed and confused with other more prominent factors if co-varying with them under the conditions of the experiment. For instance, traces of MSA and amines were found in most samples, but only during some experiments factor analysis was able to discriminate specific factors for these compounds. It is worth to mention that the amines were found in greatest concentrations in Hyytiälä and in the Po Valley, which are very different environments. The different speciation (because for example TEA was more prominent than DEA in SPC, contrary to HYY) indicates that distinct sources can contribute, including transport of marine aerosols and emissions from soil.

| IOP site (date) | # of samples | # of factors | Average contributions - % (nmolH/m$^3$) | | | | | |
|---|---|---|---|---|---|---|---|---|
| | | | MSA-containing | Amines | BioSOA-Like | Biomass Burning | HULIS | unclassified |
| **HYY (2007)** | 22 | 5 | 13% (6.5) | | 13% (6.5) | 66% (32.6) | | 8% (3.9) |
| **SPC (2008)** | 34 | 5 | 10% (9.4) | 18% (17.0) | | 27% (24.9) | Type I - 17% (15.9)<br>Type II - 28% (26.5) | |
| **CBW (2008)** | 30 | 3 | 18% (16.1) | | | | 43% (38.1) | 39% (34.4) |
| **MPZ (2008)** | 15 | 3 | | | 33% (62.7) | | 44% (83.8) | 23% (44.6) |
| **MHD (2008)** | 7 | 3 | 24% (11.2) | | | | 57% (26.4) | 19% (9.1) |
| **KPZ (2008)** | 10 | 3 | | | | | Type I - 33% (72.3)<br>Type II - 35% (75.9) | 32% (69.3) |
| **ZW (2008)** | 10 | 2 | | | | Type I - 58% (62.7)<br>Type II - 42% (45.6) | | |
| **SPC (2009)** | 29 | 4 | | 14% (10.2) | | | Type I - 38% (28)<br>Type II - 27% (19.7) | 21% (15.8) |
| **BCN&MSY (2009)** | 14 (7+7) | 3 | 31% (41.2) | | | 24% (31.8) | 45% (59.9) | |

**Table 5.2**: overview of results from the NMR factor analysis reporting the best results for each IOP.

Figure 5.11 reports the best fits found between NMR factors and reference spectra:

-Biomass Burning factors and wood burning POA from chamber experiment (carried out at Paul Scharrer Institute, PSI, Switzerland);

-Polysubstituted aliphatics factors with Suwannee River fulvic acid reference spectrum (from water sample but representative also for atmospheric HULIS) and

-bioSOA-like factors with BSOA produced in the SAPHIR simulation chamber (*Jülich Research Centre*).

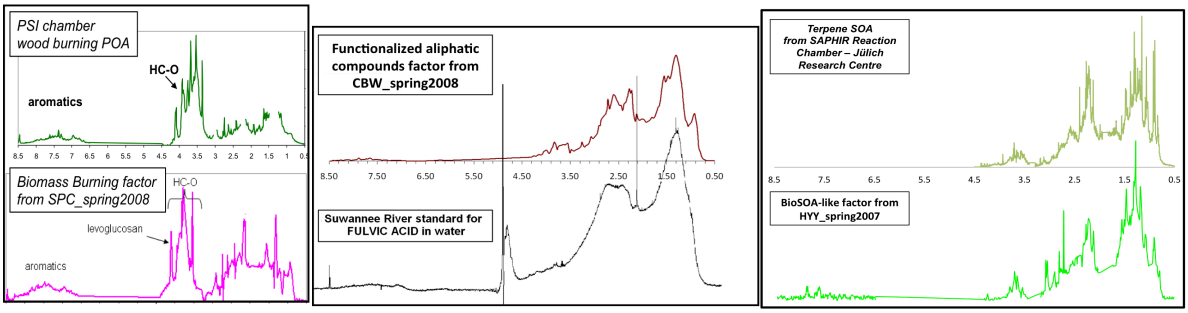


**Figure 5.11**: comparison between NMR-factors profiles and NMR-reference spectra.

Discussion about the nature of the above factors will be expanded in the following chapters. During specific IOPs, interesting correlations were found between specific NMR and AMS factors, which will be also presented for individual studies in the next three chapters.

## 5.4 Factor analysis of the whole European EUCAARI dataset

The previous section presented a comparison between the organic aerosol compositions determined at the various European sites based on a subjective clustering analysis of the factors extracted by factor analysis of the individual datasets. As anticipated, a limitation of that approach is that specific chemical classes could or could not be identified by factor analysis in the individual experiments depending on their explained variability. In other words, if the experimental (e.g., meteorological) conditions during the experiment forced distinct chemical classes to co-vary, these will be determined as a mixed factor by factor analysis. In order to overcome these problems, I lumped the individual datasets into a single global one and resubmitted it to factor analysis: this forced the analysis to identify the very same factors in the different experiments and the contributions of the resulting factors become more comparable between experiments. This second approach build up on the hypothesis that the chemical composition at the various sites can be reduced to combinations of common classes of compounds which dominate the continental background aerosol. This was contrasted by the finding of factors specific for individual sites (e.g., the PBAPs in Melpitz), but these are generally minor factors, and are supposed to fall in the residual when running factor analysis on the global dataset.

Factor analysis of the whole EUCAARI dataset required a new pre-processing of the NMR spectra with the aim of homogenize data format and blank/baseline correction: all the spectra from all individual campaigns were treated with the same baseline correction, aligned, normalized and binned in the same way (normalized to 1 and binned to 200 points, every 0.03 ppm) in order to guarantee a meaningful comparison between spectra from different campaigns and different sites.

A preliminary PCA was employed for studying the variability of the whole spectral dataset: this preliminary analysis allowed to create a more homogeneous dataset suitable for the subsequent factor analysis identifying probably outliers and any misleading source of variability in the data, both in signal peaks (loading) and in samples (scores). In particular some signal peaks isolated by PCA and recognized as contaminants peaks from quartz-fiber filters (such as peaks at 1.25, 1.31 and 1.33 ppm) and from samples treatment procedure (such as acetate peak at 1.9 ppm and Methanol peak at 3.36 ppm) were systematically removed. The peaks of contaminants (such as ethylene glycol butyl ether and 2-butoxyethyl acetate) contributing randomly in specific campaigns were removed. Finally, the peak of MSA was also removed, since not useful as explanatory variable

for discerning biogenic and anthropogenic continental sources, which are the most difficult to disentangle.

A total of 102 $^{1}$H-NMR spectra at 188 points resolution were eventually subjected to three (NMF-Gradient, NMF-Multiplicative and MCR-ALS) of the five factorization models mentioned in the experimental Chapter 4 and the solutions resulting from factors 2 up to 6 were explored. All three algorithms showed that most of the variance was explained by a limited number of factors, with the concentrations in the residual being of the order of the baseline noise for more solutions with more than 3 factors. The largest drop in the Q/Qexp ratios was registered between two and three factors, but additional factors continued to reduce Q/Qexp toward 1 until no strong change in slope was observable for more than four factors. Beyond four factors, two or more factors were found to be strongly correlated, suggesting that the measurements were not adequate to differentiate additional independent factors.

The results showed a good convergence of factor analysis models to a 3-factors solution: factor profiles are reported in Figure 5.12, whereas the correlations between factors profiles and NMR reference spectra are reported in Table 5.3:

- **Factor1** is characterized by aromatics and alcohols and its profile shows correlation only with **wood burning POA** suggesting a primary biomass burning source;
- **Factor2** is composed of polysubstituted aliphatic chains and shows a strong correlation with of **Suwannee River fulvic acid spectrum;**
- **Factor3** of less substituted aliphatics with methylenic chains and amines. Both **Factors 2 and 3** profiles show generally positive correlations with both biogenic and anthropogenic SOA and with fulvic acid standards, but the **best fit for Factor 3 is with terpene SOA**.

By comparing this 3 factor representation with the results obtained from the individual field campaigns, factor analysis of the whole EUCAARI dataset seems to capture just the main source contribution, i.e. the factors with spectral profiles with most distinguishing features and providing the greatest contributions. Other factors identified during single IOP analysis are probably “hidden” and mixed within the main three factors obtained from the analysis of the full database. Especially, Factor 3 is probably a mixture of different source contributions (BioSOA-like, Amines, etc.).

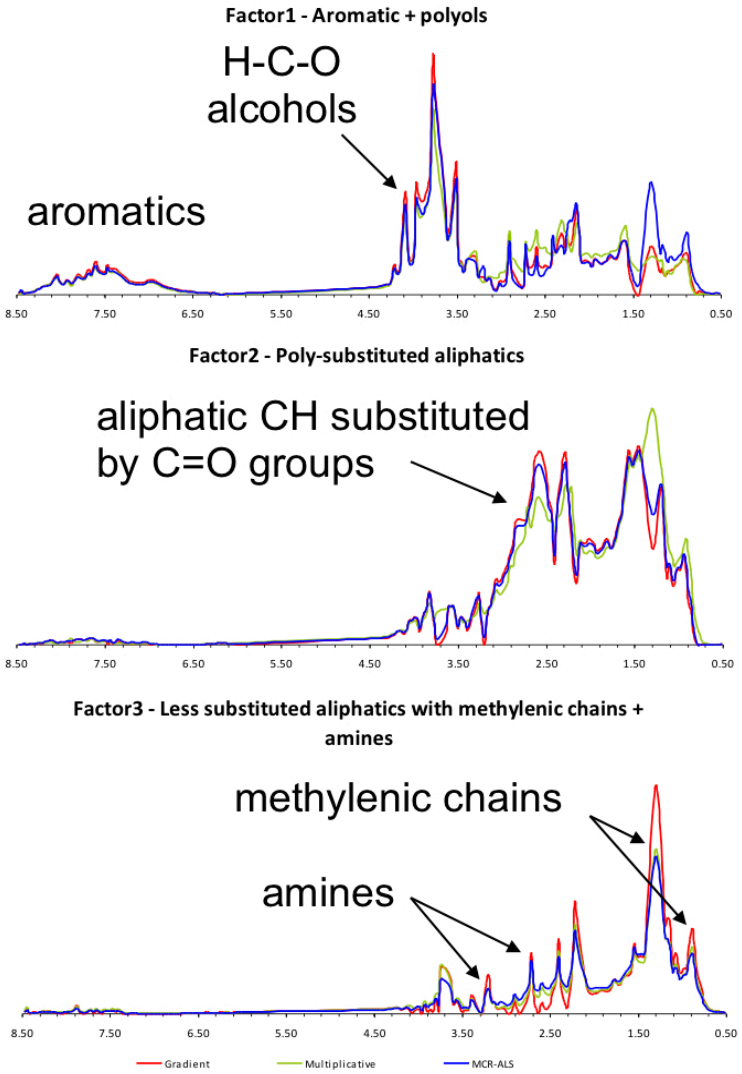


**Figure 5.12**: spectral profiles from the 3-factors solution on the whole European EUCAARI NMR-dataset. Solutions from different factor-analysis algorithms: N-NMF projected gradient (red line), N-NMF multiplicative (green line) and MCR-ALS (blue line).

| R (Pearson) | Fresh SOA | Aged SOA | α-pinene SOA | TMB SOA | Toluene SOA | Methyl-glyoxal oligomers | Wood burning POA | Suwannee Water Fulvic Acid |
|---|---|---|---|---|---|---|---|---|
| **Factor1** | 0.29 | 0.34 | 0.29 | 0.16 | 0.25 | 0.17 | 0.68 | 0.29 |
| **Factor2** | 0.81 | 0.85 | 0.79 | 0.72 | 0.75 | 0.41 | 0.21 | **0.94** |
| **Factor3** | 0.88 | 0.86 | 0.89 | 0.61 | 0.66 | 0.58 | 0.16 | 0.69 |

**Table 5.3**: correlations between NMR factors profile and some reference spectra. Fresh and aged SOA are those produced in the Julich chamber starting from monoterpene and sesquiterpene mixtures and oxidized at low NOx levels. Alpha-pinene SOA and TMB SOA are those produced in the PSI chamber at high NOX levels (POLYSOA experiment), while toluene SOA were collected in the old Ispra reaction chamber. The methyl-glyoxal oligomers were synthetized in ISAC-CNR laboratory starting from concentrated methylglyoxal aqueous solutions. Wood burning emissions are the POA injected in the PSI reaction chamber. The Suwannee River fulvic acid is the usual standard from IHSS.

However, analyzing the composition in term of functional group of the factors resolved by Factor Analysis, there are now two factors explaining the variability of functional group composition within the "SOA" range, as shown in Figure 5.13. Interestingly, the factor analysis algorithms assign the amount of aromatics purely to wood burning sources. The other two factors, more characteristic for SOA, differ from each-other especially for the amounts of carbonyls/carboxyls, with factor 2 (HULIS) being apparently more "aged".

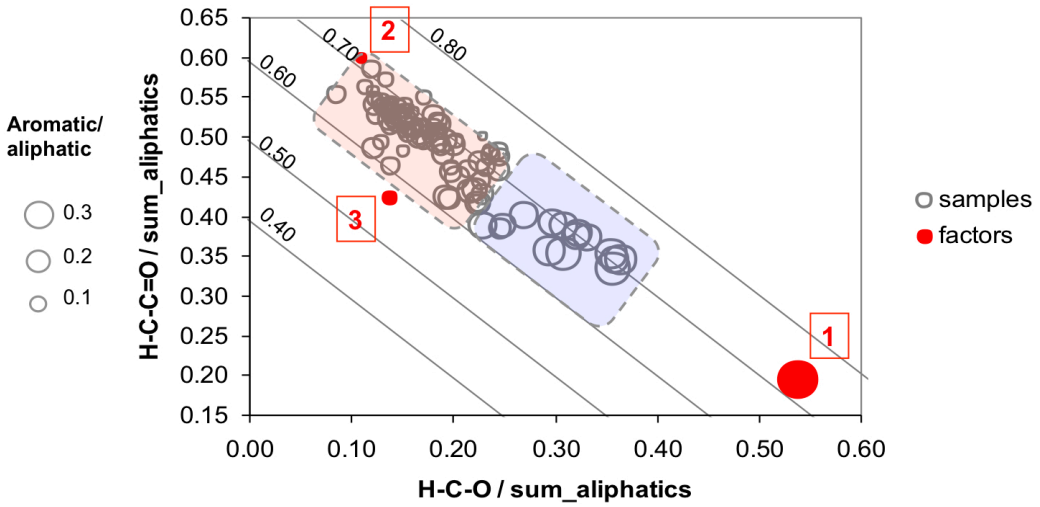


**Figure 5.13**: functional group distributions of the 3 factors from factor analysis of the whole European EUCAARI NMR-dataset.

## 5.5 Comparison between NMR and AMS results within EUCAARI project

The results of NMR factor analysis for water-soluble organic compounds were also qualitatively compared with those of AMS factors for Oxidized Organic Aerosols for specific EUCAARI intensive field studies (see following chapters). In this section, I aim to compare the results of the factor analysis on the global NMR dataset with the range of AMS chemical compositions obtained at the same sites and expressed as distribution of main AMS m/z fragments. The diagram in figure 5.14 provides a summary of such comparison. Average compositions obtained during the specific field campaigns were classified according the Ng's triangular diagram (Ng et al., 2010). This simplified representation of the oxidized organic aerosol composition (based on the plot of the relative contribution of fragment m/z 44 (f44) vs. that of m/z 43 (f43) in mass spectra of ambient aerosol) was extensively adopted in last years to yield some insights regarding the dynamic evolution of OOA in atmosphere. In fact m/z 44 and m/z 43 are prominent peaks in the OOA mass spectra, including semivolatile compounds (SV-OOA) and the non-volatile (LV-OOA), and they are representative of different oxygen-containing functional groups (f44 of carboxylic acids vs. f43 of carbonyls). What Ng et al. (2010) noted was that the ambient OOA components from all the sites

cluster within a well-defined triangular region of the plot. The dotted lines in figure 5.14 are added to guide the eye and define this space. In general, the SV-OOA and LV-OOA components at multiple sites fall into two distinct regions in this triangle: SV-OOA components are concentrated in the lower half of the triangle, while the LV-OOA components are concentrated in the upper half of the triangle. The total OOA components show an intermediate range of f44. Since photochemical oxidation is accompanied by an increase in f44 (Alfarra et al., 2004; de Gouw et al., 2005; Aiken et al., 2008; Kleinman et al., 2008), the f44 axis can be considered as an indicator of atmospheric aging. The base of the triangular region defines the range of f43 that is observed for the less oxidized SV-OOA components. Since the SV-OOA components represent photochemically "fresh" organics, the variability in f43 for these components is expected to depend mainly on the emissions rather than on atmospheric processes.

Both amount and range in f43 for OOA components decrease with increasing f44. This suggests that the OOA components become more chemically similar with increasing O:C and photochemical aged regardless of the original source of the OOA. The HULIS and fulvic acids standards, measured in Ng et al., 2010 and in various subsequently AMS studies, showed some of the highest f44 values and fall in the highest LV-OOA range of the triangle.

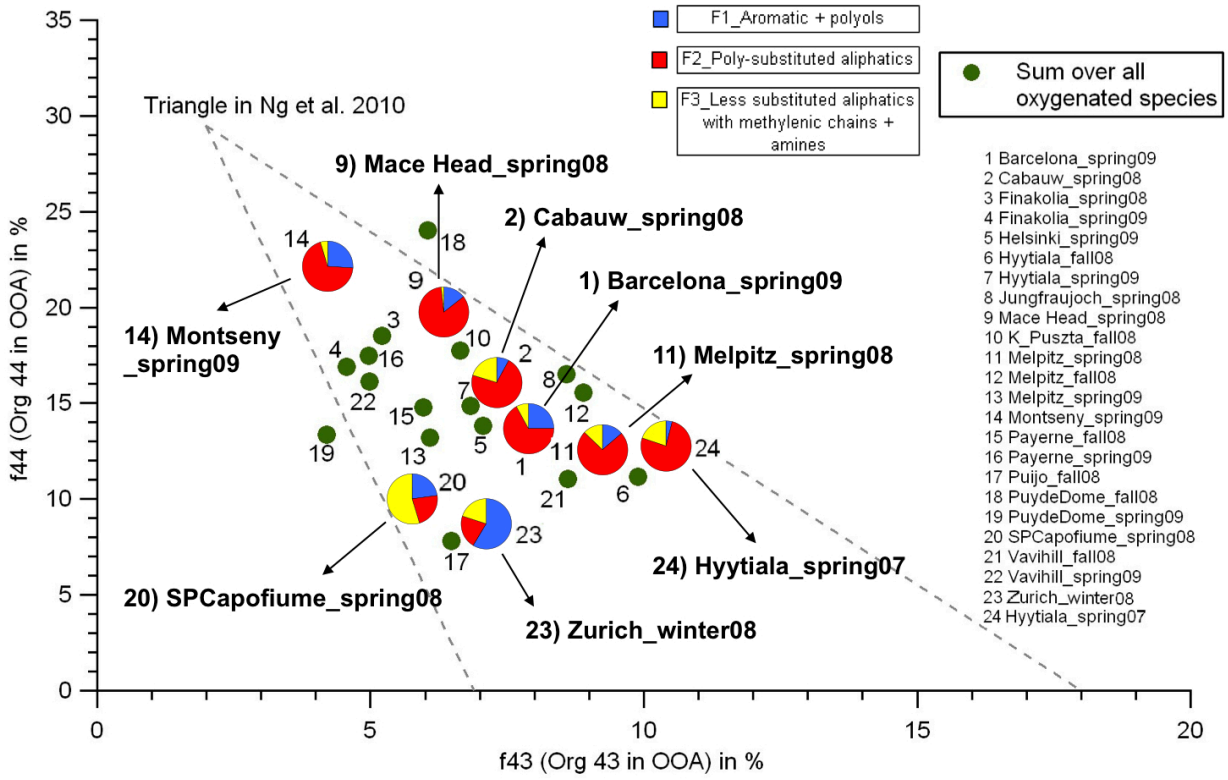


**Figure 5.14**: representation of comparison between NMR and AMS data for EUCAARI campaigns: background green points show the f44 vs. f43 position in the Ng triangular diagram calculated by AMS measurements at the different locations of EUCAARI project listed in the right part of the graph. Superimposed pie charts instead represent the average distributions of the 3 main NMR factors for Water Soluble Organic fraction for the whole EUCAARI dataset referred to the nine parallel campaigns.

Background green points in the figure 5.14 show the f44 vs. f43 position in the Ng triangular diagram calculated by AMS measurements at the various locations of the EUCAARI experiments. Superimposed pie charts report the average distributions of the 3 main NMR factors for WSOC for the whole EUCAARI dataset analyzed in this study.

In summary, the position within the triangle depends on the AMS f44 vs. f43 measurements for each individual campaign, while pie charts provide the chemical composition derived from the NMR factor analysis for the same experiments.

There is a strike difference between the NMR compositions at the lower left corner of the diagram, where NMR analysis shows large amounts of either Factor 1 (fresh Biomass Burning POA) or Factor 3 (poorly functionalized aliphatics and amines) and those at the top of the triangle, dominated by the "HULIS" NMR Factor 2. The increase of HULIS concomitant to high f44 in the AMS measurements is in agreement with the hypothesis that HULIS form prevalently along with the atmospheric oxidation and ageing of the aerosol. The poorly functionalized aliphatics (NMR Factor 3) occur in variable amounts at the base of the triangle and completely disappear at the top, providing further confirmation that oxidation reactions highlighted by AMS trigger the main compositional changes of SOA in the atmosphere.

On the other hand, the NMR Factor 2 (very functionalized aliphatics) is found in great proportions also at sites characterized by only moderate f44 and by elevated f43 values. In particular it is surprising that F2 is the main constituent in environments characterized by fresh emissions (like Hyytiälä).

There are mainly three possible reasons for these discrepancies:

1. this could be a consequence of the inability of NMR analysis to directly distinguish between carbonyl and carboxyl substitutions;
2. otherwise a portion of the SV-OOA could be in the water-insoluble fraction (not accounted for in this NMR analysis) ;
3. the backbones of the WSOC compounds, to which NMR analysis is most sensitive, is formed at early stages of chemical ageing in some environments (including the boreal and central European forests): the formation of complex branched, cyclic and substituted aliphatic compounds, which characterize HULIS, can be favored if the precursors are already cyclic and branched (like monoterpenes) compared to compounds having a linear structure (like n-alkanes). In other words, the chemical composition of precursors can impact the direction and rate of chemical ageing. Also these data seem to suggest that functionalization degree and oxidation state does not proceed at the same pace during "ageing".

## 5.6 Conclusion

Factor analysis applied to sets of NMR spectra and interpreted on the basis of a library of reference spectra can be a valuable tool for the identification of common chemical classes of Water Soluble Organic Aerosol in the continental boundary layer.

Most common types of NMR factors reflect the contributions of biomass burning POA, "HULIS-like" polysubstituted aliphatic compounds, and less substituted aliphatic SOA, comprising low molecular weight alkyl amines and biogenic SOA from terpenes.

When comparing the NMR factors to the AMS types taking the whole EUCAARI dataset, the picture appears complex: the change in NMR factor distribution doe not fully follow the prevalent AMS direction for chemical ageing triggered by the increase of oxidation state.

It is possible that functionalization degree and oxidation state does not proceed at the same pace during "ageing" and that effect of the original chemical structure of precursors is more important than the AMS measurements indicate.

With the exception of biomass burning, the 3-factor representation is unsuitable for source apportionment applications and clearly more than three factors are needed to really capture the sources contributing to the European background concentrations of WSOC.

The comparison with AMS functional groups distribution is complicated by the fact that non-negligible amounts of water-*insoluble* OOA are frequently observed in many environments and eluded NMR characterization. The nature of such "oxygenated WIOC" deserves further investigations.

Next chapters report more investigations on single EUCAARI campaigns in which NMR and AMS factor analysis results have been compared at a more quantitative level for identification and quantification of specific OA sources.

# 6 - Determination of the biogenic secondary organic aerosol fraction in the boreal forest by NMR spectroscopy

## 6.1 Introduction to the boreal forest experiment

The present chapter deals with the determination of the biogenic fraction of organic submicrometer aerosol during the intensive EUCAARI field study held in spring 2007 in Hyytiälä (Finland), employing $^{1}$H-NMR and AMS methods. The NMR analysis complements the AMS characterization by providing information on the functionalities which are not well speciated by the AMS. On the other hand, AMS permits OA to be analyzed at a higher time resolution. For the attribution of spectral fingerprints to natural and anthropogenic sources, we employed data acquired during reaction chamber experiments performed in the SAPHIR facility, Jülich (SAPHIR Simulation of Atmospheric PHotochemistry In a large Reaction Chamber, Karl et al., 2004; Bohn et al., 2005; Rohrer et al., 2005; Wegener et al., 2007; Apel et al.,2008; Ehn et al., 2012). The results of this field campaign have been published by Finessi et al. (2012) and the contribution I gave during my thesis work was to develop and apply the statistical methods of factor analysis to the NMR spectra for organic source apportionment.

## 6.2 Aerosol sampling and analysis

Submicrometer aerosol particles were sampled during a one-month campaign in spring 2007 at the Finnish Station for Measuring Forest Ecosystem-Atmosphere Relations (SMEAR II, Hari and Kulmala, 2005; http://www.atm.helsinki.fi/SMEAR/) located in Hyytiälä (61° 51' N, 24° 17' E, 181 ma.s.l.) and already described in Chapter 4. Measurements were carried out from 27 March to 17 May 2007. However, the following discussion focuses on the collection period of PM1 filter samples analyzed by $^{1}$H-NMR spectroscopy, i.e. the days from 29 March to 19 April.

Atmospheric particles were sampled by a suite of co-located online instruments throughout the campaign. Real-time measurements of the concentrations of non-refractory PM1 aerosol organic matter and inorganic ions including sulphate, nitrate, ammonium and chloride were performed by an Aerodyne Quadrupole Aerosol Mass Spectrometer (Q-AMS). A high volume sampler (HiVol) working at 850 l min$^{-1}$ and configured to remove particles with aerodynamic diameter larger than 1 μm was employed from 29 March to 19 April to collect fine particles on quartz-fiber filters (12 cm diameter, QMA grade). The quartz-fiber filters were subjected to the general procedure of extraction, filtration and off-line chemical analysis already described in Chapter 4 and so data on

TC, WSOC, WINC and main ions content in samples were provided. Aliquots of the water extracts were dried under vacuum and re-dissolved in deuterium oxide ($D_2O$) for functional group characterization by proton-Nuclear Magnetic Resonance ($^1$H-NMR) spectroscopy (see Chapter 4).
Prior to factor analysis, the original resolution of the NMR spectra was decreased by binning over 0.03 ppm and 0.01 ppm intervals, that provided matrices of 400 and 200 points, respectively. The resulting spectral datasets were processed using three of the five different factor analysis algorithms better described in Chapters 4 and 5, namely: (1) the PMF 3.0v software using the multilinear engine algorithm provided by US Environmental Protection Agency; (2) the non-negative matrix factorization (N-NMF) software with projected gradient bound-constrained optimization (Lin et al., 2007) (hereafter "Gradient"); and (3) the multivariate curve resolution-alternating least squares (MCR-ALS) software (Tauler et al., 1995). An uncertainty matrix was derived from the noise of the NMR spectra using the DLx2 approach for performing the PMF analysis. Moreover, due to constrains to the number of variables in the PMF, this algorithm could be applied only to low-resolution spectra, 200 points, while Gradient and MCR-ALS were employed for the factorization of both 200 and 400 points spectra.

## 6.3. Concentrations of main submicrometer aerosol components

Between 29 March and 19 April, the air concentrations of the major aerosol species experienced large variations (Figure 6.1). In order to evaluate the impact of air mass transport on aerosol concentration time trends, the NOAA HYSPLIT model (Hybrid Single-Particle Lagrangian Integrated Trajectory, http://ready.arl.noaa.gov/HYSPLIT.php) was used to calculate back-trajectories (BTs) every day from 29 March to 19 April. A plot of the 48 h backward BTs at 500m above ground level and calculated every 4 h, is reported in Figure 6.1.
The analysis of the BTs showed that higher PM1 sea salt levels were registered when the site was influenced by air masses originated from the Norwegian Sea and from the Arctic, while the highest aerosol mass concentrations of sulphate, nitrate, ammonium and organics occurred in concomitance with continental air masses, which is consistent with previous observations at the Hyytiälä station (Allan et al., 2006; Cavalli et al., 2006; Tunved et al., 2006; Raatikainen et al., 2010).
Figure 6.2 summarizes the chemical composition patterns averaged over periods corresponding to the main BTs typologies observed, i.e.: marine/Arctic (m/A), continental/modified marine (C/mm), continental from the West-to-NorthWest sector (C(W–NW)) and continental from the South-to-SouthWest sector (C(S–SW)).

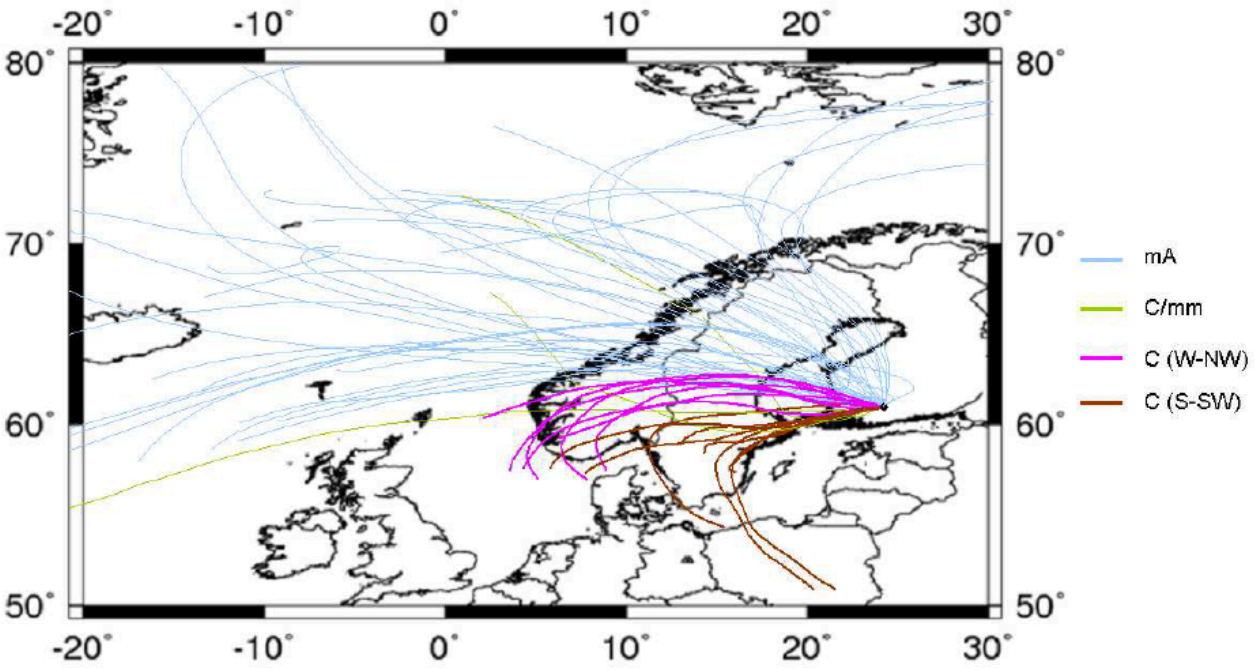


**Figure 6.1**: Back-trajectory plots (48 h backward, 500m AGL height) obtained by running the HYSPLIT model every four hours from 28 March to 21 April. Colours are used for distinct air masses typologies: marine/Arctic (mA), Continental/modified marine (C/mm), Continental from the W–NW sector and Continental from the S–SW sector.

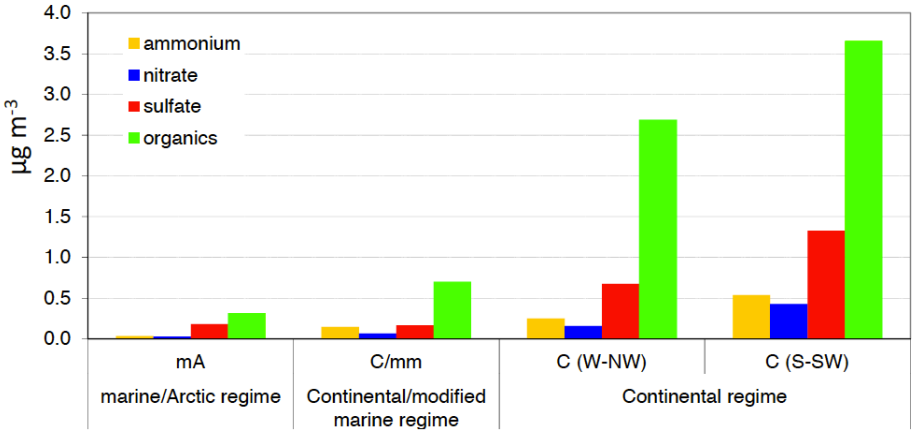


**Figure 6.2**: PM1 chemical composition (Q-AMS) averaged within the four distinct periods of Figure 6.2.

The PM1 mass concentration were derived from total carbon (TC) and water-soluble organic carbon (WSOC) analysis of the filter samples and assuming carbon-to-mass ratios of 1.4 and 1.8 for insoluble and soluble organic fractions, respectively., Total carbonaceous mass concentrations spanned from less than 1 up to 8.5 µgCm−3 (Figure 6.3, upper panel). The sampled carbonaceous mass was primarily constituted by polar, oxygenated compounds, while the water-soluble organics fraction (WSOC) being generally high, accounted on average for more than 70% of the total carbon. The Q-AMS organic concentrations, averaged over the filter sampling times, are also reported in Figure 6.3 for comparison, showing a general good correlation (R = 0.93), although during the first

polluted period and the period characterized by maritime air masses the AMS organic aerosol concentrations appear significantly underestimated compared to carbonaceous aerosol concentrations determined on PM1 filters. A more quantitative comparison will be discussed later, but the reasons for such discrepancies must be attributed to the imperfect coverage of the first period characterized by continental air masses by AMS observations, and to positive artefacts on the filters on background days (see discussion below).

The functional group distributions of the NMR-detected WSOC are also reported in the lower panel of Figure 6.3. The H/C ratios introduced in Chapter 2 were used to convert the concentrations of organic non-exchangeable hydrogen atoms into organic carbon concentrations. In addition to the main usual functional groups (i.e., "alkyls" (HC-C<, oxygen-containing aliphatic groups (HCC=O), "hydroxyls" (HC-O) and "aromatics" (H-Ar)), nitrogen- and sulfur-containing groups, such as "amines" (HC-N), and sulfonic groups (H-C-$SO_3$, such as methanesulfonic acid, "MSA", were detected.

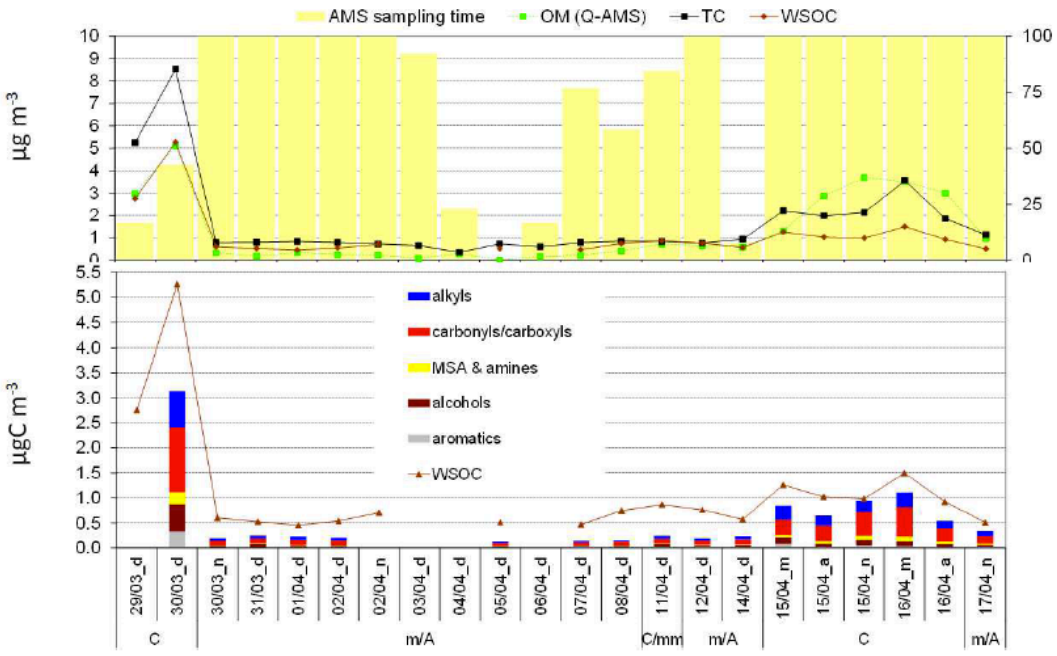


**Figure 6.3**: Upper panel, PM1 filter samples carbonaceous mass concentrations expressed as total carbonaceous (black), water-soluble organics in (dark brown) in µg $Cm^{-3}$. Q-AMS organics conc. (µg$m^{-3}$) averaged upon filter sampling times are shown in green. The coverage of filter sampling times by AMS (percentage) is reported by yellow bars. Lower panel shows functional groups distribution of the NMR-detected WSOC.

On average, the WSOC fraction comprising NMR-detectable organic carbon atoms was 50%. The missing carbon could be due to: (a) the presence of carbons not carrying protons, as in compounds containing highly branched chains or fully substituted aryls (Moretti et al., 2008), and (b) a fraction of WSOC constituted by semi-volatile organics and VOCs adsorbed on quartz-fiber filters that may be lost during the evaporation step prior to the NMR measurement.

## 6.4 Source apportionment by NMR factor analysis

A total of seventeen $^{1}$H-NMR spectra at 200 points resolution were subjected to the factorization models mentioned in the experimental section (PMF, N-NMF-GRA and MCRALS) and the solutions resulting from factors 2 up to 8 were explored. Within all the models, most of the variance turned out to be explained by a limited number of factors, the residual of the order of the baseline noise being for more than 3 factors. The largest drop in the Q/Qexp ratios was registered between two and three factors, but additional factors continued to reduce Q/Qexp toward 1 until no strong change in slope was observable for more than five factors. Beyond five factors, two or more factors were found to be strongly correlated, suggesting that the measurements were not adequate to differentiate additional independent factors. In the following discussion, the analysis is limited to the most simple and conservative solutions with three and four factors.

Profiles and loadings resulting for 3- and 4-factor solutions are shown in Figures 6.4 and 6.5. Only profiles from a single model (MCR-ALS) are reported for sake of clarity. Concerning the factor loadings, the values obtained by the three models were generally convergent, particularly in the three factor case (Figure 6.5a). Conversely, the 4-factor case appears more affected by a certain degree of rotational ambiguity of the models in splitting the F3 and F4 factors, especially for samples collected on 15 and 16 April (Figure 6.5b), with better results obtained with higher resolution, 400 points (not shown).

The isolated NMR factors are described as follows.

- **F1**: the first factor (hereinafter referred to as **"glycols" factor**) is characterized by compounds with hydroxyl (or ether) linkages and n-butyl chains, showing a spectrum similar to commercial butyl-glycols. Indeed, the observed signals show a good fit with the H-NMR spectra of ethylene glycol butyl ether and of 2-butoxyethyl acetate (Sigma-Aldrich online NMR library). Such factor contributed randomly to the set of samples (Figure 6.5) but was completely absent in blank samples, thus excluding any filter contaminations prior/post sampling. Nonetheless positive artifacts or accidental contaminations during the sampling cannot be definitely ruled out. In fact, glycol ethers are chemicals commonly used in paints and ethylene glycol butyl ether (butoxy ethanol) was identified among other VOCs of toxicological interest in urban areas (Gallego et al., 2009). If not laboratory contaminants, they may have originated from a local source at the sampling site or nearby. Their volatility is high (> 10−1 Torr), being in the VOC regime, hence if they were atmospheric costituents in Hyytiälä, they were most probably sampled as adsorption artifacts on the quartz-fiber filters.
- **F2**: the second factor (hereinafter referred to as **"HULIS-containing" factor**) has spectral features similar to those characterizing samples collected in sites impacted by anthropogenic

emissions (Figure 6.6a), and already reported in literature (Decesari et al., 2000, 2007). In terms of functional group distribution, polluted samples typically show a more pronounced band of aromatics (visible in the range between 6.5–8.5 ppm) with respect to samples collected in remote locations. Besides this feature, the HULIS-containing factor's profile retains signals of levoglucosan (visible in the spectral interval between 3.5–4.5 ppm), a well known atmospheric tracer for biomass combustion emissions. As shown in Figure 6.5, the "HULIS-containing" factor accounted for most of the signal in the 30 March sample, C(S–SW) regime, and to a much lesser extent, it contributed to the less polluted samples collected in the final part of the campaign, C(W–NW).

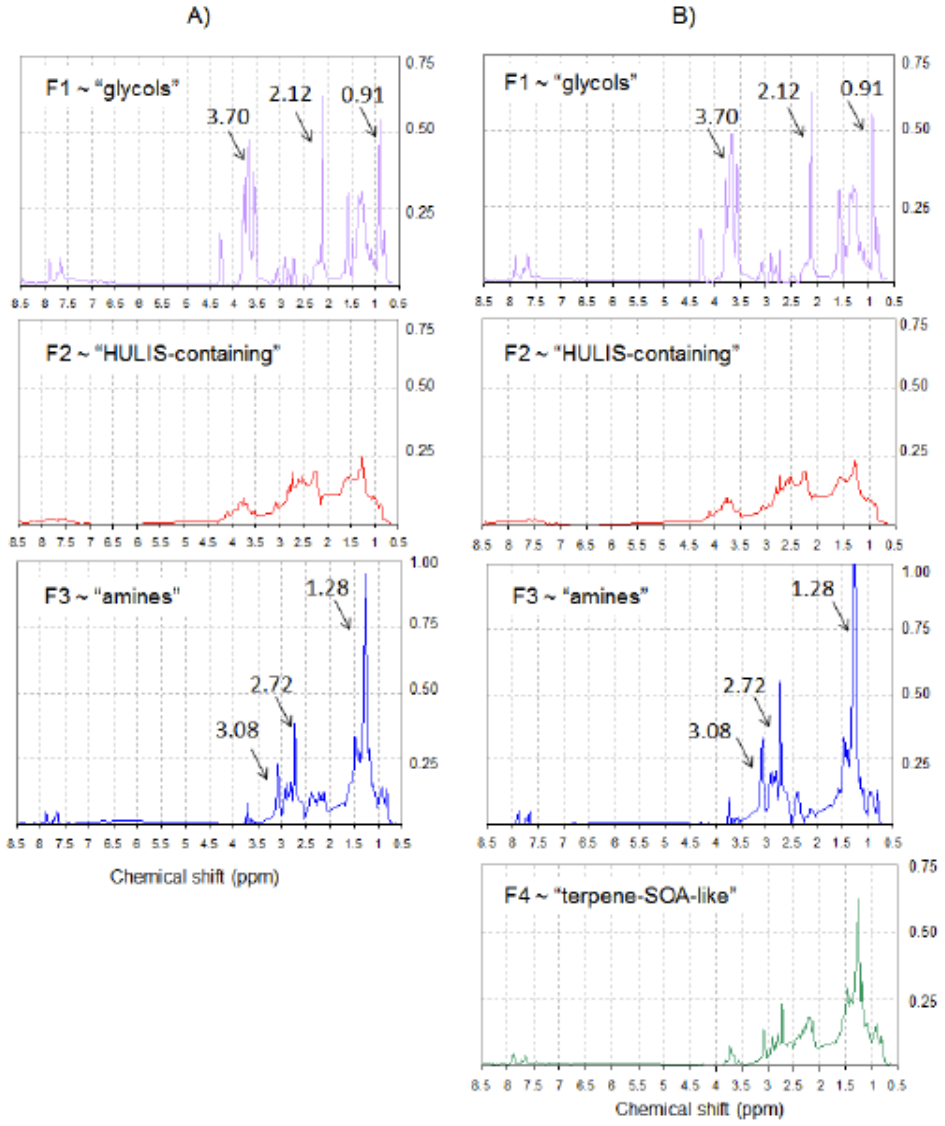


**Figure 6.4**: NMR-factor profiles isolated by applying the MCR-ALS model with a 3-factor solution (a), and a 4-factor solution (b). All factor profiles are vertically normalized to 1 and are plotted versus the NMR chemical shifts.

The concentrations for this factor were positively correlated (R = 0.99) with those of potassium ion measured by ion chromatography, pointing again to combustion sources. This is in agreement with recent results from satellite based data coupling aerosol and fires, which assess wildfires in Eastern Europe with significant impacts on the fine aerosol load even in the Scandinavian region, particularly in April (Barnaba et al., 2011). Levoglucosan was actually quantifiable in the NMR spectra of the 30/3 day and 15/4 night filter samples, and in these samples the levoglucosan-C accounted for 1.9% and 0.7% of WSOC.

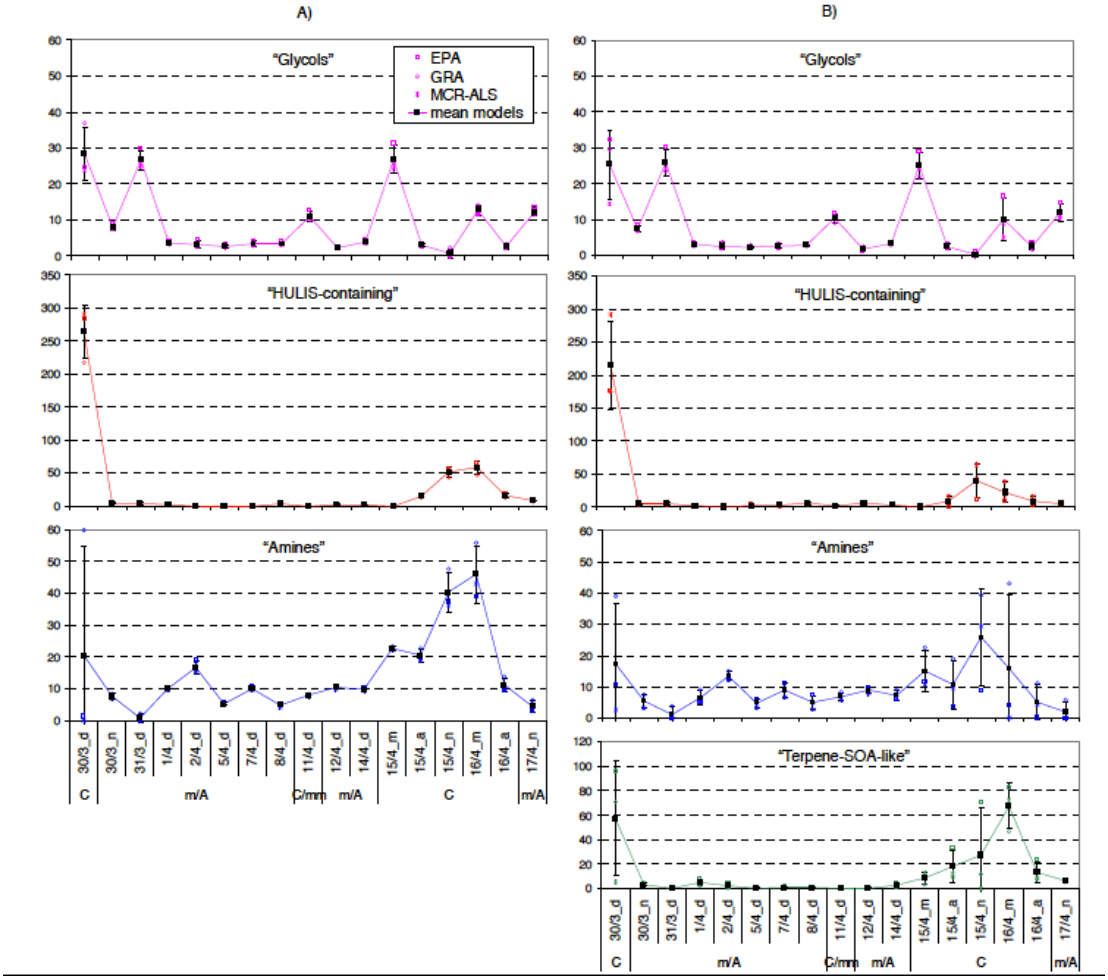


**Figure 6.5**: NMR-factor loadings generated by the models applied to the low-resolution matrix with 3-factor solution (a) and 4-factor solution (b). Within each factor, distinctive coloured symbols are used for different models while the black squared symbols represent mean values with vertical bar as standard deviations. Loadings are expressed as absolute values in nmolHm$^{-3}$.

The estimated contributions of biomass smoke to OC obtained by multiplying the levoglucosan concentrations by 7.35 as recommended by Fine et al. (2002) were 1.64 and 0.11 μgm$^{-3}$ for the Hyytiälä samples of 30/3 day and 15/4 night. Such concentrations are relevant in absolute terms (Puxbaum et al., 2007), but they accounted for about 20% and only < 10% of OM concentrations estimated for the two days of the experiment. They were also lower than the WSOM fractions

apportioned to anthropogenic combustion sources by NMR ("HULIS-containing" compounds). In summary, levoglucosan data show that biomass burning was significant source of particulate organic matter in Hyytiälä during the periods characterized by continental air masses, although such products did not account for the total WSOC fraction which was put in relation to anthropogenic sources by the NMR analysis. The anthropogenically-influenced WSOC, or "HULIS-containing" factor, must be considered rather a mix of long-range transported pollution and wood burning products.

- **F3**: the third factor (hereinafter referred to as **"amines" factor**) included intense peaks attributable to lowmolecular weight alkyl amines, i.e. diethyl and dimethyl amines (DEA, DMA), and to methane-sulphonic acid (MSA), overlapping a broad background band in the aliphatic region (0.5–4.5 ppm). Such compounds (MSA and di-alkyl amines) have previously been found by the authors in clean marine OA (Figure 6.6b) (Facchini et al., 2008; Decesari et al., 2011). Moreover, this factor accounted mainly for the OA composition when concentrations reached very low levels during the background regime (m/A), but it also contributed to the rise of concentrations during the last days of the sampling period, C(W–NW). The air mass origin from the Atlantic during the first two weeks of April, together with the presence of MSA and di-alkyl amines, suggest that the "amines" factor can be impacted by biogenic marine sources.
- **F4**: the fourth factor (hereinafter referred to as **"terpene-SOA-like" factor**) is found prevalently in the samples collected between 15 and 17 April, C(W–NW) and also, to a lesser extent, in the 30 March sample (Figure 6.5). Unlike the "HULIS-containing" factor profile, aromatic protons (H-Ar) are scarcely visible in the "terpene-SOA-like" factor, except for two weak peaks, also present in the "glycols" and "amines" profiles, which may be due to defective splitting. Besides this, main distinguishing features of this factor is the presence of single peaks overlapping the background signal in the region between 0.7–1.8 ppm which comprises un-functionalized alkyls (HC-C), e.g. methyl or methylene groups. Again, aliphatic alcohols and ethers/esters (HC-O) also contribute to characterizing the profile of such "terrestrial biogenic" factor in the range of chemical shifts between 3.3–4.5 ppm. By comparing the spectral profile of F4 with reference $^{1}$H-NMR spectra of ambient and laboratory-generated water-soluble aerosols, the best match was found with the BSOA produced in the SAPHIR simulation chamber during photo-oxidation and ozonolysis of terpene mixtures, including: α/β-pinene, limonene, $\Delta^{3}$-carene, ocimene, β-caryophyllene and α-farnesene.

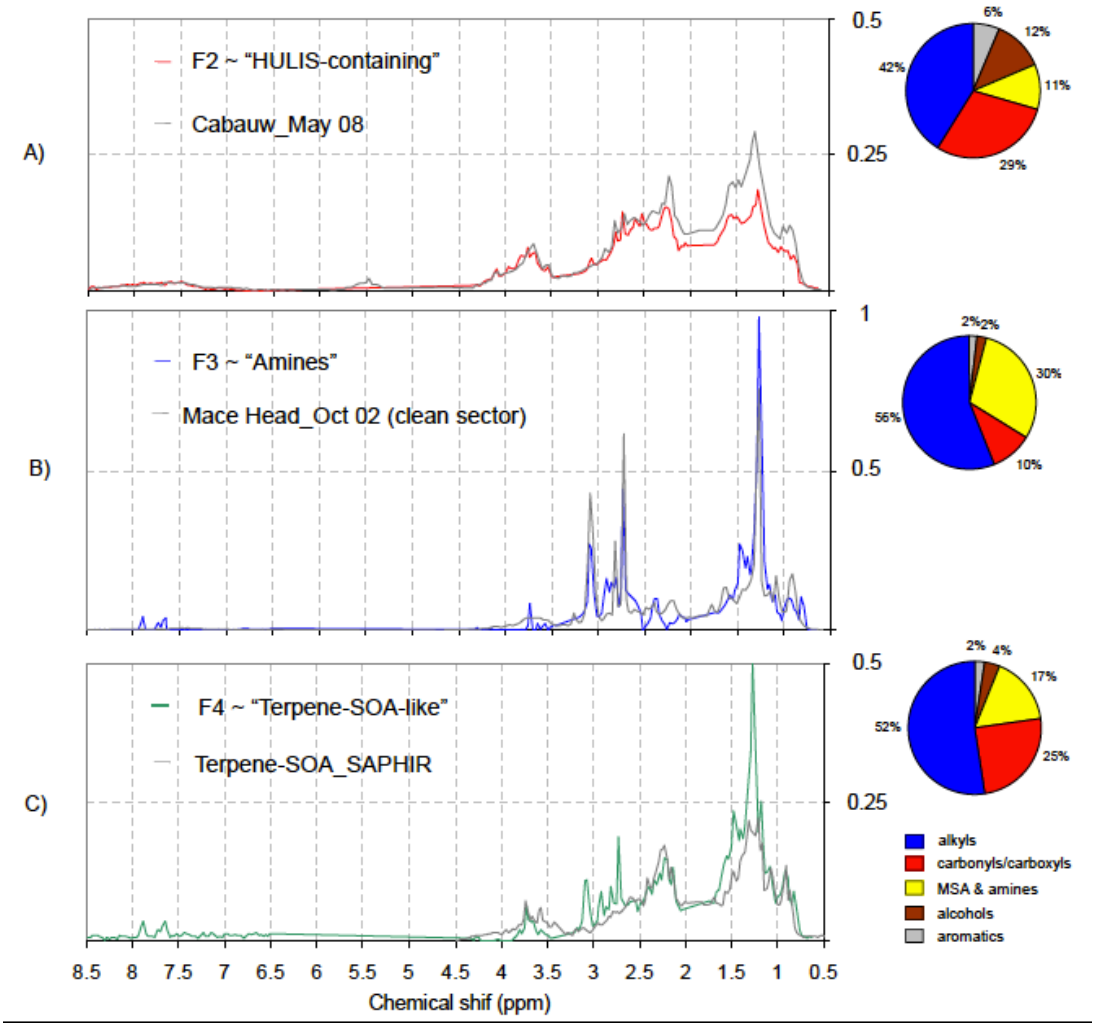


**Figure 6.6**: NMR-factors profiles (MCR-ALS) emerging from the Hyytiälä dataset (coloured lines) overlapped with reference spectra (grey lines). The comparison includes spectral signatures obtained in other field (a), (b) and chamber (c) campaigns. The functional groups patterns (%) corresponding to each factor are reported on the left.

The employ of available libraries of H-NMR spectra of reference compounds and materials (SOA) allows therefore a precise attribution of the NMR factors to WSOC source contributions. It should be noted, however, that, contrary to the "terpene-SOA" factor for which we can compare with spectra obtained in controlled laboratory conditions, our interpretation of the "HULIS-containing" factor is based on the similarities with ambient samples collected in polluted areas, however we do not know how much these fingerprints are specific for the anthropogenic sources, which certainly contributed but we do not know the extent. The same polluted conditions may have lead to the accumulation of more, and more oxidized biogenic SOA. Therefore the HULIS-containing factor should be considered a "maximum anthropogenic WSOC fraction", i.e. an upper limit, rather than exclusively anthropogenic.

## 6.5 Comparison between AMS and NMR in OA source apportionment

PMF-AMS provided two types of oxygenated organic aerosol (OOA) groups, namely OOA1 and OOA2, which were particularly stable within all tested solutions and accounted for most of the organic mass signal in both datasets (Figure 6.7).

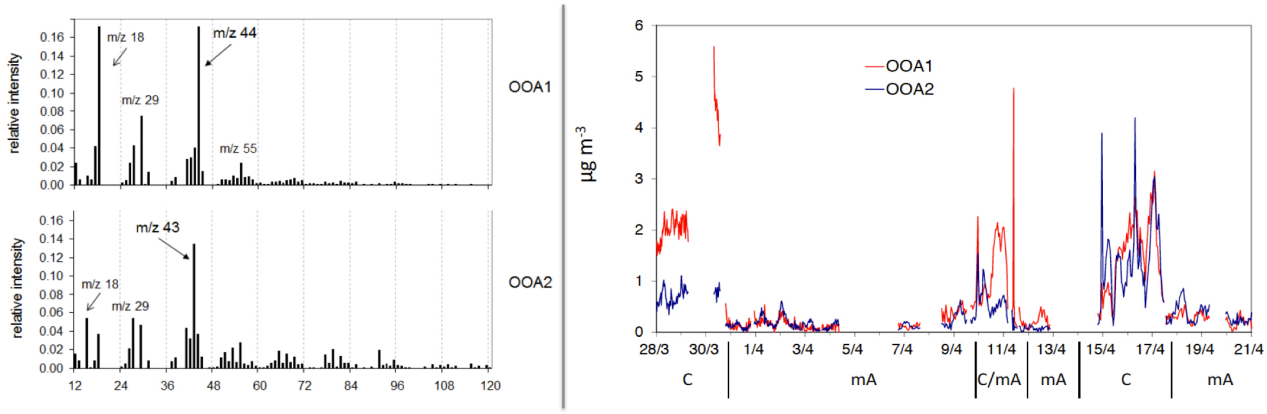


**Figure 6.7**: OOA1 and OOA2 mass spectra (Q-AMS), on the left, and time series, on the right. Labels for the observed distinct BTs regimes are reported under the time x-axis.

The mass spectra of these two OOA components, with the ions at m/z 44 ($CO_2^+$) dominating the OOA type 1 and m/z 43 (mostly $C_2H_3O^+$) dominating the OOA type 2, closely match those most commonly isolated in previous studies (Zhang et al., 2007; Lanz et al., 2007) where the OOA1 represented the more oxidized, aged organic fraction, and the OOA2 represented the less oxidized, fresher secondary organics. Other commonly found organic groups, such as hydrocarbon-like (HOA) and biomass burning organic aerosol (BBOA), were not isolated here.

The major components underlying the oxygenated organic aerosol fraction isolated from NMR data were compared to those apportioned by AMS and averaged upon filter sampling times. It should be noted that no filter samples were collected at night-time during the background period, and therefore the off-line NMR analyses did not account for the nocturnal peaks of OOA2 observed by the AMSs in such conditions.

In order to compare NMR and AMS factor loadings, the concentration metrics used by the two techniques need to be homogenized, in an attempt to retrieve equivalent organic mass concentrations from the organic non-exchangeable hydrogen concentrations provided by $^1$H-NMR analysis. As a first step, water-soluble organic carbon concentrations comprising the NMR factors were derived from hydrogen concentrations by using factor-specific H/WSOC ratios. The latter were extrapolated from WSOC and $^1$H-NMR measurements for spectral datasets representative for source types of the OA of interest to the present study. In particular, H/C molar ratios values of 0.8, 0.9 and 1 were used for the “terpene-SOA-like”, “amines” and “HULIS-containing” NMR-factors,

respectively, on the basis of the analysis of laboratory terpene SOA samples, marine aerosols in clean air masses sampled at the Irish station of Mace Head (Decesari et al., 2011), and of samples of biomass burning aerosols (Tagliavini et al., 2006). The WSOC concentrations estimated using such H/WSOC factors account for fully-substituted carbon atoms, which cannot be directly detected by $^{1}$H-NMR analysis. However, the sum of WSOC concentrations derived for the three factors is still lower than the measured WSOC, primarily because of losses of volatile compounds during sample preparation. Finally, to derive equivalent organic matter concentrations, a constant conversion factor of 1.8 was used to convert WSOC loadings into water-soluble organic mass concentrations ($\mu gm^{-3}$).

Even if the time-integrated filter samples cannot account for the great variability of OA composition observed by the online methods, when averaging the AMS factors over the filter sampling times, the OA composition patterns were comparable to those obtained by off-line measurements. The comparison between the patterns obtained by the AMS and NMR techniques is facilitated when looking at the averaged data over each distinct regime and the entire observing period (Figure 6.8). Two types of oxygenated organic components attributable to more and less oxidized organics, respectively, appeared particularly stable in all tested solutions used for factor analysis. They accounted for most of the detected mass in both methodologies and are attributable to a more and a less oxidized organic fraction. The more oxidized, aged organic fraction, represented by the AMS OOA1 and by the NMR "HULIS-containing" factors, accounted for about 50% of the detected organic mass in both cases, when considering the entire period. This more oxidized fraction shows a mass spectrum dominated by the m/z 44 ($CO_2^+$) peak, and in parallel a NMR spectrum enriched in oxidized functional groups, such as carbonyls/carboxyls and hydroxyls. Additionally, it shows high correlation coefficients with sulphate, ammonium, nitrate and potassium ions, and particularly contributed to the organic mass during the continental regime from the South-to-SouthWest sector. Thus, for all the above reasons, it has been linked to transported pollution, including wood burning products. By contrast, the second major component, is represented by the AMS OOA2 and by the NMR factors related to biogenic OA, and greatly contributed to enhancing the OA mass during the marine/Arctic and C(W–NW) regimes. The fact that only NMR analysis and not AMS highlighted a biomass burning contribution in the first, more oxygenated component can be explained by considering that the Q-AMS operated discontinuously at the beginning of the campaign when continental air masses were most clearly seen, resulting in reduced sampling time coverage (less than 50% for the 30/3 day sample, Figure 6.3, upper panel). It is likely that the Q-AMS did not sample enough biomass burning products to resolve a biomass burning organic aerosol (BBOA) factor.

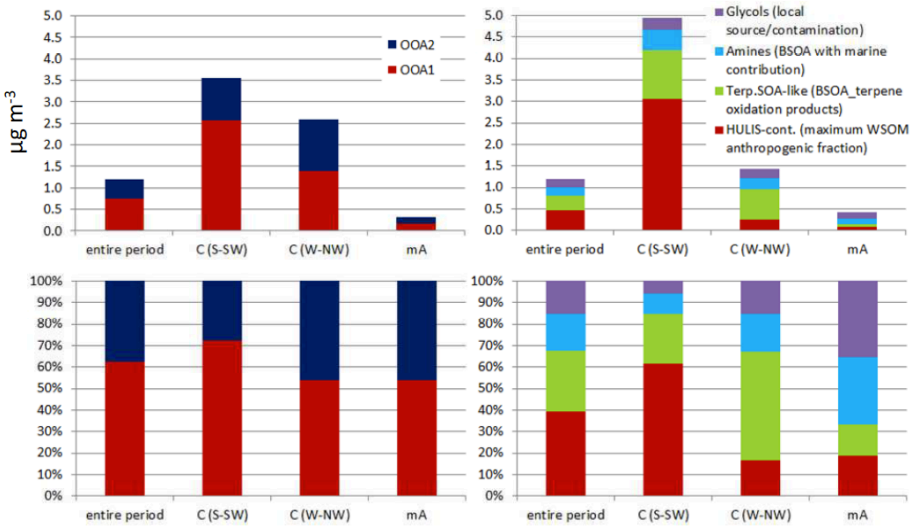


**Figure 6.8**: Percentage and absolute concentrations (μgm$^{-3}$) of the Q-AMS OOAs and filters organic components averaged upon the entire sampling period and each distinct sub-periods.

The NMR factor analysis further isolated two distinct components within the second, less oxidized OA fraction, namely the "amines" and "terpene-SOA-like" factors. Their relative concentrations appeared strongly dependent on the air mass regime. Indeed, when prevalently polar air masses reached the site (m/A regime), the NMR analysis assigned about 50% of WSOC to the "amines" factor. This was based on similarities with spectral signatures of aerosol collected in clean marine environments, including MSA and alkyl amines signals and, therefore could be linked to a biogenic OA source of marine origin. By contrast, the "terpene- SOA-like" factor is related to terrestrial secondary products originating from the gas-to-particle conversion of VOCs emitted by conifer forests, on the basis of similarities with BSOA formed in chamber experiments with monoterpenes plus sesquiterpenes. Overall, a significant fraction of WSOC can be assigned to the terrestrial biogenic factor throughout the whole period (about 30%), indicating a persistent source active in the area around the sampling site. It was also particularly enriched during the C(W–NW) regime, reaching up to 50% of the detected WSOC. The back-trajectories analysis showed that air masses influencing the site during the C(W–NW) period originated mainly from North West, undergoing a marine to continental transition over the Scandinavian forest area. Thus the BSOA enrichment in concomitance to prevailing C(W–NW) is reasonably connected to the longer time spent by the clean air masses over the boreal forest with respect to that spent by the air masses arriving from North. This is consistent with previous investigations at Hyytiälä observing aerosol properties during the marine-to-continental transition (Allan et al., 2006; Cavalli et al., 2006; Tunved et al., 2006; Raatikainen et al., 2010). Since a few short pollution episodes were still detected during this period, a higher particle concentration may be also considered as a possible explanation for the

BSOA enhancement with respect to low concentration periods, e.g. by acting as condensation sink for locally emitted gaseous precursors. However, the same composition patterns are not observed during the C(S–SW) period, when still high particle concentrations were registered but the air masses originated from Central Europe. In summary, the longer time spent over the boreal forest by the air masses reaching the site within C(W–NW) remains the most plausible explanation of the observed BSOA enrichment.

## 6.6 Summary and final remarks

During the boreal forest EUCAARI experiment, air mass origin had a strong impact on organic composition and on the distribution of NMR and AMS factors. Polluted continental air masses were associated with more oxidized organic aerosols (AMS type "OOA1") and NMR-detected water-soluble organic compounds rich of aromatic and polysubstituted aliphatic compounds similar to HULIS. Such OM component, clearly impacted by combustion sources, but including also more aged compounds of probable secondary origin, can be considered as the maximum anthropogenic fraction of OA. A second component, shown to be less oxygenated according to AMS analysis, was strongly enhanced in concomitance with air masses originating from the North to West sector, i.e. from the Atlantic Ocean crossing Scandinavia. In such less polluted conditions, NMR analyses found prevalently biogenic contributions and specifically two distinct factors that were linked to terrestrial and marine biogenic sources on the basis of similarities with spectral fingerprints and back-trajectory analysis.

Overall, such terrestrial and marine biogenic components contributed equally to OA mass (about 30% each) when averaging over the whole observing period, but showed relative abundances strongly depending on the North-to-West air-mass transition. In summary, the findings trace and quantify at least two independent sources originating biogenic secondary organic aerosols in Hyytiälä through oxidation and condensation phenomena: a first source involving products of marine origin, which is more important during low aerosol concentration regimes with predominantly polar air masses, and a second source involving reactions of locally emitted terpenes, which becomes more important with increasing time spent by air masses over the boreal forest.

In this study, we have attempted to illustrate the changes in chemical composition of particulate organic matter between air mass types making explicit links to the estimated biogenic and anthropogenic fractions, as provided by both NMR and AMS. Although there are clear overlaps between NMR and AMS chemical classes, the OA mass budget indicates that a non-negligible fraction of OOA was actually water-insoluble and eluded NMR characterization. The nature of such "oxygenated WIOC" deserves further investigations. The complementary approach exploited here

between independent source apportionment methods has proven to give a more complete and accurate picture of organic aerosol variability, and has provided the opportunity to trace biogenic SOA in the environment.

# 7 - Identification of Humic-Like Substances (HULIS) in oxygenated organic aerosol using NMR and AMS factor analysis and liquid chromatogaphic techniques

## 7.1 Introduction to the Cabauw experiment

This chapter deals with the EUCAARI intensive field campaign geld in the rural area of Cabauw, Netherlands, in springtime 2008. Contrary to Hyytiälä, the Cabauw site is not interested by important local biogenic emissions. For this reason, and because of the persistent high pressure conditions that interested central Europe in May 2008, the station turned to be a good receptor site for characterizing the aerosol chemical composition in polluted background air over continental Europe. In particular, oxygenated organic particles originated upon prolonged oxidation in the atmosphere were sampled and analyzed by both NMR and AMS techniques. In the AMS terminology, such aged organic compounds contribute to the low-volatility oxidized organic aerosol (LV-OOA) (see Chapter 2). It was also hypothesized that LV-OOA account for the *atmospheric humic-like substances* (HULIS). On the other hand, AMS spectra which are obtained by a highly destructive electron impact ionization, cannot differentiate between light and heavy molecular weight compounds. Moreover, solid-phase extraction (SPE) protocols for HULIS associate them to the *more hydrophobic* fraction of water-soluble aerosols (e.g., Varga et al., 2001), conflicting with the AMS results identifying HULIS amongst the *most oxygenated (hydrophilic)* components of aerosol organic matter (Ng et al., 2010). Clearly, the actual link between AMS "HULIS" and SPE HULIS need to be established on a more firm experimental basis. A very first investigation of this issue was carried out in the paper by El Haddad et al. (2012).

My doctoral work contributed to the aerosol experiment in Cabauw by providing the factor analysis of the NMR dataset and by comparing the results with those from PMF-AMS. The original elaboration and interpretation of the overall chemical dataset (including ion chromatographic and organic carbon data) and organic source apportionment data (NMR+AMS) are also original contributions of my work, which are now incorporated in a manuscript in course of submission.

## 7.2 Aerosol sampling and analysis

The measurements were conducted at Cabauw (Netherlands) measurement station (51° 58.223' N - 4° 55.575' E) (see Chapter 4) in the frame of EUCAARI field experiment which took place on May 2008. The evolution of the general aerosol chemical and optical properties during the EUCAARI

May 2008 IOP is discussed by Mensah et al. (2012) and by Aouizerats et al., (2010), respectively. As described in detail in Mensah et al., (2012), an Aerodyne High-Resolution Time-of-Flight Aerosol Mass Spectrometer (AMS) was located in the basement of the CESAR tower and measured submicrometer aerosol for the whole duration of the campaign.

PM1 samples for off-line analysis were sampled on pre-washed and pre-baked quartz-fiber filters (Whatman, 9cm size) using a dichotomous sampler (Universal Air Sampler, model 310, MSP Corporation) at a constant nominal flow of 300 l/min located at ground level, beneath the CESAR tower. A total of thirty samples were collected between 8$^{th}$ and 26$^{th}$ May. Typically, two filters were sampled every day, with "daytime" (D) $PM_1$ samples collected from ~10:00 to ~17:00 (local time, UTC+2), and "evening/night-time" (N) samples collected from ~18:00 to ~09:00. Exceptionally, long-time integrated samples were also taken (three samples, lasting 35, 40 and 60 hours). Samples were stored frozen until chemical analysis. The quartz-fiber filters were subjected to the general procedure of extraction, filtration and off-line chemical analysis already described in Chapter 4 and so data on TC, WSOC and WINC content in samples were provided, as well as concentrations of major inorganic ions ($NH_4^+$, $Na^+$, $K^+$, $Ca^{2+}$, $Mg^{2+}$, $Cl^-$, $NO_3^-$, $SO_4^{2-}$) and some organic acids (e.g., oxalate).

The collection of 25 NMR spectra was processed using factor analysis methodologies already described in Chapters 4 and 5 in order to find contributions and spectral profiles (loadings) of major components of WSOC. The carbon fraction not soluble in water (WINC) was not analyzed by NMR in this study as well as in previous and therefore was not accounted for by this factor analysis. The original NMR spectra were subjected to several pre-processing steps prior to the application of factor analysis in order to remove spurious sources of variability. A polynomial fit was applied to baselines and subtracted from the spectra. Careful horizontal alignment of the spectra was performed using the Tsp-d4 singlet as reference position. Blank signals, corresponding to impurities of quartz filters or $D_2O$ contaminations (at e.g. 1.25, 1.31 and 1.33 ppm), were removed. The spectral regions containing only sparse signals ($\delta H < 0.5$ ppm; $4.7 < \delta H < 5.2$ ppm; and $\delta H > 8.5$ ppm) were omitted from the data set. Binning over 0.030 ppm of chemical shift intervals was applied to remove the effects of peak position variability caused by matrix effects. Low-resolution (200 points) spectra were finally obtained, and were allowed to be processed by factor analysis. All the five non-negative factor analysis methods introduced in Chapters 4 and 5 were used.

## 7.3 Meteorological regimes and air mass origin

Standard meteorological parameters were measured during the campaign. The first half of May 2008 was anomalously warm with $T_{max}$ reaching 25°C and staying above 20°C for more than a

week after the beginning of the experiment on 8th May. Winds were consistently from East and South-Est with only a brief period in the middle of campaign (16th to 21st) characterized by northerly winds, which also brought some rain to the site. During the campaign, the prevalent anticyclonic conditions over Central Europe favored the accumulation of both primary and secondary aerosols in the planetary boundary layer, which can be regarded as a typical case of "regional pollution" (Hamburger et al., 2011).

Air mass origins were examined using the NOAA HYSPLIT model (http://ready.arl.noaa.gov/HYSPLIT.php). Periodization of the field campaign was then carried out according to meteorological regimes and clusters of HYSPLIT backtrajectories (Table 7.1, Figure 7.1).

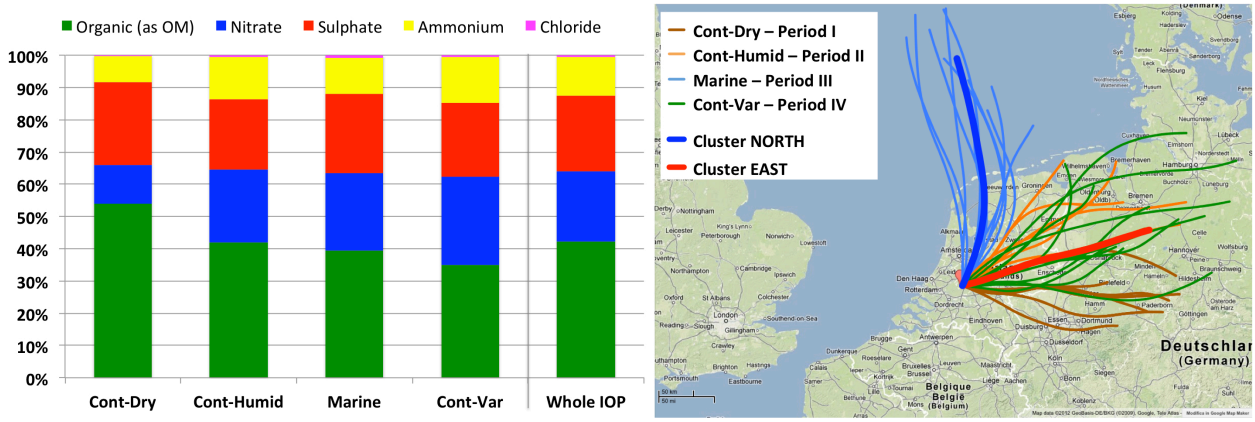


**Figure 7.1**: average PM1-filters chemical composition and back-trajectory analysis for the four periods of the campaign. Organics are reported as total organic matter (OM) calculated by relationship $OM=OC_{PM1filters}*1.6$.

| | Days | Period ID | RH % | wind (m/s) | comments |
|---|---|---|---|---|---|
| **Period I** | May 9th-12th | Cont-Dry | 40.2 | 6.1 | Continental, Windy, Dry |
| **Period II** | May 12th-16th | Cont-Humid | 71.4 | 4.0 | Continental, Calm, Humid |
| **Period III** | May 17th-21st | Marine | 68.9 | 5.8 | Marine, Windy, Humid |
| **Period IV** | May 21st-26th | Cont-Var | 66.0 | 6.6 | Continental, Variable |
| **Whole IOP** | | | 63.2 | 5.5 | |

**Table 7.1**: periods of the campaign with average meteorological conditions

The first period ("Continental-windy&dry", or Cont-Dry), lasting from 9th to 12th, was characterized by general dry and windy conditions and by Eastearly or South-Easterly air masses. Period II (Cont-Humid, standing for "Continental-Calm&Humid"), from 12th to 16th of May, showed calm and humid characteristics (with wind speeds from 1.5 to 5 m/s and a RH mean value of 71%) and a continental air mass origin, similarly to Cont-Dry but with a northerly component (Figure 7.1). The

stable meteorological conditions were interrupted by an outbreak of Atlantic cold air masses between 17th and 21st of May (third period, "Marine") accompanied by strong winds and bringing high humidity and precipitations. During the fourth and last period ("continental-variable", Cont-Var), lasting was from 21st of May to the end of the campaign, an easterly circulation was resumed but with a larger day-to-day variability in temperature and humidity compared to the first half of the campaign.

## 7.4 PM1 chemical composition from filter measurements

Atmospheric concentrations of major aerosol chemical species experienced large variations during the campaign following the changes in air mass origin. Almost the entire campaign was characterized by medium-to-high concentrations (Putaud et al., 2010) of sulphate, nitrate, ammonium, EC, potassium and oxalate (Table 7.2). Clearly, the persistent anticyclonic conditions over Central Europe favored the accumulation of both primary and secondary aerosols in the planetary boundary layer, which can be regarded as a typical case of "regional pollution" (Hamburger et al., 2011). During the third period ("Marine"), the above aerosol species experienced a marked drop in concentration, while sodium, chloride and methanesulphonate (MSA) reached a maximum in terms of relative contributions, indicating that the aerosol particles reaching Cabauw from the ocean were mainly of natural origin rather than originating from transatlantic transport of pollutants. Interestingly, the second period (Cont-Humid), even though characterized by easterly winds, showed high concentrations of marine aerosol together with the continental components, the former possibly coming from the recirculation of marine air masses traveling to Scandinavia, then turning south-west towards the Netherlands along the isobars of an Icelandic high pressure system (Hamburger et al., 2011).

| Periods | TC | OC | WSOC | EC | $NO_3^-$ | $SO_4^{2-}$ | $NH_4^+$ | MSA | Oxalate | $K^+$ | $Cl^-$ |
|---|---|---|---|---|---|---|---|---|---|---|---|
| **Cont-Dry** | 2.75 | 2.26 | 1.88 | 0.43 | 0.82 | 1.71 | 0.55 | 0.06 | 0.17 | 0.03 | 0.02 |
| **Cont-Humid** | 2.54 | 2.08 | 1.44 | 0.47 | 1.78 | 1.73 | 1.03 | 0.18 | 0.14 | 0.03 | 0.05 |
| **Marine** | **1.06** | **0.87** | **0.57** | **0.19** | **0.84** | **0.87** | **0.39** | **0.24** | **0.03** | **0.01** | 0.03 |
| **Cont-Var** | 1.77 | 1.41 | 0.99 | 0.35 | 1.77 | 1.49 | 0.92 | 0.09 | 0.10 | 0.02 | 0.03 |
| **Whole IOP** | 2.05 | 1.67 | 1.22 | 0.37 | 1.38 | 1.48 | 0.76 | 0.14 | 0.11 | 0.02 | 0.03 |

**Table 7.2**: average concentrations (μg/m$^3$) of main chemical species in PM1 filters during the four periods of campaign

PM1 TC concentration spanned from 0.62 to 3.73 μg/m$^3$ (Figure 7.2). Organic carbon (OC) concentrations, ranging from 0.48 and 2.98 μg/m$^3$, represented in average more than 80% of TC.

The water-soluble organics fraction (WSOC) was generally high, accounting for 59% of TC and for 72% of OC on average.

The distribution of the main aerosol components in PM1 was also influenced by air mass history, with greater contribution of organic compounds (54%) during the first continental period (Cont-Dry) and larger shares of ammonium nitrate in the other periods (Figure 7.1).

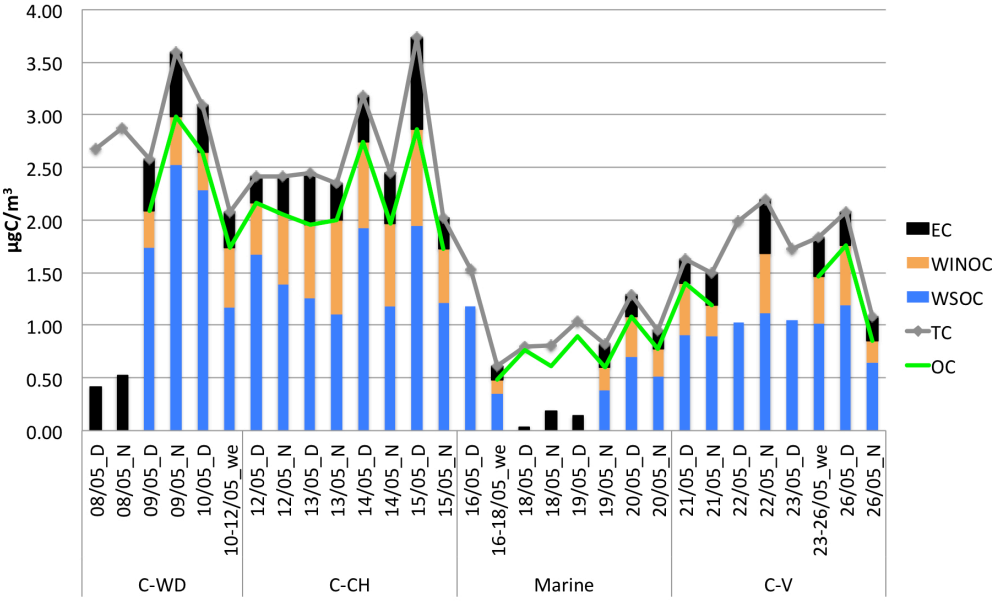


**Figure 7.2**: Carbon classes concentrations from EGA analysis (TC/OC/EC) and TOC analysis for WSOC.

The functional group concentrations measured by H-NMR spectroscopy in WSOC samples are reported in Figure 7.3. Organic hydrogen concentrations were converted to organic carbon with aim of comparison with WSOC and OC concentrations using specific stoichiometric H/C ratios (see Chapter 2, Table 2.1).

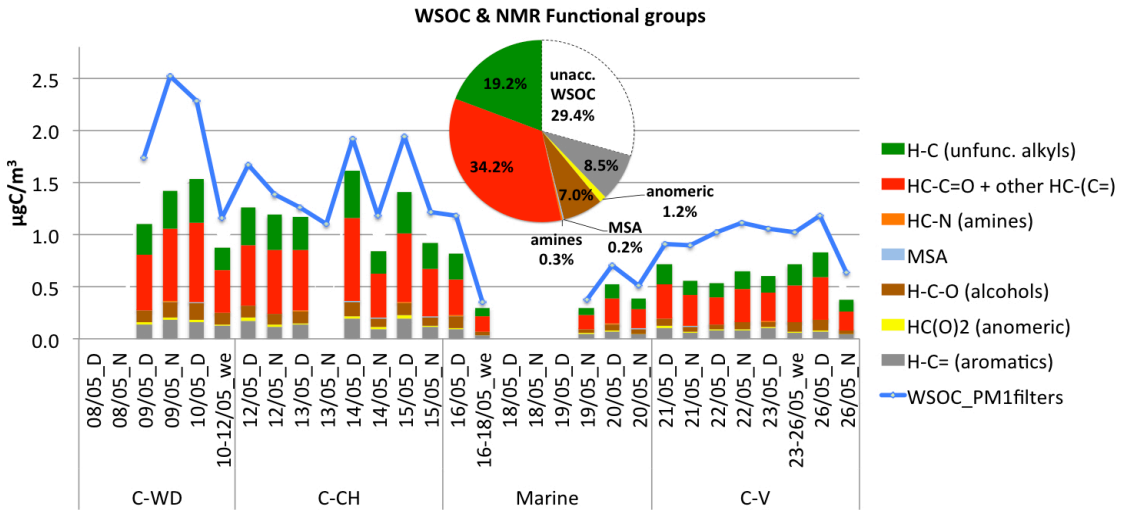


**Figure 7.3**: functional groups composition of PM1 filter samples by H-NMR analysis: pie chart represents average functional group composition for the whole campaign, while histogram their time series.

The average functional group distribution is dominated by aliphatic compounds unsubstituted or substituted by carbonyls or carboxyls, while the hydroxyl and aromatic moieties are of lesser importance. Such composition indicates that fresh biomass burning compounds did not contributed significantly to WSOC, while secondary sources are more likely (Decesari et al., 2007).

Although the sum of NMR functional group concentrations approached total WSOC in many samples, the uncharacterized fraction was significant and averaged ca. 29%. Possible reasons for the "missing carbon" are: 1) the presence of carbon atoms not attached to protons, thus invisible to H-NMR, such as oxalates and compounds containing substituted quaternary carbon atoms or fully substituted aryls (Moretti et al., 2008), and 2) evaporative losses during the evaporation of the extract prior to the preparation of the NMR tube.

## 7.5 NMR factor analysis for WSOC source apportionment

This section discusses the results of factor analysis carried out with the five algorithms presented in Section 7.2.4 starting from the set of 25 H-NMR spectra at 200-point resolution. Solutions having two up to eight factors were evaluated but, according to all algorithms, most of the variance was explained by a small number of factors. The largest drop in the Q/Qexp ratios was recorded between two and three factors, while additional factors continued to reduce Q/Qexp with a less marked change in slope (Figure 7.4).

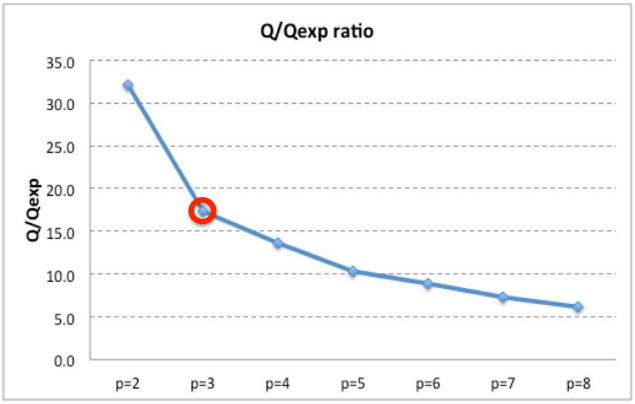


**Figure 7.4**: Q/Qexpected versus the number of factors p. Red circle denotes the chosen solution (p=3).

Starting from the four-factor solution, two or more factors were found to be strongly correlated (e.g. $R_{F3vsF4}$=0.93 as shown in Table 7.3), suggesting that the resolution of the chemical method or of the sampling was not adequate to differentiate additional independent factors.

| p=3 | R | F1 | F2 | F3 |
|---|---|---|---|---|
| | F1 | 1 | | |
| | F2 | 0.64 | 1 | |
| | F3 | 0.62 | 0.82 | 1 |

| p=4 | R | F1 | F2 | F3 | F4 |
|---|---|---|---|---|---|
| | F1 | 1 | | | |
| | F2 | 0.53 | 1 | | |
| | F3 | 0.53 | 0.81 | 1 | |
| | F4 | 0.71 | 0.78 | 0.93 | 1 |

**Table 7.3**: Pearson correlation coefficients (R) between spectral profiles of NMR-factors for p=3 and p=4 solutions. The high correlation between two factors (F3 and F4) in the p=4 solution is highlighted in bright red. Other shades of red indicate different levels of correlation, smaller but still significant.

A full examination of the outcomes of NMR factor analysis is reported in the Supplementary material, while in this section we will focus on the three-factor solution (Figure 7.5):

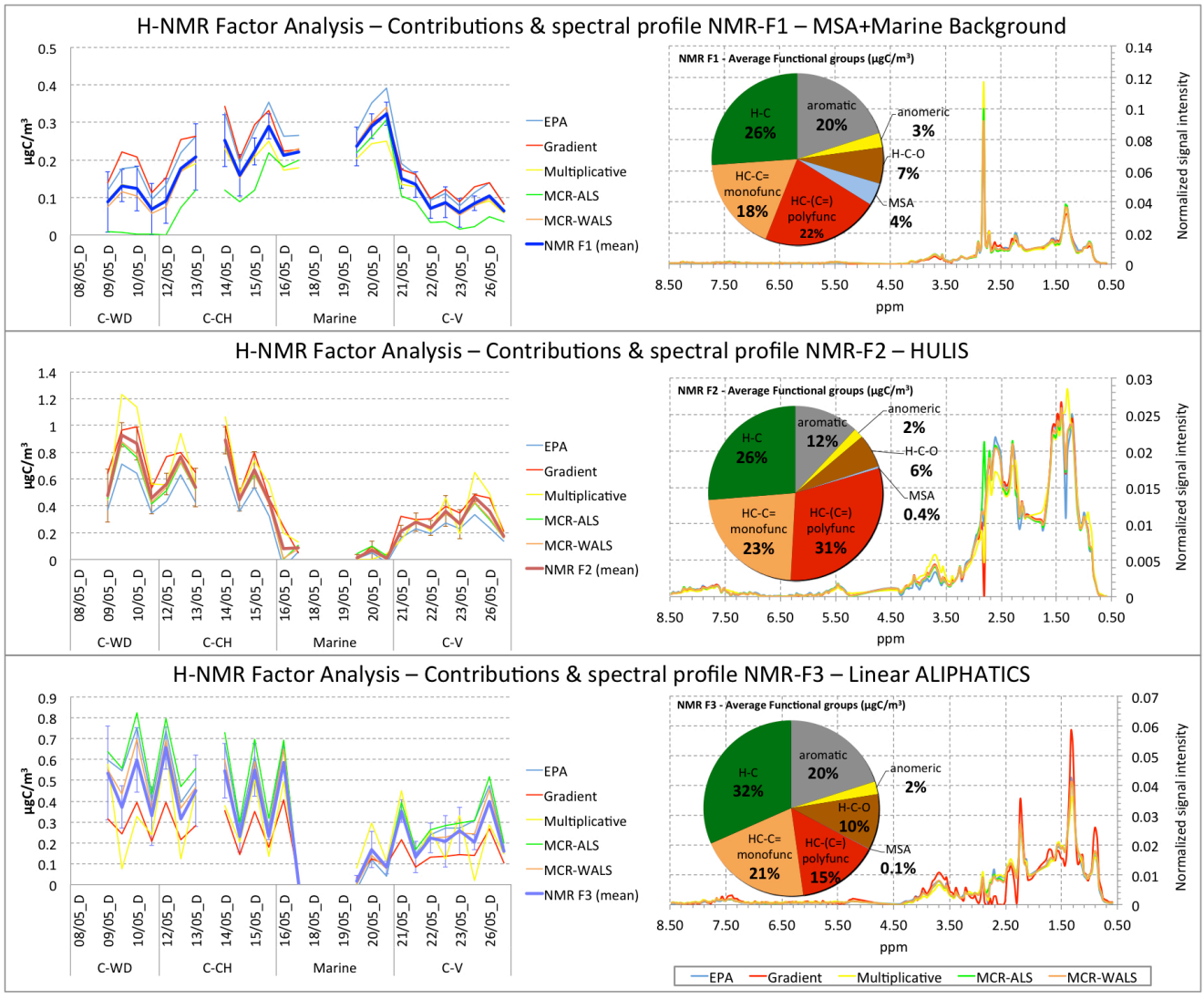


**Figure 7.5**: profiles and contributions of 3-factors solution from H-NMR spectra factor analysis. Results from all 5 different algorithms and the average between them were reported: PMF from EPA free-software (light blue line), Projected Gradient (red line), Multiplicative (yellow line), MCR-ALS (green line) and MCR-WALS (orange line) methods and average value for contribution (thick line in each graph).

1) NMR Factor 1 (F1) "MSA-containing WSOC": the peak of methane-sulphonate (MSA) at 2.81 ppm of chemical shift is most characteristic for this factor. Other spectral features include

aliphatic chains with methylenes and terminal methyls peaks at respectively 1.3 and 0.8 ppm of chemical shift. F1 concentrations ranged from 0.1 to 0.5 μgC/m$^3$, with a maximum during the marine period of the campaign, but relatively high also during the Cont-Humid period. The occurrence of MSA as major tracer compound and the characteristics of concentration time trends assign NMR-F1 to marine WSOC transported directly from the Atlantic to the Netherlands during the "marine" period of the campaigns, or recirculated over the continent in the other periods. It can be considered as a major contributor to the European continental background, becoming prominent in the days of northerly flow, as predicted by state-of-the-art CTMs (Athanasopoulou et al., ACPD 2012).

2) NMR Factor 2 (F2) "NMR-HULIS": its spectral characteristics are attributable to branched/cyclic and polysubstituted aliphatic compounds. Aliphatic chains with terminal methyls are almost absent and also the hydroxyl groups account for a very small fraction (6%) of the detected WSOC. Conversely, the aliphatic groups substituted with C=C and C=O groups (between 1.8 and 3.2 ppm) represent on average 54% of the total functionalities on a carbon basis. Such spectral features were already reported for WSOC in environments impacted by continental anthropogenic emissions (Decesari et al., 2000, 2007, 2011; Finessi et al., 2012). Most interestingly, they overlap well with the H-NMR spectrum of Suwannee river fulvic acid (Figure 7.5bis). Such "HULIS factor" accounted for the 29% of TC and 48% of WSOC and its concentration was highest during periods of continental (easterly) air masses. NMR-HULIS showed the stronger correlation with sulphate (as shown in Table 7.4) suggesting that this WSOC fraction originated from secondary continental sources at the regional scale. Since the weather regimes during the campaign were characterized by prolonged high-pressure conditions over central and northern Europe, secondary processes of SOA formation occurred prevalently in a relatively dry, cloud-free atmosphere.

3) NMR Factor 3 (F3) "Linear Aliphatics": factor characterized by compounds rich in linear aliphatic chains (peaks at 0.9 and 1.3 ppm) and less substituted compared to NMR-HULIS. Linear aliphatic compound concentrations varied from 0.1 to 1 μgC/m$^3$ with highest values in periods of continental air masses. Differently from the case of NMR-HULIS, the linear aliphatic concentrations showed a maximum in daytime samples. This factor shows moderately positive correlations with tracers of primary sources, like EC, and also with aliphatic amines (as shown in Table 7.4), especially with trimethylamine (TMA), which originates from agricultural practices. The contribution of Linear Aliphatics to WSOC seems to be linked to emissions in anthropogenic environments (heavily urbanizes or agriculturally exploited) and may correspond to a "fresher" type of SOA with respect to NMR-HULIS, and for which a positive correlation

with primary emissions originates from the effect of transport combined with short formation timescales (Russell et al., 2009).

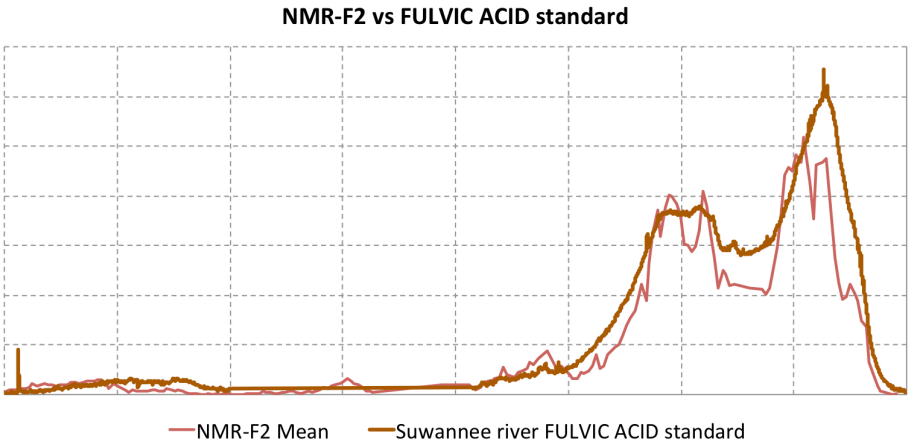


**Figure 7.5bis**: Spectral profile of NMR factor 2 compared with the spectrum of Suwannee River fulvic acid standard.

| | TC PMfilters | WSOC PM1filters | EC PM1filters | OC PM1Filters | TMA | Ammine | $NO_3$ PM1filters | $SO_4$ PM1filters | HPLC_PA |
|---|---|---|---|---|---|---|---|---|---|
| **NMR F1 (mean)** | -0.16 | -0.19 | -0.15 | -0.19 | 0.09 | 0.18 | 0.00 | -0.32 | -0.38 |
| **NMR F2 (mean)** | 0.91 | 0.90 | 0.68 | 0.94 | 0.20 | 0.35 | 0.01 | 0.62 | 0.73 |
| **NMR F3 (mean)** | 0.73 | 0.79 | 0.55 | 0.84 | 0.46 | 0.43 | -0.22 | 0.56 | 0.69 |

**Table 7.4**: correlations between NMR-Factors and chemical data from PM1 filters: white boxes indicate a lack of positive correlation between the variables; the various shades of red instead indicate different levels of correlation: from bright red to light orange (or salmon) for R>0.9 to R>0.5 respectively.

In conclusion, NMR factor analysis was able to apportion WSOC to three components, one marine and two showing continental sources. Moreover, the first two ("MSA-containing" and "HULIS") correlate with tracers of secondary aerosol, respectively MSA and sulphate, while the third one ("Linear aliphatics") showed a moderate correlation with anthropogenic primary and secondary tracers which point to processed POA or SOA with a less aged character respect to the HULIS.

## 7.6 Comparison between NMR and AMS factors for oxygenated organic aerosols

The results of the AMS-PMF analysis are shown in Figure 7.6. A 4-factor solution was chosen for this dataset and the according normalized mass spectra for each factor (F1 to F4) are shown on the left side of the figure. A whole range of mass spectra obtained during laboratory, chamber, or field measurements is presented on the AMS mass spectral database (Ulbrich et al., 2009) and can be used as reference spectra. Given their mass spectrum profiles and their time trends (showed in left and right panels of Figure 7.6 respectively), AMS factors were distinguished in:

- AMS-Factor 1 (F1) or LV-OOA, with mass spectrum dominated by m/z 44 fragment and very similar ($R^2 = 0.98$) to the Low Volatile OOA (former OOA1) spectrum measured at an urban background site in Zurich, CH, by (Lanz et al., 2007). The time series of this factor (black line in the bottom box of the Figure 7.6 right panel) corresponds well with the time series of particulate sulfate measured by the AMS (red line and axis in the same panel), another low-volatile species.
- AMS-Factor 2 (F2) or SV-OOA, with leading peak on *m/z* 43 followed by distinctive signal intensity on *m/z* 55 and *m/z* 91, typical of Semi Volatile OOA mass spectrometric pattern. The time series of this second organic factor corresponds well with the semi-volatile nitrate measured by AMS (blue line and axis).

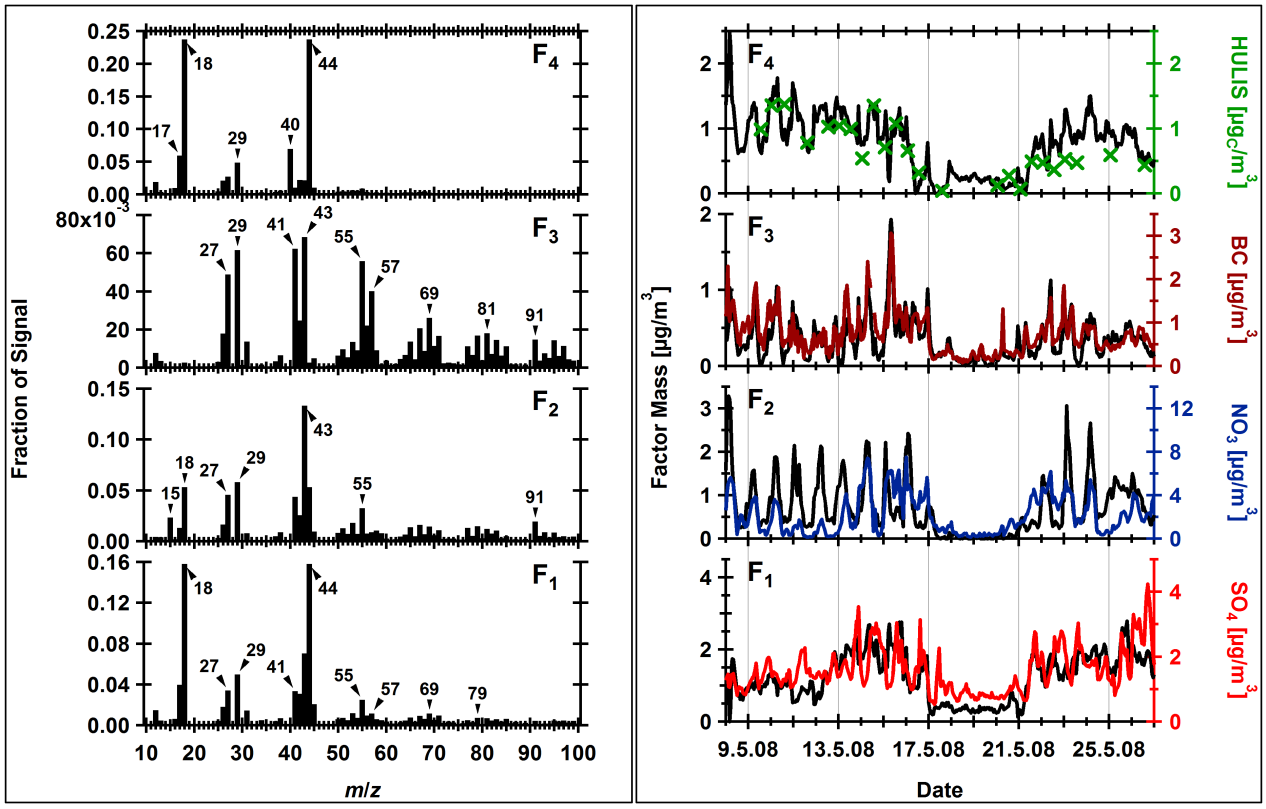


**Figure 7.6**: left: Normalized mass spectra of the four factors F1 to F4 (from bottom to top) determined by PMF analysis of the organic fraction of the 2008 measurements at CESAR tower. Right: Time series of the PMF factors F1 to F4 (from bottom to top) determined for the organic mass fraction of the 2008 measurement period at CESAR tower. Factors (black lines, left axis) and the according tracers (colored lines, right axes matching the respective trace in terms of color) are given.

- AMS-Factor 3 (F3) or HOA, with spectrum dominated by peaks separated by 14 amus, characteristic for Hydrocarbon-like Organic Aerosol (HOA), and shows high similarity ($R^2 = 0.84$) to a HOA mass spectrum measured in Pittsburgh, USA in September 2002 by (Zhang et al., 2005a). The time series of the third factor is very similar to the time trace of BC

(brown line and axis), which is expected for HOA. BC data was obtained from Multi Angle Absorption Photometer (MAAP 5012, Petzold and Schönlinner, 2004) operated by TNO.

- AMS-Factor 4 (F4) or FA-OOA, dominated by peaks on *m*/*z* 44, as well as Factor 1, and so also referred to OOA1 class but almost no signal intensity is assigned to peaks above *m*/*z* 44. This spectrum represents a highly oxygenated OA and is very similar to the mass spectrum of fulvic acid ($R^2$ = 0.97) acquired in a laboratory experiment by (Alfarra, 2004) and so named here FA-OOA meaning "Fulvic Acid-Oxydized Organic Aerosol". The time series of the NMR HULIS is shown as green crosses together with the time series of the highly oxygenated AMS-F4 in the top panel of the graph.

In the following discussion, the AMS concentrations for particulate organic compounds are compared to those derived by H-NMR analyses. Since the different techniques employ different concentration units (μg/m$^3$ of organic matter, of organic carbon and of organic hydrogen, respectively), stoichiometric ratios must be applied for quantitative comparison. In the following discussion, all AMS mass concentrations (μg/m$^3$) are converted to μgC/m$^3$ by applying the general relationships found by Aiken et al. (2008) relating the fractional abundance of m/z 44 to the O/C ratio and thereby to OM/OC ratio:

$O/C = 0.038*f_{44}+0.0794$ (1)

$OM/OC = 1.26*O/C + 1.18$ (2)

According to the above equations, OM/OC ratios of 2.0 (F1), 1.5 (F2), 1.3 (F3) and 2.4 (F4), were obtained (Table 7.5).

| AMS-Factor | f44 (%) | O/C | OM/OC |
|---|---|---|---|
| **1 – LV-OOA** | 15.8 | 0.68 | 2.04 |
| **2 – SV-OOA** | 5.3 | 0.28 | 1.54 |
| **3 – HOA** | 0.3 | 0.09 | 1.29 |
| **4 – FA-OOA** | 23.7 | 0.98 | 2.41 |

**Table 7.5**: OM/OC ratios founded for each PMF-factor by applying the general relationships found by Aiken et al. (2008) relating the fractional abundance of m/z 44 to the O/C ratio and thereby to OM/OC ratio

As already mentioned, concentrations in carbon units (µgC $m^{-3}$) for the NMR functional groups were derived from the measured concentrations in µmolH $m^{-3}$ by applying group-specific H/C ratios.

Table 7.6 reports the correlation coefficients between main chemical species and OC factors obtained by filter and AMS measurement. The modest correlation coefficient found for sulphate, which is a stable, non-volatile compound, cannot be easily explained. Uncertainties in the fluxes of the dichotomous sampler, or the non-coincident sampling height (60 m above the ground for AMS vs. ground-level for the dicothomous sampler), or sample loss due to small cracks we have found in some of the filters after sampling may have contributed to the discrepancy. It can be noticed, however, that the correlation between OC measured on the filters and that estimated by the AMS is quite satisfactory (R = 0.74). We obtained a positive correlation also between WSOC and the sum of AMS OOA types (expressed in carbon units) (R = 0.58).

| R (Pearson coefficient) | TC PM1filters | WSOC PM1filters | EC PM1filters | OC PM1Filters | $NO_3$ PM1filters | $SO_4$ PM1filters | NMR F1 (mean) | NMR F2 (mean) | NMR F3 (mean) | HPLC_PA |
|---|---|---|---|---|---|---|---|---|---|---|
| OOA AMS (µgC/m³) | 0.70 | 0.58 | 0.58 | 0.70 | 0.22 | 0.62 | -0.35 | 0.76 | 0.43 | 0.62 |
| OC AMS | 0.76 | 0.65 | 0.65 | **0.74** | 0.21 | 0.63 | -0.34 | 0.81 | 0.48 | 0.65 |
| $NO_3$ AMS | 0.16 | 0.03 | 0.37 | 0.15 | **0.52** | 0.17 | 0.01 | 0.00 | 0.03 | 0.17 |
| $SO_4$ AMS | 0.25 | 0.16 | 0.30 | 0.27 | 0.46 | **0.39** | -0.39 | 0.21 | 0.18 | 0.28 |
| AMS LV-OOA | 0.56 | 0.40 | 0.55 | 0.56 | 0.25 | 0.53 | -0.24 | 0.53 | 0.38 | 0.54 |
| AMS SV-OOA | 0.57 | 0.51 | 0.42 | 0.58 | 0.29 | 0.53 | -0.34 | 0.69 | 0.30 | 0.52 |
| AMS HOA | 0.66 | 0.52 | 0.83 | 0.67 | 0.30 | 0.42 | 0.12 | 0.44 | 0.48 | 0.61 |
| AMS FA-OOA | 0.79 | 0.74 | 0.60 | 0.82 | -0.01 | 0.62 | -0.41 | 0.89 | 0.51 | 0.70 |

**Table 7.6**: correlations between AMS analyses and chemical data from filters and NMR analyses: boxes colors follow the same scheme already described for Table 7.3. Red font highlights correlation between main aerosol components (OC, nitrate, sulphate) measured by AMS and on PM1 filters.

The comparison between the results of AMS and NMR factor analyses was conducted based on the correlation analysis of time trends (or "contributions") of the factors emerging from the two techniques (Table 7.6). This approach does not allow assessing univocal correspondences between the AMS and the NMR factors, but it rather indicates possible identifications. The best match was found between AMS-Factor4 and NMR-F2 (NMR-HULIS) with R = 0.89 (Table 7.6 and Figure 7.7). The concentrations of the two factors were also similar: 0.44 µgC/$m^3$ for AMS-Factor4 and 0.40 µgC/$m^3$ for NMR-HULIS. This finding suggests that the highly oxidized OOA of AMS-Factor4 is related to the polisubstituted aliphatic compounds identified by H-NMR analysis. We hypothesize that the same class of compounds, or "spectroscopic HULIS", was identified by both NMR and AMS in organic particles brought by continental air masses reaching Cabauw. Given the different sensitivity of the two techniques towards specific functional groups, the AMS and NMR spectral fingerprints must be considered as complementary. The H-NMR analysis is more sensitive to the aromatic rings and to the C-H groups composing the backbone of HULIS and showing that it

is mainly aliphatic and possessing no methylenic chains, while AMS fragmentation clearly provides information of the main oxygenated substituents which appear to be carboxylic acid groups.

With respect to the other AMS factors, their time trends, once integrated to the filter sampling time, show positive correlations between each other and with NMR-F2. The only factor correlating with NMR-F3 (Linear Aliphatics) is AMS-Factor1. Both have continental origin similarly to HULIS factors, but the concentrations of the latter drop steadily during the period Cont-Humid which precedes the marine air outbreak, while the concentrations of AMS-F1 and NMR-F3 remain high. However, given the time trends showing only a limited overlap and especially considering that the concentrations of AMS-F1 are much larger than those of NMR-F3, the latter may be considered rather a portion of the class of compounds identified by PMF-AMS as Factor 1.

NMR did not identify any factor matching with HOA, which is expected because HOA does not contribute significantly to WSOC, nor with AMS-F2 (SV-OOA). Further discussion about the inability of NMR analysis to account for the less oxidized AMS factor is presented in paragraph 7.3.7.

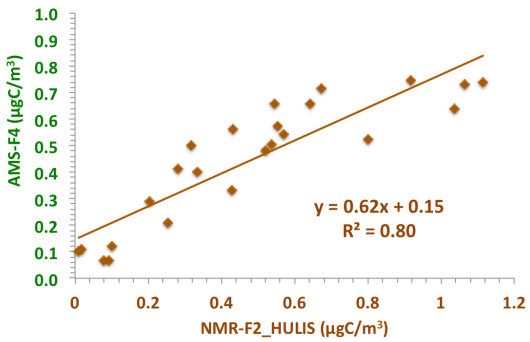


**Figure 7.7**: comparison between AMS-F4 factor & NMR-F2 (HULIS) factor.

Finally, factor analysis applied to the NMR dataset accounts for a distinct factor associated with organic aerosols from marine sources, the "MSA-containing WSOC" (NMR-F1), with no analogous resolved by the AMS-PMF analysis. It should be noticed, however, that AMS was actually able to detect a specific mass fragment of MSA, $CH_3SO_2^+$, and that its time trend was perfectly compatible with the results of off-line analysis (both IC and NMR) (Figure 7.8). In other words, the MSA mass tracer from AMS clearly showed the increase of marine SOA during the second continental period of the campaign and during the days of northerly flow towards Cabauw. At the same time, $CH_3SO_2^+$ was only a minor fragment in the AMS spectra, and its variability was not captured by PMF to identify a specific factor, equivalent to the NMR-F1. This is another example of the different NMR and AMS sensitivities towards specific functional groups, which in turn affects the outcomes of factor analysis.

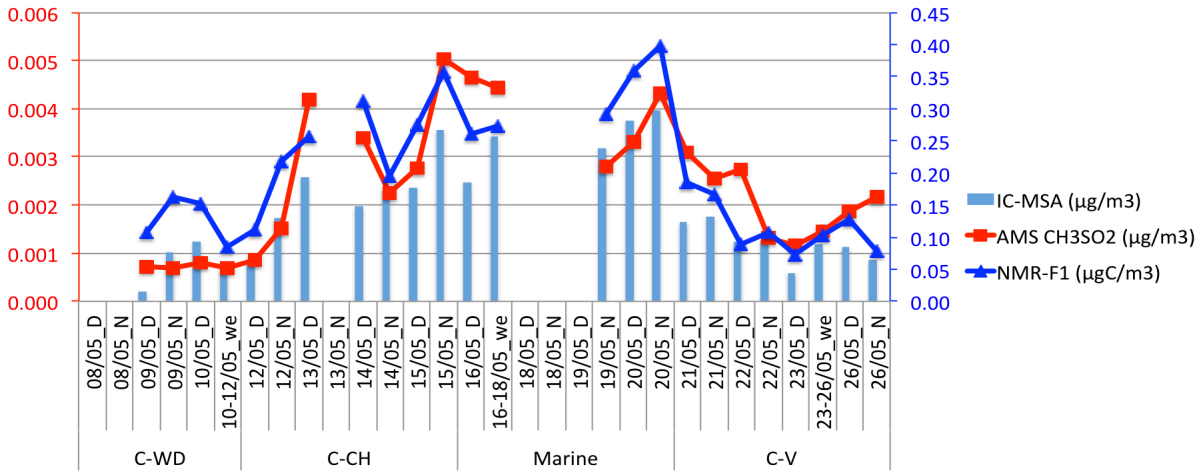


**Figure 7.8**: comparison between MSA (from IC measurements), NMR MSA-containing factor (referring to right blue axis) and AMS tracer ion CH3SO2+ (left red axis).

## 7.7 Comparison of HULIS from chromatographic and spectroscopic techniques

HULIS are determined as polycarboxylic acids using the HPLC-TOC method presented in section 7.2.2. Such technique is a derivation of the very first method used for HULIS analysis (Havers et al., 1998) and it is based on retention characteristics of fractions of WSOC with respect to a standard of aquatic fulvic acids. Therefore, polyacids or "chromatographic HULIS" must be considered as HULIS *sensu stricto*. The resulting concentrations for polyacids were compared with NMR and AMS concentrations for HULIS. Polyacids correlated with both NMR-F2 (R=0.73) and AMS-F4 (R=0.70). Nevertheless, chromatographic HULIS represented only 30% of NMR-F2 and 27% of AMS Factor4 (Figure 7.9). These results provide confirmation that the organic materials exhibiting spectral properties similar to those of fulvic acids are related to HULIS *sensu stricto* determined from chemical methods. At the same time, they also include chemical species which are not real polycarboxylic acids.

Previous studies on atmospheric HULIS (Graber and Rudich, 2006) had already highlighted differences between atmospheric HULIS and terrestrial and aquatic humic substances, including lower aromaticity (19% according to Tagliavini et al. (2005) against 31-58% from IHSS, www.ihss.gatech.edu), higher H/C molar ratios, weaker acidic nature and especially smaller molecular size for atmospheric HULIS (500-1000 Da according to Harvers et al. (1998), Krivacsy et al. (2001) and Kiss et al. (2003) versus 1000-10000 Da reported by Aiken (1984),and Marley et al. (1992). In agreement with the above studies, we observed that very oxidized carboxylic acids which are lighter than fulvic acids contributed to AMS Factor 4 and to NMR-HULIS while showing a smaller retention coefficient on SPE columns with respect to chromatographic HULIS. Since neither AMS nor NMR provide direct information on molecular size, we hypothesize that spectroscopic HULIS are actually a class of carboxylic acids spanning over a wide range of

molecular weights and whose larger homologous species correspond to the polyacids or HULIS *sensu stricto*.

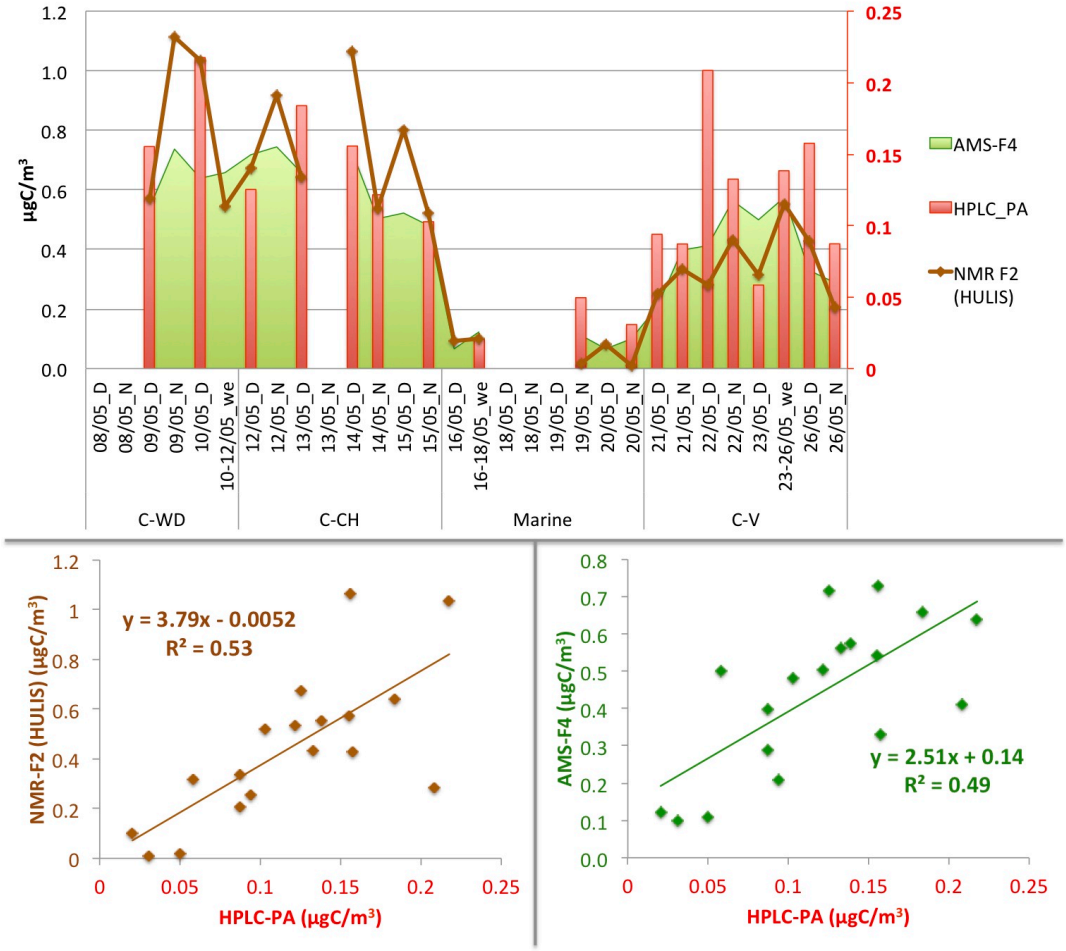


**Figure 7.9**: comparison between HPLC PA fraction, AMS-F4 and NMR-F2: the upper panel reports time series of AMS and NMR factors (left black axis) and of HPLC PA fraction (right red axis); the two lower panels show correlation between these fractions.

## 7.7 Summary and final remarks

To summarize the comparison between the NMR and AMS factors, we provide a tentative mass budget for aerosol OC including water-insoluble compounds, as a campaign average, with our best hypothesis of overlap between carbon classes derived from filter analysis and those determined by the on-line measurements (Figure 7.10). The fact that OC measured on PM1 filters was lower than the carbon associated with organic matter measured by AMS together with the low time resolution of filter collection allow only a tentative assignment between the NMR and AMS carbon classes. However, we can clearly observe that: a) there is an excess of water-insoluble carbon on filters compared to the AMS factors having low oxygen content (i.e., the hydrocarbon-like organic aerosols, HOA) suggesting that the least oxygenated fractions of AMS OOAs contributed to some

extent to WINOC; b) there were some semivolatile compounds within WSOC which were lost during sample preparation for NMR analysis; c) the less oxidized fraction of LV-OOA (Factor 1) account for a carbon fraction of WSOC that NMR characterization attributes to a heterogeneous set of compounds including MSA transported in marine aerosol (NMR-F1) and the linear aliphatic compounds which were interpreted as fresh SOA compounds (NMR-F3).

Clearly, both techniques highlighted the occurrence of water-soluble HULIS, whereas the other factors could not be reduced to a simple classification scheme common to AMS and NMR in this study.

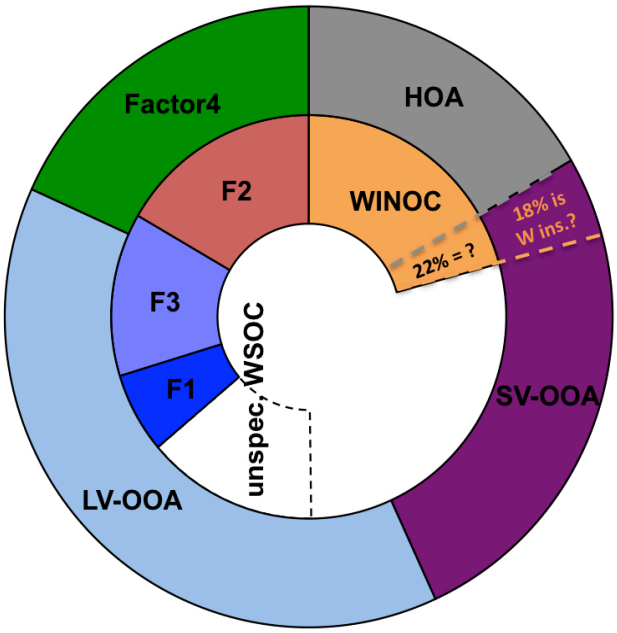


**Figure 7.10**: Organic carbon (OC) amount and comparison between the 3 different techniques used. Inner circle reports data from NMR and filters analyses; the outer one those from AMS.

Noticeably, the NMR factor analysis highlighted a marine organic aerosol component rich of methanesulphonate. No specific AMS factor for marine organics was discriminated by PMF, even if an AMS mass tracer for MSA was found, albeit in small concentrations, showing a time trend in good agreement with the results of off-line analyses. According to NMR analysis, marine organics dominate the organic composition in Cabauw on the days of strong northerly winds. Conversely, the HULIS are more characteristic of Easterly (continental) air masses. The "continental" nature of HULIS emerging from the Cabauw experiment was confirmed by additional NMR measurements at other EUCAARI stations during May 2008 showing that the NMR-HULIS factor characterized the WSOC composition in the polluted boundary layer air in easterly air masses flowing from central Europe to the British Islands: from K-Puszta (Hungary) to Melpitz (Germany) to Mace Head (Ireland) (Figure 7.11). Therefore, despite of still scarce knowledge about HULIS sources and

atmospheric fate, the oxidized organic compounds detected by NMR as HULIS were common constituents of submicron aerosols at the regional scale over Europe. Contrary to HULIS, the aliphatic-rich WSOC ("Linear Aliphatics") of Cabauw was not found in the central European stations and it can be related to different sources of oxidized organic aerosols active at that time in the North Sea area.

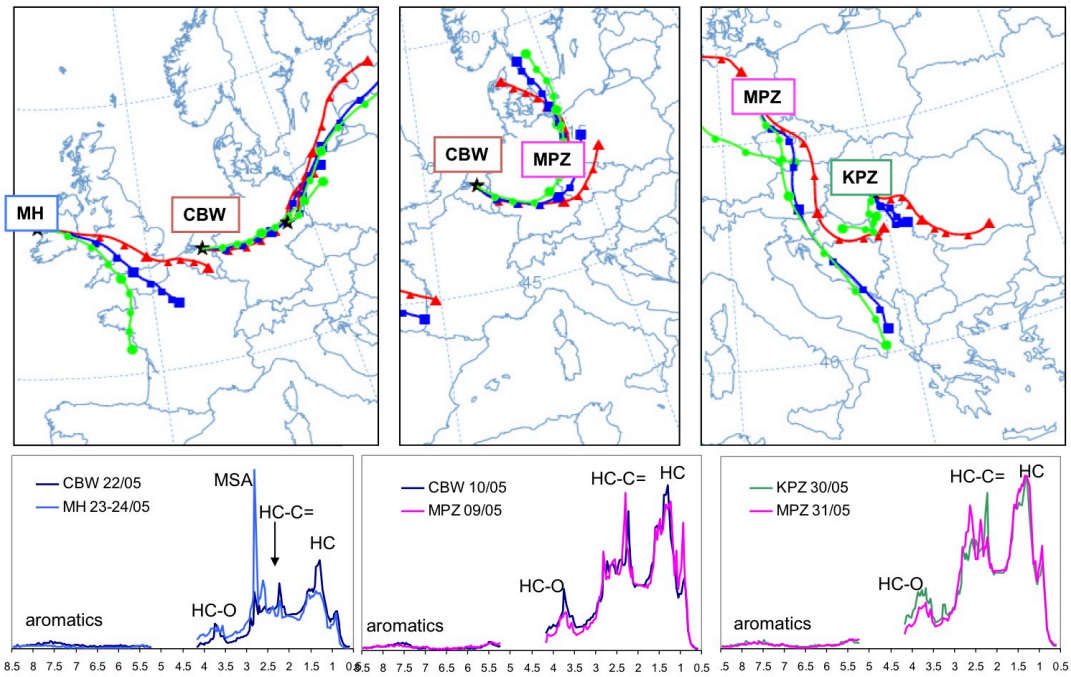


**Figure. 7.11**: Additional measurements at other EUCAARI stations during May 2008 show that the HULIS factor characterized the OOA composition in the polluted boundary layer air at the regional scale. Nevertheless, the aliphatic-rich OOA of Cabauw were not found in the central European stations and it can be related to different sources of oxidized organic aerosols active at that time in the North Sea area.

# 8 - Primary and secondary biomass burning aerosols determined by $^{1}$H-NMR spectroscopy during the 2008 EUCAARI campaign in the Po Valley (Italy)

## 8.1 Introduction to the Po Valley experiment

In this chapter, the contribution of primary and secondary biomass burning to oxygenated organic aerosols in the rural Po Valley, Italy, during another EUCAARI field campaign. The experiment was held in early spring: a period of the year which is still cold and diffuse wood burning from domestic heating systems is active in the valley, and at the same time characterized by relatively high radiation levels responsible for moderate ozone peaks (50 ppb). The paper by Saarikoski et al. (2012), dealing with the AMS measurements carried out during the same field campaign, reports that under stable meteorological conditions the diel change in atmospheric stratification following the development of the planetary boundary layer was responsible for drastic changes in submicron aerosol composition, with fresh particulates rich of semivolatile compounds during the night and early morning respect to more aged particles occurring in the middle of the day and in the afternoon. Typical diurnal patterns of atmospheric concentrations of particulate organic matter including fractions apportioned to biomass burning sources could be determined thanks to the employ of high-resolution time-of-flight mass spectrometric (HR-Tof-AMS) techniques. In their recent review, Jimenez et al. (2009) showed that a factor accounting for biomass burning sources ("biomass burning organic aerosol", or BBOA) emerges from factor analysis of AMS records at a number of field sites in the north hemisphere, suggesting that a common AMS spectral fingerprint can be used to apportion organic aerosol mass to biomass burning sources in a variety of environments. On the other hand, the actual link of AMS BBOA with common tracers of wood burning, such as levoglucosan and anhydrosugars, has not been examined extensively yet. Contrary to preliminary findings at other locations (Aiken et al., 2010), BBOA concentrations were too low and did not correlated well with the levoglucosan concentrations during the EUCAARI field campaign the Po Valley and the correlation improved only by including other OOA factors (Saarikoski et al. 2012). Such results suggested that BBOA were not the only constituents of biomass burning POA and that a more sophisticated factor analysis of the residual OOA is necessary to deconvolve the excess biomass burning POA from the contributions of other sources, including biomass burning SOA. In my doctoral work, I performed the factor analysis of the $^{1}$H-NMR dataset recorded on aerosol filter samples collected in parallel to the HR-Tof-AMS, and

identified the NMR factors characterized by biomass burning spectral fingerprints. My results on organic source apportionment derived from NMR factor analysis were then used to clarify the discrepancies between AMS and organic tracers (levoglucosan) techniques in estimating the fraction of aerosol organic carbon accounted for by biomass burning. The original results included in this thesis chapter are object of a scientific paper in preparation

## 8.2 Aerosol sampling and analysis

Atmospheric particles were sampled by a suite of co-located off-line instruments throughout the campaign conducted at the San Pietro Capofiume (SPC) measurement station "G. Fea" (44°39'0'' N, 11°37'0'' E; see Chapter 4) from 30 March to 20 April 2008. A dichotomous sampler at a constant nominal flow of 300 l/min was employed from 1st to 14th of April 2008 to collect fine particles with ambient diameter < 1 μm on pre-washed and pre-baked quartz-fiber filters (Whatman, 9cm size). Typically, two filters were sampled every day, with "daytime" (D) $PM_1$ samples collected from ~10:00 to ~17:00 (local time, UTC+2), and "evening/night-time" (N) samples collected from ~18:00 to ~09:00. Exceptionally, long-time integrated samples were also taken (three samples, lasting 32, 24 and 24 hours). Samples were stored frozen until chemical analysis.
The quartz-fiber filters were subjected to the general procedure of extraction, filtration and off-line chemical analysis already described in Chapter 4, comprising the recording of 17 NMR spectra.

## 8.3 NMR characterization of WSOC

Spectral fingerprints and individual compound speciation of H-NMR spectra recorded during the 2008 EUCAARI experiment in the Po Valley are in agreement with previous findings in the same area (Decesari et al., 2001). Levoglucosan, methane-sulphonate and four low molecular weight amines, namely monomethyl-, dimethyl-, trimethyl- and triethyl-amines (MMA, DMA, TMA, TEA) were speciated and quantified. Contrary to the marine aerosol samples collected on the Irish coast (Decesari et al., 2011), diethyl-amine (DEA) was not found, while TMA an TEA were detected at ng/m$^3$ level in almost all samples. The different speciation respect to the marine site probably reflect different biogenic sources, which in the Po Valley are largely impacted by livestock farming and waste treatment activities. Wood burning is and additional source of amines in the valley, as suggested by the tendency of DMA and MMA concentrations to peak at night, but overall the correlation with levoglucosan concentrations is negligible ($R^2 < 0.1$). With the exception of TMA, whose time trend is rather flat, the other amine concentrations reach a maximum in the third period of the campaign, on the days between 8 and 10th April, characterized by western Mediterranean air masses, high humidity with fog occurrence, a very stratified atmosphere. We

observed the highest concentrations of ammonium nitrate in the same period, indicating that the high relative humidity may have promoted the gas-to-particle conversion of low-molecular weight amines by co-condensation with nitric acid or organic acids.

A synthetic representation of WSOC functional group distribution and of its variability during the campaign is provided by Figure 8.2, based on the metrics introduced by Decesari et al. (2007). Functional group concentrations are here expressed as μgC/m$^3$ upon applying group-specific conversion factors previously introduced in this thesis.

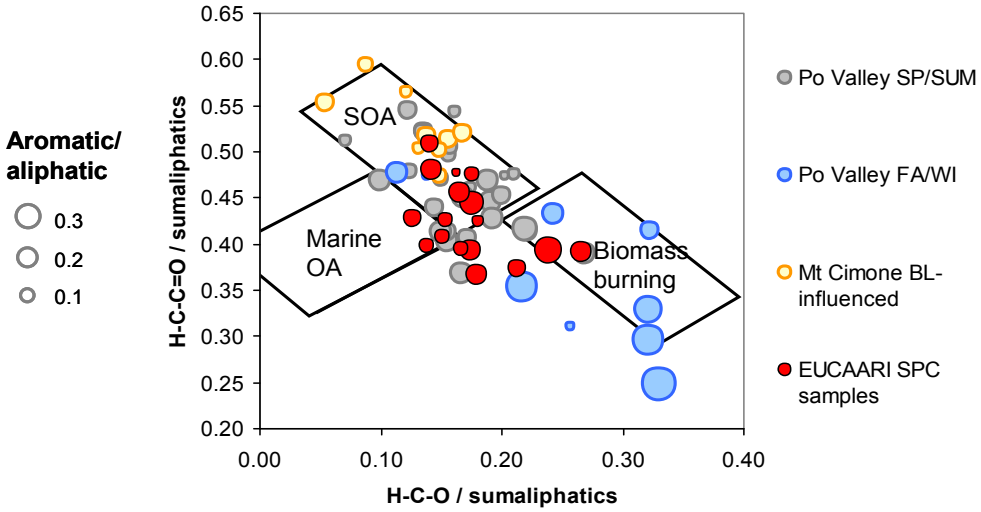


**Figure 8.2**: Functional group distribution of the SPC 2008 EUCAARI samples compared to submicron aerosol compositions derived from previous study in the same area.

The 2008 spring campaign samples exhibit an aliphatic composition stretching between the "biomass burning" and the "SOA" sectors with a prevalence of the latter. A clear biomass burning assignment was found for samples 04April_Night and 05April_Night, meaning that their composition is fully consistent with that recorded for samples taken faraway (Rondônia, Brazil) in an area directly exposed to strong biomass burning emissions (Tagliavini et al. 2006).

The aromaticity of WSOC decreased steadily during the campaign (Figure 8.3a) with a trend already observed for anhydrosugars and that can be explained by the progressive increase of minimum temperatures leading to a general decline of residential heating activities in the area (Saarikoski et al., 2012). This finding suggest that NMR-detected aromatics are mainly phenolic compounds formed by the pyrolysis of wood during combustion, together with their degradation products in the atmosphere.

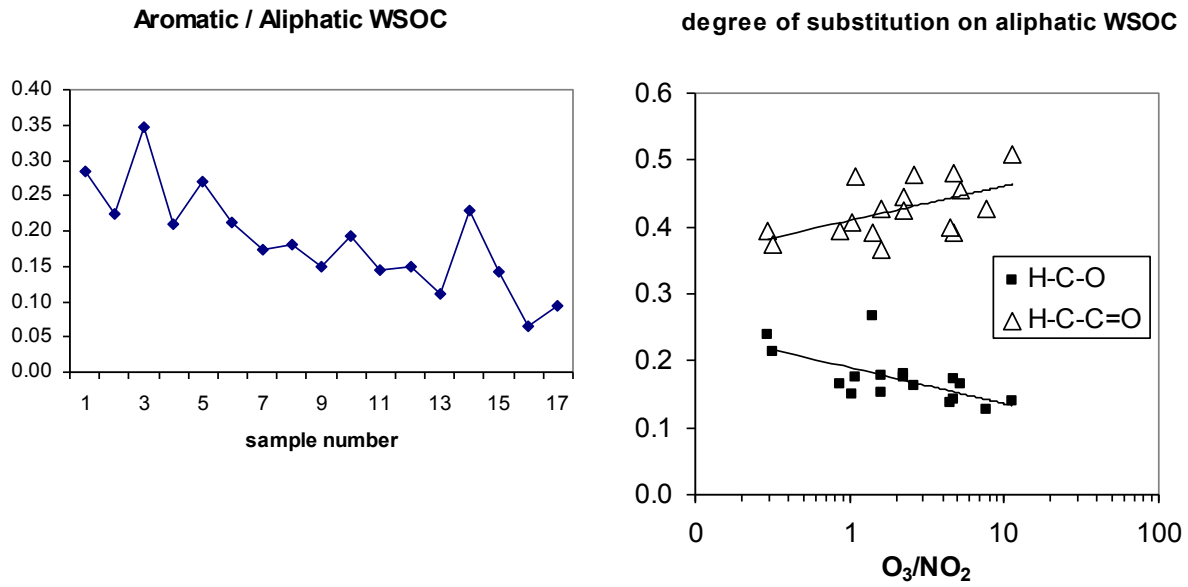


**Figure 8.3**: a) Time trend of aromaticity;
b) Content of oxygenated aliphatic functional groups as a function of trace gas composition.

The proportion of alkyl groups to the aliphatic moieties remains fairly constant resulting into a certain degree of covariance between the two main oxygenated groups, H-C-O and H-C-C=O. The conversion between hydroxylated compounds and those bearing carbonyls/carboxyls seems to be related to the air mass type and photochemical regime, since there is clear tendency to find the former at high $NO_2/O_3$ ratios and the latter in more photochemically-aged air masses (Figure 8.3b). The change is more significant for H-C-O groups, which are strongly depleted in aged samples, while H-C-C=O occurs in non-negligible amounts even at high NOx levels although reaching maxima in low-NOx conditions. It should be noted that the actual change of WSOC oxidation state consequent of the "replacement" of hydroxyl- functional groups with H-C-C=O groups cannot be accurately determined based on these data, due to the uncertainty in the split between carbonyls and carboxylic groups.

## 8.4 NMR factor analysis and comparison with PMF-AMS

The $^1$H-NMR spectra were subjected to pre-processing steps prior to undergo factor analysis: Baseline correction with a polynomial fit, horizontal alignment of the spectra and blank signals subtraction. The spectral regions containing only sparse signals ($\delta H < 0.5$ ppm; $4.5 < \delta H < 6.5$ ppm; and $\delta H > 8.5$ ppm) were omitted from the data set. Binning over 0.02 ppm of chemical shift intervals was applied to remove the effects of peak position variability caused by matrix effects. Low-resolution (400 points) spectra were finally obtained, and were allowed to be processed by four of the factor analysis algorithms described in Chapter 4: the two N-NMF models and the two

MCR ones. Solutions resulting from factors two up to eight were explored with all models. Analysis of residuals and Q/Qexp ratios were used in order to find the most robust solution. Basically all models agree on a large drop in residuals and in the Q/Qexp ratios until five factors: additional factors continued to reduce Q/Qexp with no significant change in slope. Five-factors solution presents also the best agreement between all four factor analysis methods, both in term of profiles and contributions fitting, while a number of factors greater or lesser decreases that fitting. Furthermore, beyond five factors two or more factors were found to be strongly correlated each other, suggesting that the measurements were not adequate to differentiate additional independent factors. Interpretation of factor spectral profiles was based on presence of characteristic peaks and on the comparison with a unique library of reference spectra recorded during laboratory studies or in the field at near source stations.

Based on all these considerations a 5-factors solution was chosen as the best one and discussed afterward. Figure 8.5 reported profiles and contributions of the 5-factors solution for all four methods, in order to evidence their substantial agreement.

- NMR-Factor 1 (F1) was dominated by MethaneSulphonicAcid (MSA) peak at 2.81 ppm, associated with a relative small fraction of oxidized aliphatic chains and so called hereinafter "MSA-containing" factor. Its concentrations were very small (oscillating from 0 to 0.02 ugC/m3) and became significant just in some samples (in particular one, corresponding to the night of April 4$^{th}$) that instead had a maximum of 0.06 ugC/m3. This increase was probably due to a marine air mass intrusion from Mediterranean see.
- NMR-Factor 2 (F2) showed instead characteristic spectral profile with clear signatures from aromatic compounds and polyols. This profile is very similar to reference spectrum of biomass burning primary aerosol from chamber experiment (and so it will be called "Biomass Burning" factor hereinafter, as already discussed in previous Chapter 5 and below in next section). The good correlation of its contributions with those of levoglucosan and potassium, with $R^2$ of 0.98 and 0.69 respectively, confirms the link between F2 and primary or freshly products of biomass combustion. Also its contributions time series, exhibiting diurnal trends with maxima observed in night samples during the first week of high-pressure conditions, confirmed a probable link with primary or freshly produced compounds accumulated in the surface layer under a low thermal inversion and dispersed upon formation of the mixing layer during day-time.
- NMR-Factor 3 and Factor 4 (F3 and F4) represented two oxidized aerosol types with spectral profiles characterized by polysubstituted aliphatic moieties, some hydroxyl groups (between 3.2 and 4.5 ppm) and a smaller contribution from aromatics. Aliphatic groups substituted with C=C and C=O groups (between 1.8 and 3.2 ppm) represent on average 30% of the total

functionalities on a carbon basis. They look similar but have differences in the alcohols and aliphatic regions of the spectrum even if both have specific features of secondary and processed aerosol. In particular in F4 aliphatic chains with terminal methyls are reduced to advantage of C=C and C=O groups suggesting that this factor is representative for a more processed and aged aerosol fraction.

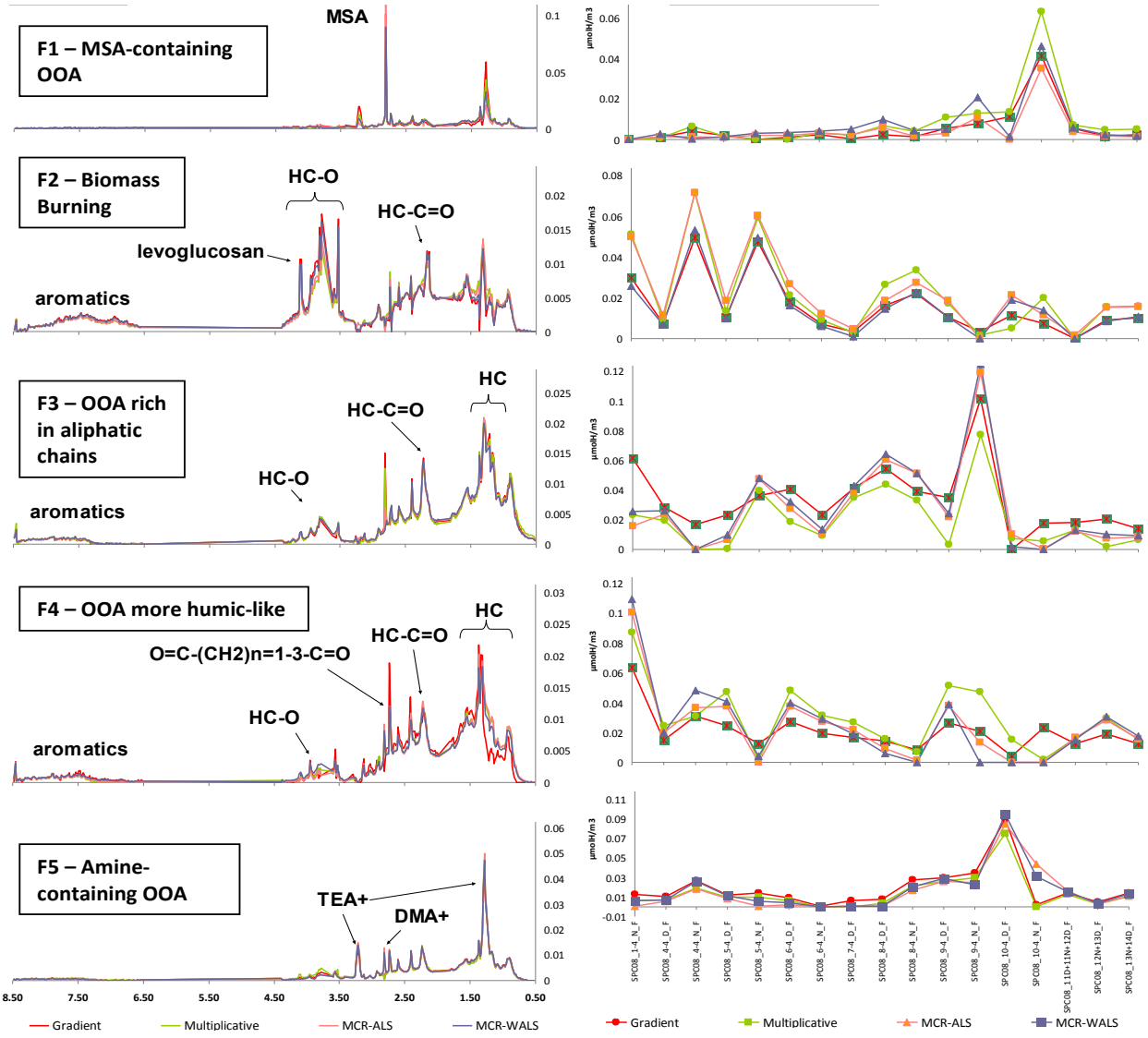


**Figure 8.5**: profiles and contributions of 5-factors solution from H-NMR spectra factor analysis. Results from all 4 different algorithms applied were reported: Projected Gradient (red line), Multiplicative (green line), MCR-ALS (orange line) and MCR-WALS (violet line) methods.

- NMR-Factor 5, finally, was characterized by low-molecular weight amines (already discussed in section 8.3.2) and some residual trace of MSA, always mixed with aliphatic compounds. In particular triethylamine (TEA) is clearly represented by its typical peaks at 3.22 and 1.29 ppm and also methylamine (MA) and di-methylamine (DMA) by their peaks at 2.60 and 2.72 ppm

respectively. All these amines are widely diffused in rural agriculture area and linked to local husbandry and agricultural practices (Xinlei Ge et al., Atmospheric Environment, 2011).

As already well described by Saarikosky et al. (2012), PMF was also applied to the high-resolution mass spectra of OA parallel measurements and a 6F-solution seemed to be the most representative. PMF factors were denoted as hydrocarbon-like OA (HOA), biomass burning OA (BBOA), nitrogen-containing OA (N-OA) and three oxygenated OAs (OOA-a, OOA-b and OOA-c) and their spectral profiles were reported in Figure 8.6 (from Saarikoski et al., 2012).

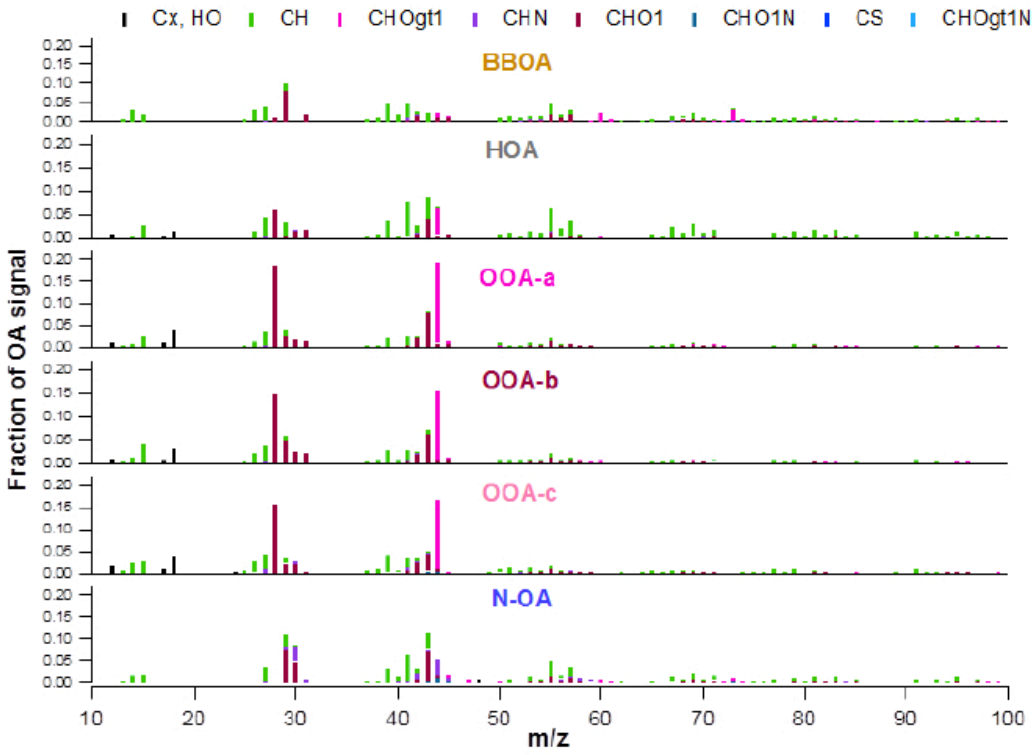


**Figure 8.6**: High-resolution mass spectra for HOA, BBOA, three OOAs, and N-OA (from Saarikoski et al., 2012).

Comparing NMR factors with those from PMF-AMS analysis, the most interesting results arise from parallelism between NMR-F2 and AMS-PMF BBOA factor, showing a positive but just moderate correlation ($R^2 = 0.18$).

NMR-factor shows a much higher concentrations with respect to AMS-BBOA ones, especially during the first period of campaign and also a much higher oxidation state. Moreover levoglucosan/OC ratios suggest that more than one factor is needed to account for the whole biomass burning fraction: levoglucosan indeed counted for 10 ÷ 15% of NMR-F2 and for 8 ÷ 25% of AMS-BBOA as carbon.

Agreement between total biomass burning fraction of OC estimated from AMS and NMR improves significantly including one of the oxygenated factors of possible secondary origin together with biomass burning factors identified: in particular the best match is found when we added up NMR-F4+F2 and compared with the sum of AMS-BBOA+OOAc, as shown in Figure 8.7.

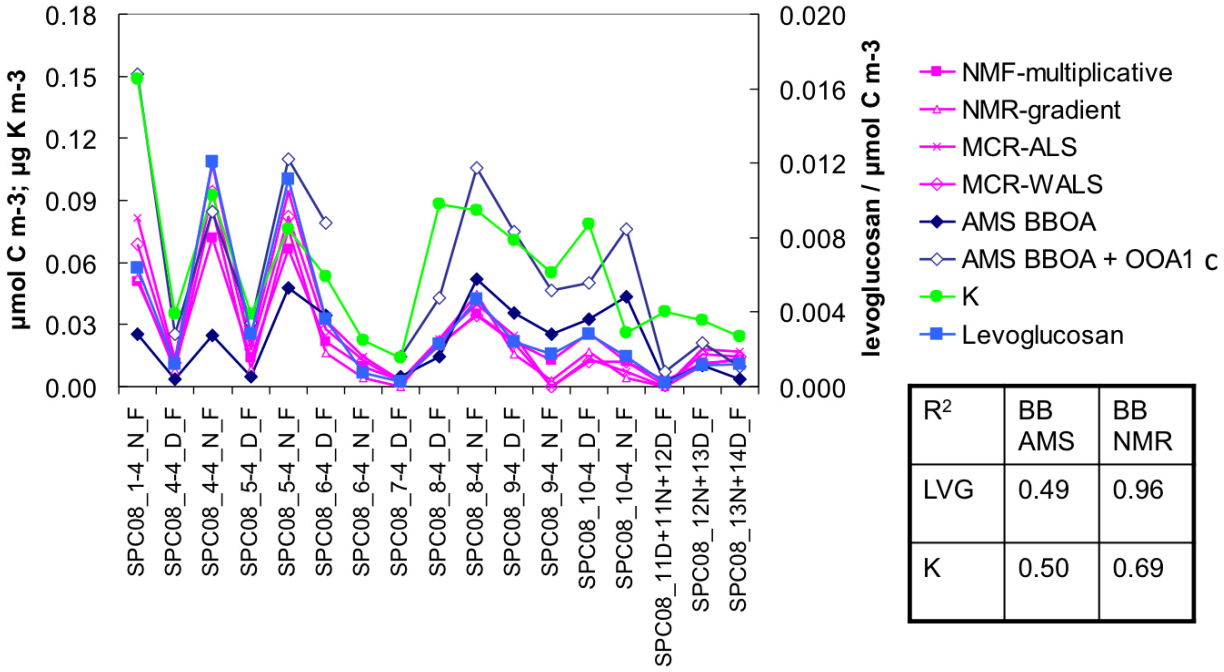


| $R^2$ | BB AMS | BB NMR |
|---|---|---|
| LVG | 0.49 | 0.96 |
| K | 0.50 | 0.69 |

**Figures 8.7**: contributions time trend of NMR-F2 from the four factor analysis methods applied (magenta lines) compared with those of biomass burning tracers (levoglucosan in blue line and potassium in green line) and AMS BBOA factors. Table summarizes correlation coefficients between tracers and factors from NMR and AMS.

## 8.5 Identification of biomass burning POA and SOA data

The examination of NMR and AMS factors in search of biomass burning aerosol components led to the following conclusions:

1. An agreement between the NMR and AMS source apportionment for biomass burning aerosol could be achieved only by considering suitable lumpings of factors.
2. Both NMR and AMS factor analyses suggest that biomass burning aerosols include a first component linked to surface sources in the Po Valley and active at night, plus a second component better mixed in the atmosphere and prevalent in daytime, that can be tagged as "fresh" and "aged" fractions respectively.
3. The AMS BBOA would then account only for the fresh component.
4. The split between the fresh and aged biomass burning aerosol is performed differently by NMR and AMS.

In the present section, the nature of the NMR factors assigned to biomass burning sources is further discussed.

Laboratory experiments are ideal tools to obtain unambiguous chemical fingerprints from specific aerosol sources and are often use for the interpretation and source attribution of ambient spectral datasets (e.g., Kiendler-Scharr et al., 2009). H-NMR spectra of biomass burning POA, i.e. freshly produced smoke particles sampled in combustion facilities (Heringa et al., ACPD 2011) shows evident resonances from aromatic moieties including phenols and from hydroxylated compounds including levoglucosan, plus a lower proportions of other aliphatic compounds (Figure 8.8a). These data are also consistent with the spectra reported by Kubatova et al. (2009), and provide confirmation that freshly produced particles account for the large fraction of aromatic and hydroxylated groups typical of water-soluble biomass burning aerosol (Decesari et al., 2007). On the basis of these NMR data recorded for fresh smoke samples, we then conclude that the NMR Factor 2, "aromatic & polyols", during the 2008 EUCAARI campaign correspond to biomass burning POA.

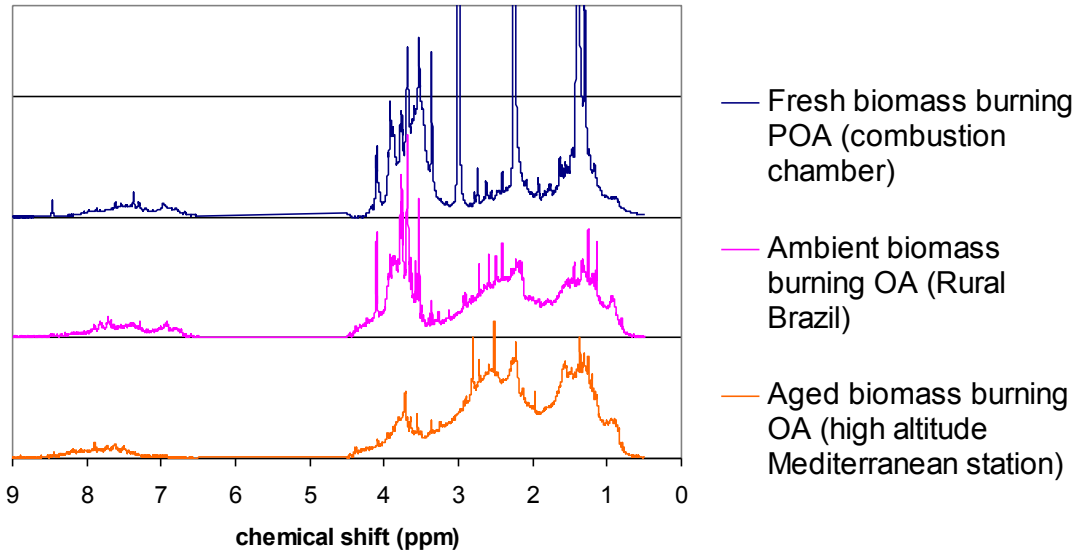


**Figure 8.8**: Reference H-NMR spectra for different stage of biomass burning aerosol ageing: a) laboratory wood burning POA (sharp peaks at 1.3, 2.2 and 3.3 ppm are from contaminants); b) ambient near-source biomass burning aerosol; c) biomass burning aerosol from long-range transport.

The spectral features of Factor 4, which we also attribute to biomass burning sources, are less characteristics and their link to chemical speciation data obtained in smoke chambers is less clear. The spectral profile suggests a mix between aromatic compounds depleted in phenols and richer in electron withdrawing substituents (like carbonylic, carboxylic or nitro- groups) mixed with a (larger) fraction of aliphatic compounds substituted with unsaturated oxygenated carbon atoms, like

carbonyls or carboxyls but with only a few alcohols. Therefore, Factor 4 is completely impoverished of compounds most characteristic of fresh smoke particles like anhydrosugars and phenols. Nevertheless, carboxylic acids were found in significant amounts in *ambient* biomass burning aerosols (Figure 8.8b; Mayol-Bracero et al., 2003; Decesari et al., 2006). Ion-exchange chromatographic techniques have been applied to separate the polyol fraction of WSOC from the carboxylic acids, including the humic-like substances (HULIS) in ambient smoke particles, showing that the concentration of the total acids can rival with that of the alcohols (Decesari et al., 2006). We have reproduced the chromatographic fractionation employed for the SMOCC biomass burning experiment in Brazil, by analysing one EUCAARI sample showing highest contributions of Factors 2 and 4. The H-NMR spectra recorded for the resulting chemical classes, namely neutral/basic compounds, mono- and di-carboxylic acids, and polyacids (HULIS), are shown in Figure 8.9.

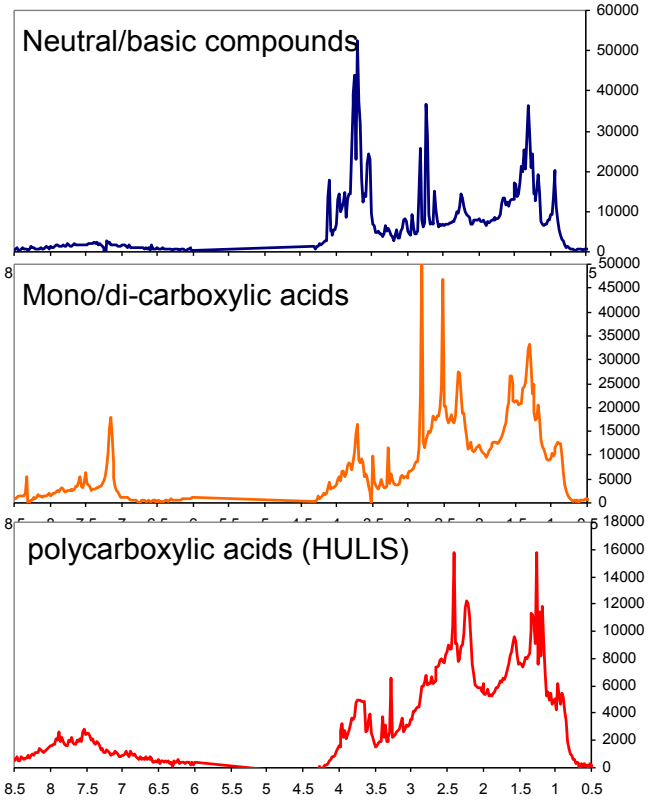


**Figure 8.9**: H-NMR spectra of WSOC fractions isolated by anion-exchange chromatography.

As during SMOCC, the fractionation of the Po Valley sample led to a clear split of the aliphatic components of WSOC, with most of the hydroxylated species and amines recovered into the neutral/basic compounds and most of the aliphatic compounds substituted with carbonyls/carboxyls falling in the acidic classes. The separation of the aromatic groups is less clear although the polyacids (HULIS) exhibit the highest degree of aromaticity. These results provides confirmation for the results of factor analysis indicating that polyols and the compounds enriched of H-C-C=O

groups belong to different chemical classes, which are here tagged as neutral/basic compounds and mono-/di-carboxylic acids + polyacids, respectively. Correlation coefficients between factor profiles and the spectra of the chemical classes actually separated by liquid chromatography indicate that the compounds responsible for Factor 4 and associated with biomass burning sources but *not* correlating with levoglucosan and phenols must be searched in the chemical class of mono- and di-carboxylic acids, operationally defined by the ion-exchange chromatographic method.

During the SMOCC experiment, a greater ratio between acids respect to polyols was found in daytime hours and was attributed to the different burning conditions in the area: more smoldering at night versus more active flaming in daytime (Decesari et al., 2006). During the first period of the EUCAARI campaign, the same behaviour was found in an area where open burning does not occur in spring, when biomass burning is essentially due to domestic heating at night-time. An alternative explanation, more suitable for the conditions encountered during EUCAARI, is that the daytime samples, richer in carboxylic acids and depleted of polyols, are the result of an atmospheric processing. Ageing would trigger the observed change in functional group distribution as a function of the $O_3/NO_2$ ratio (Figure 8.2) and Factor 4 would then correspond to biomass burning SOA.

Finding clear fingerprints for biomass burning SOA during field conditions can be challenging due to interfering source contributions. Best opportunities are large plumes from open burning in the tropics captured after several hours of transport in the middle troposphere (Capes et al., 2008). In 2007, one of such events was captured at the GAW station of Monte Cimone and the samples were analyzed by NMR spectroscopy (Cristofanelli et al., 2009). We discuss here the NMR characteristics of the aerosol sampled in those days, as it can be considered a good example of very aged ambient biomass burning organic aerosol. The spectrum, reported in Figure 8.8c, has clearly little to do with the profile of Factor 2 and with the fingerprint of fresh smoke particles determined during the EUCAARI campaign. In fact, the composition of the Monte Cimone aged biomass burning OA is impoverished of phenols and especially of alcohols, with levoglucosan nearly absent, while aliphatic compounds polysubstituted with carbonyls/carboxyls dominate. Interestingly, the spectral profile of the Monte Cimone sample shares many similarities with the polyacids (HULIS) fraction isolated from the EUCAARI sample, more than with the mono- and di-acids. These findings confirm that the compositional changes in biomass burning aerosol during long-range transport can be severe (Capes et al., 2008).

The above compilation of laboratory and ambient spectral data, although being incomplete, allows to draw first two conclusions of the nature of NMR factors linked to biomass burning POA and SOA:

1. Data from smoke chambers and from ambient samplings in near-source area agree on showing large phenol and polyol contents in fresh particles (POA).
2. Ambient data of very processed smoke particles show that phenols and polyols are strongly impoverished and that aliphatic compounds substituted with carboxylic acids plus aromatics other than phenols account for the apparent biomass burning SOA.

A third preliminary conclusion is that HULIS form and enrich with ageing. Its corollary is that specific NMR fingerprints can be derived for the fresh particles (polyols and phenols) and for the very aged biomass burning aerosol (HULIS), while less distinguishing features are available for the intermediate stage of ageing, when mono- di-carboxylic acids are formed and the composition of biomass burning SOA overlaps with that of oxidized compounds originating from other sources, like those responsible for Factor 3 during EUCAARI. It follows that in areas impacted by residential wood burning sources, the quality of the dataset and of factor analysis will be critical for the discrimination of the NMR factor for biomass burning SOA.

## 8.6 Isotopic measurements and carbon budget

Modern and fossil fuel fractions of aerosol total carbon were measured in 12 samples during periods II, III an IV of the campaign and the results are reported in Table 8.1. Contrary to period I, where a clear evolution of the aerosol composition is provided by the diurnal evolution of the boundary layer, the following periods show less clear dynamics.

| Sample | $F^{14}C$ | Error $F^{14}C$ (1 SD) |
|---|---|---|
| 080408_1D | 0.608 | 0.011 |
| 080408_1N | 0.704 | 0.014 |
| 090408_1D | 0.542 | 0.011 |
| 090408_1N | 0.588 | 0.014 |
| 100408_1D | 0.558 | 0.014 |
| 100408_1N | 0.588 | 0.011 |
| 110408_1D | 0.534 | 0.011 |
| 110408_1N | 0.573 | 0.011 |
| 120408_1D | 0.536 | 0.010 |
| 120408_1N | 0.738 | 0.014 |
| 130408_1D | 0.609 | 0.011 |
| 140408_1D | 0.572 | 0.011 |

**Table 8.1**: Results of $^{14}C$ analysis.

As a result, the small changes in modern carbon fraction between samples shown by the isotopic analysis could not be related unambiguously to any of the trends of AMS and NMR factors. The

average fraction of modern carbon for TC is 60%, an intermediate value between values typical for urban sites (Yamamoto et al., 2007; Marley et al., 2009) and those representative for rural locations (Gelencser et al., 2007; Szidat et al., 2007).

Since the biomass burning fraction of OC was already estimated using NMR and AMS factor analysis, in this section we employ the $^{14}C$ data to investigate the biogenic/anthropogenic nature of the remaining oxidized organic compounds. An aerosol carbon budget was calculated based on the following assumptions: a) the EC/OC ratio for biomass burning aerosol was set to 0.16 based on recommendations of Szidat et al. (2006); b) amine-containing compounds and AMS N-OA originate from emissions from livestock and other modern carbon sources; c) primary OC from fossil fuel combustion is fully water-insoluble. In addition, when comparing the carbon budget based on the AMS factors with that elaborated starting from filter analysis, we attributed AMS HOA to WIOC and BBOA+OOAc to the sum of NMR F2 and F4. The resulting calculations, as campaign averages, are reported in the upper panel of Figure 8.10, and, for the days covered by isotopic analysis, in the lower panels of the same figure.

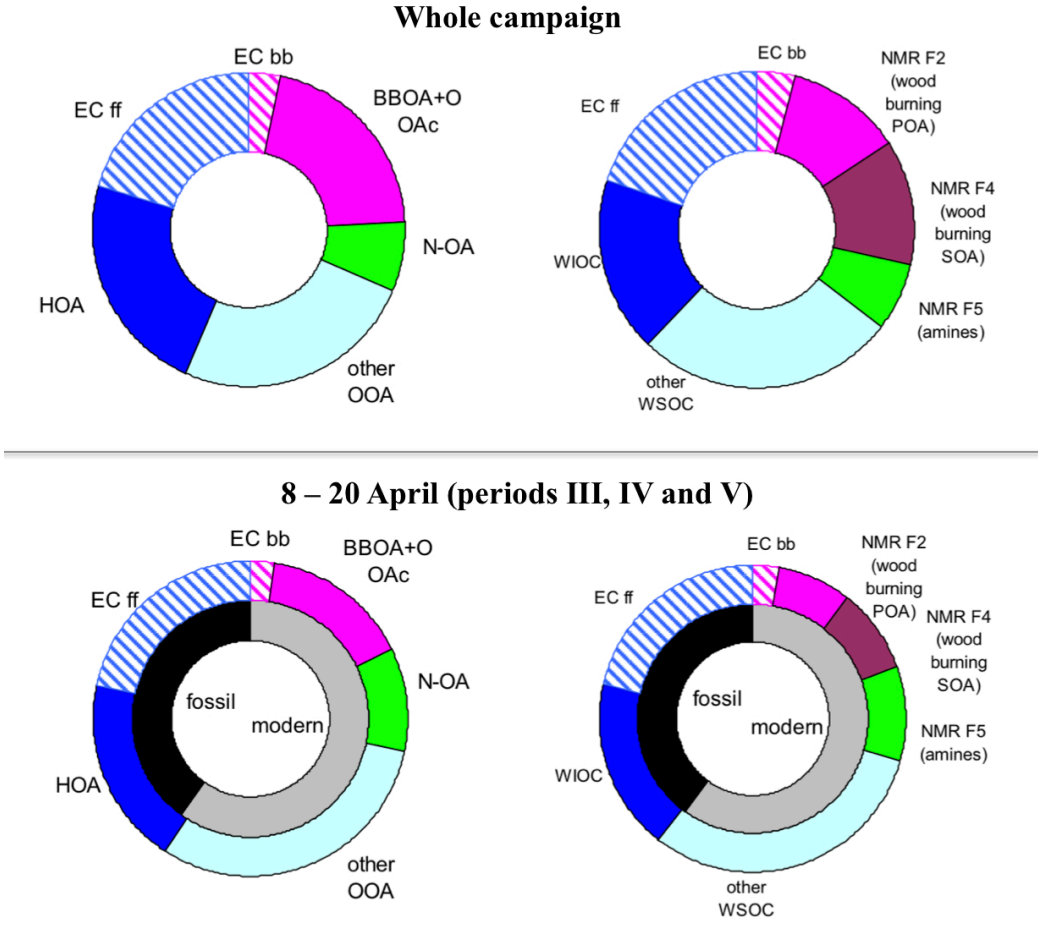


**Figure 8.10**: Carbon budget of aerosol TC for the whole campaign (upper two panels) and for the period covered by the isotopic analyses (lower panels). Budgets are reconstructed based on PMF-AMS (left) and NMR factors for WSOC (right). For more explanation refer to the text.

It can be observed that WIOC/HOA together with the fossil fraction of EC account for the totality of fossil TC, leaving no room for WSOC or OOA originating from fossil fuel combustion. As anticipated in the previous section, NMR and AMS fractionations agree in apportioning about one third of OC to biomass burning sources as a campaign average. As source intensity of wood burning decreased with time (Figures 8.2 and 8.7), the second part of the campaign, for which fossil carbon data are available, shows a lower fraction of OC apportioned to biomass burning: 20% or 22% based on respectively AMS and NMR analyses, which fall in the range indicated by the levoglucosan analyses (from 10% to 30%, Alves et al. 2012).

In summary, the **non-biomass burning WSOC (or OOA carbon) is prevalently accounted for by modern carbon, and therefore of *biogenic* origin**. The "modern" character of non-biomass burning OOA/WSOC is somewhat surprising for a polluted environment at the mid-latitudes in a period of the year (March - early April) when vegetation has just started to recover from winter dormancy. On the other hand, the occurrence of amines in large amounts in our samples suggest that biogenic processes involved by anthropogenic activities (e.g., animal farming, waste treatment) can provide a non-negligible contribution to the modern carbon fraction of Po Valley. In that case, SOA precursors originate from anaerobic processes occurring according to completely different mechanisms respect to the well-studied terpene emissions from living tissues of plants. Although some recent studies have examined the composition of VOCs emitted by animal farms and from their wastes, their SOA formation potential is poorly known, and, on the basis of the conclusions of our study, they deserve investigation.

## 8.7 Final remarks

WSOC composition in background aerosol in the Po Valley in early spring was characterized as a mix of wood burning products, amines, and substituted aliphatic compounds with a minor contribution of MSA. The occurrence of aliphatic amines in large amounts suggest that biogenic sources from anaerobic processes may have been underestimated as a sources of SOA. Moreover, this experiment highlighted the fact that a fraction of the products of biomass burning was secondary in nature, i.e., originated by the atmospheric processing of gaseous and primary particulate compounds produced by combustion. The chemical composition of such secondary combustion aerosols was shown to be markedly different from that of the corresponding POA, and at the same time, was not represented by most common organic tracers used to apportion biomass burning POA. In this context, techniques of factor analysis applied to spectroscopic methods such as AMS and NMR proved to be able to overcome the main drawbacks of the methodologies relying on molecular tracer analysis, and could be profitably used for the identification of SOA fractions.

The interpretation of the SOA factor profiles, however, is dependent on the availability of reference spectra libraries, which in turn must be provided by dedicated laboratory experiments. At the moment, none of the existing analytical techniques possesses all requirements for organic source apportionment, accounting for both primary and secondary sources. On the contrary, my doctoral work provides examples of the usefulness of a combination of multiple chemical and factor analysis methods for addressing source apportionment problems during intensive field experiments. In this respect, NMR spectroscopy, being already a "hybrid" technique, by looking at the "bulk" composition in terms of functional groups but retaining information on molecular tracers (levoglucosan, MSA, etc.), certainly deserves more attention in future applications into receptor modeling.

# *Acknowledgements*

*This doctoral thesis is based on the experimental work carried out at the Institute of Atmospheric Sciences and Climate of the National Research Council (CNR-ISAC) in Bologna, within the Atmospheric Chemistry group headed by Dr. Sandro Fuzzi and Dr. Maria Cristina Facchini. I would like to express, first of all, my gratitude to them for having given me the opportunity of this invaluable experience.*

*I gratefully acknowledge financial supports from the University of Bologna, CNR-ISAC, the Atmospheric Composition Change European Network of Excellence (ACCENT-Plus), the Emilia-Romagna Region "SUPERSITO" Project and the European projects EUCAARI, MAP, PolySOA and PEGASOS.*

*I am most grateful to Dr. Stefano Decesari for supervision and support during the preparation of this thesis and of the whole doctoral project. My work would not have been successful without his help and patience. I would like to thank him for always believing in me and encouraging me to push the limits.*

*I am very grateful to Prof. Emilio Tagliavini for believing in me from the beginning and for the helpful suggestions.*

*I warmly thanks present and past fellow colleagues which all contributed substantially to this work and in creating a cheerful atmosphere. My special thanks to Lara Giulianelli, Stefania Gilardoni, Silvia Sandrini, Matteo Rinaldi, Claudio Carbone, Fabio Moretti, Leone Tarozzi and the irreplaceable Mario C.*

*I also take the opportunity here to thank all the staff involved in the AMS measurements and data processing during the various measurement campaigns that allowed me to complete this work: Risto Hillamo and its group at the Finnish Meteorological Institute (FMI), Helsinki, Finland; James Allan and its colleagues at the University of Manchester, Manchester, UK; Thomas F. Mentel, Astrid Kiendler-Scharr and their co-workers at the Forschungszentrum Jülich GmbH, Jülich, Germany; Andrea Piazzalunga of the University of Milano Bicocca; Ari Laaksonen and its co-workers at the University of Eastern Finland (UEF), Kuopio, Finland; Markku Kulmala and its group at the University of Helsinki, Finland; finally, Douglas R. Worsnop and its staff at the Aerodyne Research, Inc. Billerica, MA, USA.*

*I would like also to acknowledge all the people I worked with during the various field campaigns.*

*Finally, I warmly thanks my parents and my friends for having always support me!*

# References


Aalto P., Hämeri K., Becker E., Weber R., Salm J., Mäkelä J., Hoell C., O'Dowd C., Karlsson H., Hansson H.-C., Väkevä M., Koponen I., Buzorius G. and Kulmala M.: Physical characterization of aerosol particles during nucleation events, Tellus B, 53, 344–358, 2001.

Aiken A.C., DeCarlo P.F., and Jimenez J.L.: Elemental analysis of organic species with electron ionization high-resolution mass spectrometry, Anal. Chem., 79, 8350–8358, 2007.

Aiken A.C., DeCarlo P.F., Kroll J.H., Worsnop D.R., Huffman J.A., Docherty K., Ulbrich I.M., Mohr C., Kimmel J.R., Sueper D., Zhang Q., Sun Y., Trimborn A., Northway M., Ziemann P.J., Canagaratna M.R., Onasch T.B., Alfarra M.R., Prevot A.S.H., Dommen J., Duplissy J., Metzger A., Baltensperger U., and Jimenez J.L.: O/C and OM/OC ratios of primary, secondary, and ambient organic aerosols with high resolution timeof-flight aerosol mass spectrometry, Environ. Sci. Technol., 42, 4478–4485, 2008.

Aiken A.C., et al.: Mexico City aerosol analysis during MILAGRO using high resolution aerosol mass spectrometry at the urban supersite (T0) -- Part 1: Fine particle composition and organic source apportionment, Atmos. Chem. Phys., 9(17), 6633-6653, 2009.

Aiken A.C., de Foy B., Wiedinmyer C., DeCarlo P.F., Ulbrich I.M., Wehrli M.N., Szidat S., Prevot A.S.H., Noda J., Wacker L., Volkamer R., Fortner E., Wang J., Laskin A., Shutthanandan V., Zheng J., Zhang R., Paredes-Miranda G., Arnott W. P., Molina L. T., Sosa G., Querol X., and Jimenez J.L.: Mexico city aerosol analysis during MILAGRO using high resolution aerosol mass spectrometry at the urban supersite (T0) – Part 2: Analysis of the biomass burning contribution and the non-fossil carbon fraction, Atmos. Chem. Phys., 10, 5315-5341, doi:10.5194/acp-10-5315-2010, 2010.

Alfarra M.R., Coe H., Allan J.D., Bower K.N., Boudries H., Canagaratna M.R., Jimenez J.L., Jayne J.T., Garforth A.A., Li S.M. and Worsnop D.R.: Characterization of urban and rural organic particulate in the lower Fraser valley using two Aerodyne aerosol mass spectrometers, Atmos. Environ., 38, 5745–5758, 2004.

Alfarra M.R., Paulsen D., Gysel M., Garforth A.A., Dommen J., Prévôt A.S.H., Worsnop D. R., Baltensperger U. and Coe H.: A mass spectrometric study of secondary organic aerosols formed from the photooxidation of anthropogenic and biogenic precursors in a reaction chamber, Atmos. Chem. Phys., 6, 5279-5293, doi:10.5194/acp-6-5279-2006, 2006.

Allan J.D., Alfarra M.R., Bower K.N., Williams P.I., Gallagher M.W., Jimenez J.L., Mc-Donald A.G., Nemitz E., Canagaratna M.R., Jayne J.T., Coe H. and Worsnop D.R.: Quantitative sampling using an Aerodyne aerosol mass spectrometer: 2. Measurements of fine particulate chemical composition in two UK cities, J. Geophys. Res., 108, 4091, doi:10.1029/2002JD002359, 2003.

Allan J.D., Alfarra M.R., Bower K.N., Coe H., Jayne J.T., Worsnop D.R., Aalto P.P., Kulmala M., Hyötyläinen T., Cavalli F. and Laaksonen A.: Size and composition measurements of background aerosol and new particle growth in a Finnish forest during QUEST 2 using an Aerodyne Aerosol Mass Spectrometer, Atmos. Chem. Phys., 6, 315–327, doi:10.5194/acp-6-315-2006, 2006.

Allan J.D., Williams P.I., Morgan W.T., Martin C.L., Flynn M.J., Lee J., Nemitz E., Phillips G.J., Gallagher M.W. and Coe H.: Contributions from transport, solid fuel burning and cooking to primary organic aerosols in two UK cities, Atmos. Chem. Phys., 10, 647–668, doi:10.5194/acp-10-647-2010, 2010.

Alves C., Vicente A., Pio C., Kiss G., Hoffer A., Decesari S., Prevot A.S.H., Minguillon M.C., Querol X., Hillamo R., Spindler G., Swietlicki E.: Organic compounds in aerosols from selected European sites - Biogenic versus anthropogenic sources, ATMOSPHERIC ENVIRONMENT 59, 243-255, 10.1016/j.atmosenv.2012.06.013, 2012.

Andreae M. O. and Gelencsér, A.: Black carbon or brown carbon? The nature of light-absorbing carbonaceous aerosols, Atmos. Chem. Phys., 6, 3131-3148, doi:10.5194/acp-6-3131-2006, 2006.

Andreae M. O. and Rosenfeld D.: Aerosol-cloud-precipitation interactions. Part 1. The nature and sources of cloud-active aerosols. Earth Science Reviews, 89, 13-41, 2008.

Anttila P., Hyotylainen T., Heikkila A., Jussila M., Finell J., Kulmala M. and Riekkola M.L.: Determination of organic acids in aerosol particles from a coniferous forest by liquid chromatography-mass spectrometry, J. Sep. Sci., 28, 337–346, 2005.

Apel E.C., Brauers T., Koppmann R., Bandowe B., Boßmeyer J., Holzke C., Tillmann R., Wahner A., Wegener R., Brunner A., Jocher M., Ruuskanen T., Spirig C., Steigner D., Steinbrecher R., Gomez Alvarez E., Müller K., Burrows J.P., Schade G., Solomon S.J., Ladstätter-Weißenmayer A., Simmonds P., Young D., Hopkins J.R., Lewis A.C., Legreid G., Reimann S., Hansel A., Wisthaler A., Blake R.S., Ellis A.M., Monks P.S., Wyche K.P.: Intercomparison of oxygenated volatile organic compound (OVOC) measurements at the SAPHIR atmosphere simulation chamber J. Geophys. Res., 113, D20307, doi:10.1029/2008JD009865, 2008

Aouizerats B., Thouron O., Tulet P., Mallet M., Gomes L. and Henzing J.S.: Development of an online radiative module for the computation of aerosol optical properties in 3-D atmospheric models: validation during the EUCAARI campaign, Geosci. Model Dev., 3, 553-564, doi:10.5194/gmd-3-553-2010, 2010.

Athanasopoulou E., Vogel H., Vogel B., Tsimpidi A., Pandis S.N., Knote C. and Fountoukis C.: Modeling meteorological and chemical effects of secondary organic aerosol during an EUCAARI campaign, Atmos. Chem. Phys. Discuss., 12, 21815-21865, doi:10.5194/acpd-12-21815-2012, 2012.

Atkinson R. and Arey J.: Gas-phase tropospheric chemistry of biogenic volatile organic compounds: a review, Atmos. Environ., 37, S197–S219, 2003.

Baduel C., Voisin D. and Jaffrezo J.-L.: Seasonal variations of concentrations and optical properties of water soluble HULIS collected in urban environments, Atmos. Chem. Phys., 10, 4085-4095, doi:10.5194/acp-10-4085-2010, 2010.

Balasubramanian R., Qian W.-B., Decesari S., Facchini M.C., and Fuzzi S.: Comprehensive characterization of $PM_{2.5}$ aerosols in Singapore, J. Geophys. Res., 108, 4523, doi:10.1029/2002JD002517, D16, 2003.

Baltensperger U., Kalberer M., Dommen J., Paulsen D., Alfarra M.R., Coe H., Fisseha R., Gascho A., Gysel M., Nyeki S., Sax M., Steinbacher M., Prevot A.S.H., Sjoren S., Weingartner E. and Zenobi R.: Secondary organic aerosols from anthropogenic and biogenic precursors, Faraday Discuss., 130, 265–278, 2005.

Barmpadimos I., Keller J., Oderbolz D., Hueglin C. and Prevot A.S.H.: One decade of parallel fine (PM2.5) and coarse (PM10–PM2.5) particulate matter measurements in Europe: trends and variability, Atmos. Chem. Phys., 12, 3189–3203, doi:10.5194/acp-12-3189-2012, 2012.

Barnaba F., Angelini F., Curci G. and Gobbi, G.P.: An important fingerprint of wildfires on the European aerosol load, Atmos. Chem. Phys., 11, 10487–10501, doi:10.5194/acp-11-10487-2011, 2011.

Belis C.A. and Karagulian F.: Source Apportionment with Receptor Models: needs, trends and prospects, Geophysical Research Abstracts, Vol. 13, EGU2011-13531, EGU General Assembly, 2011.

Belis C.A., Karagulian F., Larsen B.R., Hopke P.K.: Critical review and meta-analysis of ambient particulate matter source apportionment using receptor models in Europe, Atmospheric Environment, Volume 69, Pages 94-108, ISSN 1352-2310, 10.1016/j.atmosenv.2012.11.009, 2013.

Bernstein J.A., Alexis N., Barnes C., Bernstein I.L., Nel A., Peden D., Diaz-Sanchez D., Tarlo S.M., Williams P.B.: Health effects of air pollution, J. Allergy Clin. Immunol., 114, 1116, 2004.

Blando J.D., Porcja R.J., Li T.-H., Bowman D., Lioy P.J. and Turpin B.J.: Secondary formation And the smoky mountain organic aerosol: an examination of aerosol polarity and functional group composition during SEAVS, Environ. Sci. Technol., 32, 604–613, 1998.

Bohn B., Rohrer F., Brauers T. and Wahner A.: Actinometric Measurements of $NO_2$ Photolysis Frequencies in the Atmosphere Simulation Chamber SAPHIR, Atmos. Chem. Phys., 5, 493–503, 2005.

Bömmel H., Haake M., Luft P., Horejs-Hoeck J., Hein H., Bartels J., Schauer C., Pöschl U., Kracht M., Duschl A., The diesel exhaust component pyrene induces expression of IL-8 but not of eotaxin., Int. Immunopharmacol., 3, 1371, 2003.

Bond T.C., Streets D.G., Yarber K.F., Nelson S.M., Woo J.-H., and Klimont Z.: A technology-based global inventory of black and organic carbon emissions from combustion, J. Geophys. Res., 109, D14203, doi:10.1029/2003JD003697, 2004.

Bond T.C. and Bergstrom R.W.: Light absorption by carbonaceous particles: An investigative review, Aerosol Sci. Technol., 40, 27–67, 2006.

Braun S., Kalinowski H.-O., Berber S.: 150 and more basic NMR Experiments, Wiley-VHC, Weinheim, Germany, 1998.

Bruinen de Bruin Y., Koistinen K., Yli-Tuomi T., Kephalopoulos S. and Jantunen M.: A review of source apportionment techniques and marker substances available for identification of personal exposure, indoor and outdoor sources of chemicals (54p.). JRC—European Commission, 2006.

Buset K.C., Evans G.J., Leaitch W.R., Brook J.R., Toom-Sauntry D.: Use of advanced receptor modelling for analysis of an intensive 5-week aerosol sampling campaign, Atmospheric Environment, Vol. 40, Supplement 2, Pages 482-499, 10.1016/j.atmosenv.2005.12.074, 2006.

Calvert J.G., Atkinson R., Becker K.H., Kamens R.M., Seinfeld J.H., Wallington T.J. and Yarwood G.: The Mechanisms of Atmospheric Oxidation of Aromatic Hydrocarbons, Oxford University Press, New York, 2002.

Canagaratna M.R., et al.: Chase Studies of Particulate Emissions from in-use New York City Vehicles, Aerosol Science and Technology, 38(6), 555 – 573, 2004.

Canagaratna M.R., Jayne J.T., Jimenez J.L., Allan J.D., Alfarra M.R., Zhang Q., Onasch T.B., Drewnick F., Coe H., Middlebrook A., Delia A., Williams L.R., Trimborn A.M., Northway M.J., DeCarlo P.F., Kolb C.E., Davidovits P., and Worsnop D.R.: Chemical and microphysical characterization of ambient aerosols with the aerodyne aerosol mass spectrometer, Mass Spectrom. Rev., 26, 185–222, 2007.

Capes G., Johnson B., McFiggans G., Williams P.I., Haywood J., and Coe H.: Aging of biomass burning aerosols over West Africa: Aircraft measurements of chemical composition, microphysical properties, and emission ratios, J. Geophys. Res., 113, D00C15, doi:10.1029/2008JD009845, 2008.

Cappiello A., De Simoni E., Fiorucci C., Mangani F., Palma P., Trufelli H., Decesari S., Facchini M.C. and Fuzzi S.: Molecular characterization of the water-soluble organic compounds in fogwater by ESIMS/MS, Environ. Sci. Technol., 37, 1229–1240, 2003.

Castro L., Pio C., Harrison R. and Smith D., Carbonaceous Aerosol in Urban and Rural European Atmospheres: Estimation of Secondary Organic Carbon Concentrations, Atmos. Environ. 33: 2771–2781, 1999.

Cavalli F., Facchini M. C., Decesari S., Mircea M., Emblico L., Fuzzi S., Ceburnis D., Yoon Y. J., O'Dowd C. D., Putaud J.-P., Dell'Acqua A., Advances in characterization of size-resolved organic matter in marine aerosol over the North Atlantic, *J. Geophys. Res.*, 109, D24215, doi:10.1029/2004JD005137, 2004.

Cavalli F., Facchini M.C., Decesari S., Emblico L., Mircea M., Jensen N.R. and Fuzzi S.: Size-segregated aerosol chemical composition at a boreal site in southern Finland, during the QUEST project, Atmos. Chem. Phys., 6, 993-1002, doi:10.5194/acp-6-993-2006, 2006.

Cheng Y. and Li, S.M.: Analytical method development of long-chain ketones in PM2.5 aerosols using accelerated solvent extraction and GC/FID/MSD, Int. J. Environ. Anal. Chem., 84, 367-378, 2004.

Cheng Y., He K.B., Duan F.K., Zheng M., Ma Y.L. and Tan J.H.: Positive sampling artifact of carbonaceous aerosols and its influence on the thermal-optical split of OC/EC. Atmos. Chem. Phys., 9, 7243–7256, 2009.

Chiappini L., Perraudin E., Durand-Jolibois R. and Doussin J.F.: Development of a supercritical fluid extraction-gas chromatography-mass spectrometry method for the identification of highly polar compounds in secondary organic aerosols formed from biogenic hydrocarbons in smog chamber experiments, Anal. Bioanal. Chem., 386, 1749–1759, 2006.

Claeys M., Graham B., Vas G., Wang W., Vermeylen R., Pashynska V., Cafmeyer J., Guyon P., Andreae M.O., Artaxo P. and Maenhaut W.: Formation of secondary organic aerosols through photooxidation of isoprene, Science, 303, 1173–1176, 2004a.

Claeys M., Wang W., Ion A.C., Kourtchev I., Gelencsér A. and Maenhaut W.: Formation of secondary organic aerosols from isoprene and its gas-phase oxidation products through reaction with hydrogen peroxide, Atmos. Environ., 38, 4093–4098, 2004b.

Claeys M., Szmigielski R., Kourtchev I., Van der Veken P., Vermeylen R., Maenhaut W., Jaoui M., Kleindienst T.E., Lewandowski M., Offenberg J.H. and Edney E.O.: Hydroxydicarboxylic acids: novel markers for secondary organic aerosol from the photooxidation of α-pinene, Environ. Sci. Technol., 41, 1628–1634, 2007.

Clavero P., Martìn-Vide J., and Raso J.: Atles climatic de Catalunya, Ed. Institut Cartografic de Catalunya, Alianza, 4957, 1997.

Coury C., Dillner A.M., A method to quantify organic functional groups and inorganic compounds in ambient aerosols using attenuated total reflectance FTIR spectroscopy and multivariate chemometric techniques, Atmospheric Environment, Vol. 42, Issue 23, Pages 5923-5932, ISSN 1352-2310, 10.1016/j.atmosenv.2008.03.026, 2008.

Coury C., Dillner A.M., ATR-FTIR characterization of organic functional groups and inorganic ions in ambient aerosols at a rural site, Atmospheric Environment, Vol. 43, Issue 4, Pages 940-948, ISSN 1352-2310, 10.1016/j.atmosenv.2008.10.056, 2009.

Crumeyrolle S., Schwarzenboeck A., Sellegri K., Burkhart J.F., Stohl A., Gomes L., Quennehen B., Roberts G., Weigel R., Roger J.C., Villani P., Pichon J.M., Bourrianne T. and Laj P.: Overview of aerosol properties associated with air masses sampled by the ATR-42 during the EUCAARI campaign (2008), Atmos. Chem. Phys. Discuss., 12, 9451-9490, doi:10.5194/acpd-12-9451-2012, 2012.

Cristofanelli P., Marinoni A., Arduini J., Bonafè U., Calzolari F., Colombo T., Decesari S., Duchi R., Facchini M.C., Fierli F. et al.: Significant variations of trace gas composition and aerosol properties at Mt. Cimone during air mass transport from North Africa – contributions from wildfire emissions and mineral dust. Atmos. Chem. Phys. 9, 2009.

de Gouw J.A., Middlebrook A.M., Warneke C., Goldan P.D., Kuster W.C., Roberts J.M., Fehsenfeld F.C., Worsnop D.R., Canagaratna M.R., Pszenny A.A.P., Keene W.C., Marchewka M., Bertman S.B. and Bates T.S.: Budget of organic carbon in a polluted atmosphere: Results from the New England Air Quality Study in 2002, J. Geophys. Res.-Atmos., 110, D16305, doi:16310.11029/12004JD005623, 2005.

DeCarlo P.F., Kimmel J.R., Trimborn A., Northway M.J., Jayne J.T., Aiken A.C., Gonin M., Fuhrer K., Horvath T., Docherty K.S., Worsnop D.R. and Jimenez J.L.: Field-deployable, high-resolution, time-of-flight aerosol mass spectrometer, Anal. Chem., 78, 8281–8289, 2006.

DeCarlo P.F., Dunlea E.J., Kimmel J.R., Aiken A.C., Sueper D., Crounse J., Wennberg P.O., Emmons L., Shinozuka Y., Clarke A., Zhou J., Tomlinson J., Collins D.R., Knapp D., Weinheimer A.J., Montzka D.D., Campos T. and Jimenez J.L.: Fast airborne aerosol size and chemistry measurements above Mexico City and Central Mexico during the MILAGRO campaign, Atmos. Chem. Phys., 8, 4027–4048, http://www.atmos-chem-phys.net/8/4027/2008/, 2008.

Decesari S., Facchini M.C., Fuzzi S. and Tagliavini E.: Characterization of water-soluble organic compounds in atmospheric aerosol: A new approach, J. Geophys. Res., 105, 1481–1489, 2000.

Decesari S., Facchini M.C., Matta E., Lettini F., Mircea M., Fuzzi S., Tagliavini E. and Putaud J.P.: Chemical features and seasonal variation of fine aerosol water-soluble organic compounds in the Po Valley, Italy, Atmos. Environ., 35, 3691–3699, 2001.

Decesari S., Moretti F., Fuzzi S., Facchini M.C. and Tagliavini E.: Comment on "On the use of anion exchange chromatography for the characterization of water soluble organic carbon" by H. Chang et al., Geophys. Res. Lett., 32, L24814, doi:10.1029/2005GL023826, 2005.

Decesari S., Fuzzi S., Facchini M.C., Mircea M., Emblico L., Cavalli F., Maenhaut W., Chi X., Schkolnik G., Falkovich A., Rudich Y., Claeys M., Pashynska V., Vas G., Kourtchev I., Vermeylen R., Hoffer A., Andreae M.O., Tagliavini E., Moretti F. and Artaxo P.: Characterization of the organic composition of aerosols from Rondnia, Brazil, during the LBASMOCC 2002 experiment and its representation through model compounds, Atmos. Chem. Phys., 6, 375–402, http://www.atmos-chem-phys.net/6/375/2006/, 2006.

Decesari S., Mircea M., Cavalli F., Fuzzi S., Moretti F., Tagliavini E. and Facchini M.C.: Source attribution of water-soluble organic aerosol by nuclear magnetic resonance spectroscopy, Environ. Sci. Technol., 41, 2479–2484, 2007.

Decesari S., Finessi E., Rinaldi M., Paglione M., Fuzzi S., Stephanou E.G., Tziaras T., Spyros A., Ceburnis D., O'Dowd C., Dall'Osto M., Harrison R.M., Allan J., Coe H., Facchini M.C.: Primary and secondary marine organic aerosols over the North Atlantic Ocean during the MAP experiment, *J. Geophys. Res.*, 116, D22210, doi:10.1029/2011JD016204, 2011.

Denkenberger K.A., Moffet R.C., Holecek J.C., Rebotier T.P. and Prather K.A.: Real-time, single-particle measurements of oligomers in aged ambient aerosol particles, Environ. Sci. Technol., 41, 5439–5446, 2007.

Derksen J.W.B., Roelofs G.-J.H., Otjesb R., de Leeuw G., Röckmanna T.: Impact of ammonium nitrate chemistry on the AOT in Cabauw, the Netherlands, Atmospheric Environment, Volume 45, Issue 31, October 2011, Pages 5640-5646, ISSN 1352-2310, 10.1016/j.atmosenv.2011.02.052, 2011.

Derome A.E.: Modern NMR Techniques for Chemistry Research, Pergamon Press, Oxford, UK, 1987.

Dinar E., Taraniuk I., Graber E.R., Katsman S., Moise T., Anttila T., Mentel T.F. and Rudich Y.: Cloud Condensation Nuclei properties of model and atmospheric HULIS, Atmos. Chem. Phys., 6, 2465–2482, http://www.atmos-chem-phys.net/6/2465/2006/, 2006.

Dinar E., Taraniuk I., Graber E. R., Anttila T., Mentel Th.F. and Rudich Y.: Hygroscopic growth of atmospheric and model humic-like substances, *J. Geophys. Res.*, 112, D05211, doi:10.1029/2006JD007442, 2007.

Docherty K.S. and Ziemann P.J.: On-line, inlet-based trimethylsilyl derivatization for gas chromatography of mono- and dicarboxylic acids, J. Chromatogr. A, 921, 265–275, 2001.

Docherty K.S. and Ziemann P.J.: Effects of stabilized Criegee intermediate and OH radical scavengers on aerosol formation from reactions of α-pinene with O3, Aerosol Sci. Tech., 37, 877–891, 2003.

Donaldson K., Stone V., Borm P. J. A., Jimenez L. A., Gilmour P. S., Schins R. P. F., Knaapen A. M., Rahman I., Faux S. P., Brown D. M., MacNee W., Oxidative stress and calcium signaling in the adverse effects of environmental particles ($PM_{10}$), Free Radical Biol. Med., 34,1369, 2003.

Drewnick F., Hings S.S., DeCarlo P.F., Jayne J.T., Gonin M., Fuhrer K., Weimer S., Jimenez J.L., Demerjian K.L., Borrmann S., and Worsnop, D.R.: A new time-of-flight aerosol mass spectrometer (ToF-AMS) – instrument description and first field deployment, Aerosol Sci. Tech., 39, 637–658, 2005.

Drewnick F., et al.: Measurement of Ambient, Interstitial, and Residual Aerosol Particles on a Mountaintop Site in Central Sweden using an Aerosol Mass Spectrometer and a CVI, Journal of Atmospheric Chemistry, 56(1), 1-20, 2007.

Duarte R.M.B.O. and Duarte A.C.: A critical review on the use of advanced analytical techniques for new insights into the nature of water-soluble organic matter from atmospheric aerosols. *TrAC - Trends in Analytical Chemistry. 30, 10, 1659-1671,* 2011.

Dutton S.J., Vedal S., Piedrahita R., Milford J.B., Miller S.L., Hannigan M.P.: Source apportionment using positive matrix factorization on daily measurements of inorganic and organic speciated PM2.5. Atmos Environ 44(23):2731–2741. doi:10.1016/j.atmosenv.2010.04.038, 2010.

Dzepina K., Arey J., Marr L.C., Worsnop D.R., Salcedo D., Zhang Q., Onasch T.B., Molina L.T., Molina M.J., and Jimenez J.L.: Detection of particle-phase polycyclic aromatic hydrocarbons in Mexico City using an aerosol mass spectrometer, Int. J. Mass Spectrom., 263, 152–170, 2007.

Edney E.O., Kleindienst T.E., Conver T.S., McIver C.D., Corse E.W., and Weathers W.S., Polar organic oxygenates in PM2.5 at a southeastern site in the United States, Atmos. Environ., 37, 3947–3965, 2003.

Edney E.O., Kleindienst T.E., Jaoui M., Lewandowski M., Offenberg J.H., Wang W. and Claeys M.: Formation of 2-methyl tetrols and 2-methylglyceric acid in secondary organic aerosol from laboratory irradiated isoprene/NOx/$SO_2$/air mixtures and their detection in ambient PM2.5 samples collected in the eastern United States, Atmos. Environ., 39, 5281–5289, 2005.

Ehn M., Kleist E., Junninen H., Petäjä T., Lönn G., Schobesberger S., Dal Maso M., Trimborn A., Kulmala M., Worsnop D.R., Wahner A., Wildt J. and Mentel Th.F.: Gas phase formation of extremely oxidized pinene reaction products in chamber and ambient air, Atmos. Chem. Phys., 12, 5113-5127, doi:10.5194/acp-12-5113-2012, 2012.

El Haddad I., D'Anna B., Temime-Roussel B., Nicolas M., Boreave A., Favez O., Voisin D., Sciare J., George C., Jaffrezo J.-L., Wortham H., and Marchand N.: On the chemical nature of the oxygenated organic aerosol: implication in the formation and aging of α-pinene SOA in a Mediterranean environment, Marseille, Atmos. Chem. Phys. Discuss., 12, 19769-19797, 2012
www.atmos-chem-phys-discuss.net/12/19769/2012/, doi:10.5194/acpd-12-19769-2012, 2012.

Eldering A. and Cass G. R.: Source-oriented model for air pollutant effects on visibility. Journal of Geophysical Research, 101, (D14). doi: 10.1029/95JD02928, 1996.

Engel-Cox J. and Weber S.A.: Compilation and Assessment of Recent Positive Matrix Factorization and UNMIX Receptor Model Studies on Fine Particulate Matter Source Apportionment for the Eastern United States, J. Air Waste Manage., 57, 1307–1316, doi:10.3155/1047-3289.57.11.1307, 2007.

Escudero M., Querol X., Pey J., Alastuey A., Pérez N., Ferreira F. et al.: A methodology for the quantification of the net African dust load in air quality monitoring networks. Atmospheric Environment, 41, 5516–5524, 2007.

Favez O., El Haddad, I., Piot C., Boréave A., Abidi E., Marchand N., Jaffrezo J.-L., Besombes J.-L., Personnaz M.-B., Sciare J., Wortham H., George C. and D'Anna B.: Inter-comparison of source apportionment models for the estimation of wood burning aerosols during wintertime in an Alpine city (Grenoble, France), Atmos. Chem. Phys., 10, 5295-5314, doi:10.5194/acp-10-5295-2010, 2010.

Fine P., Cass G. and Simoneit B.R.T.: Chemical characterization of fine particle emissions from the fireplace combustion of woods grown in the southern United States, Environ. Sci. Technol., 36, 1442–1451, 2002.

Finessi E., Decesari S., Paglione M., Giulianelli L., Carbone C., Gilardoni S., Fuzzi S., Saarikoski S., Raatikainen T., Hillamo R., Allan J., Mentel Th. F., Tiitta P., Laaksonen A., Petäjä T., Kulmala M., Worsnop D. R., and Facchini M. C.: Determination of the biogenic secondary organic aerosol fraction in the boreal forest by NMR spectroscopy, Atmos. Chem. Phys., 12, 941-959, doi:10.5194/acp-12-941-2012, 2012.

Fisseha R., Dommen J., Sax M., Paulsen D., Kalberer M., Maurer R., Hofler F., Weingartner E. and Baltensperger U.: Identification of organic acids in secondary organic aerosol and the corresponding gas phase from chamber experiments, Anal. Chem., 76, 6535–6540, 2004.

Fragkou E., Douros I. and Moussiopoulos N.: The use of models for source apportionment and for assessing the contribution of natural sources in response to the Air Quality Directive. In the Proceedings of the 13th Conference on Harmonisation within Atmospheric Dispersion Modelling for Regulatory Purposes, 985-989, 2010.

Franze T., Weller M.G., Niessner R., Pöschl U.: Protein Nitration by Polluted Air, Environ. Sci. Technol., 39, 1673, 2005.

Franze T., Weller M.G., Niessner R., Pöschl U.: Enzyme immunoassays for the investigation of protein nitration by air pollutants, Analyst, 128, 824, 2003.

Fuzzi S., Andreae M. O., Huebert B. J., Kulmala M., Bond T. C., Boy M., Doherty S. J., Guenther A., Kanakidou M., Kawamura K., Kerminen V.-M., Lohmann U., Russell L. M., and Pöschl U.: Critical assessment of the current state of scientific knowledge, terminology, and research needs concerning the role of organic aerosols in the atmosphere, climate, and global change, Atmos. Chem. Phys., 6, 2017-2038, - www.atmos-chem-phys.net/6/2017/2006/ - doi:10.5194/acp-6-2017-2006, 2006.

Gauderman W.J., Avol E., Gilliland F., Vora H., Thomas D., Berhane K., McConnell R., Kuenzli N., Lurmann F., Rappaport E., Margolis H., Bates D., Peters J.: The effect of air pollution on lung development from 10 to 18 years of age, N. Engl. J. Med., 351, 1057, 2004.

Gelencsér A., T. Mészáros, M. Blazsó, Gy. Kiss, Z. Krivácsy, A. Molnár and E. Mészáros: Structural Characterisation of Organic Matter in Fine Tropospheric Aerosol by Pyrolysis-Gas Chromatography-Mass Spectrometry, Journal of Atmospheric Chemistry, Volume 37, Number 2 (2000), 173-183, DOI: 10.1023/A:1006402731340. 2000.

Ghan S.J.; Schwartz S.E., Aerosol properties and processes - A path from field and laboratory measurements to global climate models, Bulletin Of The American Meteorological Society, vol.88, issues 7, 1059–1083, DOI: 10.1175/BAMS-88-7-1059, 2007.

Gilardoni, S., Liu, S., Takahama, S., Russell, L. M., Allan, J. D., Steinbrecher, R., Jimenez, J. L., De Carlo, P. F., Dunlea, E. J., and Baumgardner, D.: Characterization of organic ambient aerosol during MIRAGE 2006 on three platforms, Atmos. Chem. Phys., 9, 5417-5432, doi:10.5194/acp-9-5417-2009, 2009.

Gilardoni S., Vignati E., Cavalli F., Putaud J.P., Larsen B.R., Karl M., Stenström K., Genberg J., Henne S., and Dentener F.: Better constraints on sources of carbonaceous aerosols using a combined $^{14}C$ – macro tracer analysis in a European rural background site, Atmos. Chem. Phys., 11, 5685-5700, doi:10.5194/acp-11-5685-2011, 2011.

Goldstein, A. H. and Galbally, I. E., Known and unexplored organic constituents in the earth's atmosphere, Environ. Sci. Technol., 41, 1514–1521, 2007.

Goldstein A.H., Worton D.R., Williams B.J., Hering S.V., Kreisberg N.M., Pani O., and Górecki T.: Thermal desorption comprehensive two-dimensional gas chromatography for in-situ measurements of organic aerosols, J. Chromatogr. A, 1186, 340–347, 2008.

Graber E. R. and Rudich, Y.: Atmospheric HULIS: How humic-like are they? A comprehensive and critical review, Atmos. Chem. Phys., 6, 729-753, doi:10.5194/acp-6-729-2006, 2006.

Graham B., Mayol-Bracero O.L., Guyon P., Roberts G. C., Decesari S., Facchini M. C., Artaxo P., Maenhaut W., Köll P., and Andreae M.O.: Water-soluble organic compounds in biomass burning aerosols over Amazonia 1. Characterization by NMR and GC-MS, J. Geophys. Res., 107 (D20), doi:10.1029/2001JD000336, 2002.

Greaves R.C., Barkley R.M. and Sievers R.E.: Rapid Sampling and Analysis of Volatile Constituents of Airborne Particulate Matter, Anal. Chem., 57, 2807–2815, 1985.

Gross D.S., Galli M.E., Kalberer M., Prevot A.S.H., Dommen J., Alfarra M.R., Duplissy J., Gaeggeler K., Gascho A., Metzger A. and Baltensperger U.: Real-time measurement of oligomeric species in secondary organic aerosol with the aerosol time-of-flight mass spectrometer, Anal. Chem., 78, 2130–2137, 2006.

Guenther A., Hewitt C.N., Erickson D., Fall R., Geron C., Graedel T., Harley P., Klinger L., Lerdau M., Mckay W.A., Pierce T., Scholes B., Steinbrecher R., Tallamraju R., Taylor J., Zimmerman P.: A global model of natural volatile organic compound emissions, Journal of Geophysical Research, Vol. 100, No. D5, p. 8873-8892, 1995.

Hallquist M., Wenger J.C., Baltensperger U., Rudich Y., Simpson D., Claeys M., Dommen J., Donahue N.M., George C., Goldstein A. H., Hamilton J.F., Herrmann H., Hoffmann T., Iinuma Y., Jang M., Jenkin M.E., Jimenez J.L., Kiendler-Scharr A., Maenhaut W., McFiggans G., Mentel Th.F., Monod A., Prévôt A.S.H., Seinfeld J.H., Surratt J.D., Szmigielski R. and Wildt J.: The formation, properties and impact of secondary organic aerosol: current and emerging issues, Atmos. Chem. Phys., 9, 5155-5236, doi:10.5194/acp-9-5155-2009, 2009.

Hamburger T., McMeeking G., Minikin A., Birmili W., Dall'Osto M., O'Dowd C., Flentje H., Henzing B., Junninen H., Kristensson A., de Leeuw G., Stohl A., Burkhart J. F., Coe H., Krejci R., and Petzold A.: Overview of the synoptic and pollution situation over Europe during the EUCAARI-LONGREX field campaign, Atmos. Chem. Phys., 11, 1065-1082, doi:10.5194/acp-11-1065-2011, 2011.

Hand J.L., Schichtel B.A., Malm W.C. and Pitchford M.L.: Particulate sulfate ion concentration and $SO_2$ emission trends in the United States from the early 1990s through 2010, Atmos. Chem. Phys. Discuss., 12, 19311-19347, doi:10.5194/acpd-12-19311-2012, 2012.

Harrison R.M. and Yin J.: Sources and processes affecting carbonaceous aerosol in central England. Atmos. Environ. 42, 1413-1423, 2008.

Havers N., Burba P., Lambertm J. and Klockow D.: Spectroscopic characterization of humic-like substances in airborne particulate matter, J. Atmos. Chem., 29(1), 45–54, 1998.

Hays M.D. and Lavrich R.J.: Developments in direct thermal extraction gas chromatography-mass spectrometry of fine aerosols, Trac-Trend. Anal. Chem., 26, 88–102, 2007.

Healy R. M., Wenger J. C., Metzger A., Duplissy J., Kalberer M. and Dommen J.: Gas/particle partitioning of carbonyls in the photooxidation of isoprene and 1,3,5-trimethylbenzene, Atmos. Chem. Phys., 8, 3215–3230, http://www.atmos-chem-phys.net/8/3215/2008/, 2008.

Henry R.C.: Current factor analysis receptor models are ill-posed, Atmospheric Environment, 21, 1815–1820, 1987.

Henry R.C., Chang Y.S., & Spiegelman C.H.: Locating nearby sources of air pollution by nonparametric regression of atmospheric concentrations on wind direction, Atmospheric Environment, 36, 2237–2244, 2002.

Hinz K.P., Kaufmann R., and Spengler B.: Simultaneous detection of positive and negative ions from single airborne particles by real-time laser mass spectrometry, Aerosol Sci. Tech., 24, 233–242, 1996.

Ho S.S.H. and Yu J.Z.: Feasibility of collection and analysis of airborne carbonyls by on-sorbent derivatization and thermal desorption, Anal. Chem., 74, 1232–1240, 2002.

Hodzic A., Jimenez J.L., Madronich S., Canagaratna M.R., DeCarlo P.F., Kleinman L. and Fast J.: Modeling organic aerosols in a megacity: potential contribution of semi-volatile and intermediate volatility primary organic compounds to secondary organic aerosol formation, Atmos. Chem. Phys., 10, 5491-5514, doi:10.5194/acp-10-5491-2010, 2010.

Hoffer A., Gelencsér A., Guyon P., Kiss G., Schmid O., Frank G.P., Artaxo P. and Andreae M.O.: Optical properties of humic-like substances (HULIS) in biomass-burning aerosols, Atmos. Chem. Phys., 6, 3563-3570, doi:10.5194/acp-6-3563-2006, 2006.

Hoffmann T. and Warnke J., Organic Aerosols, in Volatile Organic Compounds in the Atmosphere, edited by R. Koppmann, Blackwell Publishing Ltd., Oxford, UK., pp. 342–387, 2007.

Holzinger R., Millet D.B., Williams B., Lee A., Kreisberg N., Hering S.V., Jimenez J., Allan J.D., Worsnop D.R., Goldstein A.H.: Emission, oxidation, and secondary organic aerosol formation of volatile organic compounds as observed at Chebogue Point, Nova Scotia. Journal of Geophysical Research 112: D10S24, DOI:10.1029/2006JD007599, 2007.

Holzinger R., Williams J., Herrmann F., Lelieveld J., Donahue N. M. and Röckmann T.: Aerosol analysis using a Thermal-Desorption Proton-Transfer-Reaction Mass Spectrometer (TD-PTR-MS): a new approach to study processing of organic aerosols, Atmos. Chem. Phys., 10, 2257-2267, doi:10.5194/acp-10-2257-2010, 2010.

Hopke P.K., & Song, X.: The chemical mass balance as a multivariate calibration problem, Chemometrics and Intelligent Laboratory Systems, 37, 5–14, 1997.

Hopke P.K., Ito K., Mar T., Christensen W.F., Eatough D.J., Henry R.C. et al.: PM source apportionment and health effects: 1. Intercomparison of source apportionment results, Journal of Exposure Science and Environmental Epidemiology, 16, 275–286, 2006.

Huang S., Arimoto R., Rahn K.A.: Sources and source variations for aerosol at Mace Head, Ireland, Atmospheric Environment, Vol. 35, Issue 8, 2001, Pages 1421-1437, ISSN 1352-2310, 10.1016/S1352-2310(00)00368-X, 2001.

Hueglin C., Gehrig R., Baltensperger U., Gysel M., Monn C., Vonmont H.: Chemical characterisation of PM2.5, PM10 and coarse particles at urban, near-city and rural sites in Switzerland, Atmospheric Environment, Vol. 39, Issue 4, Pages 637-651, ISSN 1352-2310, 10.1016/j.atmosenv.2004.10.027, 2005.

Huffman J.A., et al.: Design, Modeling, Optimization, and Experimental Tests of a Particle Beam Width Probe for the Aerodyne Aerosol Mass Spectrometer., Aerosol Science & Technology, 39(12), 1143-1163, 2005.

Huffman J.A., et al.: Chemically-resolved aerosol volatility measurements from two megacity field studies, Atmos. Chem. Phys., 9(18), 7161-7182, 2009.

IPCC, Climate change 2007: The Physical Science Basis, Cambridge University Press, Cambridge, 2007.

Jacobson M.C., Hansson H.C., Noone K.J., Charlson R.J.: Organic atmospheric aerosols: review and state of the science. Rev. Geophys. 38, 267–294, 2000.

Jaeckels J.M., Bae M.S., Schauer J.J.: Positive matrix factorization (PMF) analysis of molecular marker measurements to quantify the sources of organic aerosols. Environ Sci Technol. 41(16):5763–5769. doi:10.1021/es062536b, 2007.

Jaffrezo J.L., Calas T. and Bouchet M.: Carboxylic acids measurements with ionic chromatography, Atmos. Environ., 32, 2705–2708, 1998.

Jaumot J., Gargallo R., de Juan A., Tauler R.: A graphical user-friendly interface for MCR-ALS: a new tool for multivariate curve resolution in MATLAB, Chemometrics And Intelligent Laboratory Systems, 76(1), 101-110, May 2005.

Jaoui M., Kleindienst T.E., Lewandowski M., Offenberg J.H. and Edney E.O.: Identification and quantification of aerosol polar oxygenated compounds bearing carboxylic or hydroxyl groups: 2. Organic tracer compounds from monoterpenes, Environ. Sci. Technol., 39, 5661–5673, 2005.

Jayne J.T., Leard D.C., Zhang X.F., Davidovits P., Smith K.A., Kolb C.E. and Worsnop D.R.: Development of an aerosol mass spectrometer for size and composition analysis of submicron particles, Aerosol. Sci. Tech., 33, 49–70, 2000.

Jimenez J.L., Jayne J.T., Shi Q., Kolb C.E., Worsnop D.R., Yourshaw I., Seinfeld J.H., Flagan R. C., Zhang X.F., Smith K.A., Morris J.W. and Davidovits P.: Ambient aerosol sampling using the Aerodyne Aerosol Mass Spectrometer, J. Geophys. Res., 108, 8425, doi:10.1029/2001JD001213, 2003.

Jimenez J.L., Canagaratna M.R., Donahue N.M., Prevot A.S.H., Zhang Q., Kroll J.H., DeCarlo P.F., Allan J.D., Coe H., Ng N.L., Aiken A.C., Docherty K.S., Ulbrich I.M., Grieshop A.P., Robinson A.L., Duplissy J., Smith J.D., Wilson K.R., Lanz V.A., Hueglin C., Sun Y.L., Tian J., Laaksonen A., Raatikainen T., Rautiainen J., Vaattovaara P., Ehn M., Kulmala M., Tomlinson J.M., Collins D.R., Cubison M.J., Dunlea E.J., Huffman J.A., Onasch T.B., Alfarra M.R., Williams P.I., Bower K., Kondo Y., Schneider J., Drewnick F., Borrmann S., Weimer S., Demerjian K., Salcedo D., Cottrell L., Griffin R., Takami A., Miyoshi T., Hatakeyama S., Shimono A., Sun J.Y., Zhang Y.M., Dzepina K., Kimmel J.R., Sueper D., Jayne J.T., Herndon S.C., Trimborn A.M., Williams L.R., Wood E.C., Middlebrook A.M., Kolb C.E., Baltensperger U. and Worsnop D.R.: Evolution of Organic Aerosols in the Atmosphere, *Science 11 December 2009: 326 (5959), 1525-1529. [DOI:10.1126/science.1180353]*, 2009.

Kanakidou M., Seinfeld J.H., Pandis S.N., Barnes I., Dentener F.J., Facchini M.C., Van Dingenen R., Ervens B., Nenes A., Nielsen C.J., Swietlicki E., Putaud J.P., Balkanski Y., Fuzzi S., Horth J., Moortgat G.K., Winterhalter R., Myhre C.E.L., Tsigaridis K., Vignati E., Stephanou E.G. and Wilson J.: Organic aerosol and global climate modelling: a review, Atmos. Chem. Phys., 5, 1053–1123, doi:10.5194/acp-5-1053-2005, 2005.

Karakach T.K., Knight R., Lenz E.M., Viant M.R., Walter J.A.: Analysis of time course $^{1}$H NMR metabolomics data by multivariate curve resolution, Magn Reson Chem. 2009 Dec;47 Suppl 1:S105-17, 2009.

Karl M., Brauers Th., Dorn H.-P., Holland F., Komenda M., Poppe D., Rohrer F., Rupp L., Schaub A., Wahner A.: Kinetic Study of the OH-isoprene and $O_3$-isoprene reaction in the atmosphere simulation chamber, SAPHIR, Geophysical Research Letters, Volume 31, Issue 5, CiteID L05117, 2004.

Katsouyanni K., Touloumi G., Samoli E., Gryparis A., Le Tertre A., Monopolis Y., Rossi G., Zmirou D., Ballester F., Boumghar A., Anderson H. R., Wojtyniak B., Paldy A., Braunstein R., Pekkanen J., Schindler C., Schwartz J., Epidemiology, 12, 521, 2001.

Kerminen V.M., Ojanen C., Pakkanen T., Hillamo R., Aurela M. and Merilainen J.: Low molecular-weight dicarboxylic acids in an urban and rural atmosphere, J. Aerosol Sci., 31, 349–362, 2000.

Kiendler-Scharr A., Zhang Q., Hohaus T., Kleist E., Mensah A., Mentel T., Spindler C., Uerlings R., Tillmann R. and Wildt J.: Aerosol Mass Spectrometric Features of Biogenic SOA: Observations from a Plant Chamber and in Rural Atmospheric Environments, Environ. Sci. Technol. 43, 8166–8172, 2009.

Kim E. and Hopke P.K.: Identification of Fine Particle Sources in Mid-Atlantic US Area, Water, Air, and Soil Pollution, Volume 168, Issue 1-4, pp 391-421, 2005.

Kleinman L.I., Springston S.R., Daum P.H., Lee Y.N., Nunnermacker L.J., Senum G.I., Wang J., Weinstein-Lloyd J., Alexander M.L., Hubbe J., Ortega J., Canagaratna M.R. and Jayne, J.T.: The time evolution of aerosol composition over the Mexico City plateau, Atmos. Chem. Phys., 8, 1559–1575, 2008.

Kroll J.H., Seinfeld J.H.: Chemistry of secondary organic aerosol: Formation and evolution of low-volatility organics in the atmosphere, Atmospheric Environment, Vol. 42, Issue 16, Pages 3593-3624, ISSN 1352-2310, 10.1016/j.atmosenv.2008.01.003, 2008.

Kubátová A., Vermeylen R., Claeys M., Cafmeyer J., Maenhaut W., Roberts G. and Artaxo P.: Carbonaceous aerosol characterization in the Amazon basin, Brasil: novel dicarboxylic acids and related compounds, Atmos. Environ., 34, 5037–5051, 2000.

Kubátová A., Lahren T.J., Beránek J., Smoliakova I.P., Braun A. and Huggins F.E.: Extractable Organic Carbon and its Differentiation by Polarity in Diesel Exhaust, Wood Smoke, and Urban Particulate Matter, Aerosol Science and Technology, Vol. 43, Issue 7, pages 714-729, DOI: 10.1080/02786820902889853, 2009.

Kulmala M., Asmi A., Lappalainen H.K., Carslaw K.S., Pöschl U., Baltensperger U., Hov Ø., Brenquier J.-L., Pandis S.N., Facchini M.C., Hansson H.-C., Wiedensohler A. and O'Dowd C. D.: Introduction: European Integrated Project on Aerosol Cloud Climate and Air Quality interactions (EUCAARI) – integrating aerosol research from nano to global scales, Atmos. Chem. Phys., 9, 2825-2841, doi:10.5194/acp-9-2825-2009, 2009.

Kulmala M., Asmi A., Lappalainen H.K., Baltensperger U., Brenguier J.-L., Facchini M.C., Hansson H.-C., Hov Ø., O'Dowd C.D., Pöschl U., Wiedensohler A., et al.: General overview: European Integrated project on Aerosol Cloud Climate and Air Quality interactions (EUCAARI) – integrating aerosol research from nano to global scales, Atmos. Chem. Phys., 11, 13061-13143, doi:10.5194/acp-11-13061-2011, 2011.

Lanz V.A., Alfarra M.R., Baltensperger U., Buchmann B., Hueglin C., and Prévôt A.S.H.: Source apportionment of submicron organic aerosols at an urban site by factor analytical modelling of aerosol mass spectra, Atmos. Chem. Phys., 7, 1503–1522, http://www.atmos-chem-phys.net/7/1503/2007/, 2007.

Lanz V.A., Alfarra M.R., Baltensperger U., Buchmann B., Hueglin C., Szidat S., Wehrli M.N., Wacker L., Weimer S., Caseiro A., Puxbaum H., and Prevot A.S.H.: Source attribution of submicron organic aerosols during wintertime inversions by advanced factor analysis of aerosol mass spectra, Environ. Sci. Technol., 42, 214–220, 2008a.

Lanz V.A., Hueglin C., Buchmann B., Hill M., Locher R., Staehelin J. and Reimann S.: Receptor modeling of $C_2$–$C_7$ hydrocarbon sources at an urban background site in Zurich, Switzerland: changes between 1993–1994 and 2005–2006, Atmos. Chem. Phys., 8, 2313-2332, doi:10.5194/acp-8-2313-2008, 2008b.

Larsen R.K. III and Baker J.E.: Source Apportionment of Polycyclic Aromatic Hydrocarbons in the Urban Atmosphere: A Comparison of Three Methods. *Environ. Sci. Technol.*, *37* (9), 1873–1881, 2003.

Laupsa H., Denby B., Larssen S., Schaug J., Source apportionment of particulate matter (PM2.5) in an urban area using dispersion, receptor and inverse modelling, Atmospheric Environment, Vol. 43, Issue 31, Pages 4733-4744, ISSN 1352-2310, 10.1016/j.atmosenv.2008.07.010, 2009.

Lee D., Seung H., Algorithms for non-negative matrix factorization. Adv. Neural Inform. Process. Systems 13, 556-562, 2001.

Lenschow, P., Abraham, H. J., Kutzner, K., Lutz,M., Preuß, J. D., & Reichenbächer,W., Some ideas about the sources of PM10, Atmospheric Environment, 35(Suppl. 1), 123–133, 2001.

Li Z., Hopke P.K., Husain L., Qureshi S., Dutkiewicz V.A., Schwab J.J., Drewnick F., Demerjian K.L.: Sources of fine particle composition in New York city, Atmospheric Environment, Vol. 38, Issue 38, Pages 6521-6529, ISSN 1352-2310, 10.1016/j.atmosenv.2004.08.040, 2004.

Lim Y.B. and Ziemann P.J.: Products and mechanism of secondary organic aerosol formation from reactions of n-alkanes with OH radicals in the presence of NOx, Environ. Sci. Technol., 39, 9229–9236, 2005.

Limbeck A., Kulmala M., and Puxbaum H., Secondary organic aerosol formation in the atmosphere via heterogeneous reaction of gaseous isoprene on acidic particles, *Geophys. Res. Lett.*, 30(19), 1996, doi:10.1029/2003GL017738, 2003.

Lin C.-J.: Projected Gradient methods for Non-negative matrix factorization. Neural Computation, 19, 2756-2779, 2007.

Liu P., Ziemann P.J., Kittelson D.B. and McMurry P.H.: Generating Particle Beams of Controlled Dimensions and Divergence: II. Experimental Evaluation of Particle Motion in Aerodynamic Lenses and Nozzle Expansions, Aerosol Science & Technology, 22(3), 314-324, 1995a.

Liu P., Ziemann P.J., Kittelson D.B. and McMurry P.H.: Generating Particle Beams of Controlled Dimensions and Divergence: I. Theory of Particle Motion in Aerodynamic Lenses and Nozzle Expansions, Aerosol Science & Technology, 22(3), 293-313, 1995b.

Liu P.S.K., Deng R., Smith K.A., Williams L.R., Jayne J.T., Canagaratna M.R., Moore K., Onasch T.B., Worsnop D.R. and Deshler T.: Transmission Efficiency of an Aerodynamic Focusing Lens System: Comparison of Model Calculations and Laboratory Measurements for the Aerodyne Aerosol Mass Spectrometer, Aerosol Science and Technology, 41(8), 721 – 733, 2007.

Lohmann U. and Feichter J., Global Indirect Aerosol Effects: A Review, Atmos. Chem. Phys., 5, 715-737, 2005.

Mancinelli V., Rinaldi M., Finessi E., Emblico L., Mircea M., Fuzzi S., Facchini M.C., Decesari S.: An anion-exchange high-performance liquid chromatography method coupled to total organic carbon determination for the analysis of water-soluble organic aerosols, J. Chromatogr. A., 18; 1149(2):385-9, 16, 2007.

Maria S.F., Russell L.M., Turpin B.J., Porcja R.J., Campos T.L., Weber R.J., and Huebert B.J.: Source signatures of carbon monoxide and organic functional groups in Asian Pacific Regional Aerosol Characterization Experiment (ACE-Asia) submicron aerosol types, J. Geophys. Res., 108, 8637, doi:10.1029/2003JD003703, 2003.

Mayol-Bracero O.L., Guyon P., Graham B., Roberts G., Andreae M.O., Decesari S., Facchini M. C., Fuzzi S., and Artaxo P.: Water-soluble organic compounds in biomass burning aerosols over Amazonia 2. Apportionment of the chemical composition and importance of the polyacidic fraction, *J. Geophys. Res.*, 107(D20), 8091, doi:10.1029/2001JD000522, 2002.

McKeown P.J., Johnston M.V. and Murphy D.M.: Online Single-Particle Analysis by Laser Desorption Mass-Spectrometry, Anal. Chem., 63, 2069–2073, 1991.

McMurry P. H.: A review of atmospheric aerosol measurements, Atmos. Environ., 34, 1959-1999, 2000.

Mensah A., Holzinger R., Otjes R., Trimborn A., Mentel Th. F., ten Brink H., Henzing B., and Kiendler-Scharr A.: Aerosol chemical composition at Cabauw, The Netherlands as observed in two intensive periods in May 2008 and March 2009, Atmos. Chem. Phys., 12, 4723-4742, doi:10.5194/acp-12-4723-2012, 2012.

Moretti F., Tagliavini E., Decesari S., Facchini M.C., Rinaldi M., Fuzzi S.: NMR determination of total carbonyls and carboxyls: a tool for tracing the evolution of atmospheric oxidized organic aerosols, Environ Sci Technol., 42(13):4844-9, 2008.

Morgan W.T., Allan J.D., Bower K.N., Highwood E.J., Liu D., McMeeking G.R., Northway M.J., Williams P.I., Krejci R. and Coe H.: Airborne measurements of the spatial distribution of aerosol chemical composition across Europe and evolution of the organic fraction, Atmos. Chem. Phys., 10, 4065-4083, doi:10.5194/acp-10-4065-2010, 2010a.

Murphy, D.M., Cziczo, D.J., Hudson, P.K., and Thomson, D.S.: Carbonaceous material in aerosol particles in the lower stratosphere and tropopause region, J. Geophys. Res., 112, D04203, doi:10.1029/2006JD007297, 2007.

Nemmar A., Hoet P.H.M., Vanquickenborne B., Dinsdale D., Thomeer M., Hoylaerts M.F., Vanbilloen H., Mortelmans L., Nemery B.: Passage of Inhaled Particles Into the Blood Circulation in Humans, Circulation, 105, 411, 2002.

Ng N.L., Canagaratna M.R., Zhang Q., Jimenez J.L., Tian J., Ulbrich I.M., Kroll J.H., Docherty K.S., Chhabra P.S., Bahreini R., Murphy S.M., Seinfeld J.H., Hildebrandt L., Donahue N.M., DeCarlo P.F., Lanz V.A., Prévôt A.S.H., Dinar E., Rudich Y. and Worsnop D.R.: Organic aerosol components observed in Northern Hemispheric datasets from Aerosol Mass Spectrometry, Atmos. Chem. Phys., 10, 4625-4641, doi:10.5194/acp-10-4625-2010, 2010.

Noble C.A. and Prather K.A.: Real-time single particle mass spectrometry: A historical review of a quarter century of the chemical analysis of aerosols, Mass Spectrom. Rev., 19, 248–274, 2000.

Novakov T. and Corrigan C.E.: Cloud condensation nucleus activity of the organic component of biomass smoke particles. Geophys. Res. Lett. 23 (16), 2141–2144, 1996.

Novakov T. and Penner J. E: Large contribution of organic aerosols to cloud-condensation-nuclei concentrations, Nature, 365, 823– 826, 1993.

Noziere B., Dziedzic P., Cordova A.: Products and Kinetics of the Liquid-Phase Reaction of Glyoxal Catalyzed by Ammonium Ions (NH4+), *J. Phys. Chem. A*, 113 (1), pp 231–237, DOI: 10.1021/jp8078293, 2009.

Oberdörster G., Sharp Z., Atudorei V., Elder A., Gelein R., Kreyling W., Cox C.: Translocation of inhaled ultrafine particles to the brain, Inhalation Toxicol., 16, 437, 2004.

Oberdörster G., Oberdörster E., Oberdörster J.: Concepts of Nanoparticle Dose Metric and Response Metric, Environ. Health Perspect., 113, 823, 2005.

Orsini D.A., Ma Y.L., Sullivan A., Sierau B., Baumann K. and Weber R.J.: Refinements to the particle-into-liquid sampler (PILS) for ground and airborne measurements of water soluble aerosol composition, Atmos. Environ., 37, 1243–1259, 2003.

O'Dowd C.D., Facchini M.C., Cavalli F., Ceburnis D., Mircea M., Decesari S., Fuzzi S., Yoon Y.J., and Putaud J.P.: Biogenically-driven organic contribution to marine aerosol, Nature, doi:10.1038/nature02959, 2004.

Paatero P. and Tapper U.: Analysis of different modes of factor analysis as least squares fit problems, Chemom. Intell. Lab. Syst., 18, 183-194, 1993.

Paatero P. and Tapper U.: Positive matrix factorization: A non-negative factor model with optimal utilization of error estimates of data values, Environmetrics, 5, 111–126, doi:10.1002/env.3170050203, 1994.

Paatero P.: The Multilinear Engine: A Table-Driven, Least Squares Program for Solving Multilinear Problems, including the n-Way Parallel Factor Analysis Model, *Journal of Computational and Graphical Statistics*, Vol. 8, No. 4 (Dec., 1999), pp. 854-888, 1999.

Paatero P., Hopke P.K., Song X.H., and Ramadan Z.: Understanding and controlling rotations in factor analytic models, Chemom. Intell. Lab. Syst., 60, 253-264, 2002.

Paatero P., Hopke P.K., Begum B.A., and Biswas S.K.: A graphical diagnostic method for assessing the rotation in factor analytical models of atmospheric pollution, Atmos. Environ., 39, 193-201, 10.1016/j.atmosenv.2004.08.018, 2005.

Paatero P. and Hopke P.K.: Rotational Tools for Factor Analytic Models, J. Chemom., 23, 91-100, 10.1002/cem.1197, 2009.

Pankow J.F.: An absorption model of the gas/aerosol partitioning involved in the formation of secondary organic aerosol, Atmospheric Environment, Vol. 41, Supplement, 2007, Pages 75-79, ISSN 1352-2310, 10.1016/j.atmosenv.2007.10.060, 1994.

Parsons M.T., Knopf D.A., and Bertram A.K.: Deliquescence and crystallization of ammonium sulfate particles internally mixed with water-soluble organic compounds, J. Phys. Chem. A, 108, 11 600–11 608, 2004.

Peltier R.E., Sullivan A.P., Weber R.J., Wollny A.G.: Holloway, J.S., Brock, C.A., de Gouw, J.A., and Atlas, E.L.: No evidence for acid-catalyzed secondary organic aerosol formation in power plant plumes over metropolitan Atlanta, Georgia, Geophys. Res. Lett., 34, L06801, doi:10.1029/2006GL028780, 2007a.

Peltier R.E., Weber R.J. and Sullivan A.P.: Investigating a liquid-based method for online organic carbon detection in atmospheric particles, Aerosol Sci. Tech., 41(12), 1117–1127, 2007b.

Penner J., Dickinson R., and O'Neill C.: Effects of aerosol from biomass burning on the global radiation budget. Science 256:1432-1434, 1992.

Poirot R.L., Wishinski P.R., Hopke P.K., Polissar A.V.: Comparative application of multiple receptor methods to identify aerosol sources in northern Vermont, Environ Sci Technol. 1;35(23):4622-36, 2001.

Polidori A., Turpin B.J., Davidson C.I., Rodenburg L.A., and Maimone F.: Organic PM2.5: Fractionation by polarity, FTIR spectroscopy, and OM/OC ratio for the Pittsburgh aerosol, Aerosol Sci. Tech., 42, 233–246, 2008.

Pope C.A., Burnett R.T., Thurston G.D., Thun M.J., Calle E.E., Krewski D., Godleski J.J.: Cardiovascular mortality and long-term exposure to particulate air pollution: epidemiological evidence of general

pathophysiological pathways of disease, Circulation, 109, 71, 2004.

Pöschl U., Atmospheric aerosols: composition, transformation, climate and health effects, Angew Chem Int Ed Engl., 25; 44(46):7520-40, 2005.

Putaud J.P., Van Dingenen R., Baltensperger U., Brüggemann E., Charron A., Facchini, M. C., Decesari S. et al.: A European aerosol phenomenology : physical and chemical characteristics of particulate matter at kerbside, urban, rural and background sites in Europe. European Commission, 2003.

Putaud J.P., Raes F., Van Dingenen R., Brüggemann E., Facchini M.C., Decesari S., Fuzzi S., Gehrig R., Hüglin C., Laj P., Lorbeer G., Maenhaut W., Mihalopoulos N., Müller K., Querol X., Rodriguez S., Schneider J., Spindler G., ten Brink H., Tørseth K., Wiedensohler A.: A European aerosol phenomenology-2: chemical characteristics of particulate matter at kerbside, urban, rural and background sites in Europe, Atmospheric Environment, Vol. 38, Issue 16, May 2004, Pages 2579-2595, ISSN 1352-2310, 10.1016/j.atmosenv.2004.01.041, 2004.

Putaud J.P., Van Dingenen R., Alastuey A., Bauer H., Birmili W., Cyrys J., Flentje H., Fuzzi S., Gehrig R., Hansson H. C., Harrison R. M., Herrmann H., Hitzenberger R., Hueglin C., Jones A. M., Kasper-Giebl A., Kiss G., Kousa A., Kuhlbusch T. A. J., Loeschau G., Maenhaut W., Molnar A., Moreno T., Pekkanen J., Perrino C., Pitz M., Puxbaum H., Querol X., Rodriguez S., Salma I., Schwarz J., Smolik J., Schneider J., Spindler G., ten Brink H., Tursic J.,Viana M., Wiedensohler A., Raes F.: A European aerosol phenomenology-3: Physical and chemical characteristics of particulate matter from 60 rural, urban, and kerbside sites across Europe, ATMOSPHERIC ENVIRONMENT, Vol. 44, Issue: 10, pp 1308-1320, DOI:10.1016/j.atmosenv.2009.12.011, 2010.

Puxbaum H., Caseiro A., Sanchez-Ochoa A., Kasper-Giebl A., Claeys M., Gelencsér A., Legrand M., Preunkert S. and Pio C.: Levoglucosan levels at background sites in Europe for assessing the impact of biomass combustion on the European aerosol background, J. Geophys. Res., 112, D23S05, doi:10.1029/2006JD008114, 2007.

Raatikainen T., Vaattovaara P., Tiitta P., Miettinen P., Rautiainen J., Ehn M., Kulmala M., Laaksonen A. and Worsnop D.R.: Physicochemical properties and origin of organic groups detected in boreal forest using an aerosol mass spectrometer, Atmos. Chem. Phys., 10, 2063–2077, doi:10.5194/acp-10-2063-2010, 2010.

Reff A., Eberly S.I., and Bhave P.V.: Receptor modeling of ambient particulate matter data using positive matrix factorization: Review of existing methods, J. AirWaste Manage., 57, 146–154, 2007.

Reinhardt A., Emmenegger C., Gerrits B., Panse C., Dommen J., Baltensperger U., Zenobi R., Kalberer M.: Ultrahigh mass resolution and accurate mass measurements as a tool to characterize oligomers in secondary organic aerosols, Anal Chem. 2007 Jun 1; 79(11):4074-82, 2007.

Rinaldi M., Emblico L., Decesari S., Fuzzi S., Facchini M. C., Librando V.: Chemical characterization and source apportionment of size-segregated aerosol collected at an urban site in Sicily, Water Air Soil Pollut., 185, 311-321. DOI 10.1007/s11270-007-9455-4, 2007.

Rinaldi M., Facchini M.C., Decesari S., Carbone C., Finessi E., Mircea M., Fuzzi S., Ceburnis D., Ehn M., Kulmala M., de Leeuw G. and O'Dowd C.D.: On the representativeness of coastal aerosol studies to open ocean studies: Mace Head – a case study, Atm. Chem. & Phys., 9, 9635-96-46, 2009.

Robinson A.L. et al.: Rethinking organic aerosols: Semivolatile emissions and photochemical aging. Science 315:1259–1262, 2007.

Roelofs G.-J., ten Brink H., Kiendler-Scharr A., de Leeuw G., Mensah A., Minikin A. and Otjes R.: Evaluation of simulated aerosol properties with the aerosol-climate model ECHAM5-HAM using observations from the IMPACT field campaign, Atmos. Chem. Phys., 10, 7709-7722, doi:10.5194/acp-10-7709-2010, 2010.

Rohrer F., Bohn B., Brauers T., Brüning D., Johnen F.-J., Wahner A., and Kleffmann J.: Characterisation of the photolytic HONO-source in the atmosphere simulation chamber SAPHIR, Atmos. Chem. Phys., 5, 2189-2201, doi:10.5194/acp-5-2189-2005, 2005.

Röhrl A. and Lammel G.: Low molecular weight dicarboxylic acids and glyoxylic acid: Seasonal and air mass characteristics, Environ. Sci. Technol., 35, 95–101, 2001.

Römpp A., Winterhalter R. and Moortgat G.K.: Oxodicarboxylic acids in atmospheric aerosol particles, Atmos. Environ., 40, 6846–6862, 2006.

Rudich Y., Donahue N.M. and Mentel Th.F.: Aging of organic aerosol: Bridging the gap between laboratory and field studies, Ann. Rev. Phys. Chem., 58, 321–352, 2007.

Russell L.: Aerosol Organic-Mass-to-Organic-Carbon Ratio Measurements, Environ. Sci. Technol., 37, 2982–2987, 2003.

Russell L.M., Takahama S., Liu S., Hawkins L.N., Covert D.S., Quinn P.K., and Bates T.S., Oxygenated fraction and mass of organic aerosol from direct emission and atmospheric processing measured on the R/V Ronald Brown during TEXAQS/GoMACCS 2006, *J. Geophys. Res.*, 114, D00F05, doi: 10.1029/2008JD011275, 2009.

Russell L.M., Bahadur R., and Ziemann P.J.: Identifying Organic Aerosol Sources by Comparing Functional Group Composition in Chamber and Atmospheric Particles, Proc. Natl. Acad. Sci., doi:10.1073/pnas.1006461108, 2011.

Saarikoski S., Carbone S., Decesari S., Giulianelli L., Angelini F., Canagaratna M., Ng N.L., Trimborn A., Facchini M.C., Fuzzi S., Hillamo R. and Worsnop D.: Chemical characterization of springtime submicrometer aerosol in Po Valley, Italy, Atmos. Chem. Phys., 12, 8401-8421, doi:10.5194/acp-12-8401-2012, 2012.

Samet J., Wassel R., Holmes K. J., Abt E., Bakshi K.: Research priorities for airborne particulate matter in the United States, Environ. Sci. Technol., 39, 209A-304A, 2005.

Sax M., Zenobi R., Baltensperger U. and Kalberer, M.: Time resolved infrared spectroscopic analysis of aerosol formed by photo-oxidation of 1,3,5-trimethylbenzene and α-pinene, Aerosol Sci. Tech., 39, 822–830, 2005.

Schauer J.J., Rogge W.F., Hildemann L.M., Mazurek M.A. and Cass G.R.: Source apportionment of airborne particulate matter using organic compounds as tracers, Atmos. Environ., 30, 3837–3855, 1996.

Schauer C., Niessner R., and Pöschl U.: Polycyclic aromatic hydrocarbons in urban air particulate matter: decadal and seasonal trends, chemical degradation, and sampling artifacts, Environ. Sci. Technol., 37, 2861–2868, 2003.

Schauer J. J., Lough G.C., Shafer M.M., Christensen W.F., Arndt M.F., DeMinter J.T., et al., Characterization of metals emitted from motor vehicles. Health Effects Institute, 2006.

Schins R. P. F., Lightbody J. H., Borm P. J. A., Shi T. M., Donaldson K., Stone V., Inflammatory effects of coarse and fine particulate matter in relation to chemical and biological constituents, Toxicol. Appl. Pharmacol., 195, 1, 2004.

Schkolnik G., Falkovich A.H., Rudich Y., Maenhaut W., Artaxo P., New analytical method for the determination of levoglucosan, polyhydroxy compounds, and 2-methylerythritol and its application to smoke and rainwater samples, Environ Sci Technol., 15;39(8):2744-52, 2005.

Schmidl C., Bauer H., Dattler Astrid., Hitzenberger R., Weissenboeck G., Marr I.L., Puxbaum H., Chemical characterisation of particle emissions from burning leaves, ATMOSPHERIC ENVIRONMENT Volume: 42 Issue: 40 Pages: 9070-9079
DOI:10.1016/j.atmosenv.2008.09.010 , 2008.

Schneider J., et al.: Mass spectrometric analysis and aerodynamic properties of various types of combustion-related aerosol particles, International Journal of Mass Spectrometry, 258(1-3), 37-49, 2006.

Seinfeld J.H. and Pandis S.N., Atmospheric chemistry and physics – from air pollution to climate change, John Wiley & Sons, New York, 1998.

Shrivastava M.K., Subramanian R., Rogge W.F., and Robinson A.L.: Sources of organic aerosol: positive matrix factorization of molecular marker data and comparison of results from different source apportionment models. Atmos. Environ. 41(40):9353–9369. doi:10.1016/j.atmosenv.2007.09.016, 2007.

Slowik J.G., Stroud C., Bottenheim J.W., Brickell P.C., Chang R.Y.-W., Liggio J., Makar P.A., Martin R.V., Moran M.D., Shantz N.C., Sjostedt S.J., van Donkelaar A., Vlasenko A., Wiebe H.A., Xia A.G., Zhang J., Leaitch W.R. and Abbatt J.P.D.: Characterization of a large biogenic secondary organic aerosol event fromeastern Canadian forests, Atmos. Chem. Phys., 10, 2825–2845, doi:10.5194/acp-10-2825-2010, 2010.

Sorooshian A., Brechtel F.J., Ma Y., Weber R.J., Corliss A., Flagan R.C. and Seinfeld J.H.: Modeling and characterization of a particle-into-liquid-sampler (PILS), Aerosol Sci. Tech., 40, 396–409, 2006a.

Sorooshian A., Varutbangkul V., Brechtel F.J., Ervens B., Feingold G., Bahreini R., Murphy S.M., Holloway J.S., Atlas E.L., Buzorius G., Jonsson H., Flagan R.C. and Seinfeld J.H.: Oxalic acid in clear and cloudy atmospheres: Analysis of data from the International Consortium for Atmospheric Research on Transport and Transformation 2004, J. Geophys. Res., 111, D23S45, doi:10.1029/2005JD006880, 2006b.

Sorooshian A., Lu M.-L., Brechtel F.J., Jonsson H., Feingold G., Flagan R.C. and Seinfeld J.H.: On the source of organic acid aerosol layers above clouds, Environ. Sci. Technol., 41, 4647–4654, 2007a.

Sorooshian A., Ng N.L., Chan A.W.H., Feingold G., Flagan R.C. and Seinfeld J.H.: Particulate organic acids and overall water-soluble aerosol composition measurements from the 2006 Gulf of Mexico Atmospheric Composition and Climate Study (GoMACCS), J. Geophys. Res., 112, D13201, doi:10.1029/2007JD008537, 2007b.

Subramanian R., Khlystov A.Y., Cabada J.C. and Robinson A.L.: Positive and negative artifacts in particulate organic carbon measurements with denuded and undenuded sampler configurations, Aerosol Sci. Tech., 38, 27–48, 2004.

Sullivan, A. P., Weber, R. J., Clements, A. L., Turner, J. R., Bae, M. S., and Schauer, J. J.: A method for on-line measurement of water-soluble organic carbon in ambient aerosol particles: Results from an urban site, Geophys. Res. Lett., 31, L13105, doi:10.1029/2004GL019681, 2004.

Sullivan, R. C. and Prather, K. A.: Recent advances in our understanding of atmospheric chemistry and climate made possible by on-line aerosol analysis instrumentation, Anal. Chem., 77, 3861–3886, 2005.

Sun Y., Zhang Q., Zheng M., Ding X., Edgerton E.S., Wang X.: Characterization and source apportionment of water-soluble organic matter in atmospheric fine particles (PM2.5) with high-resolution aerosol mass spectrometry and GC-MS. Environ Sci Technol 45(11):4854–4861. doi:10.1021/es200162h, 2011.

Surratt, J. D., Murphy, S. M., Kroll, J. H., Ng, N. L., Hildebrandt, L., Sorooshian, A., Szmigielski, R., Vermeylen, R., Maenhaut, W., Claeys, M., Flagan, R. C., and Seinfeld, J. H.: Chemical composition of secondary organic aerosol formed from the photooxidation of isoprene, J. Phys. Chem. A, 110, 9665–9690, 2006.

Suzuki Y., Imai S., Kawakami M., Masuda Y., Akasaka K., Identification and determination of low-molecular weight organic compounds in contaminated fog water using proton nuclear magnetic resonance spectroscopy, Bull. Environ. Contam. Toxicol., 60(3):355-62, 1998.

Szidat S., Jenk T.M., Synal H.-A., Kalberer M., Wacker L., Hajdas I., Kasper-Giebl A., and Baltensperger U.: Contributions of fossil fuel, biomass burning, and biogenic emissions to carbonaceous aerosols in Zurich as traced by 14C, J. Geophys. Res., 111, D07206, doi:10.1029/2005JD006590, 2006.

Szmigielski, R., Surratt, J. D., Vermeylen, R., Szmigielska, K., Kroll, J. H., Ng, N. L., Murphy, S. M., Sorooshian, A., Seinfeld, J. H., and Claeys, M.: Characterization of 2-methylglyceric acid oligomers in secondary organic aerosol from the photooxidation of isoprene using trimethylsilylation and gas chromatography/ion trap mass spectrometry, J. Mass Spectrom., 42, 101–116, 2007a.

Szmigielski, R., Surratt, J. D., Gómez-González, Y., Van der Veken, P., Kourtchev, I., Vermeylen, R., Blockhuys, F., Jaoui, M., Kleindienst, T. E., Lewandowski, M., Offenberg, J. H., Edney, E. O., Seinfeld, J. H., Maenhaut, W., and Claeys, M.: 3-methyl-1,2,3-butanetricarboxylic acid: An atmospheric tracer for terpene secondary organic aerosol, Geophys. Res. Lett., 34, L24811, doi:10.1029/2007GL031338, 2007b.

Tagliavini, E., Moretti, F., Decesari, S., Facchini, M. C., Fuzzi, S., and Maenhaut, W.: Functional group analysis by H NMR/chemical derivatization for the characterization of organic aerosol from the SMOCC field campaign, Atmos. Chem. Phys., 6, 1003-1019, doi:10.5194/acp-6-1003-2006, 2006.

Tauler R., Multivariate Curve Resolution applied to second order data. Chemometrics and Intelligent Laboratory Systems 30, 133-146, 1995.

Terrado, M., Barcelo D., Tauler R., Multivariate curve resolution of organic pollution patterns in the Ebro River surface water-groundwater-sediment-soil system, ANALYTICA CHIMICA ACTA Volume: 657 Issue: 1 Pages: 19-27 DOI: 10.1016/j.aca.2009.10.026, 2010.

Topping, D.O., McFiggans, G.B., and Coe, H.: A curved multi-component aerosol hygroscopicity model framework: Part 2 – Including organic compounds, Atmos. Chem. Phys., 5, 1223–1242, http://www.atmos-chem-phys.net/5/1223/2005/, 2005.

Tunved P., Hansson H.-C., Kerminen V.-M., Ström J., Dal Maso M., Lihavainen H., Viisanen Y., Aalto P.P., Komppula M., and Kulmala M.: High natural aerosol loading over boreal forests, Science, 312, 261–263, 2006.

Turpin B.J. and Huntzicker J.J.: Identification of secondary organic aerosol episodes and quantitation of primary and secondary organic aerosol concentrations during SCAQS, Atmos. Environ., 29, 3527–3544. 1995.

Turpin B.J., Saxena P. and Andrews E.: Measuring and simulating particulate organics in the atmosphere: problems and prospects, Atmos. Environ., 34, 2983–3013, 2000.

Ulbrich I.M., Canagaratna M.R., Zhang Q., Worsnop D.R. and Jimenez J.L.: Interpretation of organic components from Positive Matrix Factorization of aerosol mass spectrometric data, Atmos. Chem. Phys., 9, 2891–2918, 2009.

Varga B., Kiss G., Ganszky I., Gelencsér A., Krivácsy Z., Isolation of water-soluble organic matter from atmospheric aerosol, Talanta, 2001 Sep 13;55(3):561-72, 2001.

Vecchi R., Valli G., Fermo P., D'Alessandro A., Piazzalunga A., Bernardoni V.: Organic and inorganic sampling artefacts assessment. Atmospheric Environment 43, 1713–1720, 2009.

Veltkamp, P.R., Hansen K.J., Barkley R.M. and Sievers R.E.: Chromatographic measurement of molecular markers of sources of atmospheric aerosol particles, Environ. Geochem. Hlth., 18, 77–80, 1996.

Verma V., Ning Z., Cho A.K., Schauer J.J., Shafer M.M., Sioutas C.: Redox activity of urban quasi-ultrafine particles from primary and secondary sources, Atmospheric Environment, Vol.43, Issue 40, Pages 6360-6368, 10.1016/j.atmosenv.2009.09.019, 2009.

Viana M., Zabalza J., Querol X., Alastuey A., Santamaría J.M., Gil J. I., et al.: Comparative analysis of PMF and PCA-MLRA results for PM2.5 at an industrial site in Northern Spain, In Summit on environmental modelling and software, July 9–12, 2006, Burlington, Vermont, USA, 2006.

Viana M., Kuhlbusch T.A.J., Querol X., Alastuey A., Harrison R.M., Hopke P.K., Winiwarter W., Vallius M., Szidat S., Prévôt A.S.H., Hueglin C., Bloemen H., Wåhlin P., Vecchi R., Miranda A.I., Kasper-Giebl A., Maenhaut W., Hitzenberger R., Source apportionment of particulate matter in Europe: a review of methods and results, *J. Aerosol Sci.* 39: 827–849, 2008.

Visser H., Buring E., & Breugel P.B. v.: Composition and origin of airborne particulate matter in the Netherlands. National Institute for Public Health and the Environment, RIVM, 2001.

Volkamer R., Jimenez J.L., San Martini F., Dzepina K., Zhang Q., Salcedo D., Molina L.T., Worsnop D.R. and Molina M.J.: Secondary organic aerosol formation from anthropogenic air pollution: Rapid and higher than expected, *Geophys. Res. Lett.*, 33, L17811, doi:10.1029/2006GL026899, 2006.

Wåhlin P.: COPREM—a multivariate receptor model with a physical approach. Atmospheric Environment, 37, 4861–4867, 2003.

Warnke, J., Bandur, R., and Hoffmann, T.: Capillary-HPLC-ESI-MS/MS method for the determination of acidic products from the oxidation of monoterpenes in atmospheric aerosol samples, Anal. Bioanal. Chem., 385, 34–45, 2006.

Watson J.G., Zhu T., Chow J.C., Engelbrecht J., Fujita E.M. and Wilson W.E.: Receptor modeling application framework for particle source attribution. Chemosphere, 49, 1093–1136, 2002.

Weber R.J., Orsini D., Daun Y., Lee Y.N., Klotz P.J. and Brechtel F.: A particle-into-liquid collector for rapid measurement of aerosol bulk chemical composition, Aerosol Sci. Tech., 35, 718–727, 2001.

Weber R.J., Sullivan A.P., Peltier R.E., Russell A., Yan B., Zheng M., de Gouw J., Warneke C., Brock C., Holloway J.S., Atlas E.L. and Edgerton E.: A study of secondary organic aerosol formation in the anthropogenic-influenced southeastern United States, J. Geophys. Res., 112, D13302, doi:10.1029/2007JD008408, 2007.

Wegener R., Brauers T., Koppmann R., Bares S.R., Rohrer F., Tillmann R., Wahner A., Hansel A. and Wisthaler A.: Simulation chamber investigation of the reactions of ozone with short-chained alkenes, J. Geophys. Res., 112, D13301, doi:10.1029/2006JD007531, 2007.

Wentzell P.D., Karakach T.K., Roy S., Martinez M.J., Allen C.P., Werner-Washburne M., Multivariate curve resolution of time course microarray data.BMC Bioinformatics 7, 343, 2006.

Whitby K.T.: The physical characteristics of sulfur aerosols, Atmospheric Environment (1967), Vol. 12, Issues 1–3, Pages 135-159, ISSN 0004-6981, 10.1016/0004-6981(78)90196-8,1978.

Williams J., de Reus M., Krejci R., Fischer H., and Ström J.: Application of the variability-size relationship to atmospheric aerosol studies: estimating aerosol lifetimes and ages, Atmos. Chem. Phys., 2, 133-145, doi:10.5194/acp-2-133-2002, 2002.

Williams B.J., Goldstein A.H., Kreisberg N.M. and Hering S.V.: An in-situ instrument for speciated organic composition of atmospheric aerosols: Thermal desorption aerosol GC/MS-FID (TAG), Aerosol Sci. Tech., 40, 627–638, 2006.

Williams B.J., Goldstein A.H., Millet D.B., Holzinger R., Kreisberg N.M., Hering S.V., Allan J.D., Worsnop D.R., Jimenez J.L. and White A.B.: Chemical Speciation of Organic Aerosol during ICARTT 2004: Results from In-Situ Measurements, J. Geophys. Res., 112, D10S26, doi:10.1029/2006JD007601, 2007.

Yu J.Z., Flagan R.C. and Seinfeld J.H.: Identification of products containing –COOH, –OH, and –C=O in atmospheric oxidation of hydrocarbons, Environ. Sci. Technol., 32, 2357–2370, 1998.

Yu J.Z., Cocker D.R., Griffin R.J., Flagan, R.C. and Seinfeld J. H.: Gas-phase ozone oxidation of monoterpenes: Gaseous and particulate products, J. Atmos. Chem. 34, 207–258, 1999.

Zhang Q., Alfarra M.R., Worsnop D. R., Allan J. D., Coe H., Canagaratna M.R., and Jimenez J.L.: Deconvolution and quantification of hydrocarbon-like and oxygenated organic aerosols based on aerosol mass spectrometry, Environ. Sci. Technol., 39, 4938–4952, 2005a.

Zhang Q., Worsnop D.R., Canagaratna M.R. and Jimenez J. L.: Hydrocarbon-like and oxygenated organic aerosols in Pittsburgh: insights into sources and processes of organic aerosols, Atmos. Chem. Phys., 5, 3289–3311, http://www.atmos-chem-phys.net/5/3289/2005/, 2005b.

Zhang Q., Jimenez J.L., Canagaratna M., Allan J., Coe H., Ulbrich I., Alfarra M., Takami A., Middlebrook A., Sun Y., Dzepina K., Dunlea E., Docherty K., De-Carlo P., Salcedo D., Onasch T., Jayne J., Miyoshi T., Shimono A., Hatakeyama S., Takegawa N., Kondo Y., Schneider J., Drewnick F., Borrmann S., Weimer S., Demerjian K., Williams P., Bower K., Bahreini R., Cottrell L., Griffin R., Rautiainen J., Sun J., Zhang Y., and Worsnop D.: Ubiquity and dominance ofoxygenated species in organic aerosols in anthropogenicallyinfluenced Northern Hemisphere midlatitudes, Geophys. Res. Lett., 34, L13801, doi:10.1029/2007GL029979, 2007.

Zhang Q., Jimenez J.L., Canagaratna M.R., Ulbrich I.M., Ng S.N., Worsnop D.R., and Sun Y.: Understanding Atmospheric Organic Aerosols via Factor Analysis of Aerosol Mass Spectrometry: a Review, *Analytical and Bioanalytical Chemistry*, 401, 3045-3067, DOI:10.1007/s00216-011-5355-y, 2011.

Zhang X., Smith K.A., Worsnop D.R., Jimenez J.L., Jayne J.T., Kolb C.E., Morris J. and Davidovits P.: Numerical Characterization of Particle Beam Collimation: Part II Integrated Aerodynamic-Lens-Nozzle System, Aerosol Science and Technology, 38(6), 619 – 638, 2004.

# List of frequently used abbreviations

$^{1}$H-NMR = Proton-Nuclear Magnetic Resonance Spectroscopy

AMS = Aerosol Mass Spectrometer

BB = Biomass Burning

BBOA = Biomass Burning organic Aerosol

BC = Black Carbon

BCN = Barcelona

CBW = Cabauw

CCN = Cloud Condensation Nuclei

CPC = Condensation Particle Counter

$D_a$ = Aerodynamic Particle diameter

DEA = Diethylamine

DMA = Dimethylamine

DMPS = Differential Mobility Particle Sizer

EC = Elemental Carbon

EUCAARI = European Aerosol Cloud Climate and Air Quality Interactions

FTIR = Fourier Transform Infrared spectroscopy

GC/MS = Gas Chromatography coupled with Mass Spectroscopy

HOA = hydrocarbon-like Organic Aerosol

HPLC = High Performance Liquid Chromatography

HULIS = Humic-Like Substances

HYY = Hyytiälä

IC = Ion Chromatography

IN = Ice Nuclei

IPCC = Intergovernmental Panel On Climate Change; http://www.ipcc.ch/

KPO = K-Puszta

LC/MS = Liquid Chromatography coupled with Mass Spectroscopy

LV-OOA = Low-Volatility OOA

MAAP = Multi Angle Absorption Photometer

MARGA = Measuring AeRosol and GAses

MBL = Marine Boundary Layer

MCR-ALS = Multivariate Curve Resolution-Alternating Least Squares

MCR-WALS = Multivariate Curve Resolution-Weighted Alternating Least Squares

MHD = Mace Head

MMA = Monomethylamine

MPZ = Melpitz

MSA = MethaneSulfonic Acid

MSY = Montseny

MT = monoterpenes

MW = Molecular Weight

m/z = mass to charge ratio

N-NMF = Non-negative Matrix Factorization

OA = Organic Aerosol

OM = Organic Matter

OOA = Oxygenated (or Oxidized) Organic Aerosol

PAHs = Polycyclic Aromatic Hydrocarbons

PBAPs = Primary Biological Aerosol Particles

PCA = Principal Component Analysis

PILS = Particle Into Liquid Sampler

PM = Particulate Matter

PMF = Positive Matrix Factorization

POA = Primary Organic Aerosol

PToF = Particle Time of Flight

SAPHIR Simulation of Atmospheric PHoto oxidation In a large Reaction chamber

SMPS = Scanning Mobility Particle Sizer

SOA = Secondary Organic Aerosol

SPC = San Pietro Capofiume

SQT = sesquiterpenes

SV-OOA = semi-volatile OOA

TC = Total Carbon

TD-PTR-MS = Thermo-Desorption Proton-Transfer-Reaction Mass Spectrometer

TMA = Trimethylamine

TMB = Trimethylbenzene

TMS = tetramethyl-silane (NMR internal standard)

TOC = Total Organic Carbon

TSPd4 = sodium 3-(trimethyldilyl-)-2,2,3,3-d4-proponiate (NMR internal standard)

VOC = Volatile Organic Compound

WIOC (or WINOC or WINC) = Water Insoluble Organic Carbon

WIOM (or WINOM) = Water Insoluble Organic Matter (= WIOC * 1.4)

WSOC = Water Soluble Organic Carbon

WSOM = Water Soluble Organic Matter (= WSOC * 1.8)

WSON = Water Soluble Organic Nitrogen

ZW = Zurich Winter